Imperial College London
Institute of Chemical Biology

Particulate Organic Matter in Artificial Soils

Oliver Levers

Supervisors:

Prof. Jason P. Hallett Prof. Robert V. Law Prof. Jon Lloyd

Submitted to meet the requirements for the degree of
Doctor of Philosophy in Chemical Biology
Imperial College London, July 2019

Funding

I gratefully acknowledge the funding provided by
the Institute of Chemical Biology and Climate KIC.

Copyright Declaration

Declaration of Originality

Unless otherwise stated, all work included in this thesis is original work.

Abstract

It is estimated that around 2 $\times 10^9$ hectares of land (15% of global land area) has been degraded by human activity, and rates of soil degradation are increasing. (*1*, *2*) Soil is a precious resource, it sustains almost all terrestrial life and provides 90% of the food that feeds humanity. (*3*) New methods are needed to improve degraded soils and recover desertified soils, particularly in higher risk areas such as deforested areas in the tropics. (*1*) Waste products of industrial bio-refining may provide a convenient and abundant material for use as a soil amendment, with the added benefit of increasing the carbon sequestration potential of bio-based products. Unfortunately, knowledge of how soils can be restored in a targeted manner are missing.

This thesis aims to determine the key inter-particulate interactions which promote the formation of stable aggregates, with a focus on bio-refinery products as soil amendments. New methodologies are established in order to explore particulate interactions in the context of soils, and tested on artificial soils and aggregates with defined compositions. Abiotic artificial soils are studied, to identify the physical and chemical aggregate forming processes separately of biological processes. Particulate - clay interactions are found to be complex, and the mechanical properties of the aggregate are found not only to be dependent on surface chemistry but also on the fabric morphology, pore space and particle shape. Organosolv lignin, a biorefinery waste product, was shown to bind to the silica face of kaolinite, driven by hydrophobic interactions in suspension, and were found to strengthen kaolinite aggregates up to a percolation threshold. Video image analysis is used to determine slaking kinetics of aggregates submerged in a flow cell. The role of these interactions for soil development is also investigated, in order to determine if aggregates form by accumulating stable organo-mineral interactions over repeated wet/dry cycles. The nature of lignin-kaolinite interactions are investigated using solid-state magic angle spinning NMR and T_1 relaxation NMR. Finally, a soil microcosm experiment was carried out, in order to determine the microbial response to the addition of lignin, which present a challenging substrate for ecosystems of degraded soils. These experiments illustrate the importance of particulate interactions for forming stable soil aggregates and soil structure, and the results provide insights into how particulates may be engineered to improve soils with a targeted approach.

Contents

Abstract **v**

Terms and Symbols **1**

1 Introduction **3**

1.1 Particles in soil 3

1.2 Clay particles in soil 5

1.3 Kaolinite 6

1.3.1 Kaolinite in solution 8

1.3.2 Kaolinite as a solid material 10

1.3.3 Organo-mineral interactions 11

1.3.4 Kaolinite in soils 14

1.4 Soil organic matter and particulate organic matter 15

1.4.1 Particulate organic matter 17

1.4.2 Aggregate formation 17

1.4.3 POM in aggregates 20

1.4.4 Aggregate forming interactions between particulates 21

1.5 Soil mechanics . . . 23

1.5.1 Unconfined uni-axial compression test and inter-particle forces . . . 24

1.5.2 Percolation of particle assemblages . . . 26

1.6 Motivation and Objectives . . . 27

2 Artificial Aggregates I: Interactions Between Kaolinite and Organosolv Lignin 29

2.1 Abstract . . . 29

2.2 Introduction . . . 30

2.3 Experimental Design . . . 31

2.4 Particulate amendments . . . 32

2.5 Methodology . . . 36

2.5.1 Materials . . . 36

2.5.2 Generation of artificial aggregates . . . 36

2.5.3 Unconfined uni-axial stress test . . . 37

2.5.4 Porosity and particle size measurements . . . 38

2.5.5 Isolation of soluble lignin . . . 38

2.6 Kaolinite . . . 39

2.6.1 Kaolinite: Volume, density and porosity of artificial aggregates . . . 41

2.6.2 Kaolinite: Mechanical properties . . . 44

2.7 HDPE artificial aggregates . . . 47

2.7.1 HDPE: Volume, porosity and shrinkage of artificial aggregates . . . 48

2.7.2 HDPE: Mechanical properties of artificial aggregates . . . 51

2.7.3 HDPE: Nature of the inter-particulate binding. 56

2.8 Organosolv lignin 57

2.8.1 Lignin particle size 57

2.8.2 Lignin: Volume, density and porosity. 58

2.8.3 Lignin: Mechanical properties 59

2.8.4 Lignin: Bonding interactions 61

2.8.5 Lignin: Porosity and drying rate 63

2.8.6 Lignin: Nature of binding 64

2.9 Lignin: Added electrolytes 66

2.10 Lignin: Influence of pH on the mechanical strength of lignin:kaolinite aggregates . . 70

2.10.1 Lignin solubility at raised pH 71

2.10.2 Lignin cohesion at increased pH 72

2.10.3 Lignin: Porosity, volume and mechanical strength of neutralised lignin aggregates 73

2.11 The role of dissolved organic matter in particulate interactions 78

2.12 Bentonite 80

2.13 Quartz silt 82

2.14 Discussion 82

2.15 Conclusions: Part I 83

2.15.1 Methodology 83

2.15.2 Kaolinite 85

2.15.3 HDPE 86

2.15.4 Lignin 87

2.15.5 Bentonite and silt 88

2.15.6 Electolyte 89

2.15.7 Humic acids 89

3 Artificial Aggregates II: Interactions of Cellulose, Biochar and Wood Fragments with Kaolinite 90

3.1 Introduction 90

3.1.1 Cellulose 92

3.1.2 Biochar 93

3.1.3 Wood fragments 94

3.2 Experimental design 94

3.3 Materials 94

3.4 Cellulose 95

3.5 Biochar 98

3.5.1 Biochar: mechanical properties 99

3.6 Artificially decayed wood 103

3.7 Discussion 108

3.8 Conclusion 109

3.8.1 Cellulose 109

3.8.2 Biochar 110

3.8.3 Wood fragments . . . 110

3.8.4 Part I and II: Relevance to soil science . . . 111

4 Water Stability of Artificial Aggregates 114

4.1 Abstract . . . 114

4.2 Introduction . . . 115

4.2.1 Determining soil aggregate stability and slaking. . . . 117

4.2.2 Aggregate composition . . . 118

4.2.3 Inter-particle forces . . . 119

4.2.4 Imaging analysis . . . 121

4.2.5 Slaking kinetics . . . 122

4.3 Methodology . . . 123

4.3.1 Slaking apparatus . . . 124

4.3.2 Interpretation of images . . . 124

4.3.3 Gompertz model . . . 128

4.4 Results . . . 129

4.4.1 Influence of restraining mesh on breakdown kinetics . . . 130

4.4.2 Bound electrolytes in kaolinite aggregates . . . 132

4.4.3 HDPE . . . 133

4.4.4 Lignin . . . 140

4.4.5 Influence of restraining mesh on breakdown kinetics . . . 144

4.4.6 Humic acids . . . 144

4.4.7 Cellulose . . . 145

4.4.8 Biochar . . . 147

4.4.9 Beech wood fragments . . . 149

4.4.10 Hydrogen peroxide bleached pulps . . . 150

4.4.11 Gompertz model . . . 152

4.5 Conclusions . . . 155

5 Are Particulate Interactions Able to Generate Stable Aggregates over Wet/Dry Cycles in an Artificial Soil? 159

5.1 Abstract . . . 159

5.2 Introduction . . . 161

5.3 Experimental design . . . 163

5.4 Methodology . . . 163

5.4.1 Artificial soils and wet and dry cycles . . . 164

5.4.2 Characterisation techniques . . . 164

5.5 Results . . . 165

5.5.1 The formation of soil structure with wet and dry cycles . . . 165

5.5.2 Aggregation and lignin loading . . . 167

5.5.3 Lignin distribution within soil fractions . . . 169

5.5.4 Mineral composition of aggregates . . . 169

5.5.5 Particle size distribution . . . 172

5.5.6 Iron oxide and aggregation . . . 172

5.5.7 Bentonite . . . 175

5.5.8 Spectroscopic evidence of inter-particulate interactions . . . 175

5.5.9 SEM of artificial aggregates . . . 177

5.5.10 Cation exchange capacity . . . 179

5.6 Conclusion . . . 179

6 How lignin modifies the microbial communities in a sandy soil 181

6.1 Abstract . . . 181

6.2 Introduction . . . 182

6.2.1 Fungal/microbial degradation of lignin . . . 182

6.2.2 The role of soil consitutents . . . 183

6.3 Experimental design and methodology . . . 184

6.3.1 CHNS, moisture content . . . 185

6.3.2 Metabolic activity . . . 185

6.3.3 HSQC of lignin extracts . . . 186

6.4 Results . . . 186

6.4.1 Microbial response to lignin addition . . . 186

6.4.2 Moisture content . . . 188

6.4.3 Elemental analysis and mass loss . . . 188

6.4.4 Lignin HSQC . . . 189

6.5 Conclusion . . . 190

7 Investigating Organosolv Lignin - Kaolinite Interactions using Solid Statets NMR192

7.1 Abstract . . . 192

7.2 Introduction . . . 193

7.3 Methodology . . . 194

7.4 Statement of originality . . . 194

7.5 ^{1}H MAS NMR of synthetic soils . . . 194

7.6 T_1 relaxation NMR of synthetic soils . . . 198

7.7 T_1 and T_2 relaxation of synthetic aggregates on wetting . . . 198

7.7.1 Kaolinite, lignin and bentonite . . . 198

7.7.2 Kaolinite-lignin blends . . . 201

7.8 Conclusion . . . 204

8 Conclusion 206

8.1 Integrating knowledge . . . 211

8.2 Future Work . . . 211

Bibliography 212

A Appendix 236

A.1 Lignin characterisation . . . 236

A.1.1 Gel permeation chromatography . . . 236

A.1.2 Elemental analysis . . . 237

A.1.3 Lignin HSQC . . . 237

A.1.4 ^{31}P NMR analysis 237

A.1.5 Soluble lignin NMR 239

A.2 Adsorption isotherms 241

A.2.1 Absorption isotherms 241

A.2.2 Artificial Humic and Fulvic Acids 242

List of Tables

2.1 The span as measured by static lightscattering measurements of HDPE particles in DI water. 48

4.1 The slaking characteristics of kaolinite artificial aggregates with a finer mesh. Slaking time was calculated from the intersect of the two tangents formed by the initial more rapid slaking and the second slow rate of slaking, due to the blockage formed in the mesh. 132

5.1 Mineral mixtures which were added to make up the artificial soils used in these experiments. 164

A.1 Molecular weight distribution by GPC of beech and spruce Organosolv lignin. Peak molecular weight (Mp) , number average molecular weight (Mn), number average molecular weight (Mw) and polydispersity (PD). 236

A.2 CHN elemental analysis for beech and spruce Organosolv lignin. 237

A.3 Quantitative ^{31}P NMR analysis of organosolv beech and spruce lignin. 239

A.4 Residual sum-of-squares (RSS) values for isotherms fitted with Langmuir and Freundlich models 243

List of Figures

1.1 The USDA Textural triangle, soil type is characterised by the clay, silt and sand content. Clay, silt and sand is defined by USDA particle size diameters rather than the mineralogy. Particulate organic matter is not included on the soil textural triangle. 4

1.2 Montmorrilonite is a typical 2:1 swelling clay. It contains an octahedral alumina sheet, sandwiched between two silica tetrahedral sheets. The 2:1 sheets stack, and the space between the layers swell when hydrated. Individual montmorrilonite lamella are 0.98 nm thick, but form larger structures around 1 - 5 µm in diameter. 5

1.3 Kaolinite is made up of stacked alumina and silica sheets. The crystal layer is about 0.72 nm thick, but forms strong bonding interactions between sheets, platelets are around 0.05 – 2.0 μm thick. The diameter of kaolinite platelets can be between 0.2 -10 µm. 7

1.4 The variable charge of the silica and alumina faces as determined by AFM as reported by Gupta et al.(*16*) 8

1.5 The colloidal behaviour of kaolinite particulates can take many forms depending on solution pH and the electrolyte type and concentration. Figure redrawn from "Particle interactions in kaolinite suspensions and corresponding aggregate structures"(*16*) 9

1.6 The aggregate hierarchy model as described by Tisdall and Oades, which describes larger aggreagates being made of smaller microaggregates, which are in turn made of primary particles. Figure adapted from 'The Nature and Properties of Soils' by N. C. Brady and R. R. Weil. (*74*) 19

1.7 The percolation threshold corresponds to a volume loading whereby the probability of long-range networks of the additive component are more likely, which results in a large change in mechanical properties. The black line represents a continuous network of additive particulates which form a continuous network. 26

2.1 **A:** Lignin is deposited in the secondary cell wall of plant cell tissues, particularly vascular and support tissues, and plays an important role in transporting water. **B:** Lignin is deposited around cellulose, hemi-cellulose and other biopolymers such as pectin. Its exact structure and morphology is not completely understood, and the nature of the interactions are likely to be both covalent linkages and non-covalent associations. (*112*, *113*) 33

2.2 Lignin is synthesised from three hydroxy-cinnamyl alcohols (left), which form three different aromatic subunits once incorporated into the lignin polymer (middle). Lignin is synthesised via oxidative radical polymerisation. Radical coupling of the monomers is favoured at the β-position. The most common linkage (β-O-4') represents around 50 - 65 % of the total linkages present in most wood lignins. (*105*, *114*) 34

2.3 Lignin routes to soil. Lignin rich biomass is broken down by a number of processes, including the breaking down of material by physical processes (attrition), digestion by wood eating organisms and microbial/fungal digestion. This results in the formation of water soluble aromatic molecules, macromolecular lignin fragments (insoluble) and recalcitrant lignin rich fragments. 35

2.4 XRD spectra of kaolinite, characteristic reflections at d_{001} 0.72 nm and d_{002} 0.36 nm of kaolinite are observed. Smaller peaks appear to be from similar clays from the kaolinite family. 39

2.5 The particle size of kaolinite dispersed in DI water as determined using static light scattering. The particle size was small, with a large dispersity. 40

2.6 Suspensions of kaolinite at different pHs displayed different suspension and settling characteristics. The suspensions on the left (pH $<$ 6) were unstable and very white, they settled out quickly. Above this pH the particles became creamy coloured and more stable in solution. 41

2.7 The change in zeta potential of kaolinite suspended in DI water was measured as a function of pH. Zeta potential reached a minimum at neutral pH, as the result of negative charges forming on the alumina and silica faces. 42

2.8 The physical properties of kaolnite aggregates. **A**: The greatest change in any dimension was observed in the thickness dimension (became less flat in the mould with increasing pH). **B:** The volume of the artificial aggregates therefore increases as a function of pH. **C:** The porosity increases linearly resulting in **D**: A large reduction in bulk density. Some data points were not measured at intermediate pH for C and D. There was a linear relationship between pH and porosity. Lines are linear regression fitting. Error bars represent one standard deviation (n = 3-5). 42

2.9 Scanning electron microscopy image of kaolinite at pH 4 showing face-face type interactions and blocky tactoids around 10 μm in diameter. 44

2.10 The mechanical properties of kaolinite aggregates over a range of pH values. **A:** The peak stress at failure increased linearly from 4.76 to 6.06 MPa, at which point it reached a plateau. **B:** No significant change in toughness was observed, however the data was very noisy, the result of fragmentation. **C:** The change in Modulus was most dramatic indicating a large increase in stiffness as pH increased. Error bars are one standard deviation (n = 3-5). 46

2.11 The particle size distribution for HDPE particles with different surface modifications. Unmodified particles are shown in blue, particles with COOH groups on the surface are indicated in red. The d(0.5) is shown in **A**, the particle size distributions are shown in **B**. The particle sizes are referred to by their d(0.5) in the text. 47

2.12 **A**: The skeletal density decreases as HDPE loading increases, with no differences between particles. **B**: Bulk density decreases non-linearly, reflecting a change in porosity. **C**: Artificial aggregate volume was almost identical with all treatments. **D**: The porosity of the kaolinite artificial aggregates amended with different HDPE particles decreased due to the replacement of a volume of fine clay material with larger non-porous beads. All lines are guides to the eye, except **C** where lines are linear regression. Error bars represent one standard deviation either side of the mean (n = 3-5). 49

2.13 Measurements from uniaxial compression tests of artificial aggregates containing HDPE. **A:** The decrease in strength for the HDPE artificial aggregates is linear and proportional to the volume loading of HDPE. The slight deviation from a linear decrease may reflect the decrease in porosity. **B:** Surface modification of the HDPE artificial aggregates resulted in the strengthening of the composites with only a marginal size dependence. **C:** The toughness decreases in a linear fashion, reflecting the change in strength for HDPE artificial aggregates. **D:** Modification of the artificial aggregates results in artificial aggregates which are more tough, larger particles impart greater strength. **E:** The modulus for HDPE artificial aggregates was small, and a small but marked decrease in modulus was observed. **F:** Modified HDPE were much stiffer, and smaller particles formed artificial aggregates with much higher modulus. **A, C, E** are fitted to linear models, whereas **B, D, F** are guides to the eye only. Error bars are one standard deviation (n= 3-5). 53

2.14 The mechanical properties of a series of artificial aggregates made with increasing HDPE content. **A:** The increase in strength due to the surface modification was calculated by subtracting the modified particle artificial aggregate strength from the unmodified particle artificial aggregate strength. Smaller particles reach a maxima at smaller volumes. Lines are guides to the eye only. **B:** The same increase in strength is plotted against the surface area of HDPE particles in a 1 cm-3 artificial aggregate, dotted lines are fitted to the initial increase in strength. The linear fit (black dashed line) for the 122 ^{2}m is for the first 4 points (y = 0.3634x - 0.4325, R^2 = 0.9821), the linear fit for 45 ^{2}m (black dashed line) is for the first 3 points (y = 0.1849x - 0.5667, R^2 = 0.9487), the red dashed line is for the first 2 points only (y = 0.2478x - 0.8619). **C:** The calculated surface area contribution of each component in each aggregate. 55

2.15 Particle size distribution of beech organosolv lignin before (**A**) and after sieving (**B**) as determined by static light scattering. Particles were dispersed in DI water. Kaolinite is also shown for comparison (purple). 58

2.16 The densities, volume and porosity of artificial aggregates made with increasing lignin content. **A:** The skeletal density decreases with increasing volume with both lignin types. **B:** The bulk densities were much lower than the skeletal densities. **C:** The artificial aggregate volumes increased linearly with an increase in lignin, due to the reduced density of the lignin and additional porosity. **D:** Porosity was very high (> 40%) and increased strongly as lignin was added. Straight lines are linear regression, others are guides to the eye. Error bars represent one standard deviation (n = 4-5). 60

2.17 The mechanical properties of lignin artificial aggregates. **A**: Maximum compressive strength reached a maxima for the lignin artificial aggregates between 20-50% lignin loading, with beech lignin forming stronger artificial aggregates than the spruce lignin. **B**: Toughness followed a similar trend, reaching a maxima at 20% loading for both lignins. **C**: The increase in modulus was much greater for the beech lignin. Lines are guides to the eye only, error bars are one standard deviation (n = 4-5). 62

2.18 The 900 - 1200 cm^{-1} region of the ATR-FTIR spectra of lignin:kaolinite artificial aggregates showing the major absorptions of Si-O in plane stretching. Spectra is baseline corrected and normalised to the inner surface -OH bend at 910 cm^{-1}. The FTIR of the beech lignin in artificial aggregates were not observed in the FTIR spectra, pure beech lignin is presented for reference. 65

2.19 **A:** ATR-FTIR spectra of the 900 - 1200 cm^{-1} region, showing the major absorptions of Si-O iand Al-OH stretching and bending absorptions. Signals for lignin were not observed, but a strong reduction in intensity and a shift to lower wavenumbers was observed on addition of soluble lignin. **B:** The region 3500 - 3800 cm^{-1} showing the OH surface stretching absorptions, the lowest peak at 3619 cm^{-1} is due to inner OH between tetrahedral and octahedral sheets, and should not be affected by surface adsoptions. The other absorptions are modified suggesting an interaction at both the octahedral face and edge sites. 66

2.20 The mechanical strength of different lignin amended aggregates containing salts. The effect of NaCl and $CaCl_2$ solutions on the τ_f of artificial aggregates containing only kaolinite, 25% mass loading beech lignin, and 50% mass loading lignin. Error bars represent one standard deviation from the mean (n=3), lines are guide to the eye only. 69

2.21 **A:** Initial pH of kaolinite:lignin powder mixtures with 1:10 solid, DI water mixture (mass ratio). Lines of fit for beech and spruce have $R^2 = 0.99$ and 0.98 respectively. **B:** The pH for artificial aggregates formed from these powders after crushing and slaking in DI water at the same 1:10 solid:water ratio. Lines are as guides to the eye only. 72

2.22 The zeta potential measured over a range of pH for beech organosolv lignin, measurements were made by adding NaOH from the initial solution which had a pH of 2.99. Lignin was measured as 5 g in 20 ml water. The zeta-potential goes from low when the suspensions are unstable, and become more negative as the pH is raised. Above pH 7, there is some partial lignin dissolution, towards pH 8, lignin appears to become largely soluble. 73

2.23 The porosity of both beech lignin (**A**) and spruce lignin (**B**) at low pH and neutral pH. Error bars represent one standard deviation from the mean, lines are a guide to the eye only. Errors were calculated using three repeats at a single representative volume loading. 74

2.24 The strength, toughness and modulus for beech (**A,C,E**) and for spruce (**B,D,F**) organosolv lignin as added to kaolinite. The strength of the artificial aggregates increased dramatically on neutralisation due to the formation of a soluble, or gel-like component. Neutral artificial aggregates are around 5 times stronger than the low pH artificial aggregates, however the effect of initial water content is considerable. The addition of lignin creates stronger artificial aggregates at all volume loadings, despite 100% lignin artificial aggregates forming weak and brittle composites. Lines are guides to the eye only, error bars represent one standard deviation (n = 3-5). . . 76

2.25 A comparison of the mechanical strength of pure kaolinite and 42% volume beech lignin cubes made pH 7 and pH 4.5 made with the same initial water content. pH 7 aggregates were stronger, although the difference was smaller once the initial water content had been corrected. 77

2.26 The mechanical properties of kaolinite and lignin amended aggregates, with the addition of a commercial humic acid. **A:** Humic acids increased the strength of a 42% beech lignin composite, more complex behaviour was observed with kaolinite artificial aggregates, strength increased to a maxima at intermediate humic acid loading, decreasing again at higher loadings. **B:** The toughness increased with the increase in strength for composites containing lignin. However, no increase in strength was observed for the kaolinite. A background electrolyte of 0.1 M NaCl was used to maintain the salinity of the neutralised humic acid. The humic acid concentrations reported here are not accurate, as some material was found to be insoluble. Lines are linear or polynomial fits, errors are standard deviations (n=3-4) 79

2.27 **A:** The increase in total volume of the artificial aggregates as the percentage of lignin within the composite is increased. This can be attributed to an increase in porosity. **B:** The increase in porosity as the volume loading of lignin is increased. A solid bentonite aggregate could not be made at this water content, but is likely that it would contain no internal porosity if formed. This means that all the porosity present is porosity within the lignin particles or pores created between bentonite and lignin. Lines are linear fits, error bars are standard deviation (n = 4-5) 80

2.28 The mechanical properties of bentonite artificial aggregates amended with beech lignin. The strength of the lignin:bentonite composites was high. Since pure bentonite aggregates could not be formed, it is difficult to determine if the amendment results in a strengthening of the cube. **A:** Strength decreases around 50% volume beech lignin, corresponding to a percolation threshold. **B:** The toughness followed the trend observed with the strength data. The overall strength and toughness was an order of magnitude greater than that of kaolinite composites. Lines are guide to the eye only, error bars represent standard deviation (n = 4-5) 81

2.29 At low pH, kaolinite forms blocky tactoids with low adhesion between tactoids (left). On raising the pH, the platelets form a more open structure with longer range connectivity (right). 86

2.30 The formation of an artificial aggregate is influenced by the interactions which form in the suspension, which are retained in the sediment and may also be retained in the dry solid. 88

3.1 **A:** The volume of cellulose artificial aggregates increased as low density cellulose fibres were added, decreasing again after 60% volume, due the densification of cellulose particles. **B:** Porosity of cellulose artificial aggregates with different fibre lengths. Lines are guide to the eye. Error bars are one standard deviation from the mean. . . 96

3.2 **A:** The addition of cellulose to kaolinite resulted in an almost exponential increase in strength, with a particle size dependence which may reflect the difference in porosity. **B:** The same as A but for the change in volume 0 – 40% for comparison. **C:** The toughness reflected the increase in strength. **D:** Youngs modulus reflected the increase in strength and toughness, suggesting the addition of cellulose fibres helps to from more stronger and more rigid composites. Lines are guide to the eye only, error bars represent one standard deviation (n = 3-5). 97

3.3 The addition of a concentrated glucose solution had no effect on the mechanical properties of kaolinite or a composite containing cellulose. Lines are linear fitting, error bars represent one standard deviation (n = 3). 98

3.4 **A:** The skeletal density decreased linearly as biochar is added, **B:** the bulk density decreased linearly. **C:** The artificial aggregate volume increased sharply after 60% volume loading. **D:** The porosity increased linearly with biochar loading. The porosity was lower than other amendments, especially considering biochar has inherent porosity. Error bars represent one standard deviation from the mean, lines are guide to the eye only. 100

3.5 Artificial aggregates formed by mixing biochar with kaolinite resulted in a much lower porosity than that for beech lignin. Biochar is more porous than lignin, identifying interparticle porosity as the key form of porosity in these experiments. Lines are guide to the eye only, error bars represent one standard deviation (n = 3-5). 101

3.6 **A:** The strength of the biochar composites increases in comparison to that of pure kaolinite, but appears to plateau, before reaching the percolation threshold. **B:** The change in toughness is similar to that of the strength. **C:** Modulus is also increased by the presence of biochar. Lines are guide to the eye only, error bars represent one standard deviation (n = 3-5). 102

3.7 The ATR-FTIR spectra of the beech wood, and two treatments with peroxide of different strengths. The peroxide treatment removed two peaks associated with lignin and hemi-cellulose. The absorption at 1723 cm^{-1} corresponds to a carbonyl group, the absorption at 1226 cm^{-1} corresponds to a C-O stretch, associated with hemicellulose and lignin. Lines are guide to the eye only, error bars represent one standard deviation (n = 3-5). 104

3.8 Surface area analysis using the BET method, **A:** The BET surface area shows total surface area decreases with bleaching, **B:** The t-plot external surface area and **C:** The micropore area. 105

3.9 **A:** The artificial aggregate volume increased linearly regardless of the peroxide treatment, suggesting that the drying behaviour was unaltered by the surface modification. **B:** The porosity of the artificial aggregates increased with a slight inflection at 15% volume loading, and was not significantly altered by the peroxide treatments. Lines are guide to the eye only, error bars represent one standard deviation (n = 3-5). . . 106

3.10 **A:** The maximum compressive strength of composites containing beech wood and semi-bleached beech wood plateaued around 15% volume, after which the compressive strength decreased, becoming non-cohesive. Fully bleached wood did not strengthen the composites and dropped rapidly in strength after 10% volume loading. **B:** The maximum strength increased to a maximum at 15% volume, except for that of the bleached pulp which decreased after 10% volume loading. **C:** The modulus followed the changes in strength, but the data was far noisier. Lines are guide to the eye only, error bars represent one standard deviation (n = 3-5). 107

3.11 fibre-like particles can form a scaffold within the aggregate, making the composite more spongey, thereby increasing the toughness. 107

4.1 Technical drawing of imaging cell, consisting of 1: Exchangeable mesh to containing sample. 2: Clear acrylic front panel, 3: Clear acrylic viewing window with 4: white acrylic diffuser for incoming light. 125

4.2 Technical drawing of assembled slaking cell with inlet and outlet hoses included. 5: Inlet hose from syringe pump, 6: sample cell, 7: outlet hose to waste. 126

4.3 A photo of the experimental set-up consisting of a camera and the flow cell. The whole set up is kept in the dark whilst recording in order to block out stray light. . . 127

4.4 An example of Gompertz fitting to the slaking profile of kaolinite, the red line indicates the fitted function, the linear line represents the maximum slaking rate defined by μ. The lag-phase λ, is the point that the linear function crosses the x axis. 128

4.5 The particle size distribution of kaolinite as received (purple) and slaked kaolinite (blue) dispersed in DI water, showing a reduction in particle size following slaking. . 130

4.6 **A:** The cumulative particle counts are higher for kaolinite slaked using a mesh sample holder, due to the mesh retaining larger particles. **B:** The onset for both samples was similar and the plateau for the three wires samples occurred at a similar point for the intersect between the initial rapid rate of slaking and the slower rate of slaking. Errors are plotted as standard deviations and visualised as purple ribbons (n=3). . . 131

4.7 Kaolinite made with additional salt solutions showed very different slaking behaviour. **A:** The culmulative particle counts was highest for sodium salts and lowest for calcium. **B:** The slaking percentage is shown to illustrate line shapes, but is not quantitative since the samples did not slake in the timescale of the experiment. All samples represent three repeats except for 0.1 M NaCl which is a single measurement. Standard deviation either side is visualised as ribbons. Kaolinite without added salt is in purple, $CaCl_2$ is in green, NaCl is pink and dark red. 134

4.8 HDPE particles with and without COOH surface modification added at 55% volume loading were compared. **A:** The percent slaked showed that the slaking profile for the modified HDPE and kaolinite were similar **B:** The cumulative total particle counts for the modified HDPE were much higher for both, with kaolinite forming larger, more discrete particulates. **C:** The dispersion was measured to be considerably higher in artificial aggregates containing modified HDPE. The dispersion reached a maximum around 160 seconds. (A and B errors for kaolinite shown as purple ribbon, n = 3). . 137

4.9 24, 55 and 65 % volume loadings of surface modified HDPE artificial aggregates as compared to pure kaolinite, is shown as a percentage of material slaked **(A)** and as total particle counts **(B)**.Unmodified particles at 24, 55 % volume loadings are shown here, as percentage slaked **(B)** and total particle counts **(C)**, higher loadings (65%) were found to be stable to slaking and so no particles were imaged. 138

4.10 The dispersion of the COOH modified HDPE cubes. Dispersed material was observed more quickly at lower HDPE loadings. At loadings where modified HDPE was the main component (> 50%) the dispersed material was very similar. Pure kaolinite had almost no dispersed material. 139

4.11 The slaking rates of COOH modified HDPE as a function of HDPE volume loading, the slaking rate transitioned from a more kaolinite-like slaking rate below 50% volume loading, to a slower rate at higher loadings. This is indicative of a percolation threshold.139

4.12 The cumulative particle counts for the lignin:kaolinite aggregates for which slaking rate and duration was calculated. Errors are omitted for clarity. 141

4.13 **A:**The initial slaking rate, appears to drop rapidly as the amount of lignin is added. **B:** The duration of the initial rapid slaking drops at around 50% lignin volume loading. **C:** Total particle counts at 900 seconds drops almost linearly with lignin loading, reaching a minimum around 50% loading. 142

4.14 The particle size distribution of kaolinite and a 25% volume lignin aggregate, following complete slaking in DI water. Particle sizes increase with the addition of lignin, resulting in a d0.5 increase of 27%. 143

4.15 Comparing the slaking behaviour of a 42% beech lignin aggregate slaked using either a mesh or wire restraint. The plateau for the wire indicating complete slaking corresponds to a reduction in slaking rate for the aggregate held by a mesh restraint (indicated by black crossed lines). 144

4.16 The addition of a concentrated humic acid solution to a 42%volume beech lignin cube was found not to change the slaking kinetics. 145

4.17 Slaking was very similar for all cellulose containing aggregates. **A:** The particle counts for cellulose containing aggregates was much higher than that for kaolinite. **B:** The slaking profile was not too disimilar from kaolinite, although there was a slight stabilisation in slaking rate. **C:** Dispersed material increased with increasing cellulose content, dispersed material reached a peak between 100 and 150 seconds, again, increasing with cellulose loading. 146

4.18 Biochar slaking, **A:** The cumulative particle counts at 200 seconds were extremely similar until loading approaches 50% volume biochar when particle counts increased dramatically, the highest loading (67.3%) produced a stream of dispersed material. **B:** Slaking profile of biochar loadings below 34%, slaking proceeded more slowly than pure kaolinite. **C:** There was a significant amount of dispersed material produced with increasing biochar loading, 67.3% volume loading biochar continued to produce biochar with a mean grey value exceeding 40 at 600 seconds. 148

4.19 **A:** The onset time decreased with biochar loading. **B:** The duration of rapid slaking increased substantially as the volume of biochar exceeds 50% volume, due to the formation of a large amount of small particles. 149

4.20 **A:** Wood pulps formed lots of material and counted particles far exceeded that of kaolinite (not shown) **B:** The slaking profiles are very different with wood amended kaolinite with a more distinct slaking profile. 150

4.21 30% hard treatment wood pulp formed a semi-stable aggregate which produced a constant stream of slaked material but retained its shape. 151

4.22 **A:**The cumulative particle counts were very similar, however, the values for the beech with soft and hard treatments may be artificially low, as the content of dispersed material may have masked the presence of particles. **B:** The percentage slaked showed that slaking duration was extended by the presence of treated and untreated wood particles, the harshest treatment resulted in a very different lineshape. **C:** Dispersion was high, and highest for the most bleached wood chips. **D**: Dispersed material observed in C was accompanied by an increase in the particle size of the slaked particles. 153

4.23 **A:** The maximum slaking rate, μ, was obtained via Gompertz line fitting. Slaking rate was highest in kaolinite samples, and those containing COOH modified HDPE. Biochar and cellulose particles had very similar slaking profiles. **B:** Lag time, λ, is also calculated using the same model and can be considered equivalent to the slaking onset mentioned previously. The offset was found to increase with samples containing HDPE particles, both modified and unmodified. Biochar and cellulose had a reduced offset. **C:** The offset was found to correlate strongly with porosity (here a third order polynomial has been fitted). 154

5.1 An artificial soil containing 5% beech lignin was subjected to repeated wet and dry cycles and rigourous mechanical disruption using a sieve shaker. The sieved material exceeding 420 μm (green) consisted of aggregated material, the middle size fractions containing material between 420 - 177 μm (sandy colours) contained predominantly coarse sand, the smallest size fractions $<$ 177 μm contain fine powders. 166

5.2 Photograph of the aggregated material which forms after wet and dry cycles and sieving. Blocky aggregates were formed which resembled real soil aggregates. 167

5.3 The increase in the mass of soil in the aggregated size fractions (2000 – 420 μm) increases with increasing lignin loading, shown here for three wet/dry cycles. The rate of increase is higher between 0 and 2.5 % lignin than between 2.5 - 5 % lignin. Error bars represent one standard deviation (n=3) and lines are a guide to the eye only. 168

5.4 The lignin distribution between size fractions as measured by CHNS and UV-visible spectrscopy. Lignin content is higher in the aggregated size fraction, and the un-aggregated size fractions, as compared to the material enriched in sand. Lignin determined by CHNS was much lower than that determined by UV-vis spectroscopy. Considering the mass balance of each fraction, total lignin was overestimated by UV-vis by 1 – 1.5 % for 5 % lignin samples, CHNS underestimated by 1 % for 5 % loading. This may be due to a slight bathochromic shift in the lignin spectra due to an increase in pH. In CHNS, complete combustion of soil organic matter with high ash (or mineral) content is often incomplete. The errors were higher for CHNS, possibly reflecting the heterogeneity of the smaller sample masses sampled. Both measurements were complimentary. 170

5.5 Elemental distribution with XRF, concentrations go from high (top left) to low (bottom right). Fe, representative of the iron oxide distribution was highest in the most aggregated size fraction. The exchangable cations Mg and Ca were enriched in more aggregated size fractions, with Ca significantly enriched in comparison to K. Mg was enriched in the smaller of the aggregated size fractions, indicating high levels of mica. The alumina/silicon ratio was used to indicate the clay content, a higher ratio suggesting an enrichment in kaolinite 171

5.6 Static light scattering was used to determine the particle size distributions of minerals, following a DMSO wash to remove lignin. **A**: The size fraction relating to coarse sand was used to determine the sand content of each size fraction. Sand accounts for 86 % and 93 % of the material in the central sieves, and appears to be normally distributed within the sieve fractions. **A**: The d(0.5) of each fraction was calculated, ommiting material which is sand sized ($>$ 100 µm). The largest material was observed in the sieve, corresponding to material enriched in quartz silt. 173

5.7 The total specific surface area or each sieve fraction, calculated from particle size measurements, were found to correlate with the lignin measured by UV/vis to be present in each sieve fraction. This suggests that lignin is associated with smaller particles due to the small surface area, and the specificity of this interaction may be minimal 174

5.8 Artificial soils where kaolinite was replaced by bentonite resulted in large changes to the soil structure and lignin distribution. Lignin was found to accumulate in aggregated size fractions, concentrations of lignin were higher than in the bulk of the soil, suggesting a stable interaction between bentonite and lignin was formed. . . 176

5.9 SEM image of the surface of a sand grain, which is encrusted with material which resembles lignin, quartz silt and kaolinite. 178

6.1 ATP counts were reduced drastically by the addition of lignin, conversely, ATP counts were much higher in soils with additional N. Soils with no lignin and high N additions were recorded to have the highest ATP counts. 187

6.2 The moisture content of soil microcosm experiments increased with both lignin addition and urea added. 188

6.3 Increasing the amount of lignin added to the soil increased the amount of carbon lost by the soil, indicating that likely lignin was slowly degraded in these microcosm experiments, despite the very low ATP counts. There was extremely high variance in the values obtained for 5% lignin loading which could not be explained by other measured variables such as N, cellobiose or moisture. Similarly the dry mass loss was higher when lignin was present, dry mass loss did not exceed 0.5 % of the soils mass. 189

6.4 A negative correlation between ATP counts and dry mass loss was observed, suggesting microbial communities were able to metabolise some material, but that this had a negative effect on overall microbial function or abundance. 190

7.1 The ^{1}H MAS NMR spectra of the size fractions of the synthetic soils, normalised to the proton concentration present, obtained from CHNS measurements. The broad line-shape originates from protons on the lignin, with some minor contributions from clays. 196

7.2 The ^{1}H solution state NMR spectra (dark brown) of beech organosolv lignin as compared to the solid state ^{1}H MAS NMR spectra (dark blue), showing the significant broadening effects. The y axis is an arbitary intensity unit which has been scaled to see both spectra. Signals above 5.5 ppm are from aromatic protons, below 5.5 the protons are generally more aliphatic. Sharp peaks are from residual water (3.35 ppm) and DMSO which was used to reference the spectra at 2.50 ppm. 197

7.3 The T_1 for kaolinite and lignin as water content was increased from 0 - 20$\%_{wt.}$. **A**: Kaolinite appears to reach a maxima when the number of protons contributing to the signal contributes 50%. **B**: Adding water to the lignin reduced the T_1, the water molecules cause rapid relaxation of the majority phase - lignin. 199

7.4 **A**:The T_1 for bentonite, which drops dramatically around 30% moisture content. This appears to correspond to a transition from monolayer to multilayer water coverage as indicated by calculations made in **B**. 200

7.5 **A**:The T_1 and **B**: FWHM of for kaolinite:lignin artificial aggregate blends. 201

7.6 **A**:The T_1 data replotted as a function of the percentage protons originating from lignin. A 1:1 ratio would be expected if there was no changes in T_1 for the individual components (grey line), however, the data suggests that lignin has a reduced T_1 in the presence of kaolinite. 202

7.7 **A**:The T_1 data as measured, showing line shapes and features which are similar to the majority phase. **B**: The calculated T_1 data if the T_1 was just a combination of the T_1 from each component. The difference between **A** and **B** is the change in T_1 due to an interaction 203

7.8 The difference between the recorded and the calculated T_1 values for kaolinite-lignin mixtures at different moisture contents. All values are negative, meaning the recorded T_1s are much smaller (faster) than expected. 204

A.1 The 2D HSQC NMR of beech organosolv lignin dissolved in *d*-DMSO, showing the aromatic region (left) and the oxygenated aliphatic regions (right) with colour coded chemical structures. The main subunits, syringyl (S) and guaiacyl (G) are shown along with the main linkages, β-O-4' aryl ether linkage and the $\beta - \beta'$ resinol linkage.238

A.2 Soluble extracts of aqueous lignin at various pH were extracted and redissolved in *d*-DMSO for ^{1}H NMR. Top: The ratio of signal intensity aromatic/fatty(aliphatic) increases, acid-soluble lignin is therefore more aliphatic than aromatic. Middle: Methoxy groups are found on aromatic rings, and are present in solution at higher pH. Lower: The signal from β-0-4' is much higher at lower pH too, indicating less chemically modified lignin are acid soluble. Additionally the peak for COOH also increases with pH. Note: at low pH the amount of soluble material was extremely low and repeated washings were used to obtain enough material for NMR. It may be that this material was fine particulates, rather than fully dissolved. 240

A.3 The adsorption isotherm for organosolv lignin dissolved in acetone on kaolinite clay, the data was fitted to a Langmuir model (red) and a Freundlich model (blue). Langmuir model was used to obtain the equilibrium constant K_L and the maximum absorption Q_e per g of kaolinite where as Freundlich model was used to determine equilibrium constant K_F and the dimensionless heterogeneity factor n. 242

A.4 The adsorption isotherm for lignin derived 'humic' and 'fulvic' acids on kaolinite clay, the data was fitted to a Langmuir model (red) and a Freundlich model (blue). Humic acids were found to have a higher adsorption. Langmuir model was used to obtain the equilibrium constant K_L and the maximum absorption Q_e per g of kaolinite where as Freundlich model was used to determine equilibrium constant K_F and the dimensionless heterogeneity factor n. Measurements were made in triplicate. 244

A.5 The adsorption isotherm for lignin derived 'fulvic' acids on kaolinite and iron oxide, the data was fitted to a Langmuir model (red) and a Freundlich model (blue). Kaolinite was found to be a stronger adsorbent of fulvic acids. Measurements were made in triplicate. 244

Terms and Symbols

Artificial aggregate : In the context of this thesis an 'artificial aggregate' is a term used to describe particulate composites formed by drying a wet paste in a cubic mould, the composites are generally formed by mixing two powders.

Shear stress (τ) **or shear stress at failure** (τ_f): shear stress (stress perpendicular to cross section) given in units of N/m^2 or Pa, is the force applied to the solid over a unit area.

Normal stress (σ): Loads applied normal to the stress are called the normal stress and are also given in units of N/m^2 or Pa.

Strain (ε) = strain is a measure of deformation / unitless although sometimes % or mm^{-1}.

Hardness: The hardness of a material describes the resistance of a material to plastic deformation.

Toughness (U_T): Describes the amount of energy an object can absorb before it fails. It is the area under the stress strain graph and requires both strength and ductility to obtain a high toughness. Given in $J.m^{-3}$.

Strength: Ability to withstand an applied load without failure or plastic deformation, per unit area. In this context, strength is used interchangeably with ultimate compressive strength.

Yield strength: Is the minimum amount of applied stress that can result in permanent deformation

Yield point: At this point the material is no longer elastic and undergoes plastic deformation

Ultimate compressive strength: The stress which is reached at complete failure, equivalent to shear stress at failure, (τ_f).

Effective stress: The normal intergranular contact, force between particles. (force per unit area). Often used in soil science to describe the stress that allows a heap of powders to retain its structure. Gives rise to the angle of internal friction.

Friction angle(φ) (angle of internal friction): The angle of repose (the mount angle) gives the

angle of internal friction. Firm soil will have a steeper angle. tan to the line of the failure envelope in a graph of shear vs normal stress.

Young's Modulus: Youngs Modulus is reported for materials with measurable elastic regions in the stress/strain curve. Elastic deformation in the solids described here were extremely small to none, and so are not reported.

Modulus: (M) Modulus here is used as a measure of the stiffness in the plastic region. Therefore it is a measure of the particles resistance to reorganisation and deformation. Deformation in the plastic region is usually non-linear, but for almost all samples described here a linear fit was applicable.

Cohesion and adhesion: cohesion describes a sticking of a material to itself, adhesion is the property of different materials sticking together, although in particulate solids, the distinction is not always made.

Porosity (φ): The empty space within a solid, often defined as a percentage of the total volume. Often porosity is given in terms of the void ratio, but percentage porosity is used here.

Anhedral: a mineral grain without characteristic crystalline faces.

Atterberg limits: The water content at which a soil's consistency and behaviour change from being either solid, semi-solid, plastic and liquid.

Chapter 1

Introduction

Soil can be considered, at its most fundamental level, to be a collection of particles. These particles coalesce, and the particles which stick together and remain stable are called soil aggregates. These aggregates may be held together by forces between particles or surfaces, or by cementing agents which are biotic or abiotic in origin (*4*). Within these associations of particles exist pore space. This pore space is essential for soil functioning; porosity can hold water, an electrolyte, dissolved organic materials and provide an environment for the soil ecosystem (*5*). These aggregates and the pore space they create form the soil structure, which is constantly changing and evolving, and is fundamental to the health and character of the soil.

1.1 Particles in soil

It is well known that the material properties of soil are governed to a large extent by the particle size and particle size distribution of the minerals present (*6*). The soil textural triangle (Figure 1.1) demonstrates this, with each axis of the triangle representing a different mass percent of a particle size present. In this case, the definitions of 'clay', 'silt' and 'sand' are commonly defined by the particle size range, rather than the composition or mineralogy of the material. That said, the sand and silt fractions are generally dominated by silicates, whereas the clay fraction contains more diverse mineralogy, generally consisting of aluminosilicates and metal oxides and hydroxides. (*7*)

Soil texture can be used diagnostically, and is commonly used to suggest the suitability of land for agriculture. (*8*) Soil texture measurements can be done by hand, or by more sophisticated methods such as particle size measurements. Regardless of the method of particle size measurement used, the application and usefulness of the soil textural triangle has remained unchanged for decades. (*9*) This illustrates the importance of particulates as functional components of soil. The mineral fraction is often the least transient of the materials that make up soil and so in heavily cultivated soils where organic matter has been depleted; soil texture is likely to define the properties of that soil. The moisture content, the dissolved ions and dissolved organic matter present in the soil is ephemeral in comparison, and although important, can to a certain extent, only modify the properties of the mineralogy already present.

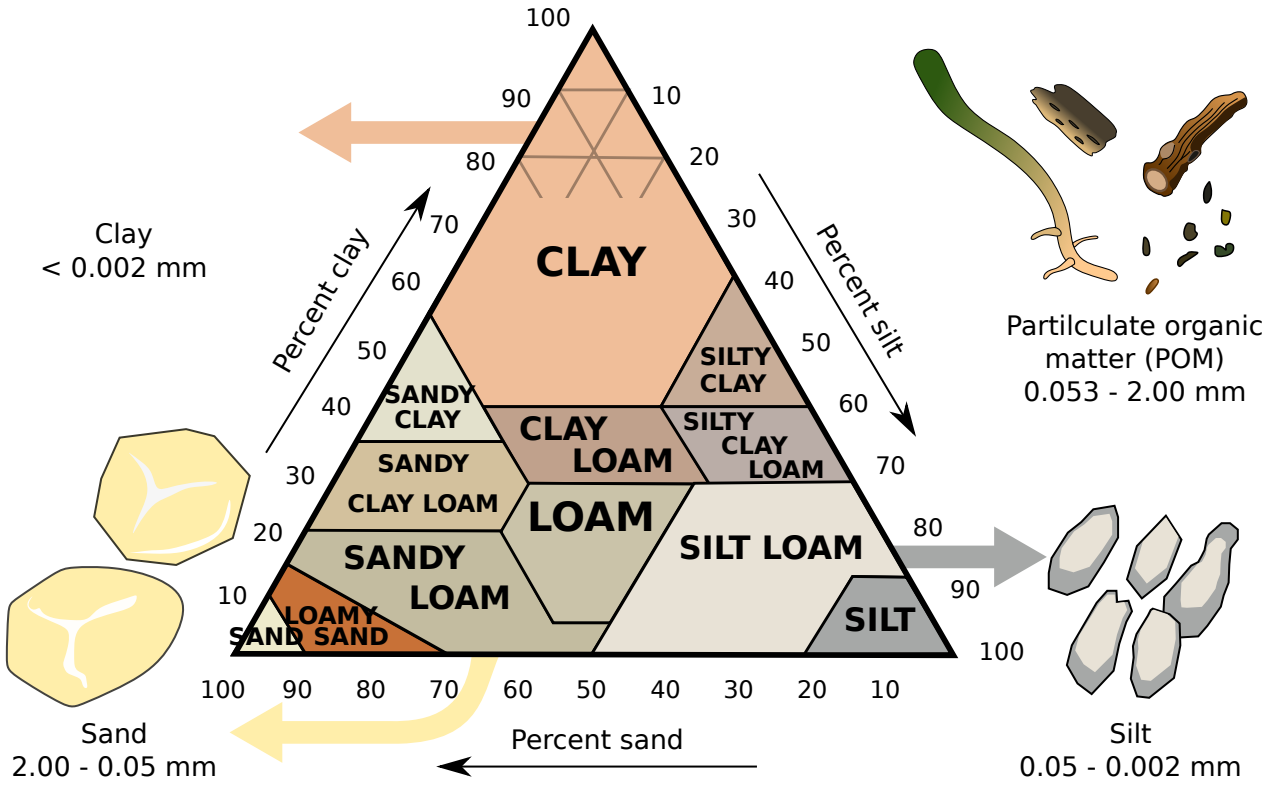

Figure 1.1: The USDA Textural triangle, soil type is characterised by the clay, silt and sand content. Clay, silt and sand is defined by USDA particle size diameters rather than the mineralogy. Particulate organic matter is not included on the soil textural triangle.

1.2 Clay particles in soil

Clays are often divided into expansive and non-expansive clays; these types of clay are very different and can modify the properties of the soil significantly. Expansive clays swell significantly, some more than half the dry volume when hydrated, and soils containing as little as 5% expansive clays can show shrink/swell behaviour. Highly expansive clay soils can cause havoc with structural foundations and agricultural land, which become cracked and hard when dry, and sticky when wet. (*10*) Clays such as phyllosilicates, smectite and montmorillonite are expansive clays. Non-expanding clays such as kaolinite, talc or mica exist in soils which are older and more highly weathered. The difference in physical/mechanical properties between these clays can be attributed to the crystal structure of the clay plates. Expansive clays have an octahedral alumina or magnesia fused between two sheets of silicate tetrahedra (Figure 1.2). Expansive clays are known as 2:1 clays, indicating the ratio of silica to alumina in the crystal structure. The stacking of these sheets leads to the formation of a gallery, or interlayer, which can expand on hydration. These layers are held together by hydrogen bonds, dipolar interactions, and van der Waals forces and are easily hydrated. The non-expansive 1:1 clays, such as kaolinite, have a single octahedral alumina sheet fused to only one silica layer. This strong a-symmetry gives rise to a large dipole, which gives rise to strong Van der Waal type bonding interaction between the sheets which can resist hydration forces and excessive swelling (1.3).

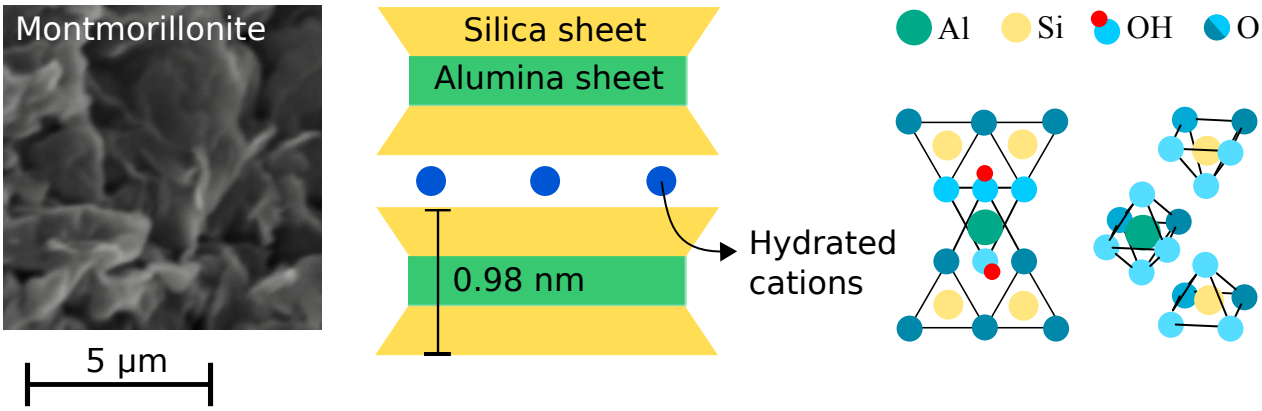

Figure 1.2: Montmorrilonite is a typical 2:1 swelling clay. It contains an octahedral alumina sheet, sandwiched between two silica tetrahedral sheets. The 2:1 sheets stack, and the space between the layers swell when hydrated. Individual montmorrilonite lamella are 0.98 nm thick, but form larger structures around 1 - 5 µm in diameter.

Because of their small size and flat plate-like shape, clays often have extremely large surface areas and usually comprise the most reactive portion of the soil mineralogy. Clays are known to be important for the formation of soil structure, holding moisture, nutrient ions and are thought to play a primary role in locking up carbon in the soil. Dispersed clay can exist as singular exfoliated platelets under some circumstances but are more likely to exist as tactoids which are agglomerations of clay particles in natural systems. These tactiods can be stacked into well-defined layers, or exist as jagged associations. The structural role of clays in soil is two-fold, first, they may act as primary particles which aggregate, or they may act as cementing agents, bridging larger particles, such as sand, together. (*11*)

1.3 Kaolinite

Kaolinite is an extremely common aluminiosilicate clay of the 1:1 type and is the most common mineral in the kaolin group of minerals. It is a clay with many industrial applications, and is obtained as a white to off-white powder, more commonly known as china clay. As with many natural minerals, the structure and form of kaolinite can be quite variable, as can associated impurities, however, kaolinite clays are generally of high purity and quality compared to other clays (*12*) (*13*) . Individual kaolinite particles are commonly pseudo-hexagonal in shape and may be nano- to micron sized.

Kaolinite contains two 0 0 1 basal plane surfaces, a gibbsite layer (an aluminium (hydr)oxide ($Al_2(OH)_4$)) and a silica sheet (Si_2O_5) fused together (1.3). These sheets are stacked with a basal spacing of around 7.37 Å. Unlike swelling smectite clays of the 2:1 type, kaolinite is noncentrosymmetric. As mentioned, this asymmetry creates a large superimposed dipole which culminates in a large cohesive energy between the lamella sheets (*14*). Additionally, there are hydrogen bonds between the aluminol groups of the gibbsite layer and siloxane groups on the surface of the silica layer. These interactions make kaolinite a non-expandable or non-swelling clay, and has low chemical reactivity in the interlayers. This also means that despite its plate-like shape, kaolinite has a low surface area (as measured by gas absorption methods – BET) and often a higher thickness compared to 2:1 clays (*15*).

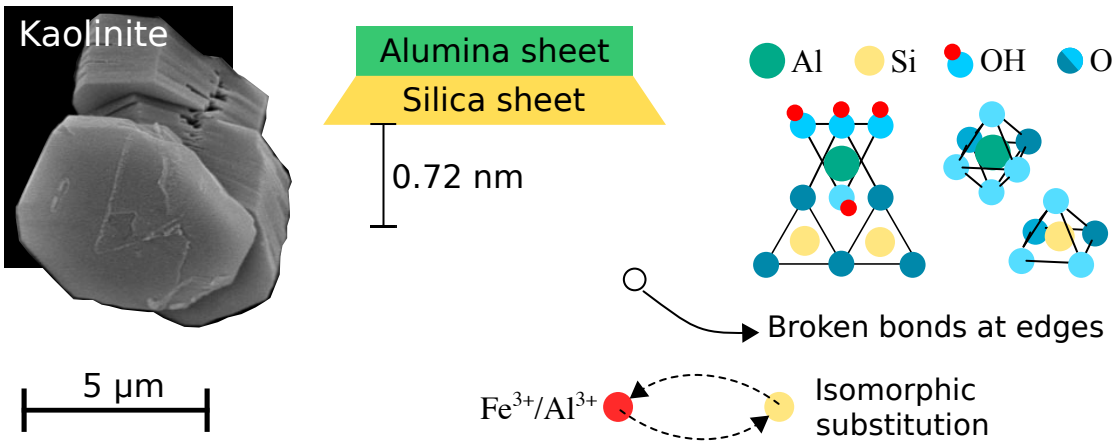

Figure 1.3: Kaolinite is made up of stacked alumina and silica sheets. The crystal layer is about 0.72 nm thick, but forms strong bonding interactions between sheets, platelets are around 0.05 – 2.0 μm thick. The diameter of kaolinite platelets can be between 0.2 -10 µm.

Unlike 2:1 clays with only silica faces exposed, kaolinite contains both an exposed gibbsite and an exposed silica surface on either face of the flat clay particle, which bestows on it, some unusual colloidal and structural properties. For example, kaolinite is particularly sensitive to pH, owing to the amphoteric nature of the exposed gibbsite face. (*16*) Kaolinite surfaces have variable and permanent charge. The permanent negative charge in clay is due to isomorphic substitution predominantly within the silicate layer, but also within the gibbsite layer. Silica faces undergo exchange of Si^{4+} with Al^{3+} or Fe^{3+}, and Mg^{2+} for Al^{3+} in the alumina layer. The substitution of a Si or Al with a lower valence cation results in a permanent negative charge (*16*). Isomorphic substitution in kaolinites is often modest, and the surface charge is often small, compensated by adsorbed K^{+}, Na^{+} or H^{+} ions. Kaolinite is only weakly hydrophilic, as kaolinite contains both a strongly hydrophilic gibbsite surface and a strongly hydrophobic silica surface, which makes kaolinite an unusual particle having both hydrophilic and hydrophobic surfaces (*17*).

The most reactive sites on a kaolinite platelet are the edges where broken aluminium or silicon bonds end with a hydroxyl group, which have variable charge depending on pH. The edge sites of some kaolinites are recognised to be the source of the majority of variable charge, behaving as amphoteric functional groups and are also attributed to kaolinites apparent acidity in solution. Edge sites account for around 12 – 34 % of the kaolinite surface area, depending on the particle dimensions, but play a disproportionate role in the reactivity of clays and their solution behaviour. (*18*) (*19*).

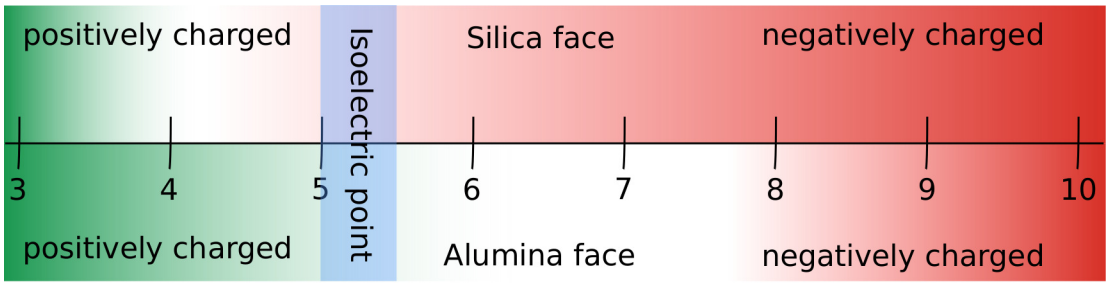

Figure 1.4: The variable charge of the silica and alumina faces as determined by AFM as reported by Gupta et al.(*16*)

1.3.1 Kaolinite in solution

Kaolinite is a clay used extensively in paper manufacturing and ceramics, and is frequently encountered in oil extraction activities. For this reason, controlling the colloidal and rheological behaviour of kaolinite is of much industrial interest (*16*). The stability of a kaolinite suspension, the rate of settling, and the volume of the sediment are dependent on solution pH and the electrolyte present. Unfortunately, a definitive consensus as to nature of the interactions between kaolinite particles has not been reached, and some studies have been contradictory as to the effect of pH. This may be as a result of the variability within kaolinite, or the difficulty in observing solution behaviour with current techniques. (*20*, *21*)

Recently, AFM colloidal force measurements were used to measure the variable charge on the face surfaces of kaolinite in response to solution pH (*22*). They showed that the silica tetrahedron has a negative charge $>$ pH 4, whereas the alumina is positively charged at pH $<$ 6, switching to a negative charge above pH 8 (Figure 1.4). This places the isoelectric point for the surfaces around pH 5 - 5.5. The mismatch of charges on the two face surfaces (and on the edges) is the origin of the complex colloidal and sediment behaviour. A variety of interactions between surface and edge sites can occur depending on the charges present, causing individual kaolinite particles to aggregate in a number of different morphologies (Figure 1.5).

Below the isoelectric point, silica face – alumina face interactions can occur, driven by Coulombic interactions between a negatively charged silica face and positively charged alumina face. As a result, the individual plates stack together, creating what is known as a ‘stack of cards’ structure in the resulting sediment. These columbic interactions cause kaolinite to aggregate and settle quickly

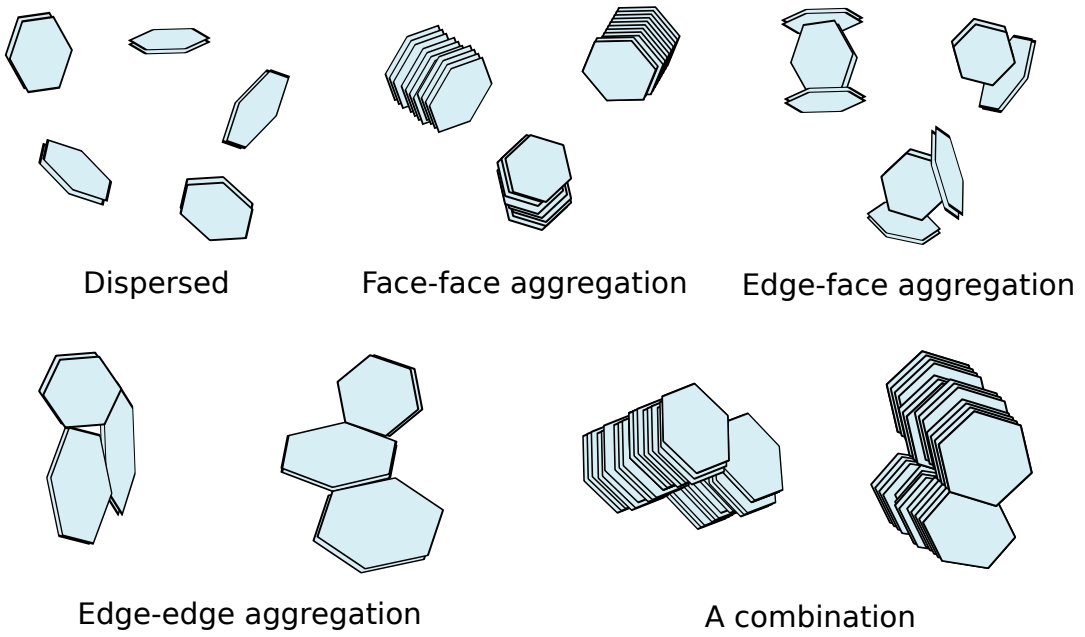

Figure 1.5: The colloidal behaviour of kaolinite particulates can take many forms depending on solution pH and the electrolyte type and concentration. Figure redrawn from "Particle interactions in kaolinite suspensions and corresponding aggregate structures"(*16*)

forming a dense sediment. The edge sites of kaolinite are also extremely pH dependent, with edge faces developing a positive charge at low pH (*21*). Recently it was determined that the charge density of the edge surfaces of kaolinite exceeded that of the face surfaces by over an order of magnitude, and were found to carry a positive charge at pH < 4, which become more and more negative after pH 5. The interaction between edge sites and the alumina faces were found to be positive between pH 5-6, becoming repulsive outside this pH range. Edge-silica face interactions were found to be positive only below pH 4. This work by Gupta et al. demonstrated that these interactions determined the rheological and colloidal behaviour. Kaolinite was shown to grow by face-face associations, to form tactoids, as pH increases. These tactiods form larger and larger edge surfaces which promote edge -face interactions with other tactoids. At higher pH, the repulsive forces caused by a switch to negative surface sites, tends to cause the kaolinite to disperse in solution (*23*). The aspect ratio of the kaolinite particles also has an influence on the behaviour, those particles with a higher aspect ratio are more likely to organise in a face-face interaction, smaller aspect ratios favour more edge-face interactions (Figure 1.5).(*24*)

The pH effect is also complicated by the presence of soluble cations such as Na^{+}, K^{+}, Mg^{2+}, Ca^{2+} or Al^{3+}, which are present in soils and as impurities in clay minerals. (*25*) Soluble ions adsorb

strongly to charged surfaces such as clays. Charged surfaces in an electrolyte form an electrical double layer. Ions of the opposite charge to the surface charge adsorb strongly to the surface in what is known as the Stern layer, forming an immobile layer of adsorbed counter ions. Negatively charged clay surfaces gain a layer of positive ions. A second layer of loosely bound ions also forms, which effectively screens the remaining charge from the rest of the electrolyte, and the remaining particles. As the electrolyte concentration increases, the screening of this charge in enhanced, and the distance the electrical potential reaches out into the solution is reduced. This has a strong effect on the colloidal properties of particles in solution. pH effects can effectively be reversed in the presence of an electrolyte, especially di -or tri- valent cations such as Mg^{2+}, Ca^{2+} or Al^{3+}, found in soils and natural environments, as they can strongly modify the surface charge of clay particles. Additionally kaolinite suspensions are acidic, and the addition of coordinating ions such as Ca^{2+} can increase this acidity by the exchange of labile protons. (*26*)

1.3.2 Kaolinite as a solid material

Kaolinite suspensions are of interest for those studying clays in aqueous environments such as streams, lakes or oceans and these studies can tell us much about inter-particle interactions and surface charge. However, much of the kaolinite on earth and in soils is present in terrestrial environments as a solid or composite material with low moisture contents. The material properties of kaolinite rich materials are well studied for civil engineering purposes and in the field of soil mechanics. Kaolinite rich soils can be extremely strong and stable in dry conditions, but can fail dramatically when wet, causing structural damage to buildings or even landslides. (*27*) In the field of soil mechanics, kaolinite is often studied in the context of a saturated subsoil under drained or undrained conditions. Kaolinite is also compressed before or during mechanical testing (dependent on the test). However, the interactions between kaolinites in dry conditions have not been studied, despite abundance of kaolinite soils in dry arid areas. This study is particularly interested in particulate interactions which occur without external pressures, mimicking those likely to form in top-soils.

The continuous material formed by the association of clays with each other is called the ‘fabric’. The

term fabric is also used to describe the geometric arrangement of particles in the soil. The term soil structure describes both the fabric and the pore space. Dry clay has been studied and imaged using SEM, and a variety of fabric structures in natural kaolinite has been observed. These fabrics often form as the result of interactions which occur in suspension. The edge-face association results in the most visually dramatic 'card-house' arrangement forming large pores and a wide extended network. (*16*) Alternatively, kaolinite forms stacks or layers, this is known as the 'deck of cards formation'. For this reason dried clays can be considered to be anisotropic at the microscale under certain circumstances such as consolidation. Kaolinite suspensions can align under compression creating lamella layers. The arrangement and densification of particles influences the clays behaviour as a material. However, it has been shown that despite the anisotropy that can form due to the stacking of kaolinite plates, kaolinite structures which form without compressive forces are found to have isotropic responses to consolidation and shearing when dried. It has been suggested that dried kaolinite has a tendency to form domains or microaggregates without continuous anisotropic planes, and the material properties are defined by the interaggregate interactions. (*20*) A study on the stress strain response of kaolinite structures found that kaolinite formed a strong microfabric, retaining the same deviatoric and effective stresses, despite different void ratios. This study clearly suggested that the strength of the material derived from the interactions between aggregated domains, rather than a continuous network of clay. (*28*)

1.3.3 Organo-mineral interactions

The surface chemistry of clays is well studied, and the reactivity of clays has been exploited in order to generate novel materials such as polymer clay composites. (*13*, *29*) Kaolinite acts as a weak absorbent of soluble organic molecules such as sugars, organic acids and alcohols, and has also been investigated as a sorbent for materials such as pesticides and fertilisers due to its presence in soil. (*30*) Many substances such as sugars are only weakly adsorbed, and are preferentially adsorbed at low concentrations. (*31*) More complex mixtures of substances such as those extracted from soil and termed 'humic acids' or similar have historically been of interest to soil scientists. (*32*) The effects of solution chemistry and pH have been extensively explored in regards to the sorption of

humic acids. (*33*, *34*) Dissolved organic matter, with functional groups such as carboxylates and sulphates are known to adsorb on the kaolinite surfaces dependent on solution pH. Within humic acids, larger molecules are preferentially adsorbed on to kaolinite surfaces, as are those which are more aliphatic.(*35*, *36*)

Much is known, or can be inferred from the structure of kaolinite, about the behaviour of kaolinite as a sorbent for soluble molecules. The exposed silica plane is relatively unreactive and only strong proton donors (such as R-NH_2) will form hydrogen bonds with bridging Si-O-Si, as the oxygens in the silica plane are poor electron pair donors. Silica however, has strong hydrophobic character, and may absorb more hydrophobic molecules. Phenol and derivatives have been shown to be weakly absorbed on the silica surface by hydrophobic interactions. (*19*, *37*) The edge sites and aluminium octahedral surface has exposed hydroxy-groups which are much more suited to adsorb more polar soluble molecules. Studies of gibbsite showed that it was a much stronger sorbent than kaolinite, indicating the importance of the aluminium octahedral surface. (*31*) Because these sites on kaolinite are sensitive to pH, adsorption of organic molecules is equally sensitive to pH. The adsorption of soil humic acids were found to decrease with increasing pH (towards neutral pH), indicating the role of electrostatic repulsion. (*19*, *36*) At very high pH, electrostatic repulsion may prevent adsorption of negatively charged solutes, and hydrophobic interactions may predominate.

Recently, a study attempting to quantify the strength of interactions between a variety of functional groups and the surfaces of mica and goethite using a functionalised AFM tip was reported. (*38*) Methyl groups were found to have very weak binding interactions with a mica surface, whereas charged carboxylate groups (COO^-) were reported as having a binding strength an order of magnitude greater. This study, carried out at pH 6, showed that strong binding occurring between mica (negative surface charge) and the carboxylate group could result in strong binding energies comparable to those of covalent bonds. Bonding strengths between geothite and NH_3, both positively charged at pH 6, were found to be strong. This study demonstrated that functionality with the same charge as the surfaces do not necessarily repel, and can form strong interactions.

It has also been found that an electrolyte can increase adsorption in some cases, with the effects of Ca^{2+} observed to be greater than that of Na^+. (*36*) Although electrolytes such as these are

effective for shielding surface charge and reducing electrostatic repulsion, binding has also been shown to increase in strength due to Ca^{2+} cation bridging. (*38*) In the handful of studies to consider the impact of drying on organo-mineral interactions, soluble organic matter bound by Ca^{2+} to clay surfaces have also been shown to increase in strength on drying, with Na^{+} bound organic matter thought to weaken on drying (*39*, *40*). Interactions of soluble molecules with clays are likely to be different in nature due to the interactions that occur between insoluble particulates. For example, small soluble molecules are able to penetrate the surface of clays forming stable inner-sphere interactions. (*39*) Larger particles may form stronger interactions by the cumulative nature of many interactions occurring over a large area.

It has been proposed that soluble molecules are able to assemble into multilayers, with discrete hydrophobic and hydrophilic zones on the surfaces of clays and minerals. Humic substances have been observed to aggregate and self-assemble into macromolecular structures in solution, soils have also been shown to display reversible water repellency, which may be due to amphiphilic molecules or associations which reorientate on drying. (*41–44*) However, little spectroscopic evidence exists for single or multilayer coverage of adsorbed molecules on clays, some studies have shown only patchy surface coatings (*45*).

The uptake of particular fractions of humic acids to clays has been widely studied, as this gives insight into the kind of materials likely to be protected from microbial decomposition, as molecules bound to clays are physically protected from hungry microorganisms. (*46*) Studies such as these form the basis of what is known or discussed regarding organo-mineral interactions in soils. However, there is little relevance of these studies to soil structure and function, it has not been suggested how these findings might be applied to build carbon in soil. Most notably, the amount of organic matter adsorbed on surfaces is often small (of the order of μmol/g), which is unlikely to be substantial enough to glue together aggregates of minerals into stable structures, or sequester large amounts of carbon. Total uptake of humic substances on clays is low, about 1.0 μmol/g humic acid has been reported for kaolinite, montmorillonite is less, around 0.7 μmol/g. Uptake is thought to be much higher in soils containing amorphous oxides. Organic matter in temperate soils, especially in the topsoil, accumulate carbon at levels inconsistent with a monolayer coverage, which suggests insoluble carbon is important. (*47*) Over time, coatings of humic acids may accumulate, but the

transitory, fluctuating nature of aggregation suggests that the interactions of clay with insoluble particulates may explain more about how soils can function and store organic matter. Biological exudates, polymeric substances excreted by microbes and fungi, mucus and digestive substances from soil invertebrates and material entrapped in earthworm castes are known to be extremely important drivers of soil aggregation in healthy soil ecosystems. (*48*) However, in an agricultural context or in soils with large amounts of weathering or degradation, particulate interactions may far exceed that of biological processing in terms of the nature of soil structure and behaviour. It has also been shown that the biological ecosystem, in particular the bacterial and fungal communities, are extremely sensitive to their physical environment. (*49*) This suggests that although microbial communities are able to modify their surroundings, particulate interactions may dictate the initial community structure and function of the ecosystem via the formation of a particular environment.

1.3.4 Kaolinite in soils

Kaolinite particles in soils tend to be much smaller and contain a greater proportion of smaller anhedral particles, compared to the more hexagonal kaolinite particles found in sedimentary or hydrothermal deposits. (*50*) Kaolinte in soils tend to contain more isomorphic substitution and a greater particle size distribution. Kaolinite rich soils are predominantly found in hot and humid regions in the tropics, although kaolinite is present in most soils.(*51*) The soils found in semi-arid, sub-humid and humid regions are mainly Alfisols, Ultisols and Oxisols (around 60-70% of soils in the tropics are kaolinite rich), and these contain kaolinite as the dominant clay in the topsoil. (*51–53*) These also contain high levels of sand, have low fertility and are particularly susceptible to soil degradation and erosion. Soils of this kind do not make particularly good agricultural soils, and do not respond well to cultivation. They are generally on the acidic side, with low nutrient holding capacity, and have low organic matter content.Organic matter is turned over more quickly in tropical environments, but organic matter associated with kaolinite is also found to turnover more quickly (*54*, *55*) They commonly occur with amorphous oxides of iron or alumina.

Soils with low clay contents are more reliant on healthy levels of soil organic matter (generally above 2% mass) to maintain good soil function (particularly for agriculture). (*56*) The rate of

soil organic matter breakdown and mineralisation is rapid in tropical regions, and so high levels of organic materials are required to maintain productive agricultural soils.(*57*) That said, kaolinite rich soils have been reported to be more stable than those containing a high proportion of swelling clays evidence that if managed correctly, kaolinite rich soils of the tropics may form soils with stable soil structure. (*58*) It has also been shown that kaolinitic soils may form aggregates via abiotic means more strongly. (*59*) This means that the nature and properties of the organic matter that is added needs to be optimised to build soil structure, to last, and to boost the nutrient and nutrient retention properties of the soil, especially in regions where access to mulch and agricultural residues are limited.

1.4 Soil organic matter and particulate organic matter

Soil organic matter (SOM) is a term used to describe an extremely diverse and complex group of materials found in soil which are carbon-rich, this term includes the previously mentioned humic substances. Soil organic matter accounts for 2400 PgC (10^{15}) globally, exceeding that of land plants 1600 PgC and representing one of the largest carbon stores anywhere on earth. (*60–62*) Essentially SOM can include any organic matter present in soil from any origin at any stage of decomposition and is as a result, exceptionally diverse and complex. In natural ecosystems soil organic matter can include material deposited from plants or animals above ground or by roots or organisms below ground. The soil organic matter that accumulates in a particular soil is dependent on the nature of the inputs and the rate of the loss of this material. This encompasses the accumulation of material from plants and other organisms versus the leaching to subsoil, carbon which is metabolised or lost by processes such as erosion. Organic matter is dynamic and thermodynamically unstable, seasonally and spatially variable and responds to a variety of environmental stimuli. It is also alive, soil organic matter contains within it a multitude of organisms continually producing and destroying SOM. SOM is in a state of continual transformation and is therefore very complex. Despite this complexity, it has been observed that this continuum of diverse molecules can be separated into functional pools based on some differentiating property and pools are extracted by physical and chemical means in order to test the size and longevity of these pools. This property can be based on the chemical

nature of the compound, the lifetime or recalcitrance of the compound, or the association with other soil components. This has historically given rise to the somewhat unhelpful fractions called humus, humic and fulvic acids, operationally defined pools based on pH solubility. (*63*) These terms are extremely common but may not provide any additional insight into soil function and are subsequently being replaced by new methods of soil fractionation with more relevance to soil function and carbon cycling. (*64*) Additionally, theories based on the inherent chemical recalcitrance of some materials in soil are being lost (some naturally derived compounds such as lignin and tannins were thought to resist biological degradation and are therefore stable) in favour of a model whereby soil accumulates materials which are physically protected in soil by mineral interactions alongside the accumulation of materials of microbial origin. (*46*, *65*) Biopolymers such as lignin which are chemically recalcitrant, are now known to be broken down by a variety of organisms. Large plant fragments are slowly degraded predominantly by a process of attrition, that is they are gradually broken down by biological (enzymatic or mechanical grinding/chewing) or abiotic processes such as wet/dry or freeze/thaw cycles. Substances greater than 600 Da cannot be transported through cell walls, so soil microbiology has developed an impressive suite of tools in order to break down and internalise larger polymers. (*63*, *64*) Alongside these biological transformations, chemical reactions between soluble residues may still form humified compounds, but their contribution to total soil carbon is likely to have been over-estimated.

The nature of the cycling of soil carbon is complex, and clearly related to variables such as soil temperature, soil hydrophobicity, soil aggregation and soil biological activity. The aim of many studies on soil carbon has been to elucidate the origins and (broadly) the chemical species which are present in stable aggregates, or carbon which remains stable over extremely long timescales. Increasing the amount of organic matter in soils, especially carbon which is long-lived (persistent), is often cited as the key to maintaining soil health. Persistent organic matter, and carbon which encourages soil to aggregate, increase the stability of soils to erosion. Increasing the amount of stable persistent carbon is also one way in which soils can be used as a carbon sink and may play an important role in sequestering carbon.

1.4.1 Particulate organic matter

Particulate organic matter (POM) is a term used to describe discrete particles of plant residues or other carbon-rich matter. POM is a fraction commonly isolated in the study of carbon cycling. POM is commonly defined as the fraction of soil 53 – 2000 μm in size and is separated from the mineral component of this same size fraction by density, using a sodium hexametaphosphate solution. (*66*) POM is insoluble and generally described to be in an intermediate stage of decomposition between fresh plant residues and humified matter (decomposed until its origin is unrecognisable). POM is somewhat like clay, it can exist as small particles, can absorb nutrient ions and water and may be critical to the function of a healthy soil. Many studies have shown that POM is one of the most sensitive indicators of land use change, and the first carbon pool to decrease in abundance after conversion of land to agriculture. (*67*) Because POM is generally made up of relatively unmodified plant residues, the metabolic and nutritional value of these materials are relatively high, and may be turned over quickly in healthy ecosystems. A link between mineralizable N and POM content has been indicated several times, suggesting it is important for N cycling. (*68*, *69*) Particulate matter is also thought to be important for forming the primary structures which bring about the formation of water stable aggregates, the fundamental building blocks of stable soil. Clays and minerals can coalesce around larger organic debris, and the process of biological and chemical degradation can help cement these interactions until stable aggregates are formed. The role of POM in forming soil structure or changing bulk soil properties is not fully understood. POM makes up a large (often the largest) proportion of total soil carbon in many soils (42-74%) (*68*), SOM is largely responsible for vast increases in cation exchange capacity, water holding capacity and soil stability, and it is likely that these properties are attributed to the presence POM, rather than the 'humified' small molecular weight molecules which have been studied so extensively.

1.4.2 Aggregate formation

Aggregates are a fundamental part of soil structure, although the term describes a hugely variable material formed by the association of organic materials with minerals. An increase in aggregation in soils is used as a primary indicator of soil health. Soil scientists have used soil aggregate size,

shape and number to indicate soil health, as aggregation tends to correlate strongly with organic matter content and biological function in field trials. As mentioned, aggregation is likely to be due to the result of a number of abiotic and biotic factors, and the importance of these variables is highly dependent on the soil type. For example, in organic soils (where soil organic matter exceeds 20%), biological processing via earthworms and other macrobiota may be dominant. Mineral soils with low organic matter contents, such as those found in the tropics (oxisols, ultisols), still contain aggregations as their basic structural component and are stabilised largely by abiotic processes such as the precipitation of cementing agents such as iron or aluminium oxides. (*4*) Wet and dry cycles, or freeze and thaw cycles are known to change soil structure, but these cycles have been shown to both increase and decrease soil aggregate stability. (*70*)

Current theories commonly evoked by soil scientists to describe the formation or breakdown of soil aggregates are based on the soil aggregate hierarchy model as described by Tisdal and Oades.(*71*) The model describes a hierarchy of structures, with macroaggregates being made up of smaller micro-aggregates and sub-microaggregates, which are formed from primary soil minerals and organic matter (Figure 1.6) The terms 'soil structure' and 'aggregates' can describe structures which occur over very large range of spacial scales, including aggregates mm in diameter to interactions that occur between micron-sized particles and smaller. The hierarchy model is useful, linking primary interactions between clays to larger structural entities such as macroaggregates and has shown to be useful in describing the change in soil structure following changes in soil management. The aggregate hierarchy model looks to be less applicable to tropical soils however, as there is evidence to show that the hierarchy model does and does not apply to oxisols for example.(*72*, *73*) Regardless, the formation of soil structure is linked strongly to the interactions which occur between primary minerals and particulates, and aggregates remain a useful concept for describing changes in soil health and function.

Wet and dry cycles are important for the formation of soil structure though both abiotic and biotic processes. Denaf et al. describes aggregate formation in wet and dry cycles to be a balance between interactions formed between organic matter and clay surfaces on drying, and differential shrinkage, which encourages the formation of failure planes on drying which cause aggregate breakdown. (*70*) One study reported aggregate stability in pasture soils to increase on drying whereas arable soils

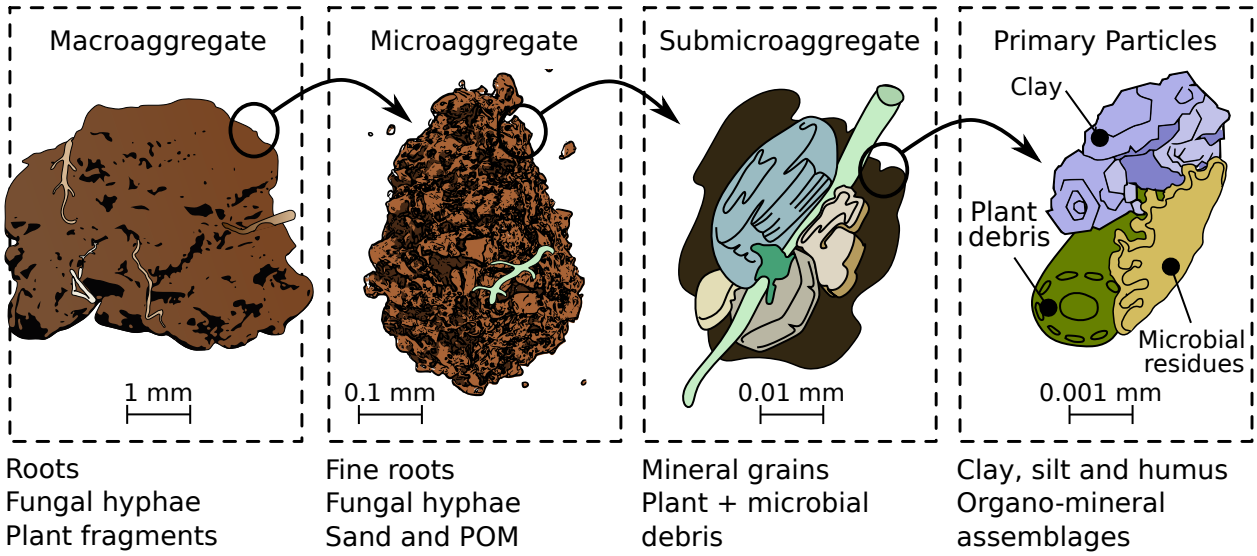

Figure 1.6: The aggregate hierarchy model as described by Tisdall and Oades, which describes larger aggreagates being made of smaller microaggregates, which are in turn made of primary particles. Figure adapted from 'The Nature and Properties of Soils' by N. C. Brady and R. R. Weil. (*74*)

reduced in stability. This was thought to be due to the higher SOM content in pasture soil, which increases the hydrophobicity of soil, and increases the amount of organo-mineral interactions on drying. (*75*) Evidence that SOM increases aggregate stability in temperate soils is substantial, and this is due to combined abiotic and biotic effects. Wet and dry cycles are also thought to be extremely important for aggregate formation in soils or arid to sub-humid regions of the tropics, where soil organic matter content is lower and the importance of cations and precipitates is greater.

Oxisols and Ultisols generally have a less aggregated structure, the aggregates are held together predominantly by non-crystalline alumina hydroxide precipitates, whereas Aridasols derive aggregate stability from high carbonate content. Soils dominated by variable charge clays such as kaolinite and oxides show strong aggregation at low SOM contents, but in these warmer environments, SOM is turned over more quickly. Kaolinite rich soils have been shown to form more stable aggregates than those rich in 2:1 swelling clays, possibly due to the strong swelling behaviour of 2:1 clays which can disrupt dry materials by differential swelling. (*67*, *72*, *73*, *76*) Kaolinite rich soils often lack organic matter in cultivated soils, whereas under forest, organic matter is abundant. Cultivation puts these soils at high risk of erosion and degradation. However, they also provide the best opportunity to increase soil organic matter and soil function to sequester carbon and increase agricultural output. In order to do this carbon must be added which is stable and forms soil structure via predominantly

abiotic means.

1.4.3 POM in aggregates

POM has been shown to be a highly sensitive indicator of land use change, with the disruption of stable aggregates (by tillage for example) leading to rapid decomposition of POM. This leads to strong changes in the soil properties and function. Not all POM is found in aggregates and POM can be divided into the subgroups free POM (fPOM), or POM occluded within aggregates (aPOM). Occluded aPOM is associated with clays and minerals. It has been shown that the larger class of aggregate 'macro aggregates', often contain fresh POM (recently deposited residues), a fraction of this, that which is protected from microbial decomposition by association with clays may persist in the soil and may form stable microaggregates. POM is often thought to be the nucleus for aggregate forming processes, as both a surface on which minerals can bind, and as a food source for soil microbiology. Residues with with higher C:N ratios tend to persist for longer with reduced rates of (microbial) decomposition. POM with low C:N ratios are likely to form more transient aggregates, those with higher C:N contents, are likely to be longer lasting, POM associated with clay or minerals may persist the longest. (*67*, *77*)

The chemical composition of POM clearly has an effect on the aggregation process, with some materials engaging in stronger inter-particle interactions. However, some materials may have stronger effects on the soil ecology, or may be more resistant to biological decomposition. However, the abiotic and biotic components of aggregate formation and POM stability are rarely considered separately, and it is difficult to separate physical/chemical contributions from biological ones . Most studies of aggregate carbon look at the material present in aggregates following incubation in mesocosm experiments, with a variety of plant residues. (*49*, *78*, *79*) Studies often show that there is a strong role for polysaccharide based, proteinaceous and lipid-based materials for microaggregate formation and stabilisation on a longer timescale in temperate soils. (*53*) These are biological compounds from root, fungal and microbial exudates, and provide little practical information for those who want to increase soil aggregation via the application of specific residues. Residues high in lignin are known to persist for longer, due to its chemical recalcitrance, as do chars from fires.

(*61*, *77*) Although these studies are important, the abiotic mechanisms are still poorly understood, specifically the initial formation of aggregate structures and the mechanisms in which particulates assemble. To optimise the application of organic materials, and to enhance carbon sequestration, more mechanistic information is required.

Determining the magnitude and nature of the binding interactions between particulate organic matter and minerals is a considerable technical challenge. (*80*) Adsorption studies of soluble organic matter on mineral surfaces are often used as evidence to suggest the type of interactions occurring between SOM with clays, but may under-represent particulate interactions. Since the forces binding two particles together are likely to be weak and disperse, individual interactions are unlikely to be measurable except by very specialised spectroscopic methods such as atomic force microscopy. (*81*) Instead, the behaviour of bulk soil following a change in particulate composition may provide an easier means to understanding particle-particle interactions and also may be more relevant to systems such as soil where a network of interactions is important.

1.4.4 Aggregate forming interactions between particulates

The interactions that occur between particles arise from the same physio-chemical phenomena of those that occur between surfaces and soluble molecules. However, these forces manifest themselves differently in particles, particularly as the additive effects of interactions over a large surface area can lead to dramatic increases in the magnitude of an interaction. For example, the additive effects of multiple Van der Waals interactions along surfaces result in a strong attractive force between particles, whereas molecular scale Van der Waals are relatively weak.(*82*) Clay materials contain highly polarisable surface functionality and the Van der Waals interactions between clays are therefore strong and are often considered to be among the primary attractive interactions between clay particles in suspension. (*82*) Soluble charged molecules can diffuse easily to the surface of charged surfaces and bind tightly to mineral surfaces. Particles are more constrained due to steric effects, and charged particles have to overcome repulsive forces if their charges are matched. Electrostatic forces occur due to the overlap of charged ions which accumulate at the surface of charged surfaces. The concentration of charged ions is high near the surface, and exponentially decreases until it reaches

the concentration of the bulk ions in solution as the distance from the surface increases. This is called the diffuse electric layer or double layer, and is another major interaction which determines particle interactions in suspensions. The nature of this charged layer is highly dependent on the solution electrolyte, its concentration and the particle surface charge. Most soil particles have a negative surface charge, and electrostatic repulsion is thought to be the dominant repulsive force in aqueous environments in natural systems.

The energy of interaction is highly dependent on the distance between the surfaces. So called 'long range interactions', such as electrostatic and Van der Waals forces are dominant at distances of around 20 Å, at shorter distances repulsive forces such as the hydration force can dominate. (*83*, *84*)

Direct measurement of these forces is a technical challenge. DLVO theory (named after Boris Derjaguin, Lev Landau, Evert Verwey and Theodor Overbeek) provides a theoretical treatment for the calculation of surface forces between particulates in solution, describing the attractive and repulsive forces present between particles dispersed in an aqueous media. DLVO describes the interactions between particles in terms of their electrostatic and Van der Waals forces, which are the longer-range interactions which dictate the suspension behaviour of particulates. (*84–86*) Most suspensions of particles are thermodynamically unstable, and are prevented from aggregating primarily by kinetic effects and electrostatic repulsion. DLVO theory is robust for relatively simple systems, but more complex systems require modifications, and the addition of other forces to explain physical measurements. DLVO has been applied to a number of clay and soil systems, however, the introduction of other forces such as the 'hydration force' and 'hydrophobic forces' are needed to explain experimental observations. (*87*) Non-spherical particles or particles with heterogeneous surface charge are difficult to model and calculations of the surface charge potential for clay materials is particularly difficult. (*88*) The interactions of particles such as clays with organic matter is likely to be extremely complex. Particles of natural organic matter are unlikely to be discrete and smooth with homogenous surface characteristics, a requirement for accurate DLVO calculations. The interaction between montmorillonite particles in soil was modelled using modified DLVO theory. The drying of particles, and the removal of water, often draws particles together via forces such as capillary action, and this can help overcome stronger repulsive electrostatic forces which keep particles dispersed in

a solution. (*86*) It has been suggested that the electrostatic force was not sufficient to disrupt Van de Waals forces formed as particles were dried and then rewetted. (*84*) The strength (2×10^4 atmospheres) deemed to be irreversible unless an additional hydration force was added which could allow the particles to be separated to a distance whereby electrostatic repulsion would cause the slaking observed in real samples.

Accurate DLVO calculations are reliant on the accrual of a number of constants obtained through measurements of particle properties, which have to be measured correctly. The attractive Van der Waals force is calculated using a Hamaker constant, which is higher in materials which have stronger Van der Waals interactions. The Hamker constants have been calculated for many inorganic materials, but not for many organic materials. Calculation of the electrostatic forces requires an accurate measurement of the particle surface potential, which is a technical challenge. Zeta potential measurements, commonly used to approximate surface charge, have been shown to give inaccurate estimates for clays. Additionally determination of surface charge by cation exchange or titration gives poor estimates when materials have both fixed and variable charge. (*88*) Theoretical treatments are becoming more powerful but are still limited to only modelling interactions between similar particles and surfaces. DLVO calculations for materials such as kaolinite, which have heterogeneous surface chemistry, or interactions between vastly different particles such as clays and POM is not yet feasible. These calculations however, provide the basis on which to discuss particulate interactions and colloidal stability. Computational simulations of clay micro-structures are also beginning to accurately describe mechanical properties and observed rheological behaviour, which may help link inter-particle forces to larger macro-scale properties. (*89*, *90*)

1.5 Soil mechanics

In the field of soil mechanics, soil is treated as a semi-cohesive solid. The properties of the bulk soil are tested under compression until shear stresses develop internally, leading to failure. This is often carried out in what is known as a triaxial shear test. This is used to measure the mechanical properties of soil by applying pressures in three dimensions to a block of soil. A triaxial shear test

treats the soil (subsoil) as a structural deformable solid, but because the cohesive nature of the particles are weak in comparison to the shear forces acting on the soil, the cohesion of the particles assumed to be near-zero, except under special circumstances. (*20*) In soil mechanics it is common to test larger masses of subsoil where the degree of water saturation is higher and the volume of pore space is smaller than that found in topsoil. The stress-strain relationships can be extremely complex and soil specific, and are only used to determine how the soil may act under loads relevant to civil engineering applications. Amendments designed to improve the stress/strain behaviour of soils are commonplace but are usually focused on structural engineering applications, rather than engineering better soils for agriculture or soil restoration. With cohesive soils, a uni-axial compression test can be used where the confining pressures perpendicular to the compressive force are removed. This causes the soil sample to bulge outwards and is analogous to the tests applied to those measuring the strength of concrete. Uniaxial compression tests are carried out on agricultural soils, in order to determine the loads that give rise to soil compaction (almost all loads give rise to some compaction), but these are barely correlated to soil properties, and do not correlate well with simple measures such as soil texture. (*91*) The application of these tests to topsoil for agricultural applications is limited. The improvement in soil structure or aggregation with the addition of an amendment has been made previously but not in great detail, as have studies on the mechanical strength of aggregates. (*11*, *91*) However, these studies have not tried to correlate structural strengthening of soil aggregates to mechanistic elements such as a change in binding interactions in any meaningful way. Soil contains a massive variety of particle materials, and the interactions between them are likely to be multifaceted. However, almost nothing is known about which interactions are strongest, or are the most stable.

1.5.1 Unconfined uni-axial compression test and inter-particle forces

The unconfined uni-axial compression test is a stress test with no lateral confining stress. A uni-axial compression results in the crushing of a composite with the sides free to bend and deform. A vertical stress (σ) is applied until the soil fails. The unconfined compressive strength, given as force per unit area, is often denoted as (q_u). Cracks form and propagate from existing failure points

perpendicular to the direction of the compressive force. The energy released from the formation of a fracture surface will generate more fractures unless the energy can be dissipated within the material. The test ends when the material fails. (*92*) The unconfined uni-axial compression test can be used to define a strength, toughness and stiffness, which can be derived from the plot of stress vs strain. The nature of failure in cohesive solids has been studied in soil mechanics and in formulation science. The unconfined compressive crushing force has not previously been used to infer the magnitude or nature of the interactions between particles. However, the strength of the material is intrinsically linked to the inter-particle forces. There are a number of factors which can influence the compressive strength of a three-dimensional porous block. In granular solids, cohesion can be complex. In over-compressed (consolidated) materials, frictional forces and interlocking strength may increase the apparent compressive strength. Some materials spontaneously phase separate due to large differences in density or even particle size, and de-mixing of particles of different types is a very common problem in solids mixing. (*93*) Ideally, bonding interactions between particulates or surfaces should be measured by tensile forces, however, the tensile and compressive strength of particulate solids are related. Bonding interactions between particles must be stretched to cause failure as compressing a bond cannot cause breakage of that bond. Therefore, the compression of a solid made of particles actually leads to the development of tensile forces which occur along faults in the solid. Thus, the unconfined uni-axial compression test can indicate the strength of bonding interactions between particles indirectly. For this to hold true, the solids must not be over consolidated, as to not cause additional strengthening by particle frictional forces and interlocking of particles. The spreading of material by crushing, termed dilatation, is caused by over consolidation and can influence the measured strength of a composite. Large flaws, of the size and shape that cause catastrophic failure should not be introduced.

One of the aims of this study is to investigate whether unconfined uni-axial compressive stress tests can be used to indicate if interactions between particulates and kaolinite are stronger or weaker than those between particles of kaolinite in an artificial aggregate. Additionally, it is investigated if the magnitude and line shape of a strength/modulus/toughness vs particulate loading can be used to infer the nature or strength of this interaction in order to inform future research into soil amendments and soil aggregation. Mathematical treatment of particles is complex and deviates strongly from

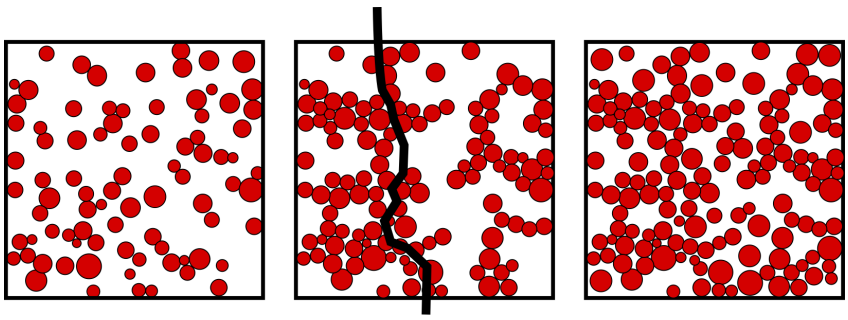

Figure 1.7: The percolation threshold corresponds to a volume loading whereby the probability of long-range networks of the additive component are more likely, which results in a large change in mechanical properties. The black line represents a continuous network of additive particulates which form a continuous network.

established relationships when non uniform spherical particles are used, and was not attempted here.

1.5.2 Percolation of particle assemblages

Note: The term percolation in soil science refers to the movement of water within a soil matrix, however here it is used to describe the connectivity of particles, used within composite science. Percolation describes the phenomenon in which a binary mixture of randomly mixed particles, or pores in a solid may form continuous structures, which usually results in a large change in the properties of the solid. (*94*) It is a statistical description, describing the likelihood that a continuous network of connected particles or pore space is likely to form (Figure 1.7). Percolation can result in a step-change in properties (i.e. strength) as an additive, for example, is suddenly statistically more likely to be connected through a dimension of the solid. Percolation is known to be dependent on porosity and the size of particles and may have significant effects on the strength of a solid. For example, a change in observed volume of sand/clay mixture was found to occur roughly around the theoretical percolation threshold of rounded spheres, suggesting percolation of the sand particles was important. (*95*) Also the percolation threshold was lower for particles with a higher polydispersity. Percolation can also be used to describe the effect of smaller particles moving between larger ones, causing de-mixing and is an important parameter to consider in particulate mixtures.

1.6 Motivation and Objectives

There appears to be a lack of understanding in regards to the processes which are responsible for soil aggregate formation and stability. To date, there has been no systematic study of the interactions of different types of particulate organic matter with clay or minerals found in soil. These studies only exist for interactions of soluble organic matter such as humic and fulvic acids. As a result, the fundamental drivers which lead to the initial formation of stable soil aggregates are poorly understood. The initial formation of soil aggregates is likely to be driven by physical and chemical drivers. Understanding these processes and identifying the functional groups or surfaces which enhance these processes could allow scientists to engineer better soils. There does not yet exist strategies to design soil amendments that can strategically build up soil structure and create healthier soils. These strategies could be used to effectively design more stable or resilient soils, quickly restore degraded soils, and speed up the soil formation process. Unfortunately, it appears that the techniques and methodologies are lacking to design these strategies. Determining interactions between particulate matter is a technical challenge, as interactions are weak and there are limited spectroscopic methods which can deal with solid materials.

The central motivation of the research within this thesis is to develop new methodologies to investigate particulate interactions in complex and mixed systems such as those in soil, and to gain insight into the interactions which form stable aggregates in soil. It is proposed that these methodologies may aid in the design of soil amendments engineered to build soil aggregates, bind clays and sequester carbon for soil restoration applications. This may reduce the need for extensive and time-consuming field trials, and inform studies looking at the role of particulate organic matter in soil function. This study will focus on particulates obtained from industrial bio-refineries, which present an opportunity to obtain large quantities of material which could be used as a soil amendment. Lastly, the role of these extracts will be assessed for their potential to ameliorate degraded soils. The role of POM in soil aggregation processes is thought to be important for overall soil health, but as yet, few studies have attempted to measure interactions between insoluble particulate matter and clays. In particular the following chapters will aim to answer the following questions:

- Chapter 2 and 3: **Can mechanical strength testing of artificial aggregates be used to quantify binding between clay particles and particulate organic matter with different surface chemistries?** These chapters explore the use of uni-axial compression tests to investigate particulate interactions in artificial soil aggregates. The artificial aggregates are made of two components, and these are mixed at varying ratios in order to infer the nature of the particulate interactions.

- Chapter 4: **Can particulate organic matter enhance the water stability of kaolinite based aggregates?** This chapter expands on chapters 2 and 3, in order to investigate these interactions in relation to water stress. Slaking is the process of the breakdown of solid composites when submerged in water. Artificial aggregates are used in order to investigate specific interactions and the resistance to water ingress.

- Chapter 5: **Do aggregates in soils accumulate particulate organic matter through abiotic processes spontaneously on mixing and wetting and drying?** Artificial soils, made from a well-mixed blend of minerals, build structure over wet and dry cycles. This chapter aims to see if this structure is formed by the preferential accumulation of certain minerals in aggregates, because of particular surface chemistries or material properties.

- Chapter 6: **Consider the effects of adding technical lignin on the microbial community and functioning of a degraded sandy soil.** Much of this work has been focused on the application of technical lignins as a soil amendment. This study aims to investigate how the addition of a technical lignin will modify the microbial community structure of a degraded soil.

- Chapter 7: **Solid state NMR is used to determine the interactions of lignin with clay, and of these materials with water.** Solid state NMR is a technique which is particularly suited to studying amorphous particulate solids and their interaction with water. This chapter summarises some investigations made using the technique, which aim to identify the some of the aggregate forming interactions.

Chapter 2

Artificial Aggregates I: Interactions Between Kaolinite and Organosolv Lignin

2.1 Abstract

Particulate organic matter is an essential component of healthy soils, but the nature of its interactions with clays and other soil mineralogy has not been determined in the context of topsoil. By manipulating the composition of artificial soil aggregates, and subjecting the mixtures to mechanical testing, interactions between the particulate components of a soil can identified. Specifically, these experiments have focused on how agricultural residues and biorefinery waste products interact with clays to form stable structures. Particle-particle interactions are inferred by changes in strength, toughness and stiffness of artificial aggregate made via a wet/dry cycle from a clay and an organic particulate. The maximum strength and modulus are strongly affected by the composition and surface chemistry of particulates. The percolation threshold is dependent on both the porosity and additive volume, and is indicated by a step-wise change in material properties. Amendments with very small particle sizes that do not create large pore volume when drying are likely to be strong up to 50% volume percent additive. Large particles are likely to reach the percolation threshold before becoming the majority phase. Unconfined uniaxial strength tests may be a crude and relatively unsensitive technique but qualitative trends are observed, which are relevant to topsoil engineering

applications and soil amendment design. The changes in modulus and strength did not strongly correlate with porosity, suggesting that the soil fabric strength is more important than the porosity in dry conditions. It is likely that hydrogen bonding interactions are responsible for large increases in aggregate strength. Electrostatic interactions, particularly repulsive interactions, which occur in the suspension or sediment phase, did not play a large role in determining the strength of artificial aggregates, as they are not present in the dry material. These findings can be used to help instruct the design of more effective soil amendments and provide insight into the physio-chemical interactions that occur within soil aggregates.

2.2 Introduction

The mechanical strength of aggregates is recognised as an important physical property of a soil, although few studies have attempted to quantify or measure aggregate strength in a meaningful way. Model systems have been used to identify some basic mechanistic aspects which result in an increase in mechanical strength, using mixtures of sand, silt and clay. (*11*, *96*) Studies on clay/sand mixtures showed that wetting and drying cycles increased aggregate strength by the formation and development of clay bridges between sand particles. This has since been observed in natural soils (*97*, *98*). The formation of bridges, or the rearrangement of the solid continuum into a stronger structure (the fabric) increases aggregate strength. The changes in fabric of artificial aggregates made from clay/silt mixtures was investigated via scanning electron microscopy. The fabric arrangement was found to strongly effect the water slaking properties although the mechanical breakdown (tested by sieving) was also affected. Strengthening was deemed to be a result of greater cohesion between silt and clay particles. The strongest interactions occurred via the formation of a suspended clay paste, which was mixed into the silt, maximising the contact and coating of the silt particles. (*11*)

In real soils, aggregates were found to decrease in strength as porosity increased, the porosity was determined by micro-computed tomography, but correlations were found to be weak. This suggests that porosity may not be the only factor dictating aggregate strength. (*99*) In this study they used the aggregate crushing test, an indirect tension test carried out by crushing aggregates, first

described by Dexter and Kroesbergen (*100*). The methodology is severely limited by the difficulty in accounting for aggregate shape, and obtaining natural aggregates of similar dimensions. Aggregate shape has also been investigated in real soils, something that appears to be strongly effected by soil management practices, although no clear trend has emerged to explain changes in aspect ratio, roundness and sphericity. (*99*) Aggregate strength in a real soil was found to decrease on the addition of organic matter, in this case peat moss), due to the increase in porosity. However, these aggregates were formed via kneading and heavy manipulation, so the origin of the resulting porosity is not clear. (*101*) Using a single source of 'organic matter' such as peat moss is problematic and is unlikely to represent the huge variety of residues present in real soils. Without a mechanistic description, studies such of this are difficult to build on.

Studies of these kind aim to infer changes in aggregate characteristics from changes in soil management practices. An understanding of the deeper mechanistic processes has not been attempted using mechanical strength testing, although some attempts have been made using DLVO theory. (*102*) Although these theoretical treatments tend to focus on colloidal interactions in water, they do offer an explanation of the forces which cause particles to aggregate.

2.3 Experimental Design

In these experiments, uni-axial compressive strength testing is used to measure the magnitude and character of interactions formed between particulates and clays. Simple 'artificial aggregates' are synthesised with varying clay:particulate ratios, expressed as a percentage volume loading. In part I, the behaviour of pure kaolinite artificial aggregates is investigated over a wide pH range, and the mechanical properties explored in context of the kaolinite fabric. Next, spherical particles of hydrophobic HDPE and hydrophilic surface modified HDPE particles are added at increasing loadings and compared, in order to demonstrate the role of surface functionality in creating inter-particle bonding. Organosolv lignin, a technical lignin extracted from beech wood, is a heterogenous particulate with hydrophobic and hydrophilic functionality, and is of interest both as a soil amendment and a component of natural soils with high biological recalcitrance. The role of lignin is then studied

as a component of a kaolinite-based artificial aggregates, and the role of salts and pH on these interactions are also investigated. The 2:1 clay, Bentonite, is also compared, as is quartz silt. Finally, the role of dissolved organic matter is considered, in order to characterise the interaction between organic particulates, DOC and clay in soils. Findings from this section are built upon in Chapter 3.

2.4 Particulate amendments

Lignin

Lignin is an aromatic biopolymer which accompanies cellulose and hemi-cellulose in lignified plant cells, acting to enhance the hydrophobicity and structural stability of plant cells (Figure 2.1). It makes up around 10- 30 % of lignocellulosic materials as a major component of cells used for structural support and the transport of water (*103*, *104*). In damaged cells, it is also produced by the plant to protect against bacterial and fungal attack, in order to prevent against disease. (*105*) The molecular structure of lignin is highly variable. The structure can differ considerably with regards to its location in the plant and there are even larger differences between plant species. Angiosperms are synthesised from coniferyl and sinapyl alcohols, forming guaiacyl (G) and syringyl (S) lignin, gymnosperm lignin contains predominantly coniferyl alcohol forming G rich lignins, and both contain small amounts of *p*-hydroxyphenyl (H) subunits from the incorporation of p-coumaryl alcohol (Figure 2.2) (*106*) These alcohols are polymerised via oxidative radical polymerisation to form heterogenous and often branched macromolecules. (*105*) Lignin has been studied most extensively in the context of forestry products, most of what is known about lignin structure comes from commercially relevant species. (*107*, *108*) The extraction of lignin is technically challenging, and isolated lignin is commonly obtained via the depolymerisation and solubisation of lignin fragments, resulting in a number of modifications and condensation reactions. (*109–111*)

Lignin is one of the major biopolymers present in lignocellulosic biomass and is therefore likely to be a major component of soil organic matter. (*77*, *115*, *116*) Once deposited into soil, lignin is

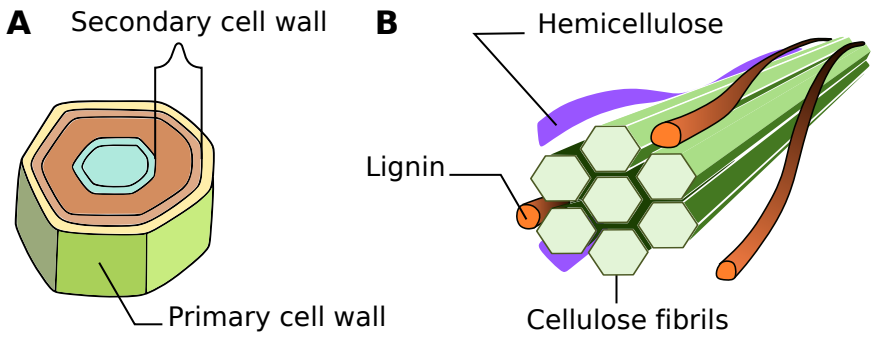

Figure 2.1: **A:** Lignin is deposited in the secondary cell wall of plant cell tissues, particularly vascular and support tissues, and plays an important role in transporting water. **B:** Lignin is deposited around cellulose, hemi-cellulose and other biopolymers such as pectin. Its exact structure and morphology is not completely understood, and the nature of the interactions are likely to be both covalent linkages and non-covalent associations. (*112*, *113*)

likely to be liberated from biomass in a number of different forms (Figure 2.3). Fungi are known to be the predominant lignin degraders in soil and are the most studied,(*117*), however a number of bacterial species are also known to degrade lignin. (*118*). Lignin is a difficult substrate to degrade, and few species have demonstrated the ability to survive on lignins as the sole carbon source. (*119*) Macroorganisms such as wood eating insects and worms, excrete lignin enriched frass or casts, and have specialised gut biota which chemically degrades wood lignin. (*120*, *121*) Lignin is also present in manure, although more extensive modifications to the structure are likely, although analysis of complex heavily processed material such as manure is a technical challenge. (*122*) These studies suggest that a whole range of lignin products can be produced by degrading processes. Small soluble fragments, short oligomers with associated biomolecules and large recalcitrant fragments are likely to be common after extensive biological processing. The contribution of physical/mechanical grinding and fragmentation via weathering to lignin fragments in soil is not known.

The reduced rate of decomposition, compared to other plant biopolymers makes lignin a prime candidate for a source of stable SOM in soils, and is therefore thought to enhance aggregation. SOM in tropical soils where decomposition of organic materials can be rapid, large macroaggregates, microaggregates and free pom have been found to be enriched in lignin. (*123*) Additionally, evidence that iron oxides specifically protect lignin from degradation has been demonstrated. (*124*) Mucilage, hyphae and exudates from the fungal species which use lignin as a food source are also thought to enhance aggregate forming factors, although the mechanism of lignin-clay aggregation has not been

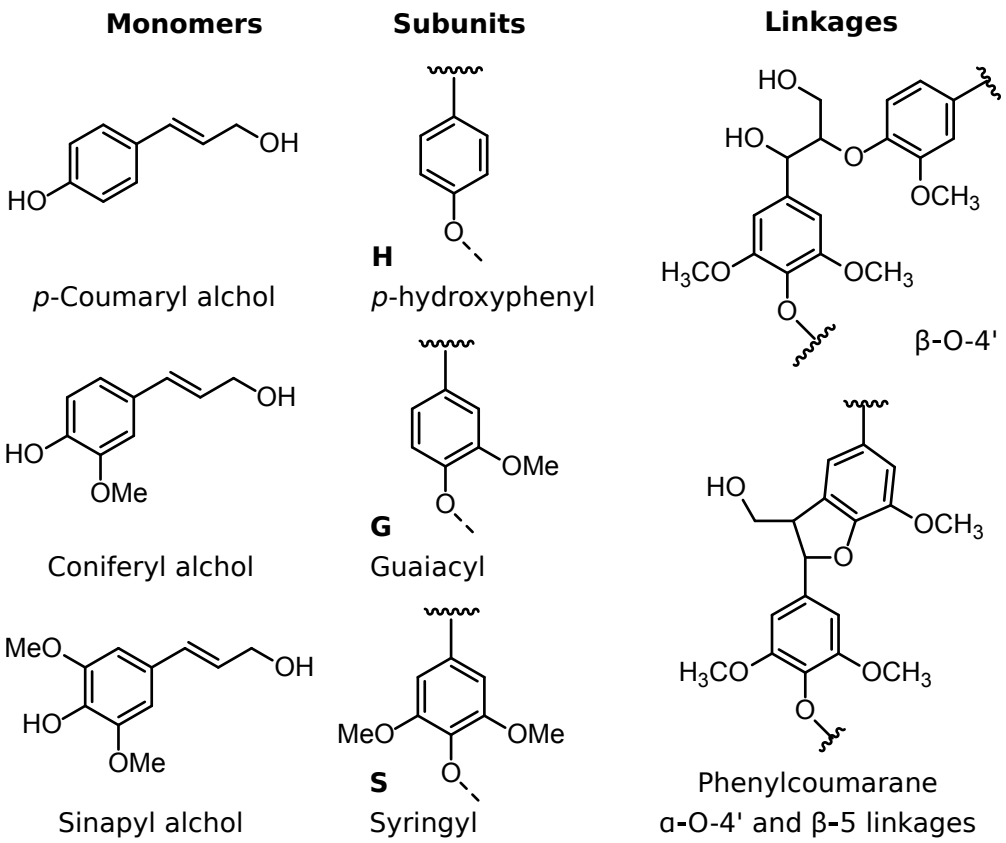

Figure 2.2: Lignin is synthesised from three hydroxy-cinnamyl alcohols (left), which form three different aromatic subunits once incorporated into the lignin polymer (middle). Lignin is synthesised via oxidative radical polymerisation. Radical coupling of the monomers is favoured at the β-position. The most common linkage (β-O-4') represents around 50 - 65 % of the total linkages present in most wood lignins. (*105*, *114*)

studied. The effect of adding lignin to soil has only been considered with respect to civil engineering purposes, although the materials used in these studies can only be described as containing lignin or lignin derived, and are heavily modified residues from biomass processing operations. (*125*) Extracting 'native' lignin – lignin which has undergone only very mild chemical modification requires extensive chemical and physical extractions and yields are extremely low. For this study, lignin extracted using the organosolv method was used, as it is a technical lignin with low to moderate chemical modification, much preferred to Kraft or sulphonated lignins. (*108*, *126*) Additionally, a softwood lignin (beech) and a hardwood lignin (spruce) was compared, as they represent the two most distinct lignin types encountered in the context of a biorefinery.

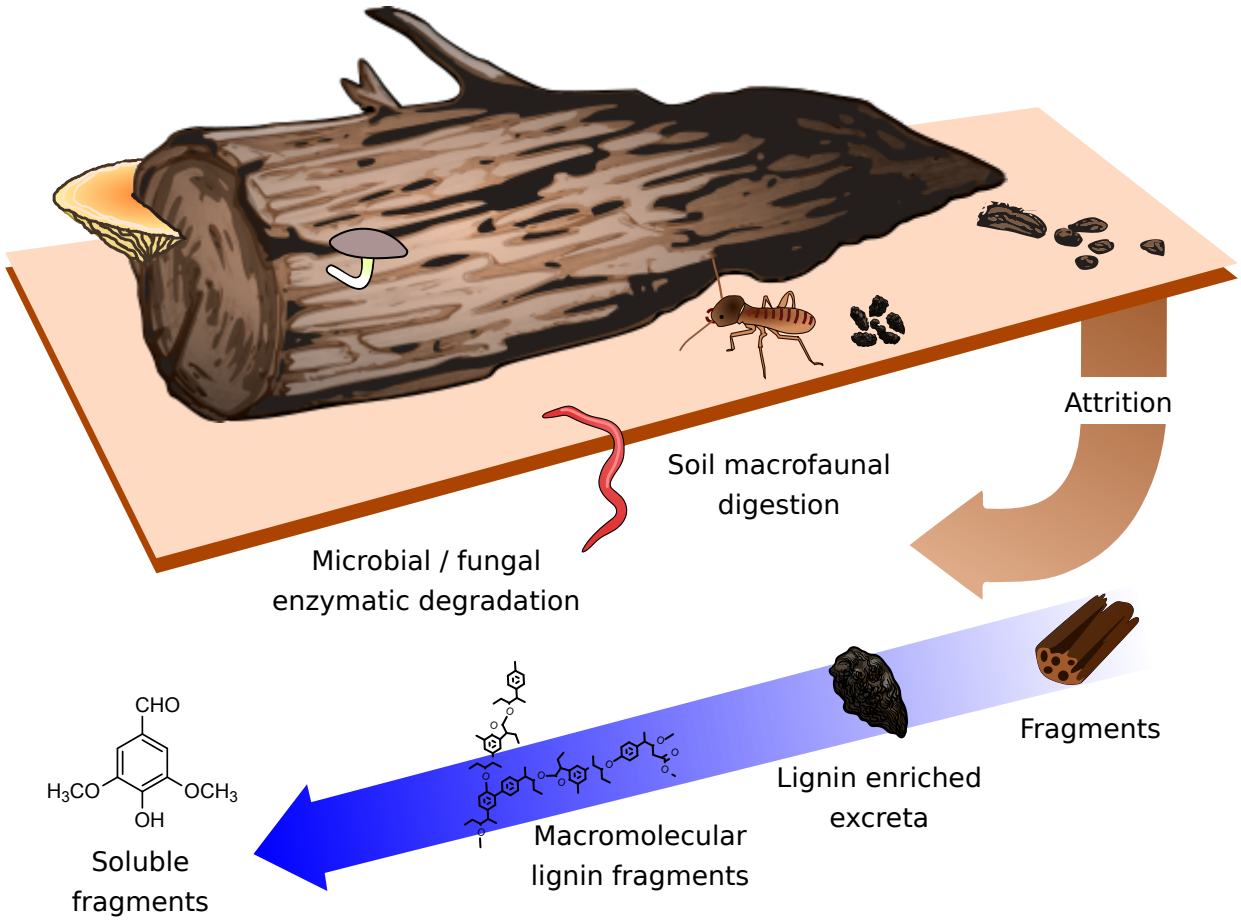

Figure 2.3: Lignin routes to soil. Lignin rich biomass is broken down by a number of processes, including the breaking down of material by physical processes (attrition), digestion by wood eating organisms and microbial/fungal digestion. This results in the formation of water soluble aromatic molecules, macromolecular lignin fragments (insoluble) and recalcitrant lignin rich fragments.

2.5 Methodology

2.5.1 Materials

Kaolinite, bentonite and fine quartz was purchased from PotteryCrafts Limited, Stoke-on-Trent ST4 4ET, United Kingdom. All minerals were used as received. The following plastic particles were purchased from Sigma Aldrich:

- High density polyethylene PDPE (particle size 4—48 μm) COOH Modified.
- High density polyethylene PDPE (particle size 125 μm) COOH Modified.
- Polyethylene - U.H.M.W. 150 μm, sieved into two size fractions.

Beech and spruce organosolv lignin was provided in 1 kg tubs from Fraunhofer Centre for Chemical-Biotechnological Processes CBP, Stuttgart. Lignin was oven dried at 40°C and sieved to below 63 μm for use in these studies. Concentrated humic acids were made by dissolving 1.028 g of humic acid in 0.1 M NaOH solution overnight, then adding 0.1 M HCl solution and leaving to stir until the solution was neutralised. The resulting solution was centrifuged and the filtrate was used as a concentrated humic acid solution, approximate concentration was 400 mg/L. The solutions were diluted with 0.1 M NaCl in order to retain equivalent salt content in the dilutions.

2.5.2 Generation of artificial aggregates

Blends of additives (particulate organic matter) and clay (kaolinite/bentonite) were made by mixing the dry powders at increasing mass loadings to obtain mass percentage loadings of 0, 10, 20, 30, 40, 50, 70, 100 % of the additive, single component samples were still treated as if they required mixing. The powders were mixed using a vortex mixer for 100 seconds and inspected to ensure no material remained unmixed. Samples were then left on a vortex shaker for 60 minutes. 6.5 ml of ultra-pure deionised water (18 Ω) was added to 5 g of the samples to form a paste. The water content was selected by trial and error, and was modified for subsequent experiments, in order to

form a workable wet paste. The wetted material was then hand mixed on a vortex for 100 seconds and inspected to ensure all material was wetted. The paste was further vortexed for 100 minutes on the vortex shaker and was left overnight to soak and equilibrate. Samples were always in sealed 15 ml centrifuge tubes to prevent evaporation. Before use, mixtures were again hand vortexed for 100 seconds and the resulting paste was spread into clean and dry silicone trays with 1 cm^3 artificial aggregate moulds. The mixtures in the mould were then knocked on a flat surface 100 times to remove trapped air, this was continued until no further air could be seen escaping the paste. The mould was then added into an oven and dried at 35 °C for 18 hours. The dimensions of the artificial aggregates were measured using a Vernier Calliper ($\pm$ 0.1 mm) before crushing. The dried artificial aggregates were placed into vials and sealed with parafilm, then placed in a sealed plastic bag to limit atmospheric uptake of water. Artificial aggregates were crushed within a day of removing from the oven. To modify the pH of the artificial aggregates the procedure was modified. An extra 5 ml of DI water was added to the paste and the pH was adjusted with 1.0 M and 0.1 M NaOH solution. The mixtures were vortexed, left overnight, centrifuged and the pH readjusted until the pH has stabilised. Water was removed by freeze-drying and the powders re-wetted with 6.5 ml water. The artificial aggregates were then made as mentioned above.

2.5.3 Unconfined uni-axial stress test

The unconfined uniaxial stress test was carried out on a Lloyd EZ 50 with a 100 kN cell in compression mode at 5 mm/min. Soils were crushed until the artificial aggregate failed completely. The measured values were extracted from stress/strain curves using Origin Pro. If a sample from a set of soil artificial aggregates exceeded the 100 kN limit, a new cell at 1000 kN was used instead, and the same cell was used for samples of the same type where possible. When crushing, the artificial aggregate was observed to ensure the major failure plane formed perpendicular to the load. However, it was not uncommon for some material from the edges to disintegrate and fall away, but the main point of failure occurred through the bulk of the artificial aggregate. Any artificial aggregates which crushed abnormally or had any irregularities were discarded for analysis.

2.5.4 Porosity and particle size measurements

Pycnometric density measurements were carried out using a Micromeritics AccuPyc II 1340 using helium gas. Helium is able to penetrate the pores, and the skeletal sample volume can be obtained. Prior to analysis, samples were accurately weighed, and densities were calculated from an average of 10 runs per sample. These measurements were used to obtain measurements for the envelope or bulk density. Measurements of bulk density were carried out using a Micromeritics GeoPyc 1360. The GeoPyc uses a principle of displacement of a dry solid powder to determine the bulk volume of a solid. The mass of the sample, and the skeletal density allow for a porosity to be calculated. Values for skeletal density were then used as inputs for the AccuPyc calculations. A representative triplicate measurement was made per experiment.

Particle size measurements were carried out using a Mastersizer 2000 instrument using materials dispersed in DI water. SEM measurements were carried out using a JEOL JSM-6010LA under ultra-high vacuum. The pH of the powders and artificial aggregates was measured using 1g:10ml DI water ratio, and confirmed with pH paper. Aggregates were vortexed to achieve maximum slaking, and left to settle before particle size measurements were made. Attenuated total reflectance Fourier transform infrared spectroscopy (ATR-FTIR) was carried out using an Agilient Cary 630 FTIR Spectrometer using 32 scans and a resolution of 2 cm^{-1}.

2.5.5 Isolation of soluble lignin

Soluble lignin was isolated by suspending lignin in a centrifuge tube, and adjusting the pH with 0.1 M NaOH solution. Once the pH had stabilised (adjusted over 3 days), the lignin suspension was centrifuged and filtered to extract a clear solution. These solutions were freeze dried to obtain soluble lignin which was dissolved in *d*-DMSO for NMR. At low pH, large amounts of lignin and large volumes of water were used to isolate a very small (mg) sample of soluble lignin. At low pH, the extracted lignin may have been extremely small particles of lignin, rather than lignin which was strictly dissolved.

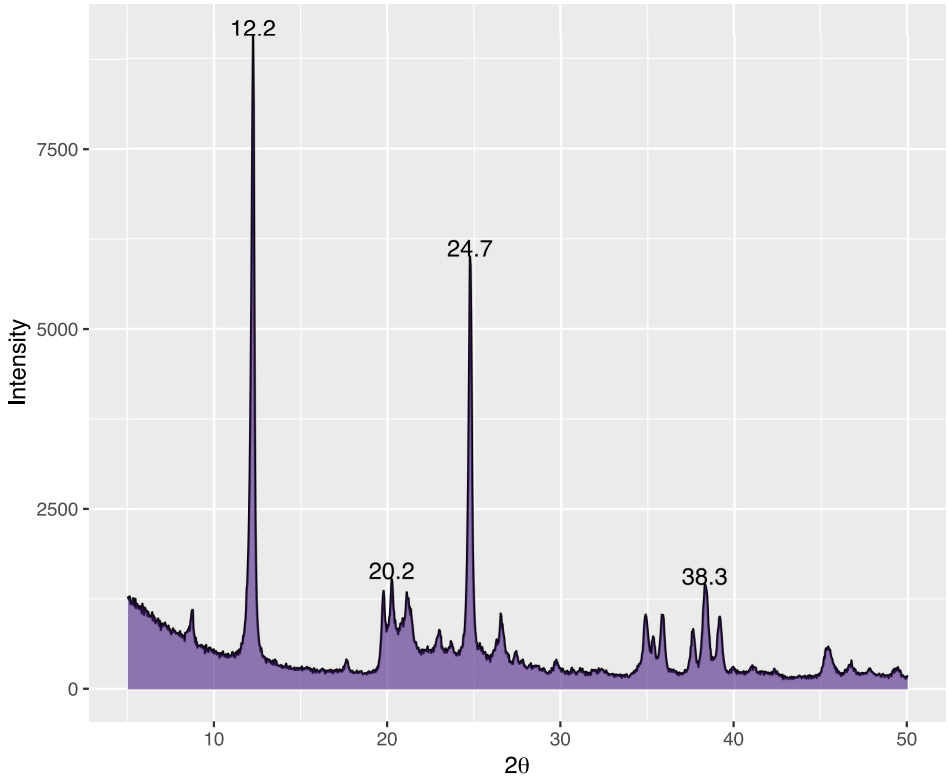

Figure 2.4: XRD spectra of kaolinite, characteristic reflections at d_{001} 0.72 nm and d_{002} 0.36 nm of kaolinite are observed. Smaller peaks appear to be from similar clays from the kaolinite family.

2.6 Kaolinite

XRF was used to determine if the elemental analysis was consistent with that of kaolinite. The signal for Si was higher than predicted for a pure kaolinite, suggesting some impurities were present (likely quartz). Impurity elements above the ppm range was determined to be Mg, K and Fe, which could be present as isomorphic substitution, or as isolated impurities. FTIR of the kaolinite showed no absorptions typical for Fe bearing kaolinites (865-875 cm^{-1}) Studies on kaolinite have shown that minor impurities have little effect on mechanical properties. (*127*)

XRD was used to confirm that kaolinite was the main component and to identify impurities. Characteristic peaks at 12.2 2θ (d_{001} 0.72 nm) and 24.7 2θ (d_{001} 36 nm) confirmed the presence of kaolinite, smaller peaks at 20.2 and 38.3 2θ are likely to be from halloysite, or other related minerals from the kaolinite family (Figure 2.4). FTIR indicated no peaks for halloysite (*19*), impurites were attributed to amorphous kaolinite or unidentified kaolinite minerals from the kaolinite family.

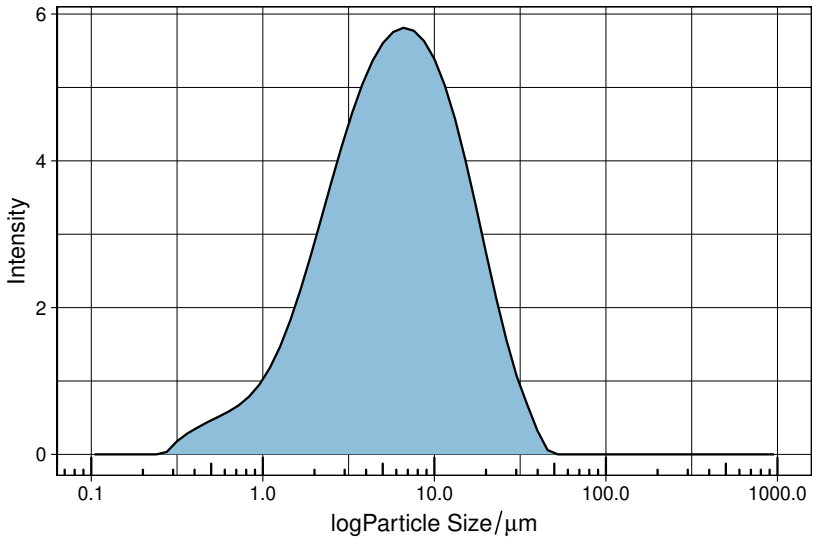

Figure 2.5: The particle size of kaolinite dispersed in DI water as determined using static light scattering. The particle size was small, with a large dispersity.

Kaolinite in suspension

Kaolinite was dispersed in DI water and was found to have a particle size dispersity common in natural materials. Kaolinite has been shown to have particle sizes which range from the nano-meter scale to the micron scale. This kaolinite had a d(0.5) of 5.76 µm and a span of 2.46 (Figure 2.5), there was some material present that was smaller than 1 µm.

The pH of kaolinite dispersed in DI water was modified drop-wise using a 0.1 M NaOH solution. The behaviour of the kaolinite changed from a fine powder which settled rapidly at low pH, to a cream coloured solution which was stable in suspension as the pH was raised (Figure 2.6). The colour change indicates a change in size of the particle associations due to Mie/Tyndall-Mills colloidal scattering. The settling rate indicates the rate of densification of particles in solution, but is also related to the strength of electrostatic repulsion. The creamier colour is indicative of larger particles being formed more quickly. (*16*) The increase in suspension stability indicated an increase in electrostatic repulsion at higher pH. Between pH 4.76 and 5.06, it is likely that coulombic associations are formed as a result of positive and negative charges present on the Al and Si surfaces respectively. This leads to a faster rate of settling with smaller denser particles due to face-face interactions. It appears pH 6 marks the transition between face-face stacked kaolinite and dispersed and negatively charged kaolinite where electrostatic repulsion prevails. This means settling is slow, and particle associations

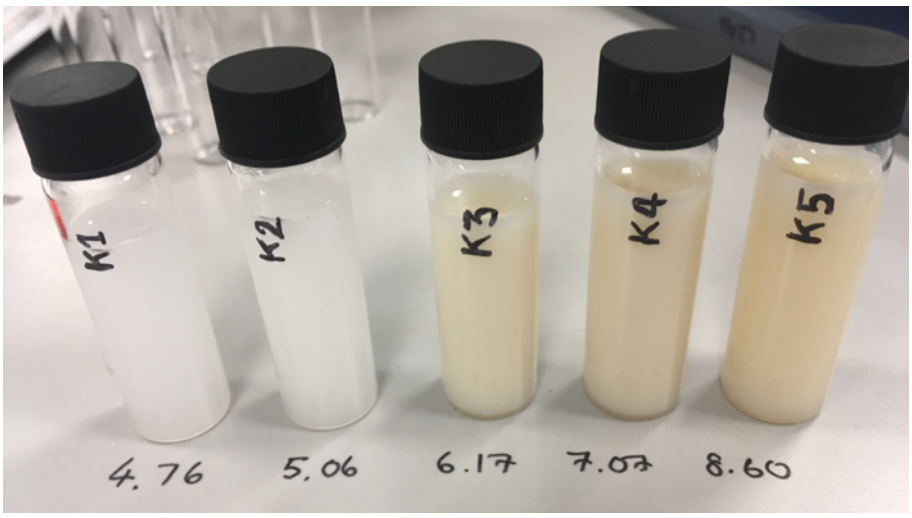

Figure 2.6: Suspensions of kaolinite at different pHs displayed different suspension and settling characteristics. The suspensions on the left (pH < 6) were unstable and very white, they settled out quickly. Above this pH the particles became creamy coloured and more stable in solution.

may be less dense forming larger particles. Face-face interactions at low pH have been observed previously, with edge-edge and edge-face interactions occurring at higher pH. (*16*)

The charge which exists around the kaolinite particles in suspension was measured by zeta potential to confirm this hypothesis. Here, low pH kaolinite has a small zeta potential, which increases dramatically between pH 5 and 6 (Figure 2.7). This increase in zeta potential can be attributed to the deprotonation of the alumina face. It is not clear what causes the apparent decrease in zeta potential above 7, however, it has been shown that zeta potential is not a true measure of surface charge, and may only be valid for qualitative measurements. (*88*)

2.6.1 Kaolinite: Volume, density and porosity of artificial aggregates

Kaolinite formed well defined smooth artificial aggregates with clean edges and no visible porosity. Kaolinite artificial aggregates could be removed from the mould with ease due to some shrinkage and no sticking interaction with the silicone mould. The volume of the artificial aggregates increased as a function of pH (Figure 2.8, **B**). This may indicate face-face stacking type interactions that occur in solution at low pH result in a higher density solid than solids formed from dispersed material at higher pH. The volume change was observed to be greatest in the thickness dimension (Figure 2.8 A), i.e. artificial aggregates were flatter in the mould at lower pH.

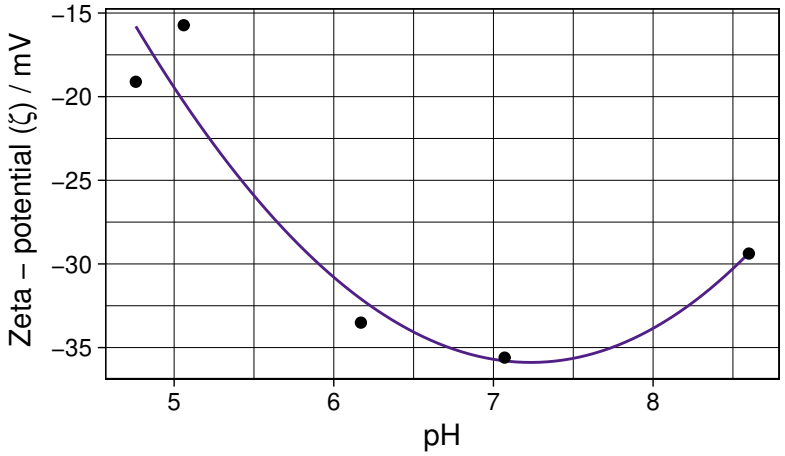

Figure 2.7: The change in zeta potential of kaolinite suspended in DI water was measured as a function of pH. Zeta potential reached a minimum at neutral pH, as the result of negative charges forming on the alumina and silica faces.

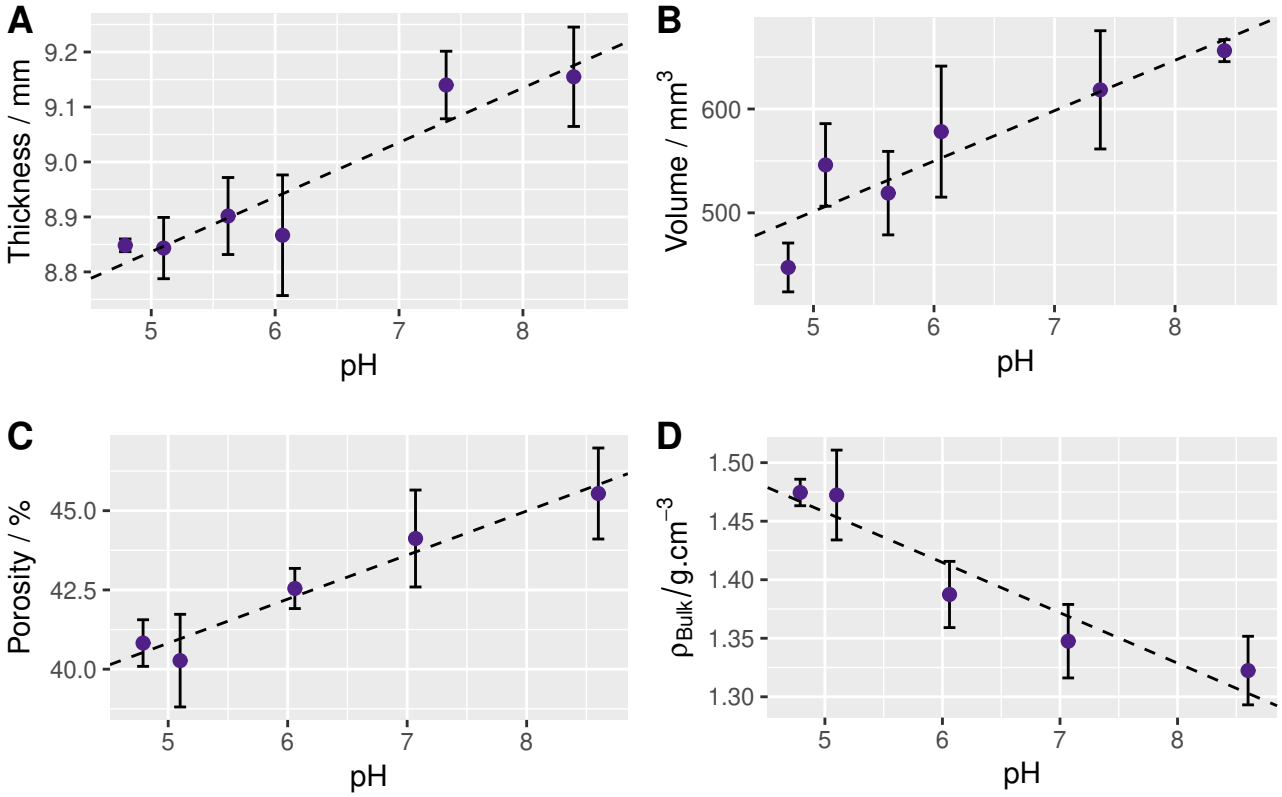

Figure 2.8: The physical properties of kaolnite aggregates. **A**: The greatest change in any dimension was observed in the thickness dimension (became less flat in the mould with increasing pH). **B:** The volume of the artificial aggregates therefore increases as a function of pH. **C:** The porosity increases linearly resulting in **D**: A large reduction in bulk density. Some data points were not measured at intermediate pH for C and D. There was a linear relationship between pH and porosity. Lines are linear regression fitting. Error bars represent one standard deviation (n = 3-5).

An increase in volume (Figure 2.8, **B**) reflected the observed linear decrease in bulk density and a corresponding increase in pore volume. A small increase in porosity (Figure 2.8, **C**) of around 5 % was found over the entire pH range, although porosity was high, above 40%. A transition from densely packed face-face kaolinite to more edge-face interactions at higher pH, reflecting the solution behaviour, can explain the increase in porosity. However, the highly linear correlation (R^2 = 0.9598) observed between pH and porosity does not reflect more complex changes in kaolinite surface charge and fabric morphology. Modifying the pH is known to change the Atterberg limits of kaolinite. For example, increasing the pH decreases the liquid limit of kaolinite (the amount of water a clay can hold before becoming liquid like), suggesting low pH kaolinite can hold more water. The reduction in water holding capacity at higher pH may mean that clays dry faster leading to an increase in porosity. A more subtle change in the drying rate may be an alternative and more simple explanation for the change in porosity.

The pore size and pore size distribution was not determined, so it was not known if this increase was due to greater pore volume between individual kaolinite particles or pores between agglomerations or aggregates of kaolinite particles. Pores between individual kaolinite particles would suggest a change in the fabric of the kaolinite, pores between agglomerations might suggest that the result was related to drying rate, if the aggregate size and morphology remained constant. A change in fabric, for example a transition from edge-face to face-face might result in a change in the skeletal density if kaolinite exists as a continuous fabric, as the densification of particles may result in a slight decrease in surface area available to the helium pycometry measurements. No change in skeletal density was observed (not shown), which suggests that the pore space between kaolinite aggregates was changed. The constant skeletal density also indicates that the water content was extremely small. This is consistent with the description of kaolinite as a collection of aggregates rather than a continuous fabric. (*28*, *128*) Measurements made by Y. H. Wang and W. K. Siu, showed that face-face aggregates had interaggregate pore sizes on the order of 0.30 μm, with edge-face pore sizes of 1.10 μm. (*21*) However, without pore size and distribution information, this hypothesis remains largely speculative. Face-face stacking interactions were confirmed by SEM (Figure 2.9).

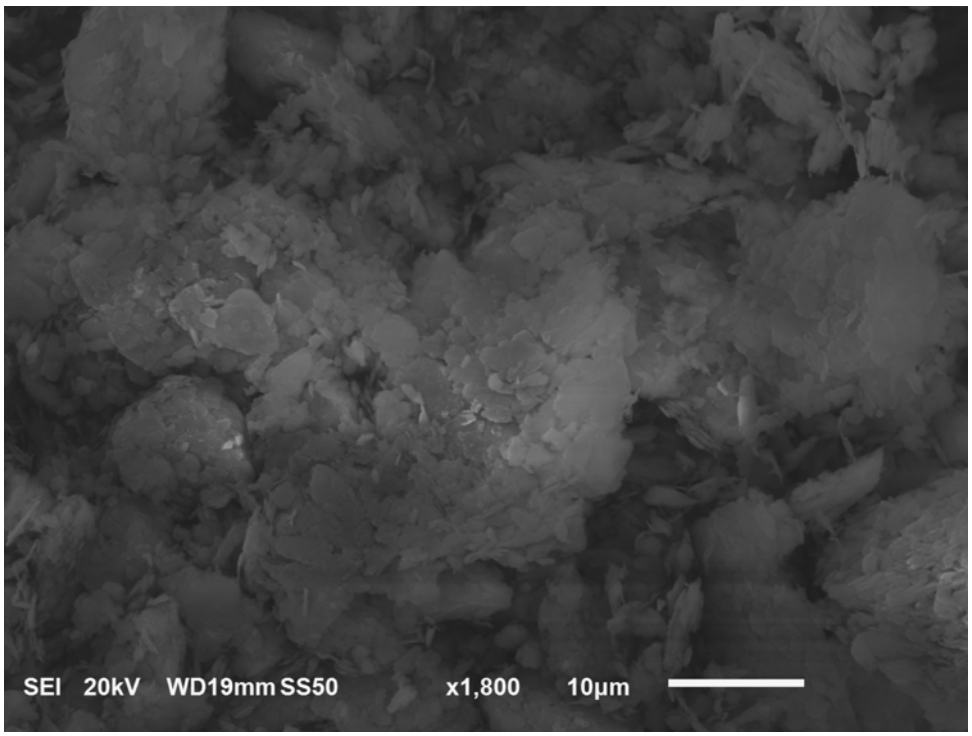

Figure 2.9: Scanning electron microscopy image of kaolinite at pH 4 showing face-face type interactions and blocky tactoids around 10 µm in diameter.

2.6.2 Kaolinite: Mechanical properties

The maximum stress at brittle failure increased in the 4.76 – 6.06 pH range, after which it reaches a plateau, despite an increase in pore volume and a decrease in bulk density (Figure 2.10, **A**). This strengthening does correlate with an increase in thickness, although since the stress is a force/area measurement, the thickness should be independent of the measured pressure. The more complex changes in fabric morphology is likely to result in changes in the artificial aggregate strength.

The most significant increase in the mechanical properties is observed with the change in modulus (Figure 2.10, **C**). The modulus ('M') increases with pH, with an apparent plateau after pH 6. The increase in modulus suggests that the kaolinite formed a more brittle network. The increase in porosity could result in a more brittle fabric, however, M correlates better with τ_f, suggesting that the kaolinite fabric has a larger influence on the modulus than the porosity.

The apparent linear increase in strength (between pH 4.76 – 6.06) occurs with an increase in modulus (Figure 2.10, **C**) suggests a stiffening and strengthening of the kaolinite fabric. The linear increase is in agreement with observations of the rheological studies of kaolinite. Additionally, the increase

in strength follows the theory described by Gupta et al. (*22*) Below pH 6, alumina-face silica-face interactions are favourable, which causes kaolinite to stack and form tactiods. This stacking promotes additional interactions between the tactiod edge and other kaolinite faces. These edge-face interactions are strong interactions favourable in the pH range 5-6. Beyond pH 6, electrostatic repulsion creates dispersed kaolinite suspensions and the strength and modulus no longer increase further in the dried kaolinite. However, this suggests that well dispersed kaolinite is able to form a stronger solid, and that kaolinite is relatively insensitive to pH above pH 6. This may be because dispersed kaolinite tends to form more edge-face interactions which occur in a larger network. This may also suggest that face-face interactions cause a weakening of the fabric, despite the increased packing density which may result. This could be due to interparticle pores (tactoids may not form strong interactions between aggregates), or the kaolinite plates may slide under stress. It is hard to know intuitively why dispersed kaolinite formed at higher pH would form a stronger cohesive solid, and why face-face interactions which form solids of higher density are weaker, but similar observations have been made for saturated kaolinite in tri-axial tests. (*27*)

The changes in mechanical properties are very large, suggesting the cohesive nature of dry kaolinitic soils could be improved by increasing the pH. This also results in the formation of larger pores, which may be beneficial for root penetration. However, the increasing porosity may be the result of much faster drying and lower water holding capacity of clay, due to the reduction in Atterberg limits. Higher pH soils will not hold the same volumes of water, but the increased porosity may allow water to permeate topsoil.

In these studies, the stress-strain behaviour is tested with dry cohesive kaolinite. Therefore, the electrostatic forces which are generated between particles are overcome on the removal of water by drying, so it may be that hydrogen-bonding and van der Waals forces become dominant in dry solids. In this case, the greater surface area afforded by a more open structure may lead to a stronger network. The toughness, U_T (Figure 2.10, **B**) represents the amount of energy the artificial aggregate could absorb before failure. Over the pH range investigated, toughness was not significantly altered. This suggests that although the artificial aggregates were stiffer and stronger a similar energy was distributed through the fabric of the artificial aggregates before they failed. This means that the kaolinite particles were well connected and force could be distributed throughout the

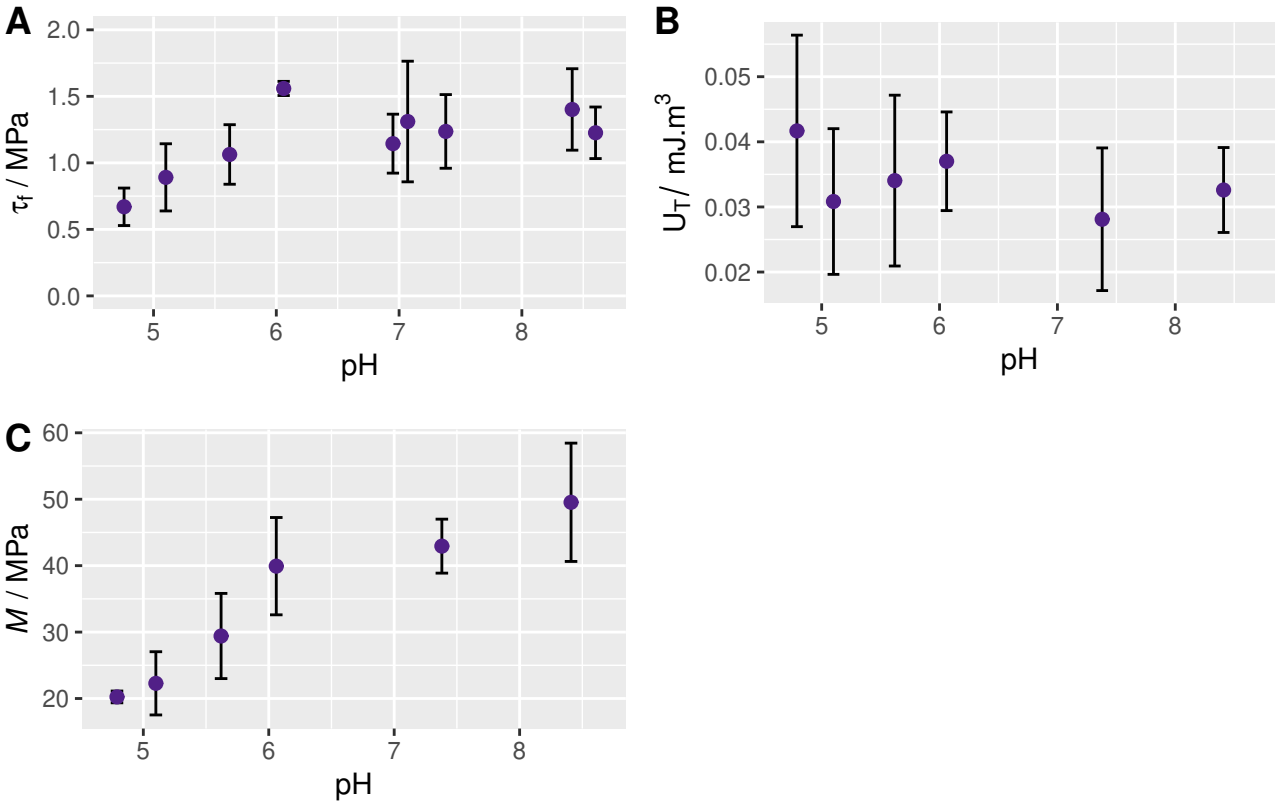

Figure 2.10: The mechanical properties of kaolinite aggregates over a range of pH values. **A:** The peak stress at failure increased linearly from 4.76 to 6.06 MPa, at which point it reached a plateau. **B:** No significant change in toughness was observed, however the data was very noisy, the result of fragmentation. **C:** The change in Modulus was most dramatic indicating a large increase in stiffness as pH increased. Error bars are one standard deviation (n = 3-5).

solid over the entire pH range.

These results indicate that the strength and modulus of the kaolinite artificial aggregates has a pH dependence. This dependence is likely to be sensitive to the kaolinite fabric formed in the sediment, and the interactions formed on drying. However, the strength and modulus was independent of the total porosity of the material even at high porosities of 40 – 46 %. This might also indicate that the pore sizes are small (no trapped air bubbles) as the formation of larger voids may significantly reduce the strength of a composite artificial aggregate as they do for other particulate solids such as concrete.

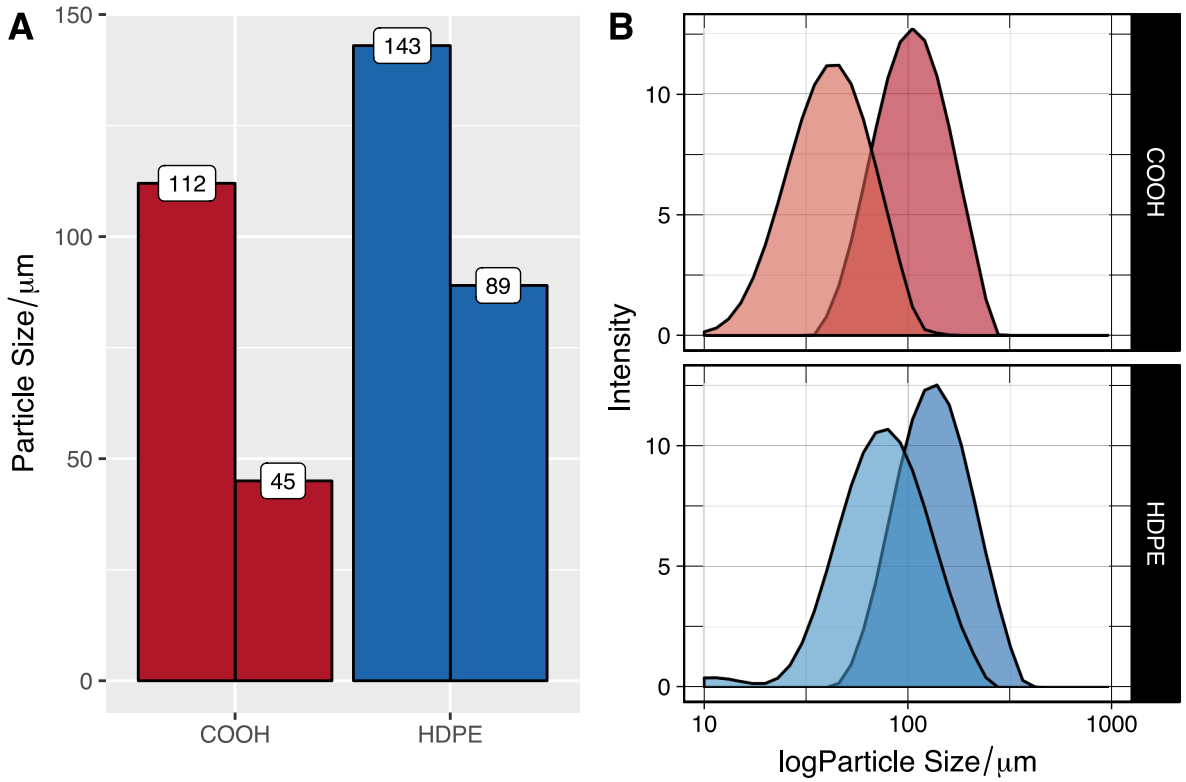

Figure 2.11: The particle size distribution for HDPE particles with different surface modifications. Unmodified particles are shown in blue, particles with COOH groups on the surface are indicated in red. The d(0.5) is shown in **A**, the particle size distributions are shown in **B**. The particle sizes are referred to by their d(0.5) in the text.

2.7 HDPE artificial aggregates

As shown in Figure 2.11 **B**, the HDPE particles have similar particle size distributions. The particles are hereafter referred to by their d(0.5) shown in Figure 20, **A**. The span values for the modified particles are 1.10 and 1.27 for the 112 μm and 45 μm particles respectively. The span values for the unmodified particles are 1.13 and 1.49 for the 143 μm and 89 μm unmodified particles respectively. Larger particles have narrowly larger spans than the smaller particles. Particle sizes are much larger than that of kaolinite which has a d(0.5) of 5.76 μm, however kaolinite has a much larger particle size distribution, with a span of 2.46 (Figure 2.11 and 2.1). Strictly speaking the HDPE could be considered 'silt-sized' rather than 'clay-sized'. pH of the dispersed particles was around 7.

Interactions between particles occur at the surfaces, and so surface area is likely to be a contributing factor to the strength and toughness. As expected, the smaller particles have larger surface areas, particle size and specific surface area relationship deviate slightly from the idea mathematical rela-

Particle size	*Span (particle size dispersity)*
112 µm (COOH modified)	1.10
143 µm	1.13
45 µm (COOH modified)	1.27
89 µm	1.49

Table 2.1: The span as measured by static lightscattering measurements of HDPE particles in DI water.

tionship for a spherical particle due to differences polydispersity but can otherwise be assumed to be spherical.

2.7.1 HDPE: Volume, porosity and shrinkage of artificial aggregates

The skeletal densities for the artificial aggregates decreased with increasing HDPE loading regardless of particle size or modification (Figure 2.12, **A**) as all HDPE particles have the same density. The envelope density decreased with HDPE loading, in keeping with the decrease in skeletal density, however the relationships were non-linear, relating to the changes in porosity (Figure 2.12, **B**). COOH modified artificial aggregates had a higher envelope density than the unmodified artificial aggregates.

Artificial aggregate volume (Figure 2.12, **C**) was not significantly affected by HDPE mass loading, or the particle surface modification. This is unexpected. Artificial aggregates are reduced in volume compared to the 1 mm^3 mould due to the loss of water and the contraction of the clay. A constant volume is unexpected as shrinkage is expected to be affected by the mass of kaolinite, and the presence of large low-density particles was expected to reduce shrinkage.

Porosity (Figure 2.12, **D**): HDPE particles are smooth and appear to contain little inherent macro-porosity on visual inspection (no air bubbles). There is a consistent decrease in porosity as HDPE is added for all samples, however, a minimum porosity is reached after 50% volume loading at which point there is an inflection and porosity increases again. Increasing the HDPE loading is effectively replacing a volume of fine-grained kaolinite with large particles, thereby removing pore space. However, if this was the only mechanism of porosity reduction, the greatest reduction in particle size would be expected to occur with the addition of the larger particles, which contain less

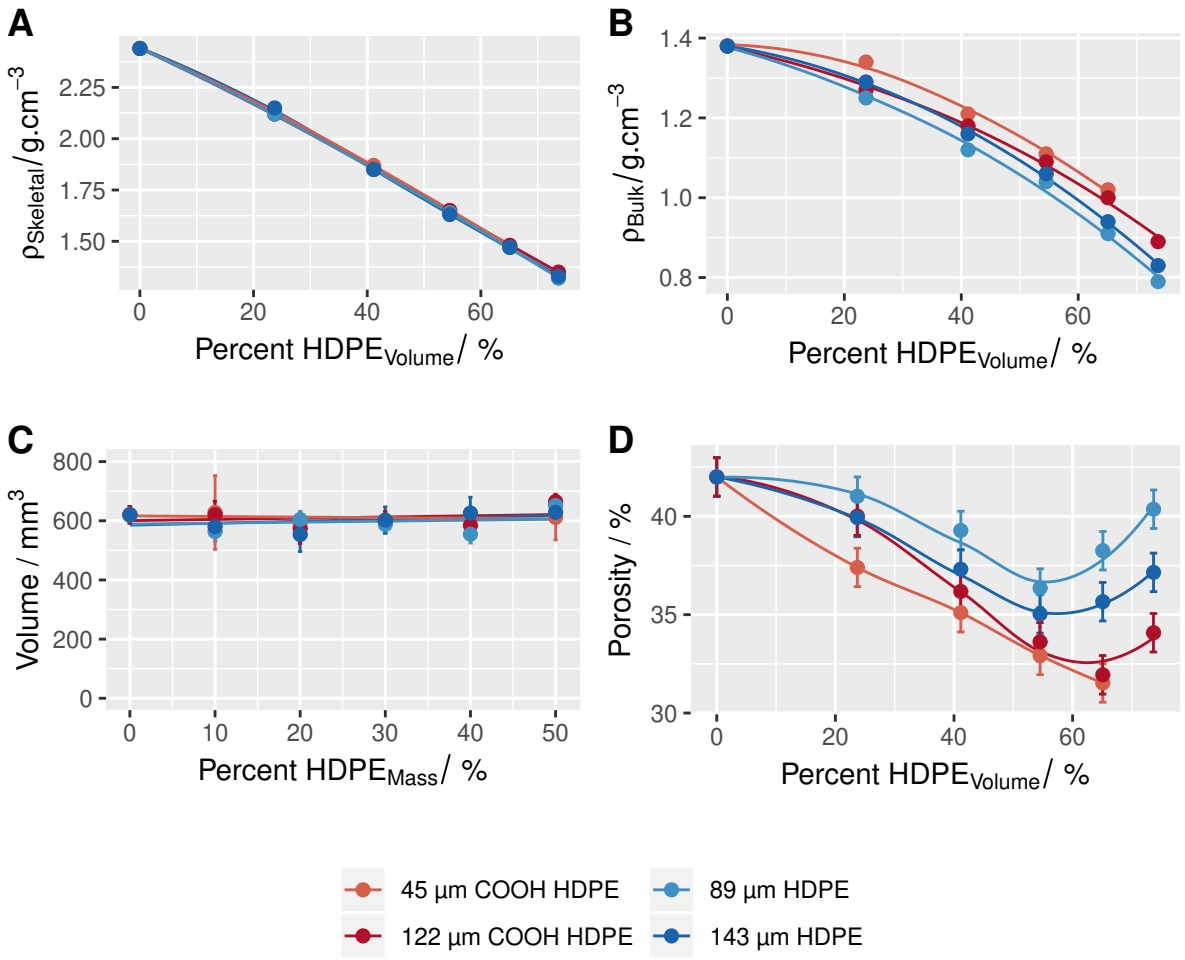

Figure 2.12: **A**: The skeletal density decreases as HDPE loading increases, with no differences between particles. **B**: Bulk density decreases non-linearly, reflecting a change in porosity. **C**: Artificial aggregate volume was almost identical with all treatments. **D**: The porosity of the kaolinite artificial aggregates amended with different HDPE particles decreased due to the replacement of a volume of fine clay material with larger non-porous beads. All lines are guides to the eye, except **C** where lines are linear regression. Error bars represent one standard deviation either side of the mean (n = 3-5).

pore space per unit volume. This is not the case. As the volume of HDPE particles is increased, the packing of these particles must also be considered. Theoretical modelling has shown that a well packed matrix of spheres results in a porosity of 38%, a similar porosity is observed for the HDPE artificial aggregates. At the maximum loading, the volume percent of HDPE is over 70%, suggesting a solid consisting of closely packed HDPE particles is likely, with kaolinite filling the interstitial pore space.

There are clear differences between the particles relating to surface modification and particle size in regard to porosity. Unmodified HDPE particles have higher porosities than those with surface modification, suggesting that the particles are less well packed or are not interacting strongly in order to increase the density of the particles. This could also reflect the drying rate, with modified particles retaining water, allowing kaolinite to reorganise into a denser sediment. The highest porosity artificial aggregates are found with the smaller unmodified particles, as smaller particles contain more inter-particle porosity per volume than a mixture of larger particles. The decrease in porosity for the smallest modified HDPE particles exceed 24 %. The lowest porosity artificial aggregates contain modified HDPE, and unlike the unmodified particles, the smaller size particles form artificial aggregates with less porosity. This may suggest a stronger interaction between the modified HDPE and kaolinite particles resulting in an increased particle density and reduced porosity. The porosity is slightly larger with larger particles. This suggests strong interactions with the smaller modified particles and the kaolinite, especially at lower loadings. The inflection point, the volume or mass of HDPE added where porosity reaches a minima, is different for modified and unmodified particles. A large change in porosity was expected to represent a change from a artificial aggregate where HPDE was dispersed in kaolinite, to a regime where HDPE formed the bulk and pore space can no longer be filled by kaolinite. However, the inflection point for the modified particles extends beyond that of the unmodified particles. Instead, the surface modification allows a further densification of the artificial aggregates. The reduction in pore volume by stronger interactions may extend the amount of HDPE that can be added before HDPE particle-particle interactions start to form voids.

It is also possible that the surface modification allows the modified artificial aggregates to retain more water, the unmodified artificial aggregates were visibly hydrophobic, which may speed up drying. The drying rate of the artificial aggregate is slower for those containing COOH modified particles

and smaller modified particles. The slower drying allows particles to reorganise to form more dense packing and to minimise the internal porosity. The inflection point could therefore represent the mass% of HDPE that can be added before pore space is created by more rapid drying. This is higher for the hydrophobic particles, especially the smaller ones with more surface area.

2.7.2 HDPE: Mechanical properties of artificial aggregates

Unmodified HDPE: Unmodified HDPE seems to decrease linearly in strength and toughness. R^2 values for linear regression are > 0.94, and the lines cross 0 MPa before 100% volume loading, reflecting the inability of unmodified HDPE to form cohesive artificial aggregates. The decrease is roughly equivalent for both particle sizes, showing no strong particle size dependence. This follows the trend of a decrease in density, and the effect of the reduced porosity is only reflected as a small bump in the linearly decreasing strength, toughness and modulus.

The linear decrease in strength represents a reduction in the strength or number of interparticle interactions with the addition of the unmodified HDPE. The linear decrease, whereby the strength is proportional to the volume ratio of the two components, shows that the HDPE is replacing the stronger kaolinite-kaolinite interactions for weaker kaolinite-HDPE interactions. Composites made with the larger HDPE particles have greater toughness as a result of the reduction in failure planes by a replacement of a volume of fine kaolinite with larger HDPE particles. The modulus is extremely low, reflecting a significant loss in stiffness.

Modified HDPE: It appears that the strength at 23% volume loading (10% mass loading) of all artificial aggregates is roughly equal, and lower than that of kaolinite. This is likely to be because a low loading of particles disrupts the network of kaolinite. At this loading, the percent strain was higher than the other artificial aggregates, meaning that the artificial aggregates were deformed more at 10% than the others before breaking, which results in an apparent reduction in strength. On increasing the HDPE loading, the composites become stronger, with the strength equalling or exceeding that of kaolinite at 20% loading. Smaller particles appear to form stronger artificial aggregates, possibly due to the reduced porosity or a higher surface area, increasing the density of

strengthening interactions in the artificial aggregate. It appears that there is a significant difference between the strength of the modified and unmodified artificial aggregates. Although it is true that the strengthened composites made from COOH modified HDPE have lower porosity, the trend cannot be explained by a reduced porosity alone. The maxima and subsequent decrease in strength observed with the modified particles may represent the percolation threshold, as the volume of the HDPE now exceeds that of the kaolinite and porosity is high.

Smaller particles were higher in strength, but not as tough. This means the network of interactions formed between the particles are strong, but do not deform easily, as shown by the huge increase in modulus. The smaller particles formed more bonds, which made the artificial aggregate more brittle, which meant that the artificial aggregate could absorb less energy, before a fracture was formed and the composite failed. It appears that the toughness is unaffected by the addition of the larger modified HDPE particles. The deformability doesn't change, which is reflected in the modulus. Larger particles are able to deform and are far less brittle than the smaller particles. At 10% loading, the composite artificial aggregates are weakened in comparison to a pure kaolinite composite, this could be because a network of strengthened particles has not yet formed fully, and the structure of the pure kaolinite artificial aggregate has been disrupted, reducing the strength.

The difference in strength and porosity observed for the unmodified and modified particles can only be accounted for by an increase in kaolinite-HDPE interactions due to the inclusion of carboxylic functionality. By comparing the stress/toughness/modulus data of a non-interacting particle (HDPE) with the modified equivalent (HDPE surface modified), an attempt at quantifying the increase in strength due to the presence of COOH groups can be made.

The decrease in strength vs volume for unmodified HDPE particles was fitted to a straight line with an $R^2 > 0.94$ (Figure 2.14, **A**). The strength can be considered to be equivalent to the volume ratio of the components. The increase in strength of the modified particles relative to the unmodified particles can be calculated via a simple subtraction and plotted as a function of HDPE volume (Figure 2.14, **A**). A more rapid increase in strength per volume added is observed for the smaller 45 m^2 particles. The smaller particles have an increased surface area, and therefore can form a stronger network of interactions at lower loadings. The maxima may represent the volume loading

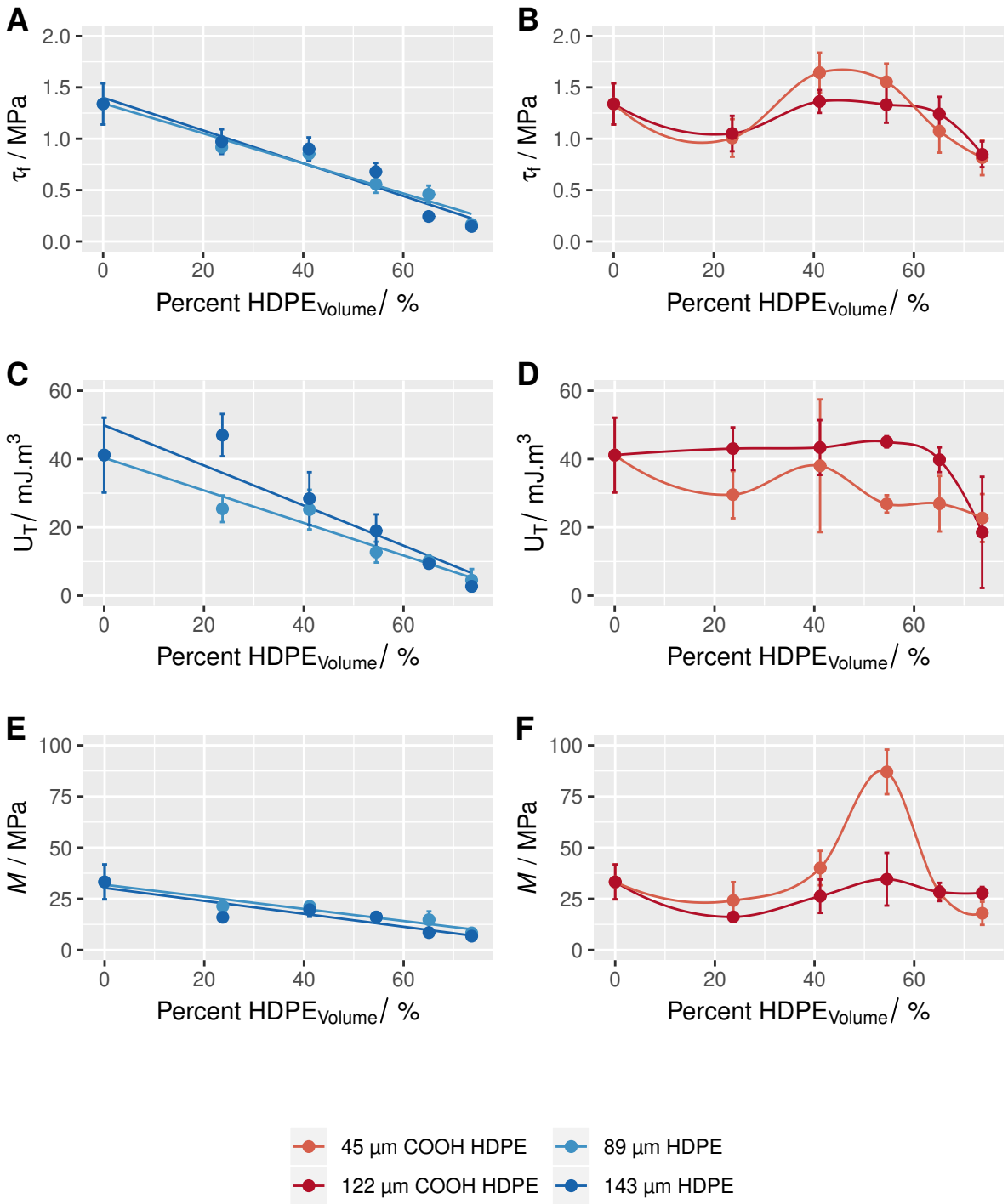

Figure 2.13: Measurements from uniaxial compression tests of artificial aggregates containing HDPE. **A:** The decrease in strength for the HDPE artificial aggregates is linear and proportional to the volume loading of HDPE. The slight deviation from a linear decrease may reflect the decrease in porosity. **B:** Surface modification of the HDPE artificial aggregates resulted in the strengthening of the composites with only a marginal size dependence. **C:** The toughness decreases in a linear fashion, reflecting the change in strength for HDPE artificial aggregates. **D:** Modification of the artificial aggregates results in artificial aggregates which are more tough, larger particles impart greater strength. **E:** The modulus for HDPE artificial aggregates was small, and a small but marked decrease in modulus was observed. **F:** Modified HDPE were much stiffer, and smaller particles formed artificial aggregates with much higher modulus. **A, C, E** are fitted to linear models, whereas **B, D, F** are guides to the eye only. Error bars are one standard deviation (n= 3-5).

where kaolinite:HDPE surface area are optimised. Beyond this point, the surface area added may not add additional interactions. Alternatively, the percolation threshold is reached and a continuous network of HDPE and pore space is formed which weakens the artificial aggregates.

The larger particles can be added at a higher volume before the decrease in strength is observed because the surface area added is smaller (larger particles have smaller surface area per volume added) and interactions with kaolinite may not yet be saturated. Both modified particles plateau at 1 MPa. This may represent the maximum strength fabric that can be formed by a network of kaolinite particles with particles modified with COOH groups, which may be independent of particle size. However, particle size has a more significant effect on the modulus, which can impact strength. Porosity also begins to increase after 60% HDPE volume. The increase in strength can also be replotted against surface area (Figure 24, **B**). The gradient of the fitted lines for the initial increase are observed to be roughly equivalent, indicating that strength increase / surface area added is also equivalent for the two particles.

HDPE modified with COOH groups gave :

- 112 μm = 0.36 MPa/m^2 added
- 45 μm = 0.18 MPa/ m^2 added

The offset from zero on the x axis of Figure 2.14, **B** represents a surface area which does not contribute to an increase in strength. At low loadings, particles are dispersed in the kaolinite and do not form strong networks. The offset (3.06 - 3.47 m^2 for 45 μm, 1.19 m^2 for 112 μm) is larger for the smaller particle size, suggesting much more of the initial surface area added does not contribute directly to strength. Smaller particles will disperse more evenly in the kaolinite matrix, reducing the probability that strong networks will form. This is why larger particles form stronger interactions at lower loadings and the increase in strength is observed at a lower value for surface area added. The maximum strength is also equal for both particle sizes suggesting that the increase in strength may be proportional to the strength of the interparticle interactions when their ratios are optimised. The surface area at which the strength increases from the offset to the maxima is 2.75-5.40 m^2 , which may correspond to the surface area forming interactions with kaolinite particles to form the

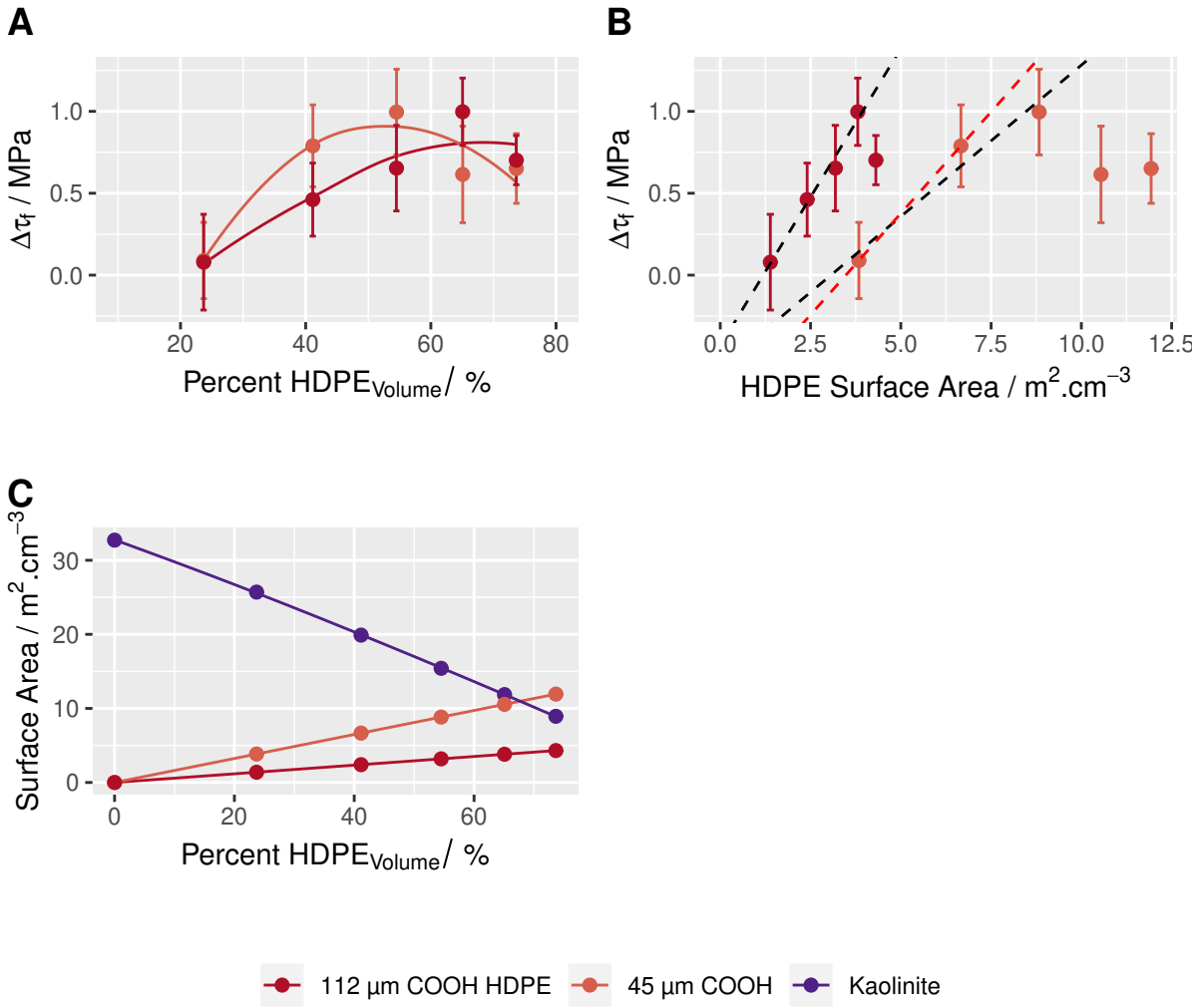

Figure 2.14: The mechanical properties of a series of artificial aggregates made with increasing HDPE content. **A:** The increase in strength due to the surface modification was calculated by subtracting the modified particle artificial aggregate strength from the unmodified particle artificial aggregate strength. Smaller particles reach a maxima at smaller volumes. Lines are guides to the eye only. **B:** The same increase in strength is plotted against the surface area of HDPE particles in a 1 cm-3 artificial aggregate, dotted lines are fitted to the initial increase in strength. The linear fit (black dashed line) for the 122 ^{2}m is for the first 4 points (y = 0.3634x - 0.4325, R^2 = 0.9821), the linear fit for 45 ^{2}m (black dashed line) is for the first 3 points (y = 0.1849x - 0.5667, R^2 = 0.9487), the red dashed line is for the first 2 points only (y = 0.2478x - 0.8619). **C:** The calculated surface area contribution of each component in each aggregate.

strongest network. The surface area of kaolinite always exceeds that of the HDPE particles (Figure 2.14, **C**), which could indicate that the HDPE surface area is limiting. However, the total surface area of kaolinite may not be available for binding interactions due to charge and surface functionality heterogeneity on the particle surface.

2.7.3 HDPE: Nature of the inter-particulate binding.

The presence of COOH groups are able to increase the strength of kaolinite-HDPE interactions with respect to unmodified particles. However, the pure kaolinite artificial aggregates exceeded the strength of all unmodified HDPE, and was roughly equivalent to the modified particles. HDPE contains only C-C and C-H bonds, and are able to form only weak Van der Waals interactions or hydrophobic type interactions. This suggests that particles able to form these types of interactions are not able to form particularly strong binding interactions with clay surfaces in dry soil.

COOH modified artificial aggregates are therefore likely to take part in inter-particle binding interactions of a similar strength to that between aggregates of kaolinite. Kaolinite aggregates are likely to be held together by a mixture of Van der Waal and hydrogen bonding interactions. At low pH, the COOH groups on modified HDPE remain protonated and at low moisture contents (these aggregates are very dry) acid groups are likely to retain protons. This means that the interactions are unlikely to be dominated by electrostatic effects, although this could feasibly occur at much higher pH. Electrostatic interactions may have a stronger effect for particles in suspension, effecting primarily the suspension behaviour and sediment density and are overcome on drying, but may effect the morphology of the sediment that forms on drying. Here, it is likely that modified HDPE and kaolinite are held together via predominantly hydrogen bonding interactions and Van der Waals forces. Hydrogen bonds are strong and may cause the large increase in strength, additionally hydrogen bonds are directional and may also give rise to an increase in modulus as they may resist deformation much more than Van der Waals interactions.

2.8 Organosolv lignin

Organosolv lignin of both beech and spruce wood feedstock was analysed extensively using a range of NMR techniques, GPC, elemental analysis and compositional analysis, some of the results are included in the Appendix and may be referred to in the Results and Discussion (see A.1). Attaining information about the behaviour of lignin as a solid particle from molecular information obtained using common lignin characterisation techniques is a challenge, as few studies consider (or are interested in) lignin as an aggregated particle (*129*, *130*), although some information is useful from studies investigating lignin as an additive in materials science. (*131*, *132*) It is also only recently that studies have began to investigate the interactions between lignin and cellulose and hemicellulose in intact plant cell walls in real detail, which requires advanced NMR techniques. (*112*, *113*) These studies are beginning to indicate the role of more minor linkages, and the differences in subunit composition for inter-fibril linkages, which may not be purely covalent in nature. Studies such as this may provide new ideas as to how lignin may bind to surfaces via non covalent linkages. The beech lignin was found to contain both S and G subunits, where as spruce contains only G characteristic of angiosperm wood and gymnosperms wood respectively. An abundance of G units and the higher aliphatic OH content (see Appendix A.1.4) suggests spruce lignin may form more hydrogen bonding interactions, although this is highly dependent on the molecular organisation and morphology of the lignin particles. (*129*)

2.8.1 Lignin particle size

The particle size and distribution of lignin was determined by static light scattering. The particles form a quazi-stable suspension in water which settles within minutes. Lignin decreases the pH of the solution to around pH 4.7. Kaolinite has a d(0.5) of 5.76 µm and a span of 2.46. Beech lignin has a d(0.5) around 10 µm, but is distributed around 5 – 50 µm, stable clumps were reduced by sieving through a 63 µm sieve, and were broken further by vortexing. After sieving, beech lignin had a d(0.5) of 4.59 µm and a span of 3.25 (Figure 2.15). Spruce organosolv lignin was found to have a similar particle size distribution. SEM was used to determine the morphology of lignin, and to

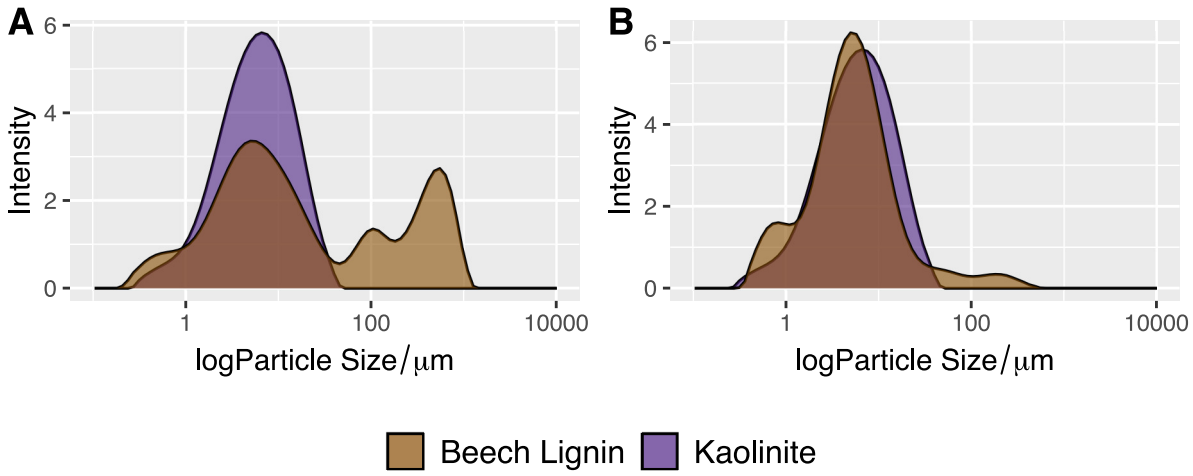

Figure 2.15: Particle size distribution of beech organosolv lignin before (**A**) and after sieving (**B**) as determined by static light scattering. Particles were dispersed in DI water. Kaolinite is also shown for comparison (purple).

confirm the particle size. Both lignins were found to be non-uniform and globular in shape. These micron sized globular structures are likely to be formed by the agglomeration of micron sized lignin colloids, the structures formed by these colloids are controlled by the precipitation kinetics, and can be very dense or open. (*130*) Therefore the particle size of lignin is determined to an extent by the precipitation kinetics. That said, control over the particle size of these lignins could not be achieved through dissolving lignin in acetone and re-precipitating in water at different rates. This is likely to be due to the large heterogeneity and polydisperse nature of the lignin molecules, which makes fine tuning difficult. (*133*)

2.8.2 Lignin: Volume, density and porosity.

Blends of lignin and kaolinite formed stable artificial aggregates with no visible pores. The volume of the artificial aggregates increased linearly with increasing lignin content (Figure 2.16, **C**), with artificial aggregates increasing in depth. The solids formed tended to cling to the walls of the mould which resulted in flatter structures which became thicker with increasing lignin. This suggests an increased interaction with the silicone mould, in comparison to the pure kaolinite and a reduction in shrinkage. Deviation from a linear relationship between lignin content and volume or porosity would be suggestive of a change in particle morphology, packing or porosity, and this was not observed

(Figure 2.16). Lignin has a lower density than clay, the densities of the artificial aggregates decreased linearly as a function of volume lignin loading (Figure 2.16), there was no clear significant difference between the two lignin types. Porosity was also observed to increase, with little difference between the lignin types, although beech artificial aggregates appeared to have a lower porosity than the spruce (Figure 2.16, **D**). The zeta potential is slightly more negative for beech lignin than spruce, which means that a difference in electrostatic repulsion does not drive this difference in porosity. With HDPE particles, a reduction in porosity was a suggestion of stronger interactions and stronger artificial aggregates, although why beech lignin may form stronger binding interactions with kaolinite is not yet understood. The increase in porosity due to the addition of lignin may be due to the inherent porosity of lignin particles, the porosity measured for both lignin and kaolinite via BET was small, 8.45 % pore space in kaolinite vs 2.31% pore space in beech lignin, suggesting that as the lignin content should decrease the porosity in a simple mixture. This suggests the added porosity is between the particles, suggesting poor packing. Poor packing may be the result of the sedimentation characteristics. Both particles are of similar sizes, but different morphologies, and the creation of inter-particle porosity is likely. The linear nature of the increase in porosity may suggest a simple phenomenon such as increase in drying rate could also be a plausible explanation. The increased hydrophobicity of the mixtures could lead to more rapid drying, resulting in a reduced reorganisation of particles on drying and the formation of pores. The increase in porosity is extremely large, around 25%, and could feasibly be a combination of these factors.

2.8.3 Lignin: Mechanical properties

The peak stress reaches a maxima at 42% beech lignin loading and 25% mass for spruce lignin (Figure 2.17, **A**). At the maxima, beech lignin makes up just less than 50% of the total solid volume, spruce at its maximum makes up only 25% solid volume (Figure 2.17, **A**). Crucially, the strength of the composites exceeds that of pure kaolinite, suggesting lignin-kaolinite interactions are stronger than kaolinite-kaolinite interactions. The addition of 42% beech lignin results in a 45% increase in strength from the pure kaolinite. This occurs despite a large increase in porosity and a reduction in density. Kaolinite and beech lignin have similar particle sizes and surface areas, and a strengthening

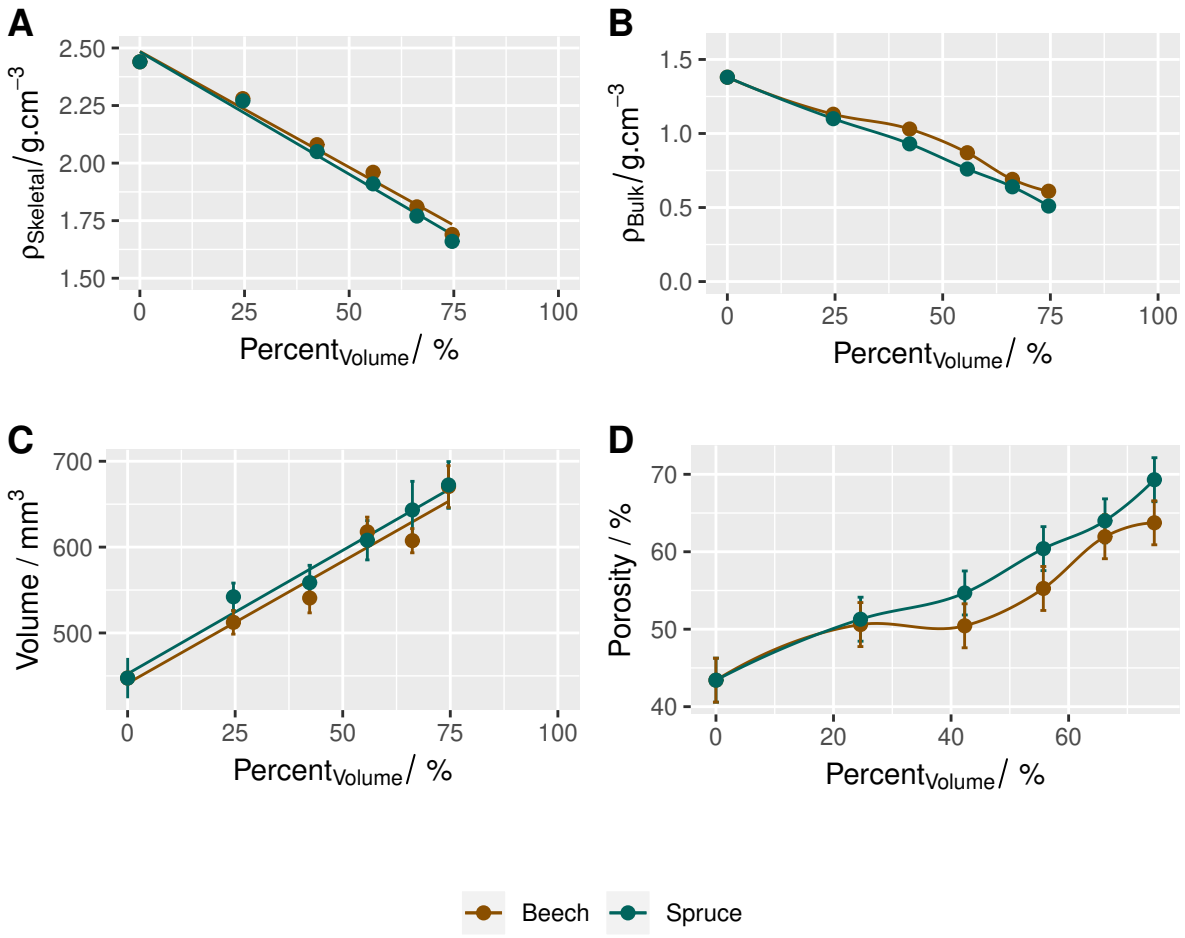

Figure 2.16: The densities, volume and porosity of artificial aggregates made with increasing lignin content. **A:** The skeletal density decreases with increasing volume with both lignin types. **B:** The bulk densities were much lower than the skeletal densities. **C:** The artificial aggregate volumes increased linearly with an increase in lignin, due to the reduced density of the lignin and additional porosity. **D:** Porosity was very high ($>$ 40%) and increased strongly as lignin was added. Straight lines are linear regression, others are guides to the eye. Error bars represent one standard deviation (n = 4-5).

at 50% volume loading would be expected if a 1:1 mixture created the strongest network within the solid. However, following the initial strengthening of the composites with lignin loading up to the maxima, further lignin loading leads to a rapid decline in strength. If this decrease in strength is extrapolated, the strength of the artificial aggregate reaches zero before 100% lignin volume. This reflects that 100% lignin artificial aggregates did not form cohesive artificial aggregates. The reduction in strength after the maxima represents the percolation threshold for the material, where the combination of additive volume and porosity starts to create connected networks of weakness in the artificial aggregate. In these artificial aggregates where porosity is high ($> 40\%$) and increases strongly with loading, a low percolation threshold is expected. The reduced porosity of beech lignin compared to spruce may explain why it has increased strength at higher loadings, as the percolation threshold may not be reached. It is likely that the cementing properties of both lignin types are similar.

The trend in modulus is equivalent or more pronounced than that of the strength, with stronger artificial aggregates also becoming more rigid (Figure 2.17, **C**). A simultaneous increase in both strength and modulus suggests that the bonding interactions and the network it forms are strong but inflexible. The artificial aggregates also seem to increase in toughness, but with both types of lignin have a maximum toughness at 10% loading (Figure 2.17, **B**). This suggests the artificial aggregates are able to take up more energy in the deformation at low loadings, possibly because of the collapse of smaller pores. The brittle nature of the bonds suggests localised bonding interactions with small and inflexible contact points between particles. Hydrogen bonding type interactions are directional at a molecular scale and may be more inflexible than van-der-Walls forces.

2.8.4 Lignin: Bonding interactions

The maxima represents a point where lignin:kaolinite interactions are maximised to create a continuous network of particles, before a percolation threshold is reached. The strengthening of the artificial aggregates is obtained because the kaolinite-additive interaction is stronger than that of a kaolinite-kaolinite interaction, or a larger continuous fabric is formed by the gluing of kaolinite tactoids. Stronger interactions will result in stronger artificial aggregates, but since the maxima

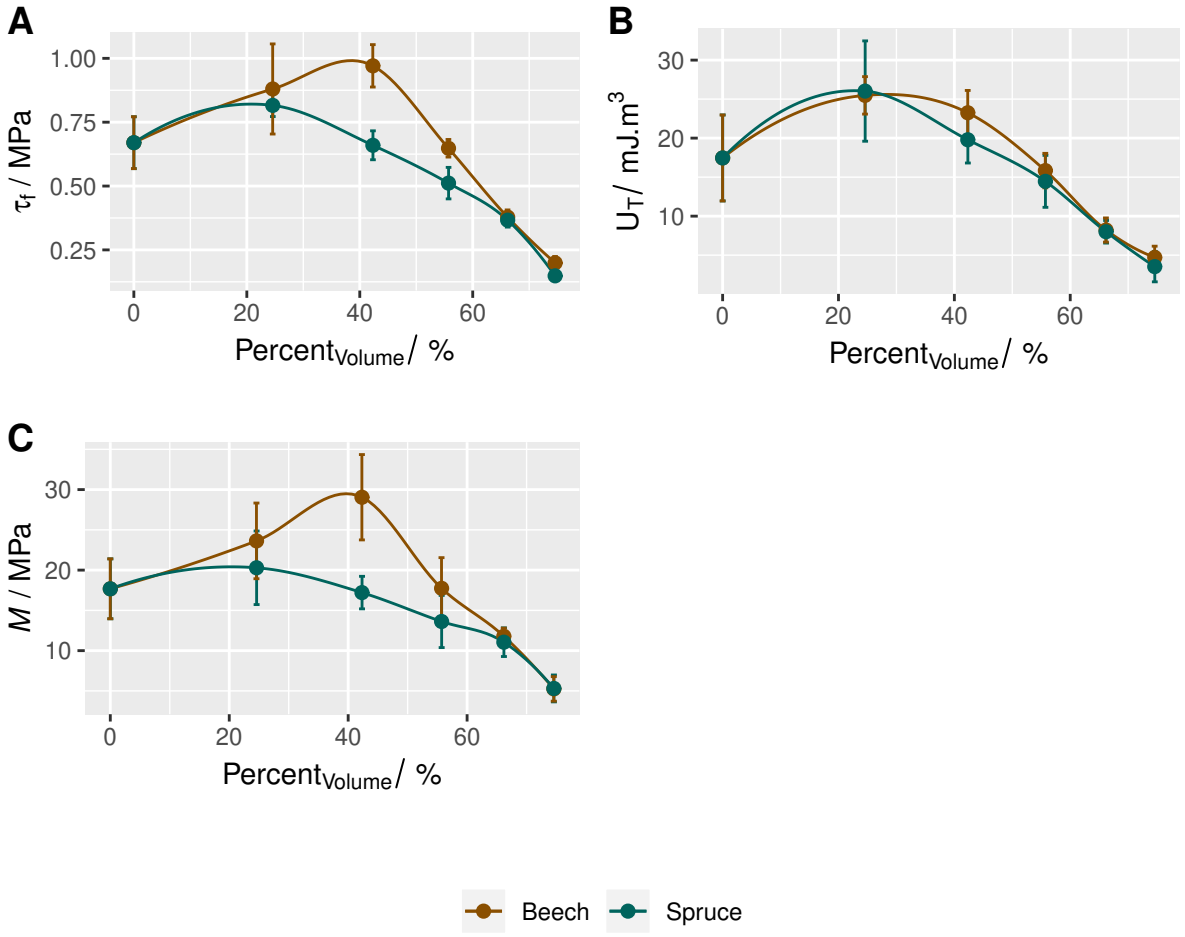

Figure 2.17: The mechanical properties of lignin artificial aggregates. **A**: Maximum compressive strength reached a maxima for the lignin artificial aggregates between 20-50% lignin loading, with beech lignin forming stronger artificial aggregates than the spruce lignin. **B**: Toughness followed a similar trend, reaching a maxima at 20% loading for both lignins. **C**: The increase in modulus was much greater for the beech lignin. Lines are guides to the eye only, error bars are one standard deviation (n = 4-5).

obtained is dependent on the percolation threshold, which is dependent on the particles shape, size, packing and density of bonding interactions, we cannot say that the maximum represents the maximum possible strength resulting from these interactions. However, as calculated for the HDPE, the initial linear strength increase per surface area, is a much better indication of the binding strength, which depends on both the surface functionality and the density of these interactions. Beech organosolv lignin resulted in an increase in strength of 2.1 kPa/m^2 of lignin surface area added, in a 1 cm^3 artificial aggregate, whereas spruce organosolv lignin resulted in an increase of 1.9 kPa/m^2 of lignin added.

The increase in strength per surface area added is much smaller than that of modified HDPE. Lignin is a much smaller particle with a much larger surface area being added, however the large increase in porosity may decrease the contact point between particles. The silt sized HDPE maximises the surface area contact, whereas smaller particles pack less effectively. (*11*) This could also suggest that the lignin binding contains very few binding sites, in comparison to the surface modified HDPE. An amendment containing very small particles with a high density of polarisable or COOH groups would therefore, be a very strong amendment. The smaller the particle, the more volume can be added before percolation, and the more surface area that can be added, to create a strong network of particles, at which point the kaolinite surface area available becomes limiting. The difference between spruce and beech lignin is very small, and this reflects the similar nature of the two particles. The maxima obtained is a result of the porosity formed, so stronger artificial aggregates may be formed by optimising extracted lignin to create a denser sediment. Alternatively, technical lignin could be optimised to hold nutrient cations, resist microbial decomposition or to hold water. Aliphatic hydroxyl groups are known to form much stronger hydrogen bonds than other functionality present in lignin, and so increasing the surface density of aliphatic hydroxyls and carboxylic acids may increase the binding strength of lignin. (*129*)

2.8.5 Lignin: Porosity and drying rate

The effect of temperature on porosity was tested, in order to investigate if drying rate could drive the large porosity increase in lignin composites. Over the temperature range of room temperature to 70

°C, porosity increased by only around 3 % (Appendix). This suggests that drying rate does not have a strong control on the porosity, but that the sediment packing is more important. Beech:kaolinite composites were also centrifuged in a modified centrifuge tube, in order to obtain composites with 10% less porosity. A decrease in porosity of 10% was found to increase strength by around 41% of a 42% beech lignin cube, suggesting consolidated aggregates would be considerably stronger.

2.8.6 Lignin: Nature of binding

ATR-FTIR is a surface sensitive technique and was used to investigate lignin-kaolinte surface chemistry and interactions. For artificial aggregates at all lignin loadings, the spectra was dominated by kaolinite absorptions, and no characteristic signals for lignin were observed (Figure 2.18). At higher loadings however, the baseline was increased, due to black-body absorption which occurs with dark materials. Aggregates at different loadings were compared after applying a polynomial background subtraction, and normalised to signals attributed to inner OH stretches (3619 cm^{-1} or 910 cm^{-1}) which are not exposed surface OH groups, and are unlikely to be modified by the presence of surface interactions. Signals were assigned based on literature values. (*19*) Kaolinite contains a number of characteristic absorptions which are used for studying organo-mineral interactions and changes in surface chemistry, (*19*, *134*) absorptions attributed to OH stretching vibrations the region 3570 to 3730 cm^{-1} are often shown to decrease in intensity due to ligand exchange reactions with soluble organic molecules. No changes in this region was observed suggesting that no ligand exchange reactions occurred and that surface hydroxyls on the octrahedral edge and surface are not significantly changed. The region between 900 - 1200 cm^{-1} are attributed to bending and stretching vibrations, and have been used to indicate changes in surface chemistry with pH. This region showed a decrease in in plane Si-O stretching vibrations at 1032 and 1012 cm^{-1}, which might indicate lignin interactions with the silica surface. (Figure 2.18)

To investigate lignin-kaolinite interactions further, lignin was dissolved in acetone added to kaolinite and dried. Dissolving the lignin facilitates strong interactions with the clay surface, acid groups have been found to form inner-sphere complexes with surface hydroxyls on drying. (*19*, *134*). Lignin dissolved in acetone was added at a range of 15 - 150 mg of lignin / g of kaolinite. The FTIR

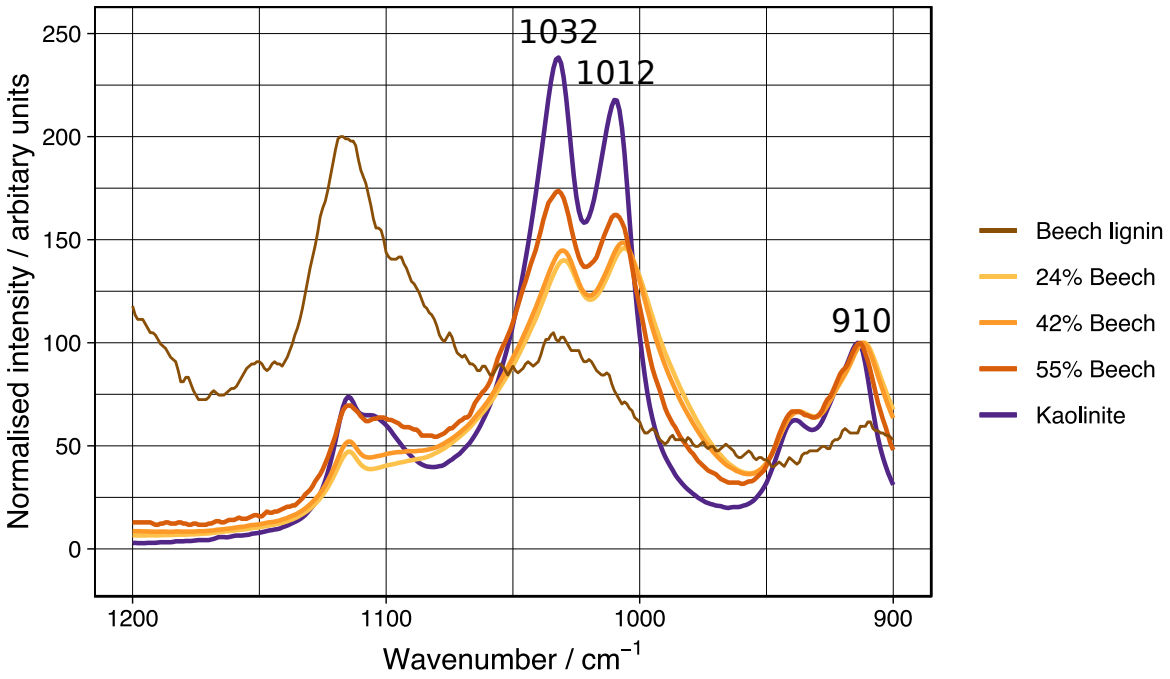

Figure 2.18: The 900 - 1200 cm^{-1} region of the ATR-FTIR spectra of lignin:kaolinite artificial aggregates showing the major absorptions of Si-O in plane stretching. Spectra is baseline corrected and normalised to the inner surface -OH bend at 910 cm^{-1}. The FTIR of the beech lignin in artificial aggregates were not observed in the FTIR spectra, pure beech lignin is presented for reference.

spectrum of kaolinite was modified on adding lignin (Figure 2.19) but did not change over the entire concentration range, suggesting that kaolinte surface interactions had been saturated at the lowest concentration. This demonstrates the low adsorption capacity of kaolinite. A UV/vis study was used to generate an absorption isotherm (see Appendix: A.2.1). Lignin appeared to follow a type I Langmuir type absorption isotherm, consistent with a mono-layer coverage giving a maximum adsorption capacity (Q_m) of 0.614 mg g^{-1} in solution, or 0.275 µmg^{-1}. For reference, the $Q_m$of humic acids are reported to be between 5 - 10 mg^{-1} in water (*19*). Lignin is a macromolecule, which makes the formation of a mono-layer more difficult, and this may be reflected in the lower (Q_m). Also acetone may be a more competitive solvent for binding sites then water. The FTIR analysis showed both evidence of interactions at the silica edge (Figure 2.19, **A**) which showed a strong reduction of the Si-O stretch and a shift to lower wavenumbers, and a reduction in Al-OH stretching vibrations at higher wavelengths (Figure 2.19, **B**). This demonstrates that lignin is able to form interactions with both surfaces in solution, however, this does not mean the same interactions occur in aqueous suspensions with undissolved lignin. The large change in Si-O stretching suggests a strong

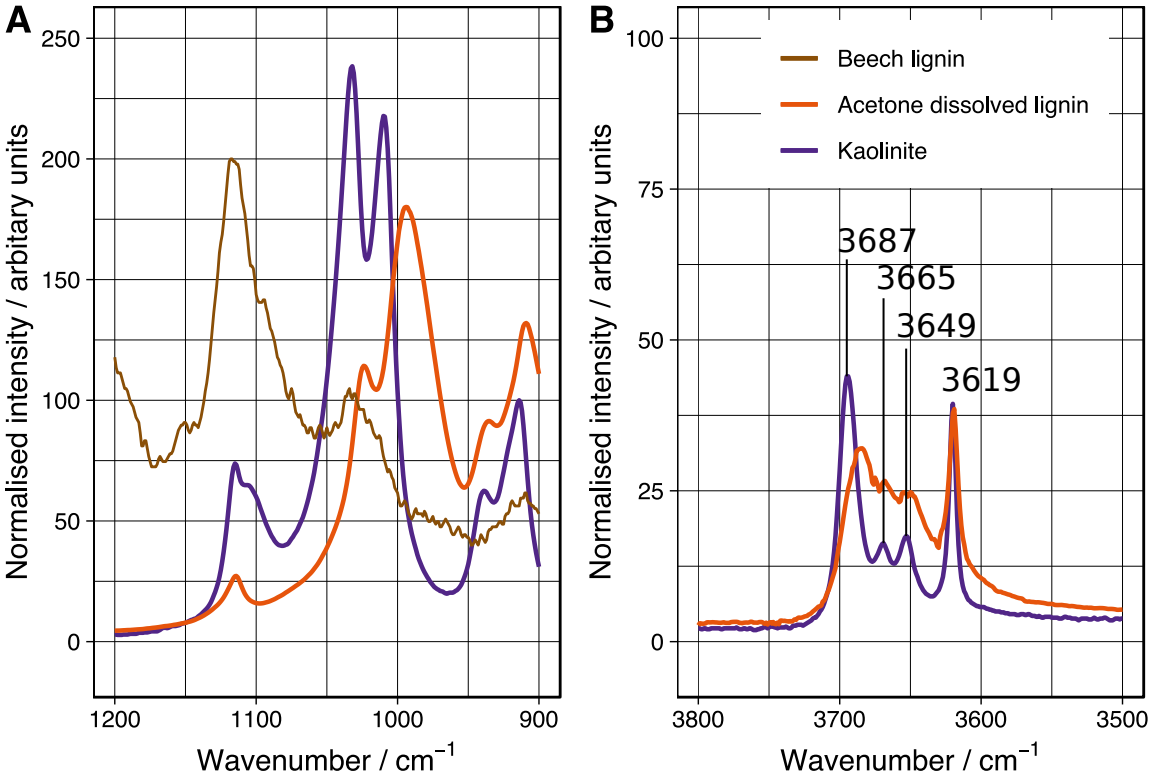

Figure 2.19: **A:** ATR-FTIR spectra of the 900 - 1200 cm^{-1} region, showing the major absorptions of Si-O iand Al-OH stretching and bending absorptions. Signals for lignin were not observed, but a strong reduction in intensity and a shift to lower wavenumbers was observed on addition of soluble lignin. **B:** The region 3500 - 3800 cm^{-1} showing the OH surface stretching absorptions, the lowest peak at 3619 cm^{-1} is due to inner OH between tetrahedral and octahedral sheets, and should not be affected by surface adsoptions. The other absorptions are modified suggesting an interaction at both the octahedral face and edge sites.

interaction with the silica surface, which has not been observed with organo-mineral interactions of kaolinite with small soluble molecules or surfactants and may therefore be a property of polymeric hydrophobic molecules.

2.9 Lignin: Added electrolytes

The solution electrolyte is known to strongly influence the behaviour of kaolinite in solution, cations such as Na^+ and Ca^{2+} reduce electrostatic repulsion by shrinking the electrical double layer or adsorbing to surfaces. (*135*) Here, salts were added to the initial water solution in order to test if electrostatic repulsion had any influence on kaolinite-lignin interactions. Figure 2.20 shows the effect of the dissolved salts NaCl and $CaCl_2$ on the compressive strength of three artificial aggregates

with increasing beech lignin at a pH < 6. At this pH, electrostatic interactions are known to be particularly sensitive to electrolytes. Also, the affinity of kaolinite for Ca^{2+} is considered to be much larger than that of Na^{+}. (*135*) Concentrations of 0.1 and 0.5 M salt are beyond the reported critical coagulation concentrations for Ca^{2+}, although the solid:solution ratio is much higher in these experiments compared to those carried out on kaolinite slurries. Preliminary data showed that high salt concentrations were needed to effect significant changes in artificial aggregate strength (data not shown). This goes contrary to the solution and rheological behaviour, in which low salt concentrations can change the properties of suspensions dramatically. Salt solutions containing only monovalent cations such as NaCl are known as indifferent electrolytes. These electrolytes do not have a strong affinity for the kaolinite surface in solution, but shrink the electrical double layer as the concentration increases. This means that electrostatic repulsion is reduced and kaolinite tends to flocculate as a result. Divalent and trivalent cations such as Ca^{2+} and Al^{3+} adsorb strongly in the Stern layer, and at increasing concentrations can effectively neutralise kaolinite surface charge, and reverse it. These effects are well known, but the effects of these salts on the fabric strength has not been reported.

The addition of an NaCl electrolyte at either concentration did not affect change in the strength of the kaolinite (Figure 2.20). This suggests that a reduction in electrostatic forces does not cause considerable change to the fabric of the kaolinite particles. Silica face – alumina face interactions may still dominate and the resulting fabric may not be modified. At high salt concentrations, shorter range interactions are likely to have a larger influence in solution and face-face stacking is favoured. Face-face stacking is observed at low pH, and so the change in fabric may be minor. The more dramatic increase in strength at 0.1 and 0.5 M $CaCl_2$ with kaolinite suggests a different method of strengthening. The high adsorption affinity of Ca^{2+} is known to cause flocculation in kaolinite suspensions. Kaolinite has heterogenous charge distribution, but remains net negatively charged over the entire pH range (Figure 2.20). Ca^{2+} can effectively neutralise this negative charge and may also promote edge-face interactions.

Salts added to artificial aggregates made with 25% beech lignin has the opposite effect to that observed in pure kaolinite. NaCl brought about no strengthening or weakening of the artificial aggregates, suggesting the strength of the artificial aggregate has no contribution from electrostatic

interactions in the dry solid or in the sediment. This is evidence to suggest that strong lignin-kaolinite interactions are not formed in solution via face or edge Al-OH_2^+ with COO^- groups on the lignin. Unexpectedly $CaCl_2$ strongly weakens the artificial aggregates containing 25% lignin at both concentrations. Ca^{2+} is known to promote adsorption of soluble organic matter with kaolinite surfaces, especially organic matter containing chelating groups such as carboxylic acids. Lignin carboxylic acids are weak chelators of Ca^{2+} but can form strong calcium bridges with clay surfaces. It is possible that high concentrations of Ca^{2+} are able to induce net positive charge on both kaolinite and beech lignin, resulting in electrostatic repulsion between the particles, making a weaker artificial aggregate. High calcium retention of lignin has also been reported, which may result in a change in the morphology of the particles. (*104*, *136*) Alternatively, it could be that the strong kaolinite flocculation caused by high concentrations of Ca^{2+} result in greater phase separation, with kaolinite aggregating into larger domains preferentially over forming bonds with lignin. Regardless of the mechanism, lignin-kaolinite interactions are evidently not strengthened via calcium bridging interactions of the kind described by the adsorption of similar soluble molecules on kaolinite surfaces.

At 50% lignin loading, the strengths of the artificial aggregates are very low, and are difficult to measure, no large strengthening was observed due to the presence of either salt, this confirms that salts do not increase the mechanical properties of lignin rich composites. 1H NMR was used to investigate whether $CaCl_2$ could induce a chemical shift in any lignin signals when dissolved in d-DMSO, none were observed, suggesting that the beech organosolv lignin does not strongly coordinate Ca^{2+}.

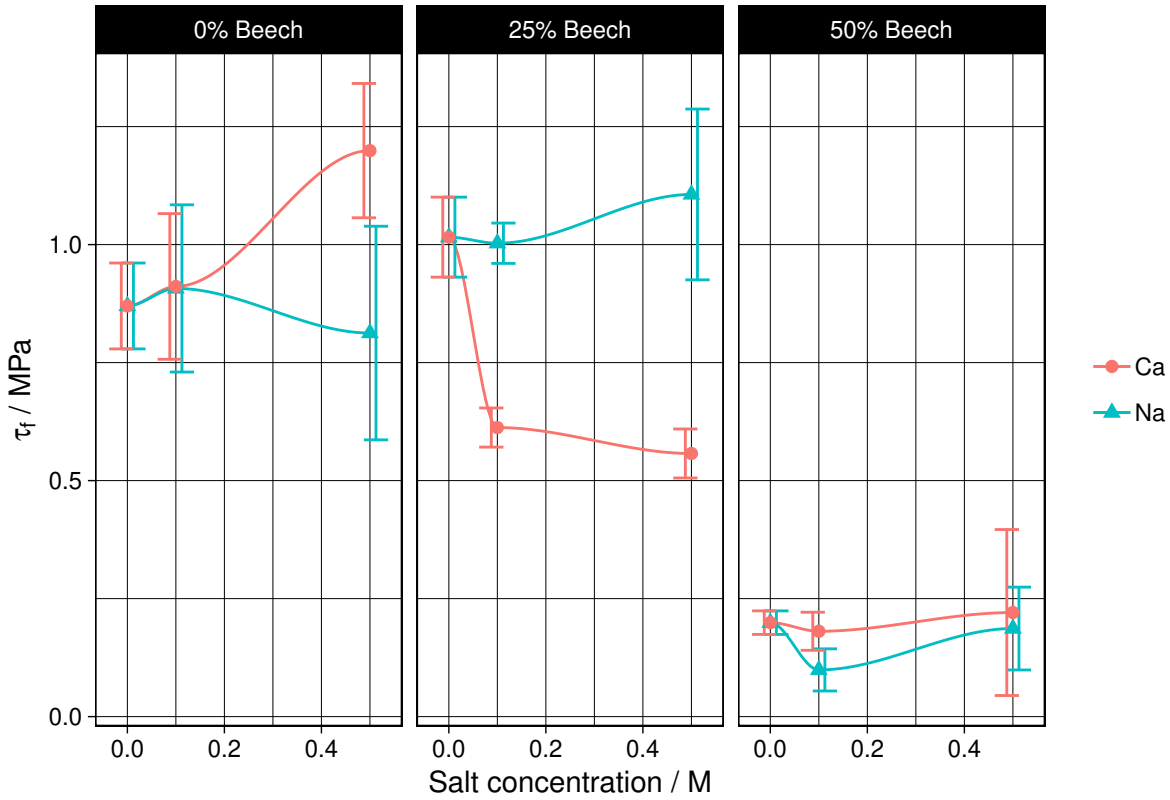

Figure 2.20: The mechanical strength of different lignin amended aggregates containing salts. The effect of NaCl and $CaCl_2$ solutions on the τ_f of artificial aggregates containing only kaolinite, 25% mass loading beech lignin, and 50% mass loading lignin. Error bars represent one standard deviation from the mean (n=3), lines are guide to the eye only.

2.10 Lignin: Influence of pH on the mechanical strength of lignin:kaolinite aggregates

The pH of soil and other particulate matter is not straight forward to measure or to interpret, as compared to solutions. Since the pH of a dry solid cannot be measured, particulate matter has to be suspended in an aqueous solution before a pH probe can be used measure the concentration of protons. When using water, it is known that there is a non-linear relationship between the pH measured and the solid:liquid ratio, and pH may drift towards equilibrium as ions are exchanged within the soil. In soils, using a solution of $CaCl_2$ is often used, Ca^{2+} is able to liberate H^+ bound to the surface of minerals and organic matter, and may give a much better representation of the amount of available protons. A 1:10 soil to water ratio is often used in standardised protocols, and is convenient for making comparisons between similar samples in soil science. Here, a simple 1:10 ratio of soil to DI water is used in order to make comparisons between samples of the same type. The dried artificial aggregates are added to the same mass:volume ratio of DI water and vortexed to ensure complete slaking was achieved. The use of electrochemical pH meters are also problematic in that these probes are designed to measure the H^+ in a solution containing no suspended solids. In these systems there is sufficient colloidal material, measurements of pH can be inaccurate or misleading, even in optically pure solutions, especially with low ionic concentrations. However, the pH readings made here were confirmed as best as possible using coloriometric tests using pH paper, which has been shown to be a better measure of pH containing suspended particulates or colloidal material. (*26*)

Kaolinite is naturally acidic in water. Studies have observed the pKa of silanols on the Si-face to have a pKa of 5.6 and the Al-OH edge sites to have a pKa of around 5.7. (*137*) These labile protons on edge sites are likely to be the source of kaolinite acidity. The pH of kaolinite in DI water was pH 4.76 (Figure 2.21, **A**), the addition of lignin reduced the pH linearly, with the beech lignin reducing the pH to a greater degree than the spruce lignin. This suggests that lignin is the stronger acid, or that small acidic fragments are present in the lignin, -COOH groups in lignin have a low pKa, around 4, whereas the phenol groups have much higher pKas above 8, and may be transferring protons to

the surface of the kaolinite [Al-OH + $H^+ \rightarrow$ Al-OH_2^+]. (*138*)

The pH is found to increase after the powders have formed a composite by drying and are then re-wetted and slaked (Figure 2.21, **B**). This occurs to the greatest extent with the pure kaolinite powders, suggesting that a simple wet/dry cycle is able to reduce the acidity of the kaolinite. The neutralisation could suggest the formation of water stable aggregates, which reduce some of the exposed acidic surface, or may be an artefact resulting from a lower particulate content in the supernatant. It is possible that face-face and edge-face interactions may trap H^+ in hydrogen bonding interactions. Adding lignin drops the acidity closer to that of the original pH. This suggests that acid sites are liberated once more from the kaolinite surface, possibly because beech lignin engages in interactions with kaolinite. Alternatively, it could be that the lignin acts a mild buffer and acid groups undergo greater dissociation without the kaolinite protons. Additionally, it is known that on drying, water molecules bound to the surfaces of minerals are further polarised and can become more acidic, and changes in pH have been observed before, in minerals after wetting and drying has occurred, although not for kaolinite.(*39*) Increased acidity may catalyse reactions at the kaolinite surface, which may change the nature of surface sites. The kaolinite fabric has been shown to be strongly affected by pH, with acidic pH resulting in weaker artificial aggregates. This means that lignin is not simply modifying the pH to strengthen the fabric, otherwise the aggregates would weaken.

2.10.1 Lignin solubility at raised pH

Lignin is an insoluble particulate material when added to water. Its properties as a suspension in water was investigated over the pH range 3 – 8 (Figure 2.22). At low pH both beech and spruce lignin forms an unstable suspension and tends to settle. At pH 3, it appears that lignin is isoelectric, with acidic groups remaining fully protonated. Raising the pH increases the suspension stability, with the zeta potential decreasing below - 60 mV. This is due to the deprotonation of acidic groups in the lignin. Increasing the pH further deprotonates the lignin and it begins to become soluble towards pH 7. At pH 6.62, the minimum zeta potentials were measured as -67.62 and -63.95 mV for beech and spruce lignin respectively, despite spruce lignin having a greater concentration of COOH and

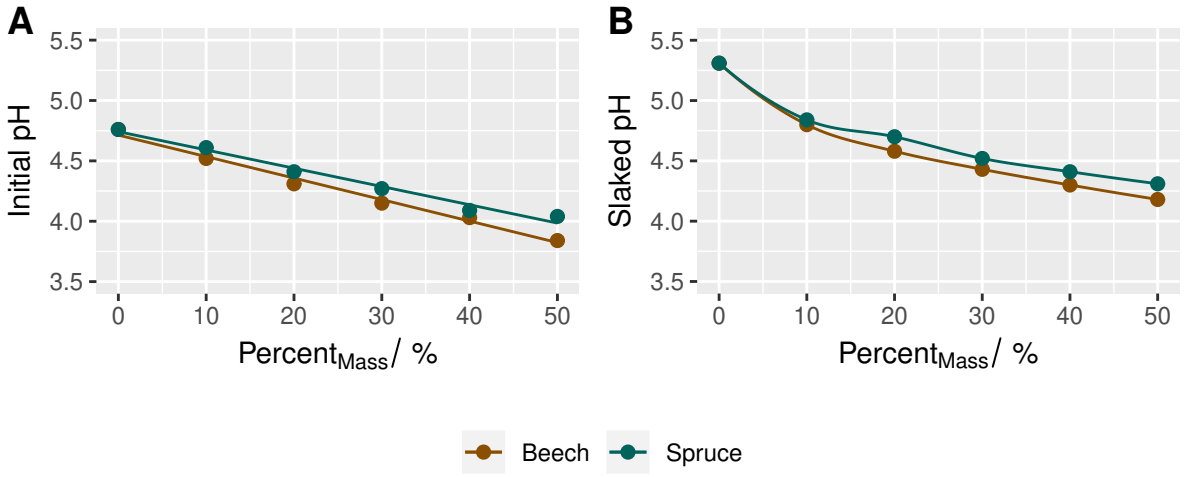

Figure 2.21: **A:** Initial pH of kaolinite:lignin powder mixtures with 1:10 solid, DI water mixture (mass ratio). Lines of fit for beech and spruce have $R^2 = 0.99$ and 0.98 respectively. **B:** The pH for artificial aggregates formed from these powders after crushing and slaking in DI water at the same 1:10 solid:water ratio. Lines are as guides to the eye only.

OH functionality. Zeta-potentials could not be measured over pH 7 because of partial dissolution of the lignin. It is likely that the change in zeta-potential is associated with a reorganisation and distribution of lignin macromolecules in the particulate solids. Studies have shown that increasing the pH gives rise to more complex particle size distribution. Soluble components may swell the particles and make them more gel like, or may be fully solvated in the solution. (*139*)

2.10.2 Lignin cohesion at increased pH

Both beech and spruce lignin could not form cohesive artificial aggregates strong enough to stay intact once recovered from the mould, over the entire pH range 3 – 8 investigated. As the pH increased, the artificial aggregates formed larger and larger internal voids within the mould on drying, indicating a densification of material at the walls of the mould. These voids are formed when lignin is dissolved and is re-precipitated as denser lignin at the edges of the mould. Despite the precipitation of dense lignin these artificial aggregates were still extremely brittle and relatively non-cohesive, something which is observed in lignin derived polymers and fibres. (*140*, *141*) Although it was not possible to form cohesive lignin aggregates at a variety of water contents, it was observed that the lignin fragments were harder at higher pH.

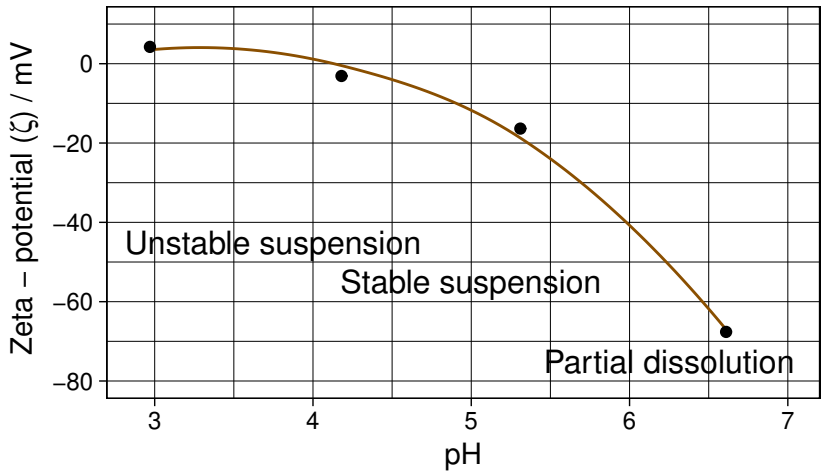

Figure 2.22: The zeta potential measured over a range of pH for beech organosolv lignin, measurements were made by adding NaOH from the initial solution which had a pH of 2.99. Lignin was measured as 5 g in 20 ml water. The zeta-potential goes from low when the suspensions are unstable, and become more negative as the pH is raised. Above pH 7, there is some partial lignin dissolution, towards pH 8, lignin appears to become largely soluble.

2.10.3 Lignin: Porosity, volume and mechanical strength of neutralised lignin aggregates

In order to test how the strength of the artificial aggregates was affected by pH, the kaolinite:lignin:water slurry was adjusted to pH 7 using NaOH. The slurry was observed to be less hydrophillic and had a lower water holding capacity forming a thinner slurry. The reduction in apparent water holding capacity is the result of the partial dissolution of lignin, which creates a lower solid:liquid ratio as well as the change in Atterberg limits of kaolinte. Initially pH 7 artificial aggregates made with 6.5 ml of water did not shrink as before, instead the artificial aggregates retained the dimensions of the mould, but a large void formed in the centre. Shrinkage suggests that the artificial aggregate is drying evenly throughout the artificial aggregate (all the particles try and retain water), a void suggests that the material dries quickly on the external edges, leaving the material on the inside to move to the edges, forming a void. This occurs due to the presence of soluble lignin in solution which precipitates before the remaining solid matter dries and the reduced water holding capacity of the clay. The neutralised solutions were instead freeze dried and remade with only 4 ml of DI water (instead of 6.5 ml) in order to form a complete set of artificial aggregates which formed no internal voids, but resulted in a higher solids loading per aggregate.

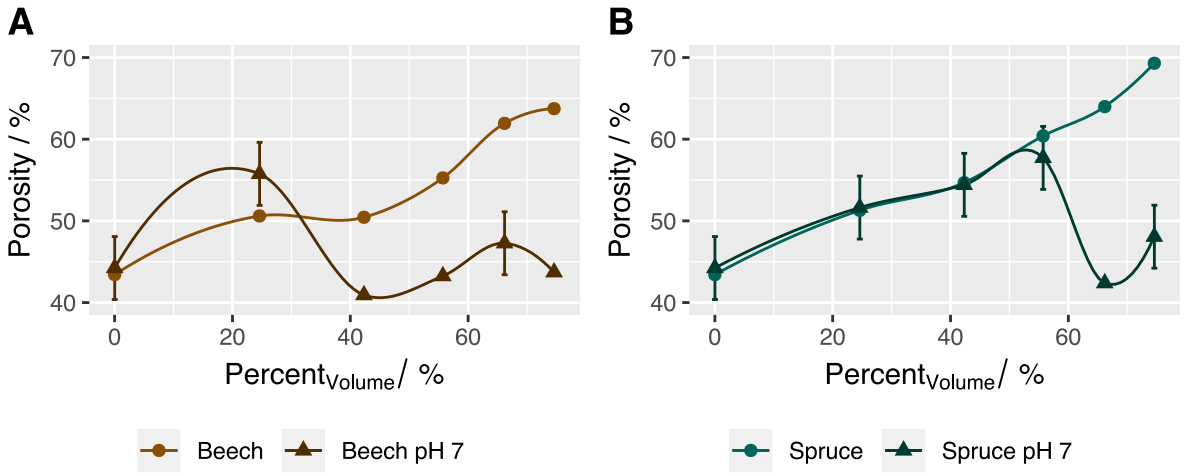

Figure 2.23: The porosity of both beech lignin (**A**) and spruce lignin (**B**) at low pH and neutral pH. Error bars represent one standard deviation from the mean, lines are a guide to the eye only. Errors were calculated using three repeats at a single representative volume loading.

The total porosity of the artificial aggregates remained high as before, $>$ 40 %, in a similar range to that of the low pH artificial aggregates (Figure 2.23). The initial porosities for beech and spruce were the same as the low pH artificial aggregates, despite the differences in initial water content and zeta potentials and the presence of soluble lignin. This indicates that porosity is dependent on the composition rather than the initial water content.

The porosity decreased dramatically for beech and spruce artificial aggregates at 30% and 50% volume loading respectively, which may be the result of soluble or more gel like lignin acting to fill the pores resulting in densification. However, if the reduction in porosity was caused by soluble material, there is no reason why this would not occur at lower loadings. This was tested, lignin was found to be more soluble at lower loadings, although the soluble component was always small (10% mass). Alternatively, the drop-in porosity is a result of overly concentrated suspensions which force particles into close proximity whilst wet (consolidation). In the wet pastes, the higher loadings contain a much higher volume loading of material, due to the low density of lignin and the gel-like lignins are compressed on drying. At this pH range, both the kaolinite and lignin reach a minimum (most negative) in the zeta potential, and electrostatic repulsion is strong, and so a dispersed and porous sediment is expected. The large change in porosity must be due to a change in the lignin morphology.

There were significant changes in the mechanical properties of the artificial aggregates with the

neutralisation of the composite mixtures (Figure 2.24). However, in the initial volume loadings where porosity was comparable, the mechanical strengths were very similar for beech and increased for spruce. Neutralised beech lignin artificial aggregates reached a maxima at 55% volume loading, 10% higher than the acidic artificial aggregates. This is the result of the reduced porosity which effectively extends the amount of lignin which can be added before the percolation threshold is reached. The spruce lignin artificial aggregates appeared to have a maxima at low loadings (25% volume loading) and an additional maxima at loadings above 50%. The second maxima corresponds to the large reduction in porosity. The toughness and modulus mirrored the increase in strength.

Low pH artificial aggregates made with a reduced water content (4 ml) were found to have increased strength in comparison to those made at higher water contents due to a higher solids loading, resulting in a lower porosity (Figure 2.25). The pastes formed at this low water content were not ideal, and did not flow well into the moulds. Despite this, the low pH composites were still reduced in strength in comparison to the neutralised lignin:kaolinite composites. The increase in strength is therefore a result of an increased binding interaction and possibly a greater clay surface area of due to a change in fabric morphology, or partially soluble lignin particles. Newcomb et. al. reported high binding strengths of COO- groups with a negatively charged basal mica surface, although these were significantly increased in strength at lower pH. It is possible that the increase in pH provides more deprotonated functionality on the lignin to bind to clay surfaces.. The type of binding interaction investigated by AFM studies may not represent interactions that could feasibly occur at surfaces, inner-sphere coordination with small molecules may not occur on particle surfaces, and other sphere interactions are more favourable at increased pH. Edge sites play a greater role here also, and these sites are neglected from these AFM studies.

The effect of pH is multifaceted with lignin composites. Firstly, the increase in pH results in a stronger kaolinite component. For beech lignin there is a well-defined maxima slightly above 50% volume beech. The reduction in porosity allows this peak to extend to over 40% volume, the maxima observed with the acidic composites because a reduction in porosity means an increase in the percolation threshold for lignin loading. The beech lignin composites are extremely strong, demonstrating the effectiveness of lignin as a cementing agent. This may be the result of a soluble component, which softens the lignin edges and allows lignin to adhere to clay with a greater surface

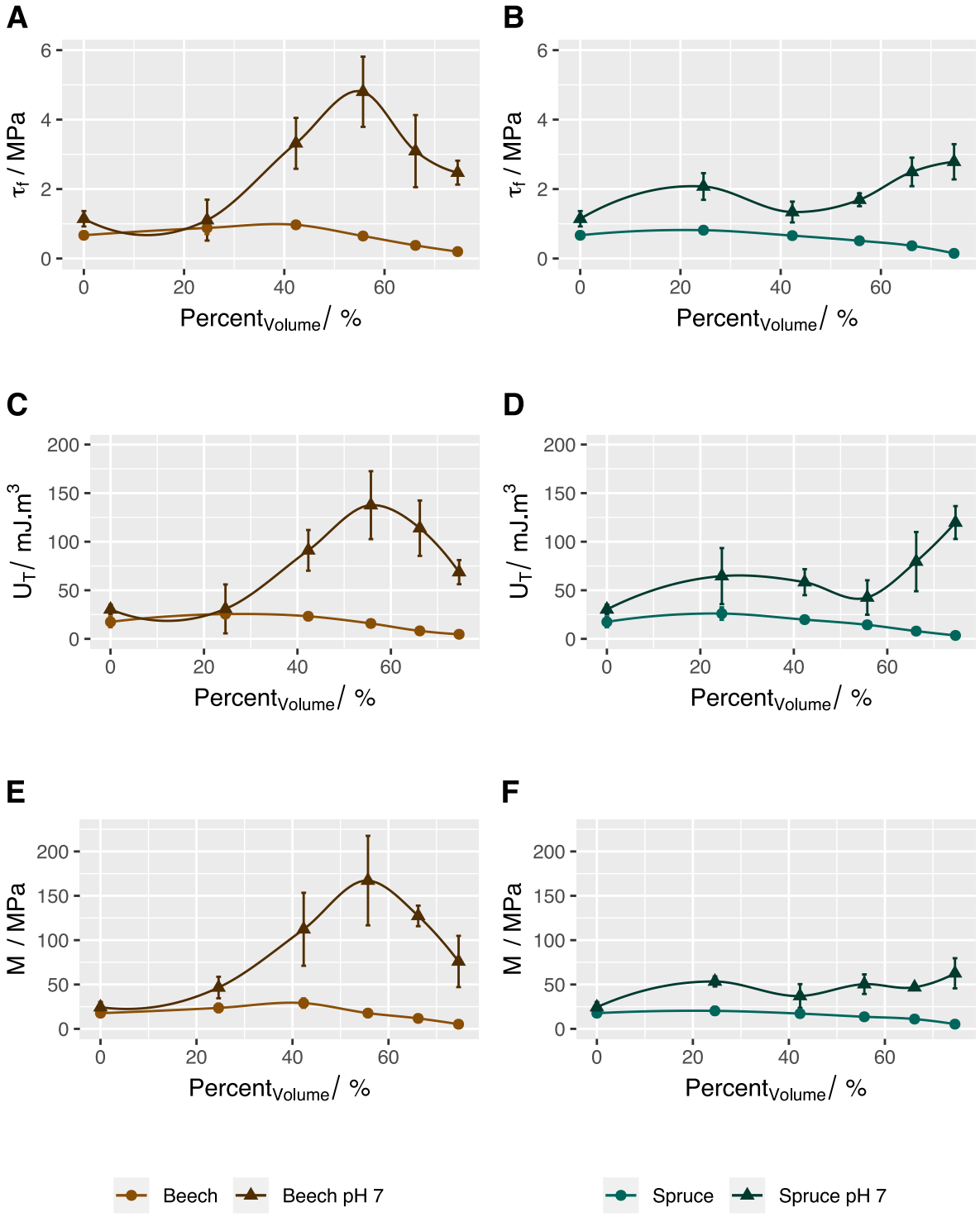

Figure 2.24: The strength, toughness and modulus for beech (**A,C,E**) and for spruce (**B,D,F**) organosolv lignin as added to kaolinite. The strength of the artificial aggregates increased dramatically on neutralisation due to the formation of a soluble, or gel-like component. Neutral artificial aggregates are around 5 times stronger than the low pH artificial aggregates, however the effect of initial water content is considerable. The addition of lignin creates stronger artificial aggregates at all volume loadings, despite 100% lignin artificial aggregates forming weak and brittle composites. Lines are guides to the eye only, error bars represent one standard deviation (n = 3-5).

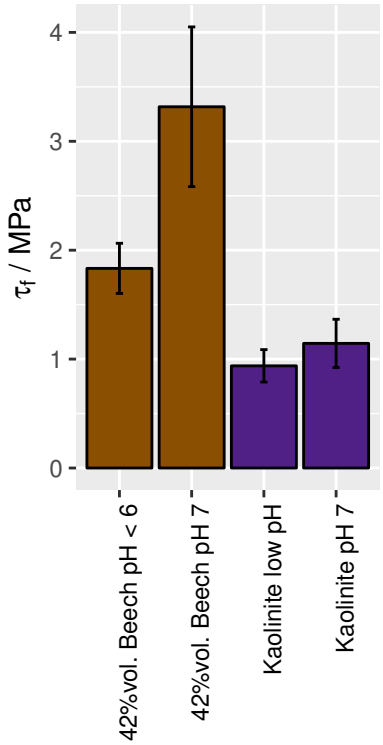

Figure 2.25: A comparison of the mechanical strength of pure kaolinite and 42% volume beech lignin cubes made pH 7 and pH 4.5 made with the same initial water content. pH 7 aggregates were stronger, although the difference was smaller once the initial water content had been corrected.

area. Studies on lignite particles have shown that pH increases can release small soluble molecules, and reduce the particle size of the insoluble ligninite. (*142*) This may increase the binding strength by enhancing the surface area available for interactions with kaolinite. The soluble component of beech lignin was determined by HSQC NMR and found to have less aromatic character than the bulk lignin and contained more β-O-4' linkages and fewer -MeO side groups. This suggests that relatively unmodified lignin fragments constitute the soluble component, with more crosslinked aromatic residues remaining undissolved. (See A.1.5)

Studies on the binding of organic matter at different solution pH have observed that adsorption of humic acids decreases with increasing pH although increased adsorption of humic acids at alkaline pH have been observed and attributed to hydrophobic interactions (*19*). This does not necessarily correlate with observations made with mixed composites, whereby van-der-Walls interactions occurring on larger surfaces and hydrogen-bonding interactions dominate short range interactions. It is therefore be unwise to compare the clay interactions of insoluble organic residues with soluble

materials dissolved in suspension. However, soluble lignins liberated at pH 7 may strongly interact with kaolinite surfaces.

2.11 The role of dissolved organic matter in particulate interactions

In soil, dissolved organic substances are continuously being generated and consumed, and during wet/dry cycles they may contribute to the strength of aggregates. Reported concentrations of DOC in soils vary greatly with soil type and sampling depth, seasonal factors and the methodology used. However, generally concentrations in soil water are reported as being between 1 to 100 mgL^{-1} in temperate soils. (*143*, *144*) Humic and fulvic acids are historical terms used to describe fractions of organic matter distinguished only by solubility at different pHs. These operationally defined fractions are used less and less. A predominant portion of the soluble soil organic matter may be exudates from plants, fungi and bacteria, residues from larger soil invertebrates as well as soluble residues from decomposition processes. These exudates have been shown to effect soil mechanical properties and aggregation. (*145*)

The role of humic acids on the mechanical properties of kaolinite and a composite containing 42% volume beech lignin was compared, using a saturated humic acid solution, applied at different dilutions. Humic acids were shown to increase the strength and toughness of a lignin:kaolinite composite, increasing linearly with the concentration of humic acid added (Figure 2.26, **A, B**). Humic acids were also found to increase the strength of kaolinite artificial aggregates before they weakened again, and toughness remained constant. Due to the method used to dissolve humic acids, these aggregates contained some dissolved NaCl, which makes comparisons with other studies in this section problematic.

The role of soluble organic matter is likely to be as important as soluble species can modify surface charge and chemistry of clays and particulates. Adding humic acids to kaolinite resulted in no change toughness but a change in strength, which is consistent with a change in the fabric of the

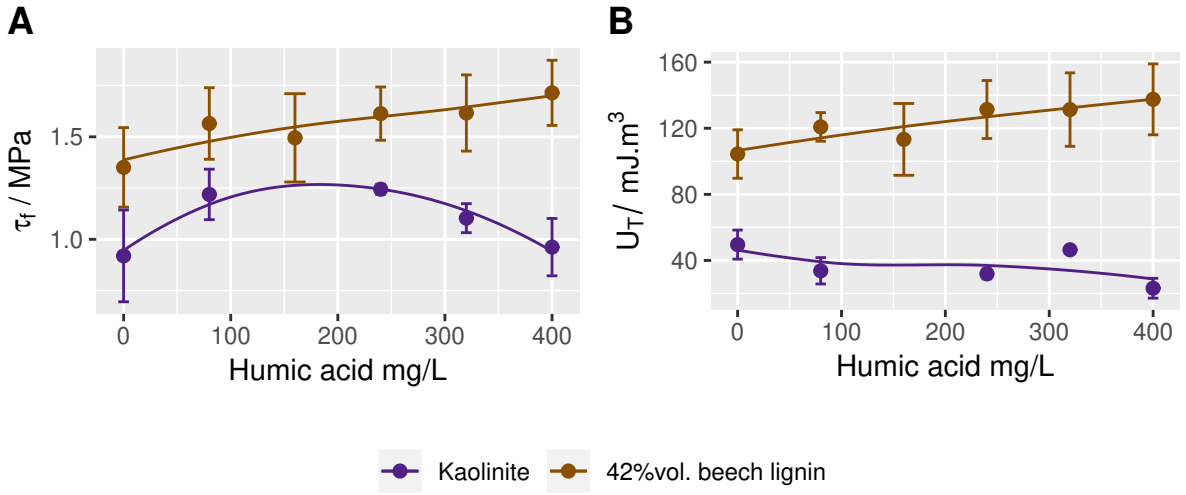

Figure 2.26: The mechanical properties of kaolinite and lignin amended aggregates, with the addition of a commercial humic acid. **A:** Humic acids increased the strength of a 42% beech lignin composite, more complex behaviour was observed with kaolinite artificial aggregates, strength increased to a maxima at intermediate humic acid loading, decreasing again at higher loadings. **B:** The toughness increased with the increase in strength for composites containing lignin. However, no increase in strength was observed for the kaolinite. A background electrolyte of 0.1 M NaCl was used to maintain the salinity of the neutralised humic acid. The humic acid concentrations reported here are not accurate, as some material was found to be insoluble. Lines are linear or polynomial fits, errors are standard deviations (n=3-4)

kaolinite. With increasing humic acid concentrations, the strength may increase because silica-face, alumina-face interactions are disrupted by adsorption of humic acids on the faces, resulting in an increase in edge-face interactions observed at higher pH values and a more open structure. Further addition of humic acid may disrupt stronger hydrogen bonding interactions between the clay surfaces, resulting in a weakening of the fabric. Material precipitating on the clay surfaces on drying may act as a slippery lubricant, creating a softer clay fabric. The mechanism of strengthening for the kaolinite:lignin composites is likely to be complex. Humic acids may decrease the pH of the composites neutralising lignin surface charge. Alternatively, humic acids may enhance binding by adsorbing to the clay surface, or act as a plasticizer which modifies the surface stickiness of the lignin particles. Determining the exact mechanism of strengthening is a substantial technical challenge, requiring an understanding of the partitioning of the dissolved organic matter between clay surfaces, precipitates and additive (lignin). Despite the potential for humic acid to bind to surfaces and disrupt particulate interactions, modest changes in strength are observed. This demonstrates that despite the presence of a saturated humic acid solution, the particulates determine the mechanical properties of the aggregate.

2.12 Bentonite

Bentonite:lignin artificial aggregates showed strong shrink-swell behaviour, on drying the moist pastes shrank significantly forming small dense aggregates. The aggregates were not significantly thinner in any dimension and shrunk evenly forming more voluminous cubes as the lignin was added, the volume increased almost linearly with lignin loading (Figure 2.27, **A**). This suggests drying occurred uniformly from all surfaces and that the formation of an initial sediment was unlikely. Pure bentonite aggregates were not able to form a cohesive solid, instead forming hard but flaky materials, which broke apart on removal from the mould. The flakey structures are indicative of face-face interactions which form a continuous fabric. The porosity increased linearly with lignin loading (Figure 2.27, **B**). The initial porosity was considerably lower for bentonite, extrapolation suggests that a pure bentonite clay has no internal porosity on drying, in stark contrast to kaolinite which has an initial porosity of 40%. The increase in porosity for kaolinite:lignin is less than that for bentonite:lignin mixtures (porosity increases 23% over 50% mass loading (75% volume loading) for kaolinite; porosity increases 35% over 50% mass loading (72% volume loading) for bentonite. This might indicate that lignin is able to interact more strongly with the kaolinite, possibly due to the alumina faces, with higher hydrogen bonding potential.

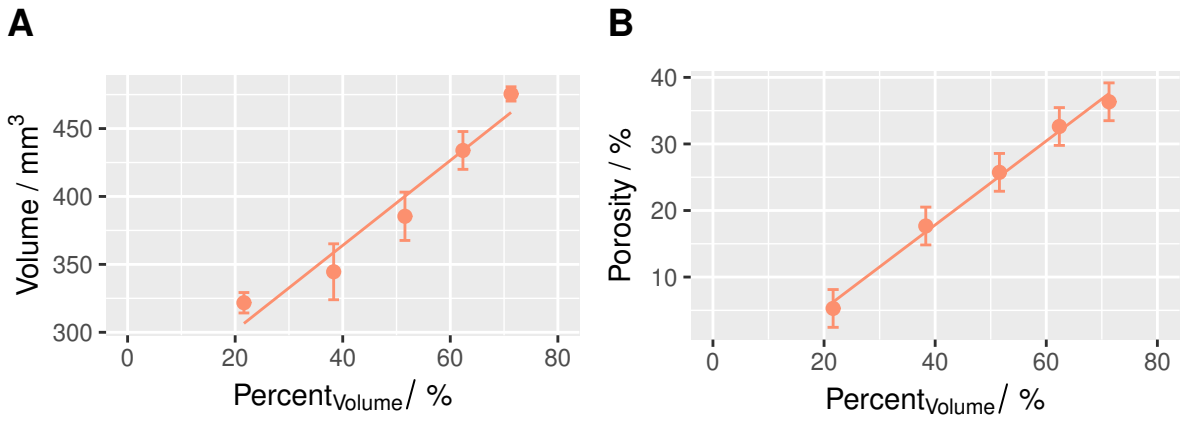

Figure 2.27: **A:** The increase in total volume of the artificial aggregates as the percentage of lignin within the composite is increased. This can be attributed to an increase in porosity. **B:** The increase in porosity as the volume loading of lignin is increased. A solid bentonite aggregate could not be made at this water content, but is likely that it would contain no internal porosity if formed. This means that all the porosity present is porosity within the lignin particles or pores created between bentonite and lignin. Lines are linear fits, error bars are standard deviation (n = 4-5)

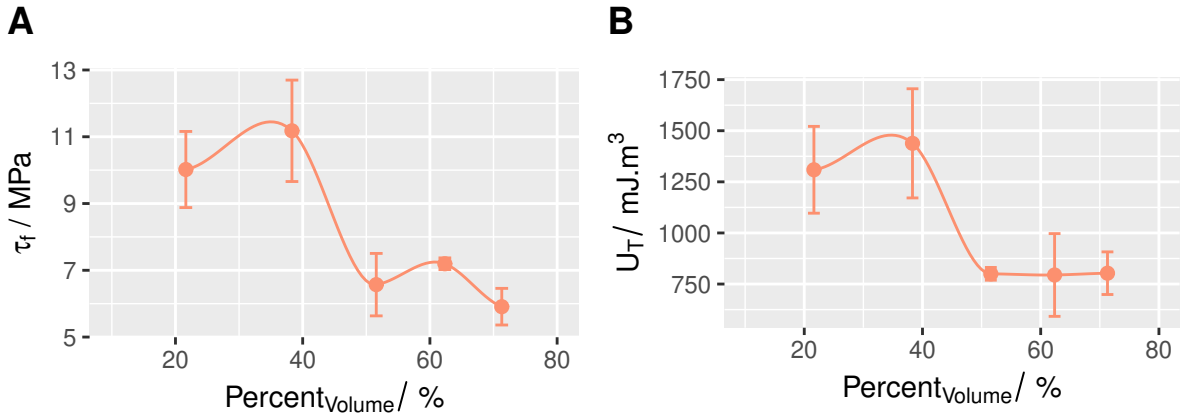

Figure 2.28: The mechanical properties of bentonite artificial aggregates amended with beech lignin. The strength of the lignin:bentonite composites was high. Since pure bentonite aggregates could not be formed, it is difficult to determine if the amendment results in a strengthening of the cube. **A:** Strength decreases around 50% volume beech lignin, corresponding to a percolation threshold. **B:** The toughness followed the trend observed with the strength data. The overall strength and toughness was an order of magnitude greater than that of kaolinite composites. Lines are guide to the eye only, error bars represent standard deviation (n = 4-5)

Bentonite contains predominantly montmorillonite, a 2:1 clay. 2:1 clays have only exposed silica faces, resulting in a reduced pH dependent behaviour with only edge sites responding significantly to pH change. Without knowing the strength of a pure bentonite cube, it is not clear if the maxima at 40% volume loading corresponds to a strengthened composite (Figure 2.28, **A**). It is clear that at lower loadings, the aggregates retain the strength of bentonite (lignin dispersed in clay). At 40% beech lignin loading, the total volume of pore space and lignin is around 60% of the total volume of the artificial aggregate, which leads to significant weakening. The strengthening observed between 20-40% volume loading is likely to be due to a disruption of the edge-edge bentonite interactions which form flat ribbon-like structures and may be very brittle, lignin may act as a filler, reducing the brittleness of the composite. SEM images could not be used to differentiate between areas rich in lignin or clay, to observe the mixing. The bentonite platelets and globular particles of lignin were not easy to distinguish from each other (see Appendix).

2.13 Quartz silt

Quartz silt is non-cohesive on wetting and drying, low loadings of lignin increased the stability of dried artificial aggregates but they appeared to phase separate despite excessive mixing of dry and wet powders, forming a lignin-rich and lignin-poor layer. Phase separation is likely to be driven by a difference in density, exacerbated by poor silica-lignin binding often called segregation in the granulation theory. 50% mass lignin blends were semi-stable. At point of failure, the maximum stress was of 0.08 ± 0.03 MPa, 50% lignin may correspond to quartz silt dispersed in a lignin phase, other lignin-silt composites were brittle and fell apart on extraction from the mould. This data suggests a large increase in mechanical strength due to lignin-silica surface is unlikely, although a weak interaction is possible.

2.14 Discussion

Uni-axial compression tests have not been used previously to determine interactions between particles, because soil aggregates are heterogeneous and the compressive strength is dependent both on aggregate shape and internal porosity. (*80*, *100*) These variables cannot be controlled in real soils. This study uses artificial aggregates to determine interactions, and uses moulds to form aggregates of uniform shape and size. Additionally, since the artificial soils are made from a simple mix of one or two particulates the effects which are observed can only be prescribed to differences in the particle-particle interactions. It is important to vary the loading in two particulate systems, because the line shape is indicative of the interaction occurring between particulates. This is not always carried out in composite science, for example concrete testing, because of the difficulty in making multiple repeats of varying loadings.

There was some difficulty in measuring any modulus measurements from the initial stress/strain curves. This was because of the cube shape of the aggregate, which tend to have a higher density of microcracks, and the edges may become spalled, before the formation of a strong central columnar crack which leads to failure. These lateral cracks appear on the stress-strain curves which mask the

shape of the initial curve. This has been observed in concrete samples, cylindrical specimens may be a better shape for further study, providing the aggregates can be formed to reach similar sizes in the height dimension(*146*). This failure behaviour was observed in all specimens, and the failure mechanism is likely to be identical in these cases.

The micro-structure that forms when particles of kaolinite interact are generally studied as a kaolinite suspension or viscous slurry (*16*, *147*). Measurements of particle size and viscosity are common, and the micro-structure is not generally studied in the solid form, unless by SEM or X-ray techniques (*16*, *128*). Previous studies, on drained and undrained tri-axial testing of consolidated kaolinite indicated a role for the micro-structure formed in suspension. They found that that dispersed kaolinite was stronger under undrained tests, but dispersed and flocculated kaolinite displayed similar shear strength under drained conditions. Direct shear tests showed that the flocculated samples had higher strength, which agrees with the findings of the experiments on dry kaolinite aggregates. (*28*) Experiments such as these verified the findings of these experiments, but this may be the first time that dry kaolinite has been used, as saturated samples are generally used in civil engineering experiments.

The interactions of HDPE with clays is relevant also to the field of microplastics. The improper disposal of plastics has resulted in the formation and distribution of microplastics in both aqueous environments and in soils (*148*). The microplastics are likely to interact with minerals in both environments, and the persistence of microplastics relates to the ability to bind and adhere to surfaces. (*149*, *150*) From this study, it is likely that microplastics do not interact strongly in dry conditions, unless the surfaces are modified, likely oxidised to include hydrogen bonding functionality.

2.15 Conclusions: Part I

2.15.1 Methodology

Mechanical strength testing of artificial aggregates may be a useful tool to determine inter-particle interactions and the role of surface chemistry in clay-rich aggregates, it may also be a useful method-

ology for determining the effects of particulate soil amendments on aggregation. The measurement of the mechanical properties over a range of additive loadings allows for the determination of the percolation threshold and the increase in strength per volume (or mass) added, which could not be determined by measuring a single loading. Forming artificial aggregates using silicone moulds with no compressive forces acting on the wet pastes allows for porosity to form which more closely replicates that which may be formed in natural systems. However, initial water content has to be changed and optimised to produce a workable paste for each additive. A careful balance between mass loadings which are too small, resulting in the formation of voids, or mass loadings which is too high, resulting in dry, unworkable pastes which retain air pockets has to be found in order to produce artificial aggregates. Further work is required to find alternative methodologies to form artificial aggregates under more comparable conditions, or to introduce a factor which can correct for differences in water content to make measurements carried out at different initial water contents more directly comparable.

The compressive strength of a material is only one of the variables that can be extracted from measurements of stress versus strain in a compressive strength test. In composite science, the modulus is often used. However, soil aggregates are brittle and the elastic strain is practically non-existent in most cases. Here the 'modulus (M)' is used to quantify a pseudo-linear region which represents plastic deformation and is used as a measure of the brittleness. A linear region was not always observed, with experimental noise originating from fracturing adding additional uncertainty to the measurements. Toughness, is another useful indicator, and is a measurement of energy/volume. The strength at compressive failure was found to be more indicative of changes in material fabric, with smaller errors between measurements. Often strength and toughness were considered in conjunction, in order to indicate changes in fabric without changes in the type of binding interactions for example. It was hoped that changes in the surface chemistry of the particles, or the particle size may result in clear changes in either strength, toughness or modulus, but this was not observed.

2.15.2 Kaolinite

The mechanical properties of dry kaolinite was found to change in response to changing pH. This was due to a change in the fabric formed on drying, which is determined by the settling behaviour of the kaolinite particles. Electrostatic forces determine the arrangement of kaolinite particles in the drying sediment, and as water is removed, these forces are overcome, and particles remain more or less fixed in their sediment configuration. The change in pH modified the artificial aggregates Atterberg limits, and the dry artificial aggregates were remarkably different in volume, strength and modulus. As the pH increased from pH 4 – 6, there was a significant increase in stiffness and shear strength, above pH 6, the kaolinite properties remain constant. Despite large changes in strength and modulus, the change in toughness was relatively modest. This suggests that the kaolinite fabric becomes more brittle but increasingly strong as pH increases, but that the energy required to fracture the artificial aggregate remains the same. This is because the fabric retains a similar amount of bonding interactions which are of mixed Van-der-Walls/hydrogen bonding type, and that the changes in mechanical properties are largely due to particle arrangement, rather than a large change in the type or number of interparticle (or inter-tactoid) interactions. At acidic pH the kaolinite forms tactoids, due to the formation of face-face stacking type interactions, which results in a dense, low porosity solid. As pH increases, the formation of edge-face interactions (which are stronger than face-face or edge-edge type interactions) is promoted, and a more open network of particles is assumed. These structures are strong but brittle, owing to the small contact area between particulates and the porous structure. At high pH, the kaolinite particles have high electrostatic repulsion, which forms a dispersed sediment. The surface area and total contact area between particles is maximised, contains large number of edge-face interactions and porosity increases, resulting in a strong but brittle kaolinite artificial aggregate. The change in Atterberg limits is likely due to the neutralisation of the alumina face and edge, which is the origin of kaolinite hydrophilicity. At low pH this face is charged and as a result, holds much more water. Critically, the fabric and inter-particle packing and bonding interactions has greater control on the mechanical properties than volume, or porosity. It is also indicated that electrostatic interactions are important in that they modify the sediment and the dry particle orientation. No evidence that electrostatic interactions contribute to the strength of dry solids was found, as kaolinite formed a strong solid when particles maximised electrostatic repulsion

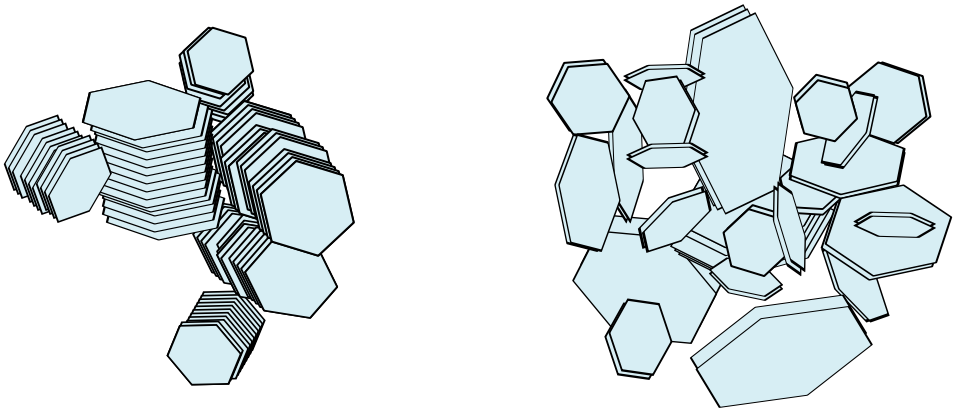

Figure 2.29: At low pH, kaolinite forms blocky tactoids with low adhesion between tactoids (left). On raising the pH, the platelets form a more open structure with longer range connectivity (right).

(high pH). In dry kaolinite, the predominant interactions are likely to be mixed van-der-Walls and hydrogen bonding.

2.15.3 HDPE

HDPE was used to identify the role of particle size and surface chemistry on the mechanical properties of dried clay-HDPE composites. HDPE particles were significantly larger than the clay particles and the influence of electrostatic interactions in the wet phase is likely to be reduced as HDPE does not form a suspension. Although HDPE is not part of natural ecosystems, microplastics are increasingly common in soils, and the interaction of these materials with clays is not understood. The mechanical strength, toughness and modulus was strongly affected by the surface chemistry of the particles, and to a minor extent the porosity present within the composites. The addition of unmodified HDPE particles resulted in a weakening of the artificial aggregates, which weakened in proportion to the volume of HDPE added to the clay. Modified HDPE formed strong artificial aggregates, owing to the presence of carboxylic and hydrogen bonding type functionality, present on the surface of the HDPE particles.

With the modified artificial aggregates, a percolation threshold was observed, corresponding to a large decrease in strength. This is due to the formation of continuous large network of pore space and HDPE particles which substantially weakens the artificial aggregate. The percolation threshold was also observed in the porosity data, corresponding to a sudden increase in porosity

as interstitial space between particles was no longer filled by kaolinite. An attempt was made at quantifying the strengthening effect per surface area of HDPE added, values between 0.18 - 0.36 MPa/m^2 were obtained, but a size dependence was indicated. Determining a quantitative measure of binding strength from these experiments, is not technically feasible, since the fabric morphology is changeable, and the effect of porosity and contact area adds additional variability.

2.15.4 Lignin

Two types of technical 'organosolv' lignin extracted from beech or spruce wood was tested. Porosity in lignin:kaolinite composites was large and increases by around 25% over the range tested. Beech lignin has low inherent porosity, and so this pore space may exist between aggregates and is created on forming the aggregates. SEM showed that materials had not separated into large distinct phases. The large porosity may be related to the sedimentation behaviour, both kaolinite and lignin particles are negatively charged, electrostatic repulsion in solution may form a fabric with large porosity. This could also be the result of very different particle morphologies. Despite the large increase in porosity, the addition of lignin increased the strength of the composites until the percolation threshold was reached. This shows that lignin is clearly able to strengthen the kaolinite acting as a cementing agent. Beech lignin was found to form stronger composites than spruce lignin due to the reduced porosity of the beech lignin composites, and the extension of the percolation threshold. It is likely that beech and spruce had very similar binding as the increase in strength/surface area added was equivalent at lower loadings.

The mechanism of binding is not completely clear. It appears that solid lignin preferentially binds to silica faces, which contain fewer hydroxide groups, and are more hydrophobic. Lignin contains phenol, hydroxyl and carboxylic acid functionality, and so the preference for the silica face is not due to a lack of hydrogen bonding interactions. Instead, hydrophobic interactions which form in solution may orientate silica faces towards more hydrophobic surfaces on the lignin, and these interactions strengthen on drying (Figure 2.30).

Increasing the pH of the lignin:kaolinite artificial aggregates resulted in partial lignin dissolution, and

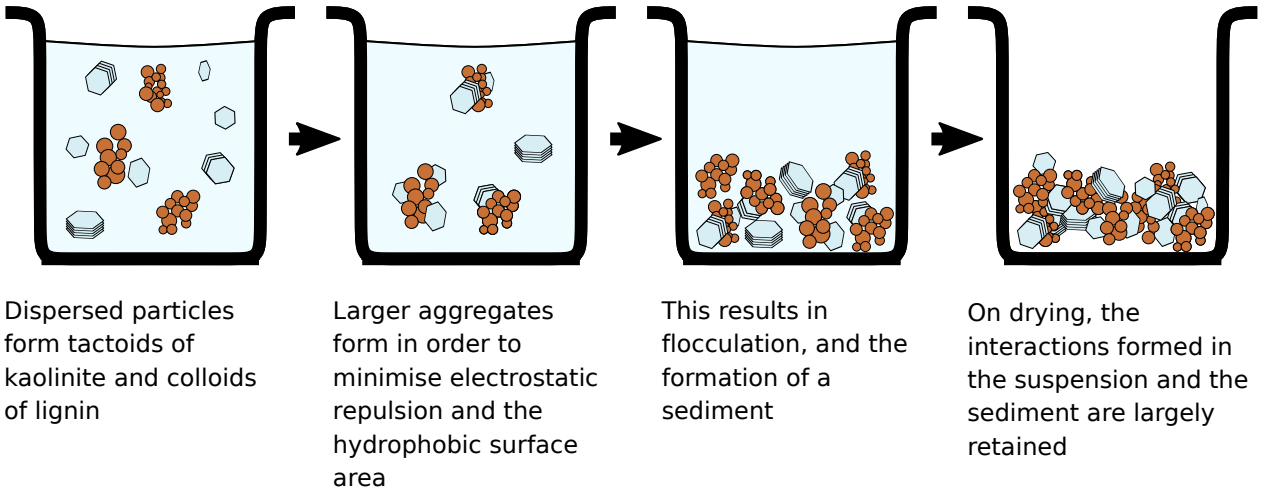

Figure 2.30: The formation of an artificial aggregate is influenced by the interactions which form in the suspension, which are retained in the sediment and may also be retained in the dry solid.

the particle size of the insoluble lignin may have decreased as a result. The soluble component can also act to soften the edges of lignin particles increasing the contact area between particles. Increasing the pH resulted in an increase in both the kaolinite and kaolinite:lignin composites mechanical strength, toughness and modulus. A large increase in strength was a result of a sudden reduction in porosity, observed for both beech and spruce at different loadings. No evidence could be found for the role of electrostatic interactions in the solution phase, although the zeta-potential of lignin reaches a minima (negative zeta) at pH 7, which would result in a very well dispersed kaolinite-lignin suspension and potentially a very porous composite.

2.15.5 Bentonite and silt

Both bentonite and quartz-silt contain exposed silica surfaces. Quartz-silt was non cohesive, and artificial aggregates could not be formed. Bentonite is a 2:1 swelling clay and on drying forms exceedingly strong composites with lignin. However, the mechanical properties of pure bentonite aggregates could not be determined because the fabric of pure bentonite formed thin brittle ribbons. The increase in strength with lignin is likely to be the result of stabilising the bentonite fabric, rather than an increase in inter particle interactions. However, since lignin has been shown to bind to the silica face, it is possible that lignin is acting as a glue in this case.

2.15.6 Electolyte

Increasing the electrolyte concentration of the solutions used to make artificial aggregates resulted in some changes to the mechanical behaviour. The indifferent electrolyte NaCl, did not change the properties of a kaolinite aggregate, evidence that at low pH, electrostatic interactions do not contribute greatly to fabric formation. $CaCl_2$ however, increased the strength of kaolinite aggregates. $CaCl_2$ bind strongly to the surface of kaolinite and effect changes in the sedimentation behaviour. Rapid flocculation may result in a more open structure and promoting more edge-face type interactions which are stronger than face-face type interactions, and result in a larger continuous fabric of connected particles. $CaCl_2$ may also promote edge-face interactions by modifying the surface charge. The addition of $CaCl_2$ does not increase the strength of lignin: kaolinite artificial aggregates. The formation of calcium bridging type interactions are known to occur between soluble organic matter and clay surfaces. Calcium bridging type interactions of the type clay – Ca^{2+} – COO^{-} are unstable without water, and so in dry solids, may not influence the strength of inter-particle interactions. It is possible that $CaCl_2$ enhances phase separation in the aggregates via increasing flocculation of the kaolinite and lignin.

2.15.7 Humic acids

Humic acids were shown to increase the strength of pure kaolinite artificial aggregates via a modification of the kaolinite fabric, consistent with a change in strength and not toughness. Disruption of the kaolinite face-face interaction observed at low pH results in the formation of a more open kaolinite fabric, which is observed to be stronger, due to the formation of more edge-face interactions. Continued addition of humic acids resulted in aggregate weakening, this is thought to be due to the precipitation of humic acids on the clay surfaces, disrupting the kaolinite fabric and forming a more slippery inter-grain boundary. The mechanism resulting in the increase in mechanical strength and toughness for lignin:kaolinite composites is likely to be complex. However, humic acids may act as a plasticiser, softening the lignin edges, or binding to alumina surfaces, creating an organic layer which more favourably interact with lignin particles.

Chapter 3

Artificial Aggregates II: Interactions of Cellulose, Biochar and Wood Fragments with Kaolinite

3.1 Introduction

In the following chapter, the interactions of kaolinite with cellulose, biochar and wood are investigated. Interactions between clays and various particulates, in particular cellulose, are not only important in soils, but in materials such as paper and tablets for pharmaceutical applications. Within formulation science, materials such as cellulose and calcium carbonates, are studied in order to form stable pellets for drug delivery. (*92*) In order to form strong interactions between particulates in the formation of tablets, mixtures are often compressed and then consolidated. Compression involves the reduction of pore space and the rearrangement of particles by the application of pressure. Further compressive forces are then applied to consolidate the material, in this case the particles form stronger interactions and the particles are deformed in order to maximise the surface area between them. Binders are also used, which reduce the need for consolidation and reduce tablet forming pressures. There are a number of overlaps between compression physics in formulation science and soil science. For example, both reference the formation of secondary aggregates from primary par-

ticles, and the formation of macromolecular structures from these secondary particles. Additionally, the often soluble drug molecules are also known to effect the tableting behaviour, and these studies may inform further studies on particulate-dissolved organic matter interactions. (*92*)

Kaolinite is often used as a cheap 'filler' additive in mixtures and materials, but is also added to improve the smoothness of films and process ability of materials. It is also an environmentally innocuous material which can be incorporated easily into new sustainable materials. New materials from cellulose nanofibrils are being developed for biomedical applications, coatings and barriers for packaging. Nano-cellulose is a potentially abundant material, with low environmental impact on disposal, and has interesting mechanical and barrier properties. It is also relatively expensive to make, and so kaolinite is of interest as a filler additive to reduce the cost of these new materials. (*151*, *152*) Adding kaolinite does have benefits however, and cellulose-clay composites, and nano-structured composites containing cellulose, clay and a polymer are under investigation for advanced flame-retardant coatings, printed electronics and biocomposites. (*152*, *153*) In order to create strong interactions between the two components, an additive is often added, or surface properties of the clay or cellulose are modified. There is low cohesion between the clay and cellulose, which reduces the superior mechanical properties of nano-clay films considerably.

Particulate composites such as those found in paints and coatings, consist of solids dispersed in a polymer matrix. These systems provide a simple system on which to test structure-function relationships and have been studied in detail. Alumina trihydrate particles dispersed within poly(methyl methacrylate), have been used to predict relationships between microstructure and physical properties. (*154*) The microstructure formed between the two components was investigated using SEM and image analysis to identify the volume distribution of each component in the matrix. This analysis was used to predict crack formation, elastic modulus and failure strength via computational modelling. In composites such as these, non-bonding particles can be considered to be large voids, which cause the formation of cracks on bending the matrix. If bonding occurs between the components, larger strains are required for the formation of cracks. Smaller particles create larger interfaces, but can agglomerate and form weak points. The applicability of this method to complex systems such as soils, with high porosity and pore size distribution is not clear. Additionally, the method requires well defined regions and phase transitions to be clearly identified by SEM. It is not clear if a mixed

particulate system could be treated in the same way, with one (smaller clay particles) component considered analogous to the PMMA phase.

3.1.1 Cellulose

Cellulose is the major component of plant materials, and residues contain around 16 – 30 % cellulose, this means a good proportion of the litter which is deposited on the topsoil contains cellulosic residues. (*116*) Cellulose is a polysaccharide, a linear glucose homopolymer joined in chains by β – 1,4 glycosidic bonds. These long polymer chains form highly aligned and rigid crystalline structures held together by inter-chain hydrogen bonds. These structures are known as microfibrils. Only the C6 of the glucose monomer, CH_2-OH, are exposed from the plane of the crystal, which makes the surface only mildly hydrophilic. (*155*, *156*) Despite this, cellulose is quickly metabolised and has been shown to be one of the most transient materials present in soils. (*156*) Residues or amendments with high cellulose contents are responsible for a phenomenon known as 'priming' when added to soil. Priming is the observed decrease in soil organic matter caused by the rapid production of bacterial enzymes which occur after the addition of an easily metabolised carbon source. The increase in available sugar brings about a race for other nutrients which are mined from more recalcitrant substances to meet nitrogen and mineral requirements of soil biota. (*157*) This is not to say that there is no role for cellulose in the formation of aggregates, cellulose is known to be found in larger aggregates as POM or intact plant residues. (*158*) The physical form of natural cellulose from plant litter origin found in soils is unknown, but likely to be as shortened or broken fibres, associated with some xylose and lignin. (*159*) Soil carbohydrate analysis is usually carried out following a hydrolysis step using strong acid, the hydrolysis breaks down the carbohydrates and they are quantified and characterised using HPLC techniques. (*160*) This breakdown prevents the size of the carbohydrates present in soil to be determined. Extracellular enzymes may help degrade or reduce the crystallinity of the cellulose. It has been thought that cellulose microfibrils around 10 – 20 nm across (Spruce wood) are thought to be coated by a hemi-cellulose (xylan) and lignin coating, which imparts further structural stability and resistance to biological attack. (*161*, *162*) However, recent evidence has suggested that cellulose may be more structurally separate (at least in non-woody plants) and bound

to lignin via a xylose bridge. (*112*) This could suggest that both lignin rich and cellulose rich residues may be easily formed in soils. Cellulose is not often employed as a soil additive. Cellulose rich waste materials such as cotton or paper are discouraged for a variety of reasons, paper can act as a sealant creating a papier-maché effect and the intrinsic nutrient value of these materials is low. Within the plant, cellulose exists as long fibrils, these impart stiffness and strength into the growing plant cell wall. When liberated and part of the soil, fibres behave very differently to particles and may impart very different properties, enmeshing smaller particles along their length. In solid mechanics, fibres aligned down the length of the material are important additives for enhancing the tensile strength of composites but often have little effect on the compressive strength. A mesh formed by a network of fibres and particles may increase mechanical properties of solids in compression, if not aligned.

3.1.2 Biochar

Charred residues are present in natural soils formed as the result of forest or grassland fires. (*61*) Chars are particularly resilient to microbial decomposition, and are long lasting. (*62*) For this reason, the addition of charred residues to soil may be an effective way to increase soil carbon in soils for carbon mitigation and increase soil properties. (*61*, *163*) Biochars are formed by the thermal conversion of biomass and agricultural residues via pyrolysis. Biochars are formed at temperatures between 300 and 1000 °C under low oxygen environment. Biochars are quite variable, porosities are sometimes high and inherited from the parent material, the acidity and pH of the material depends on the parent material composition, also pre and post treatments can modify biochars physical properties. (*164*, *165*) That said, most biochars are largely aromatic and porous, and highly hydrophobic. This means that most biochars have low CEC. (*165*) Biochar formed from biomass which is highly porous can retain its porosity, and this can create structure in soils, however there is little evidence that biochar enhances aggregation or how it may interact with clay surfaces. (*49*, *166*)

3.1.3 Wood fragments

Relatively intact plant fragments are thought to make up a large proportion of soil particulate organic matter. The external surface of residues from plant fragments are likely to be rough and porous, retaining the physiological structure of the plant. The exposed surface is likely to contain almost any chemical functionality present in a plant cell, and the process of deconstruction is likely to have caused large ruptures and breaks in the structure, exposing surfaces with a high surface energy. As the biomass is processed biologically, the surfaces are likely to increase in surface roughness due to the formation of pores and fragments. For this reason, newer plant remains are thought to retain clays less strongly, although the production of microbial exudates and polymeric glues also increases the binding of minerals to organic matter in soil as plant matter is broken down.

3.2 Experimental design

This section is a continuation of artificial aggregates I, to include additional amendments with different surface chemistries in order to test the applicability of different particle types.

3.3 Materials

Cellulose was obtained through SigmaAldrich (now Merck) as Sigmacell Cellulose Type 50, (50 μm) and Sigmacell Cellulose Type 20 (20 µm).

Biochar was obtained from Nova Pangaea Technologies. The char was formed from a technical organosolv beech lignin obtained via a steam explosion process which was then pyrolyzed at high temperatures. Biochar was dried, crushed and sieved through a 63 micron sieve before use.

Wood chips were used to represent unmodified plant debris. Wood chips were derived from beech wood which was dried, shredded using a Retch SM 100- series grinder, and then sieved to 250 - 300 mm. For the bleaching experiments, beech wood was treated with peroxide to replicate the oxidation of extracellular enzymes used to degrade plant matter, and to see if this effected the

binding of the particles, by removing surface lignin. Peroxide bleaching was carried out by soaking 10 g of beech wood in 90 ml of 10% wt. NaOH solution for 30 minutes at 80 °C in a mini-reactor. Peroxide was added dropwise over a period of 3 hrs with continuous stirring. 45 mls and 5 mls of 30 wt.% hydrogen peroxide was added to obtain bleached and semi-bleached pulps respectively. Pulps were washed in copious amounts of DI water and residual salts were removed by dialysis. Pulps and untreated material were washed extensively.

3.4 Cellulose

The solid volume of the cellulose artificial aggregates increased substantially with increasing loading of the cellulose component. The cellulose fibres can form a mesh and may resist collapsing as the pastes dry. The addition of the cellulose reduced the envelope and skeletal densities of the artificial aggregates although only two points were measured. Porosity (Figure 3.1, **B**) increased more substantially with the smaller size (20 μm) cellulose additive, reaching 60% porosity at 50% loading, suggesting a very porous composite was created. The fine mesh structure formed by cellulose fibres could have within it inherent porosity, the kaolinite acting as a filler.

Unlike previous amendments, artificial aggregates made with only cellulose were extremely cohesive and strong, reaching 13.45 +/- 1.41 MPa for the 50 μmm cellulose particles. The 100% cellulose artificial aggregates far exceeded all other amendments in terms of strength. The increase in strength was non-linear, in respect to mass and volume loading. The line shape is suggestive of the nature of the interaction between kaolinite and cellulose, which is the opposite to previous amendments in which the cohesion between particles of the amendment are less than the cohesion between kaolinite particles. The convex up shape of the graph suggests that cellulose-cellulose interactions are strong and that cellulose-kaolinite interactions are considerably weaker (Figure 3.2).

It appears that the strength of the cellulose artificial aggregates begins to increase around 20% volume loading, however once the volume exceeds 50% the strength increases almost exponentially. Since the strength of the kaolinite:cellulose composites remained high, this could indicate that the interaction of cellulose-kaolinite particles is at least, of the same binding strength as kaolinite-

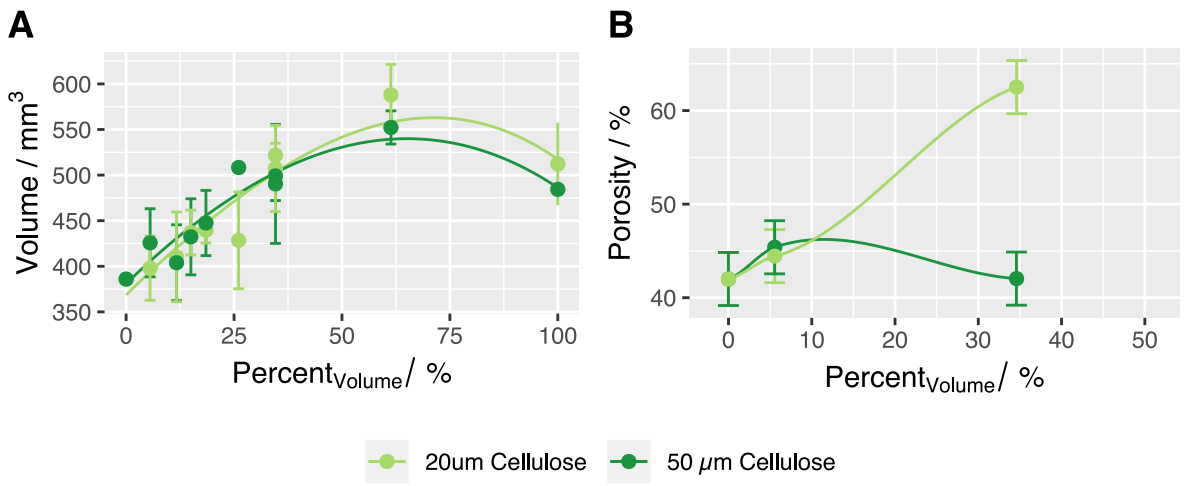

Figure 3.1: **A:** The solid volume of cellulose artificial aggregates increased as low density cellulose fibres were added, decreasing again after 60% volume, due the densification of cellulose particles. **B:** Porosity of cellulose artificial aggregates with different fibre lengths. Lines are guide to the eye. Error bars are one standard deviation from the mean.

kaolinite interactions. Otherwise, at low cellulose loadings, the kaolinite artificial aggregates would be weakened. However, as the cellulose content increases, the cellulose begins to form percolating networks and the strength of the composites increases almost exponentially. As mentioned, cellulose in this case is a more fibrous particle, and the interactions between fibres, and particles enmeshed within particles is likely to be very different from particle-particle interactions. SEM images showed that the kaolinite particles fully coated the cellulose particles leaving no exposed cellulose fibre surface at 50% mass loading (35% volume loading), which explains why the large increase in strength does not occur until higher loadings when cellulose fibre surfaces may come into contact (Appendix). The cellulose shown here resembles long blocky particles, with reasonable surface roughness, and do not resemble long smooth fibres of cotton fibres. (*167*)

A glucose solution was added to test the effect of soluble organic matter on the mechanical strength of kaolinite and cellulose. Over the entire concentration range, no significant differences were observed, suggesting that the glucose was not able to disrupt kaolinite-kaolinite interactions (Figure 3.3).

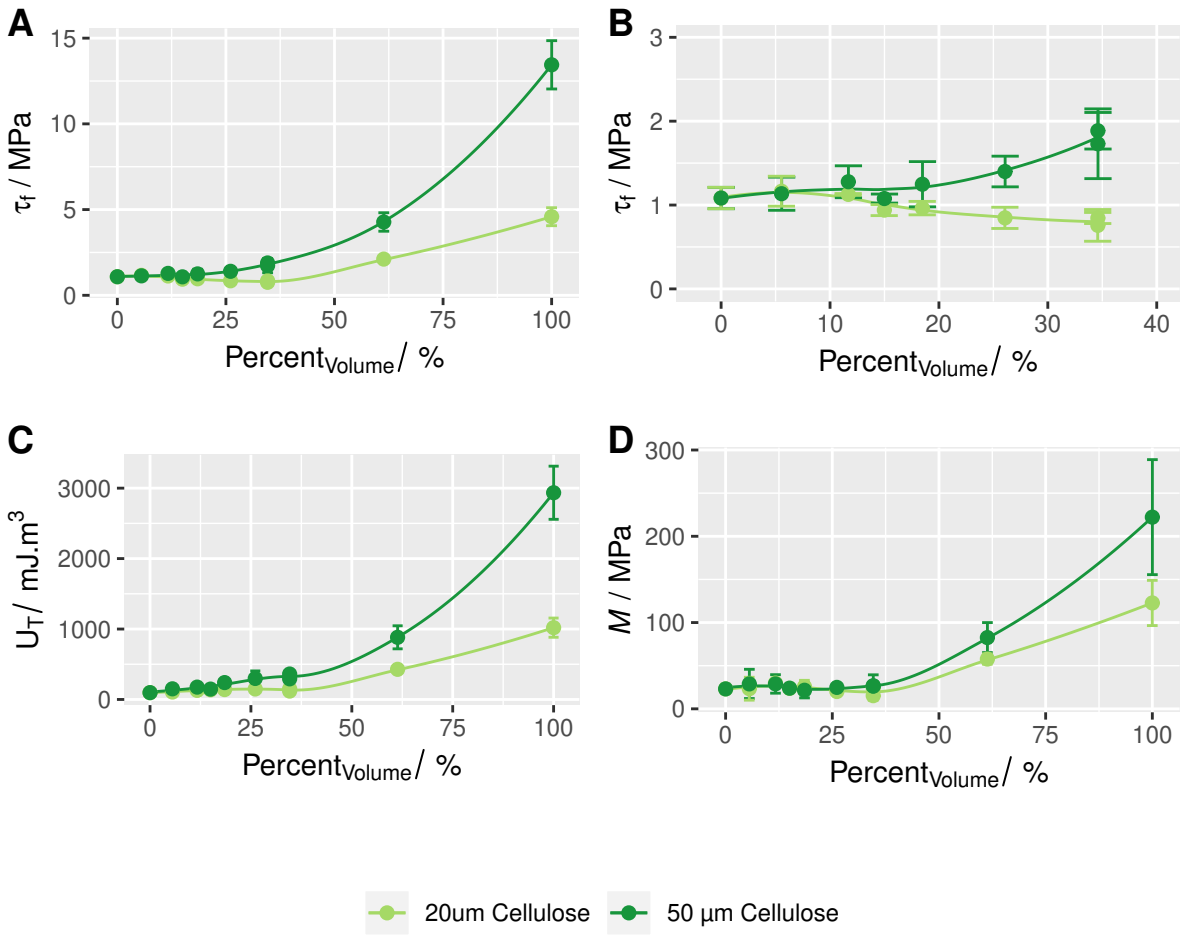

Figure 3.2: The mechanical properties of artificial aggregates made with kaolinite and cellulose. **A:** The addition of cellulose to kaolinite resulted in an almost exponential increase in strength, with a particle size dependence which may reflect the difference in porosity. **B:** The same as A but for the change in volume 0 – 40% for comparison. **C:** The toughness reflected the increase in strength. **D:** Youngs modulus reflected the increase in strength and toughness, suggesting the addition of cellulose fibres helps to from more stronger and more rigid composites. Lines are guide to the eye only, error bars represent one standard deviation (n = 3-5).

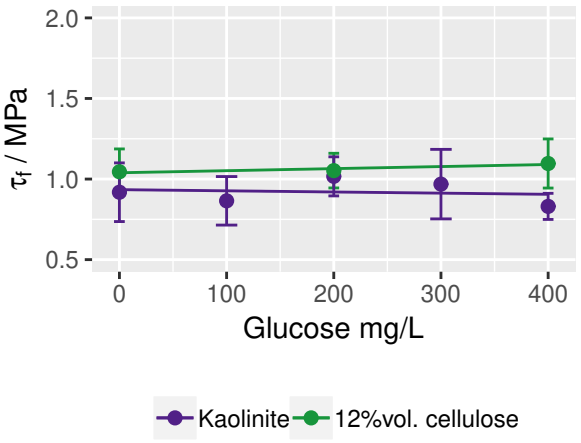

Figure 3.3: The addition of a concentrated glucose solution had no effect on the mechanical properties of kaolinite or a composite containing cellulose. Lines are linear fitting, error bars represent one standard deviation (n = 3).

3.5 Biochar

Biochar was crushed and sieved to below 63 µm. Fine particles were extremely hydrophobic and could not be dispersed in water for particle sizing. FTIR analysis resulted in spectra with a high curved baseline characteristic of black-carbon. Strongest adsorption was observed in regions for C=C and C=O stretches. The lignin derived biochar was found to be deficient in O-H adsorptions, with no signals appearing around 3000 cm^{-1}, suggesting a low hydroxyl content. The biochar was made via pyrolysis from technical lignin, the biochar contains only small pores, not retaining the micro/macro porous of the biomass it was derived from. The surface area of biochar was found to be 256.85 +/- 13.43 m^2/g using BET surface area analysis, with a pore volume between 1.7 and 300 nm to be 25.35 m^2/g. This pore volume is too small to entrap kaolinite particles, which are micrometers in diameter. The t-plot external surface area was calculated to be 54.36 +/- 4.83 m^2/g, which is likely to be closer to the surface area available for inter-particle interactions. Biochar derived from lignin is quite different from that which is derived from biomass, commonly applied in agricultural settings. (*168*) Lignin is much more recalcitrant to oxidative degradation and pyrolysis, and much higher mass yields are strongly correlated with lignin content. Acidity is also strongly correlated with lignin content, pyrolysis largely results in the cleavage of ether bonds and methoxy groups, resulting in increased aromaticity. Biochar particles formed from lignin are likely to be highly

acidic, hydrophobic and aromatic. The crushed and powdered biochar was extremely hydrophobic, but mixed well with the kaolinite forming a grey powder and phase separation was not observed in the paste.

3.5.1 Biochar: mechanical properties

The addition of biochar to kaolinite reduced the skeletal and envelope density linearly as a function of biochar mass loading (Figure 3.4, **A** and **B**). Biochar has a lower density than kaolinite. A porosity of 45% was maintained across all loadings, with a slight increase of about 5% observed over the 0 – 70% volume loading (Figure 41, D). Notably, this porosity was much smaller than that of organosolv beech or spruce lignin (Figure 42). A linear increase in porosity may only reflect the replacement of a volume of kaolinite with that of the more porous biochar, the inter particle porosity is therefor very small. The reduced porosity of biochar may be a result of the suspension behaviour. Unlike lignin, biochar is strongly hydrophobic and contains low surface charge. This means that biochar and kaolinite may coalesce via hydrophobic interactions forming a dense sediment.

The volume of the artificial aggregates (Figure 3.4, **C**) increased strongly when biochar exceeds 60% volume when the cubes transition from biochar dispersed in kaolinite, to kaolintie dispersed in biochar. The increase in volume indicates the reduction in packing between biochar particles, which is observed in the porosity measurements, although the inherent porosity of the biochar must also be considered (Figure 3.4, **D**).

The biochar was observed to strengthen the kaolinite artificial aggregates at 60% volume biochar (Figure 3.6, **A**) whereby the artificial aggregates became brittle and weak, this corresponds to a sharp decrease in strength occurring consistent with a percolation threshold. The strength increased by 36%. This consistent increase in strength coincides with an increase in toughness and modulus, suggesting that the composites are increasing consistently in their mechanical properties. The strength of the composites appears to reach a maxima and plateau, and does not appear to increase beyond 10%. The crushed and sieved biochar consists of a very fine powder with a high surface area. Between 20 – 50% biochar volume loading, the kaolinite-biochar interactions may be saturated, and

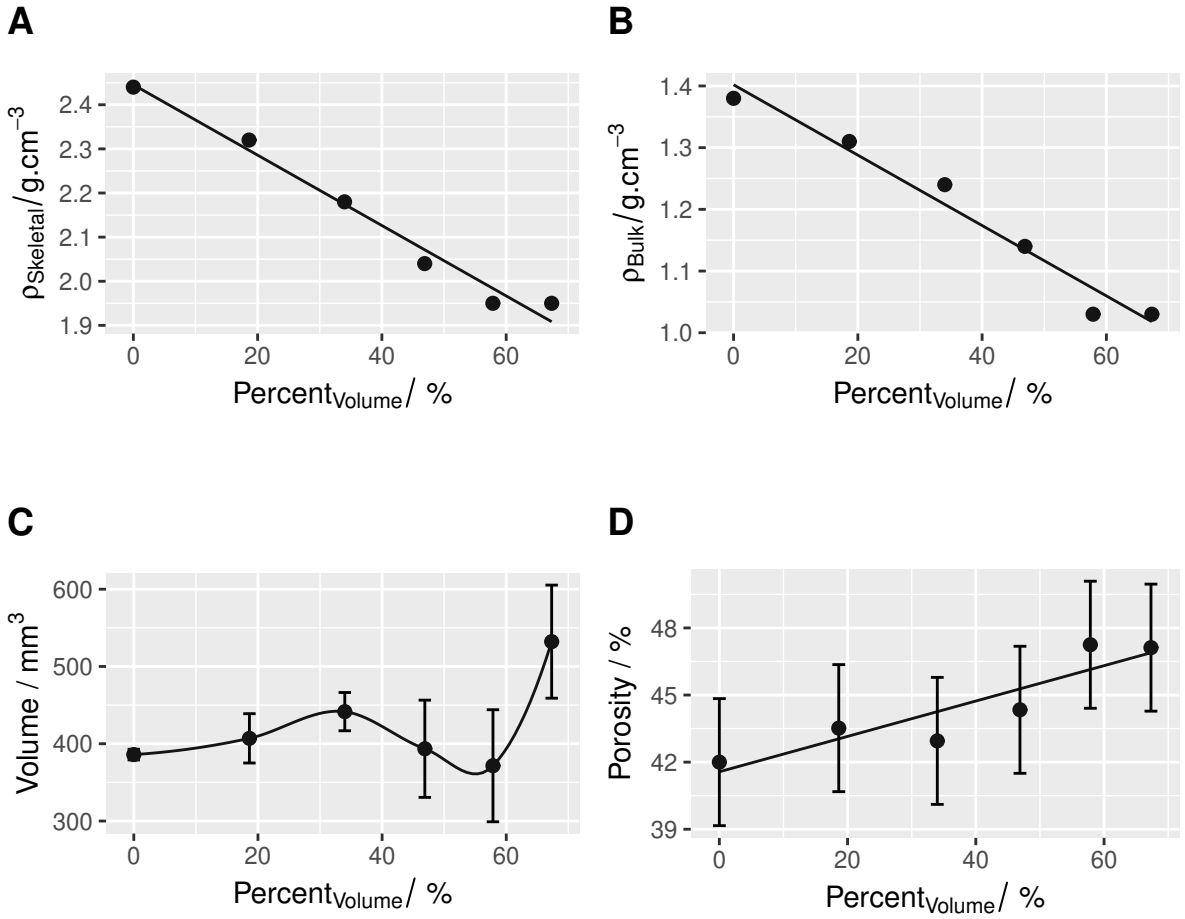

Figure 3.4: **A:** The skeletal density decreased linearly as biochar is added, **B:** the bulk density decreased linearly. **C:** The artificial aggregate volume increased sharply after 60% volume loading. **D:** The porosity increased linearly with biochar loading. The porosity was lower than other amendments, especially considering biochar has inherent porosity. Error bars represent one standard deviation from the mean, lines are guide to the eye only.

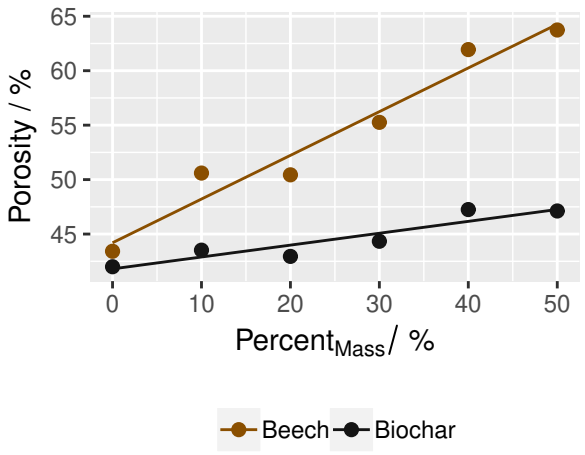

Figure 3.5: Artificial aggregates formed by mixing biochar with kaolinite resulted in a much lower porosity than that for beech lignin. Biochar is more porous than lignin, identifying interparticle porosity as the key form of porosity in these experiments. Lines are guide to the eye only, error bars represent one standard deviation (n = 3-5).

these interactions retain a strengthened network until the percolation threshold is reached. 100% biochar artificial aggregates were not able to form cohesive artificial aggregates. The surface area of biochar is extremely high (256.85 +/- 13.43 m^2/g) compared to that of kaolinite (13.40 +/- 0.04 m^2/g) which may explain why it is able to form a strong network at low loadings.

The dominating characteristic of biochar is its hydrophobicity, resulting from high aromaticity, despite the presence of some acid groups. There is little evidence to identify the type of bonding interaction between the kaolinite and the biochar, but because of the overwhelming hydrophobicity of the biochar powder, it is likely that these experiments confirm that hydrophobic interactions can increase the strength of the kaolinite considerably. The silica surface of kaolinite is hydrophobic, and it is possible that this surface preferentially binds to the biochar. This would leave the hydrophilic alumina surfaces facing outwards into the solution, or to make further binding interactions with kaolinite particles. The high surface area and small particle size mean that more interactions can form.

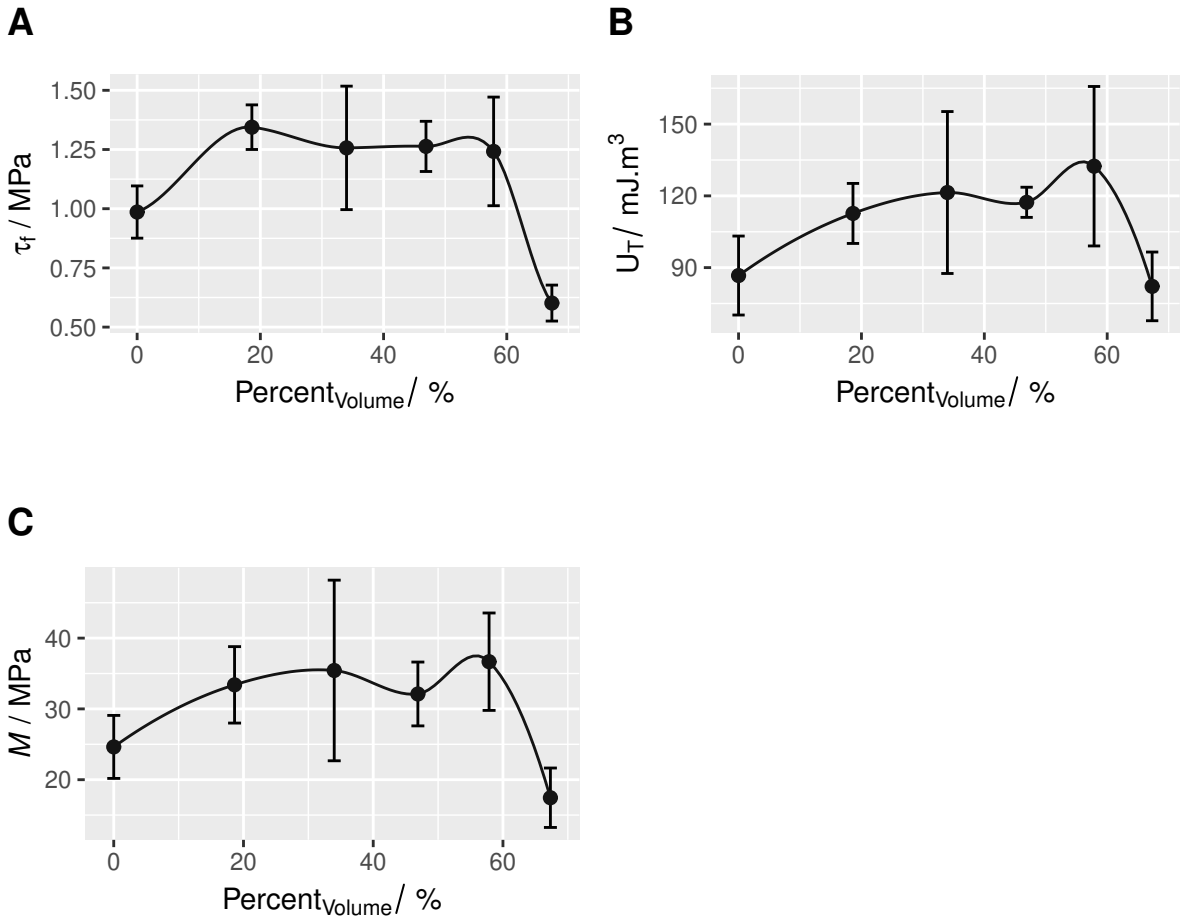

Figure 3.6: **A:** The strength of the biochar composites increases in comparison to that of pure kaolinite, but appears to plateau, before reaching the percolation threshold. **B:** The change in toughness is similar to that of the strength. **C:** Modulus is also increased by the presence of biochar. Lines are guide to the eye only, error bars represent one standard deviation (n = 3-5).

3.6 Artificially decayed wood

Wood chips contain exposed cellulosic, hemicellulosic and lignin residues which are present as fractured surfaces that are rough and contain exposed fibres. When added to soil, the woodchips are subjected to microbial decomposition. In order to simulate this decomposition and determine the effects of this surface, these wood chips were bleached using hydrogen peroxide. Wood chips were sieved to a 212-300 μm size range and these same chips were treated. The peroxide treatments whitened the pulps, the most extensive treatment turned the pulps a light yellow colour. However, peroxide treatment is not very selective and is a harsh method, the surface and structure of the wood fragments are likely to be heavily modified. Under alkaline conditions, hydrogen peroxide reacts with hydroxide to form the hydroperoxide anion. This anion is known to attack the lignin aromatic side chain at the α-position and also cause ring opening reactions. These reactions release soluble fragments into solution, gradually delignifying the surface. In addition, hydroperoxy radicals (HOO·) and hydroxy radicals (HO·) are known to attack hemi-cellulose.

ATR-FTIR is a surface sensitive technique. The biggest decreases in the FTIR spectra following bleaching occur at 1723 cm^{-1}, which corresponds to carbonyls associated with lignin and acetyl groups of hemicellulose, along with a decrease in 1224 cm^{-1} which corresponds to the C-O stretch, again associated with lignin and xylan (hemicellulose). Signals associated with cellulose such as the C-H and O-H stretching absorption around 2880 – 3330 cm^{-1} remained unchanged, as did other signals at lower wavenumbers (Figure 3.7). FTIR analysis shows a decrease in vibrations associated with lignin and hemicellulose. It also shows the removal of C=O bonds associated with lignin and hemi-cellulose. However, there was little change at other absorptions which originate from lignin alone, such as the absorption at 1575 cm^{-1} which corresponds to lignin aromatic skeletal vibrations.

The surface area and porosity of the wood was changed significantly by peroxide treatment (Figure 3.8). Bleaching reduced the total surface area, the external surface area and the microporous area. Lignocellulosic biomass is full of pores, tubular structures such as the xylem and phloem can collapse when treated (known as hornification), as can pores left by damaged cells. However, the BET seems to suggest that the external surface area is rapidly reduced, and a larger proportion of the surface area is found in micropores. This is evidence to suggest that the peroxide is likely to have attacked

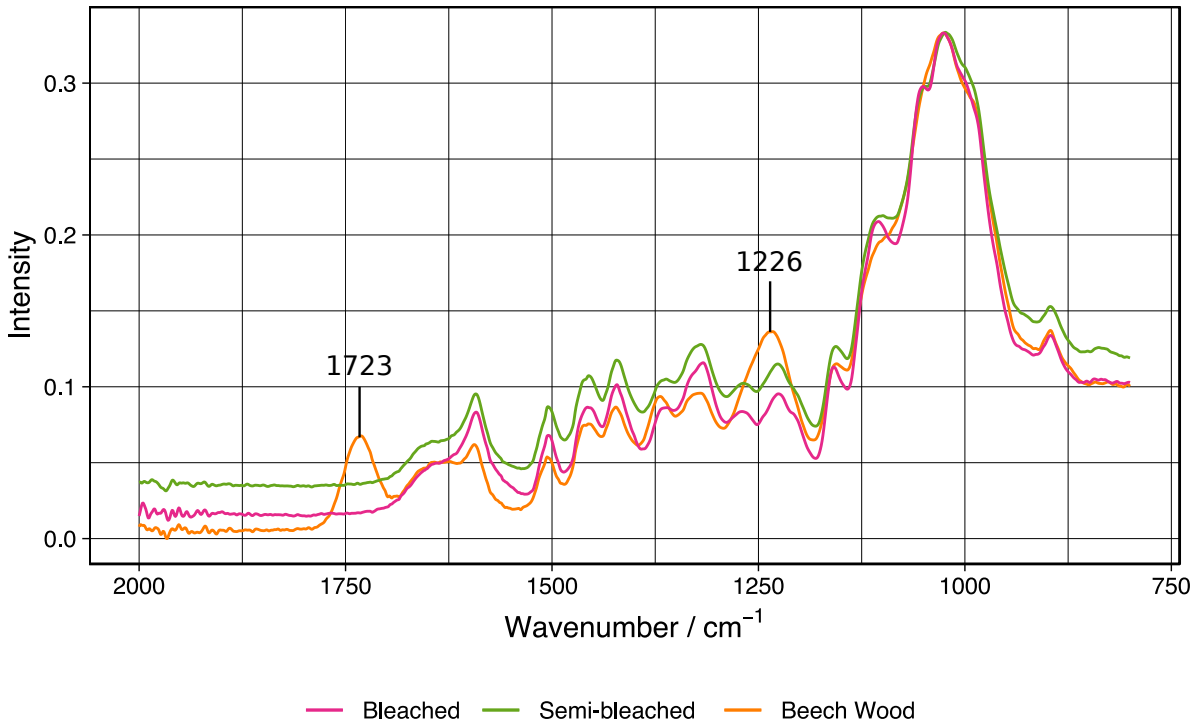

Figure 3.7: The ATR-FTIR spectra of the beech wood, and two treatments with peroxide of different strengths. The peroxide treatment removed two peaks associated with lignin and hemi-cellulose. The absorption at 1723 cm^{-1} corresponds to a carbonyl group, the absorption at 1226 cm^{-1} corresponds to a C-O stretch, associated with hemicellulose and lignin. Lines are guide to the eye only, error bars represent one standard deviation (n = 3-5).

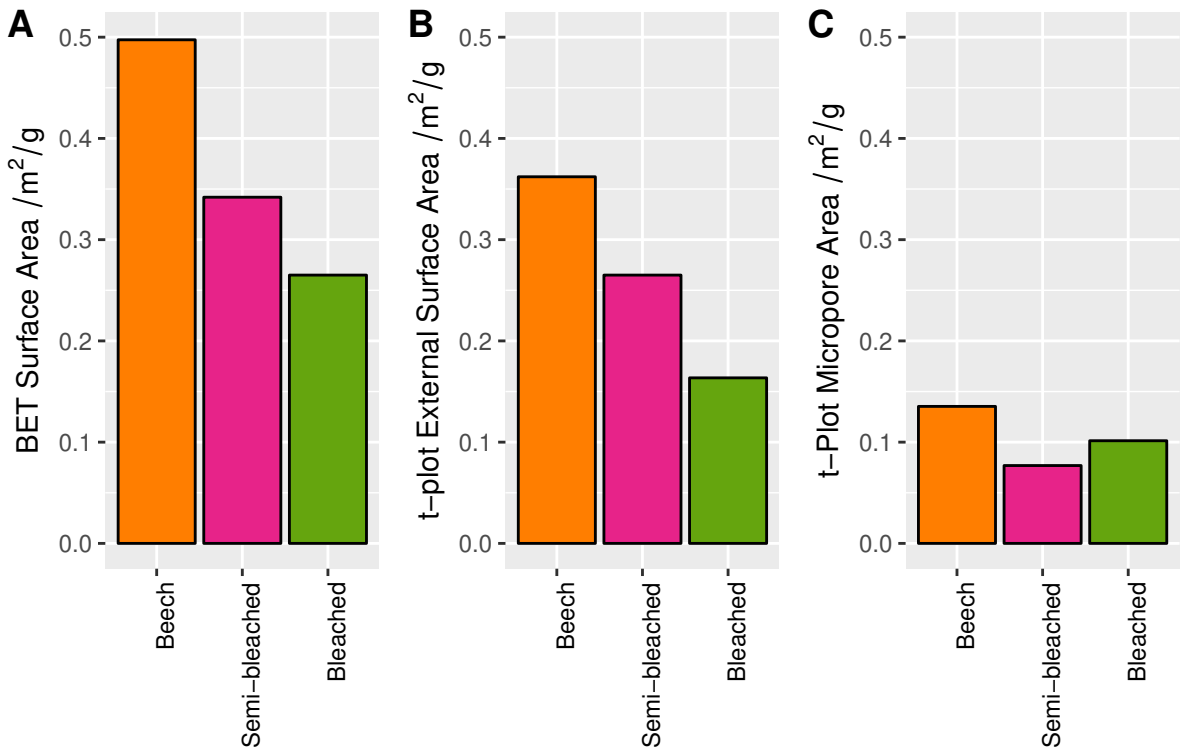

Figure 3.8: Surface area analysis of treated wood chips using the BET method, **A:** The BET surface area shows total surface area decreases with bleaching, **B:** The t-plot external surface area and **C:** The micropore area.

the surface extremely strongly and dissolved much of the surface, reducing the particle size and external surface. The large reduction in mass of the recovered material following peroxide treatment supports this. Even mild bleaching reduced the external surface area considerably, the microporous area did not change as much.

The linear increase in cube volume is due to the increasing volume of wood, which has a low bulk density and makes up a considerable portion of the total volume of the composites (Figure 3.9, **A**). The porosity increases with the volume of wood fragments added, above 15% volume loading the increase may be slightly greater, representing a change in particle packing or density (Figure 3.9, **B**) indicative of a percolation threshold. The increase in porosity is very large, but does not reflect the changes in porosity of the wood fragments following peroxide treatment. This means that a much greater additional porosity is created between the wood particles and that the change in surface chemistry does not influence this porosity. These interparticle porosities are of a similar magnitude to 50 µm cellulose, which has similar surface chemistry, but may reflect the more-fibre like properties

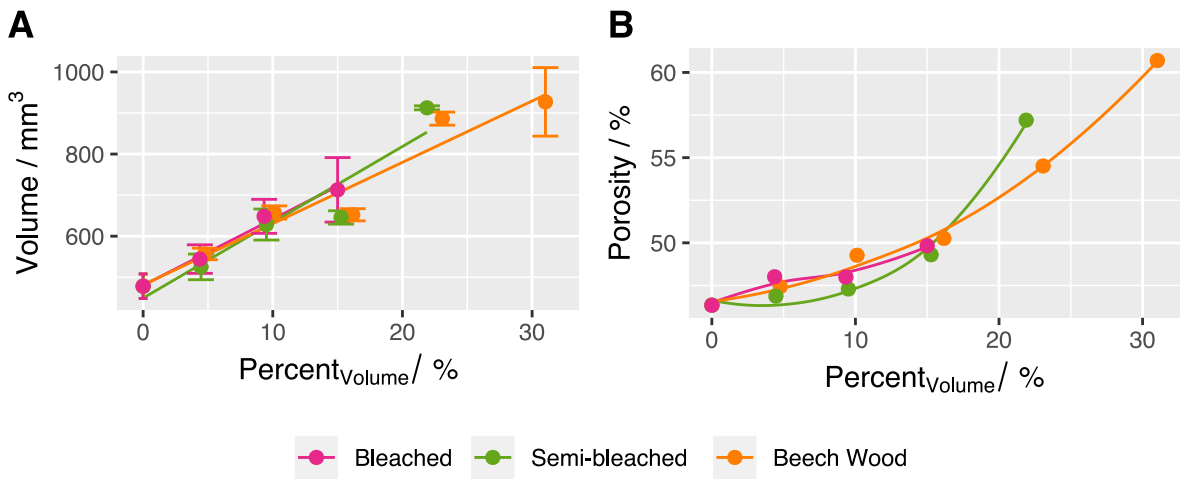

Figure 3.9: **A:** The artificial aggregate volume increased linearly regardless of the peroxide treatment, suggesting that the drying behaviour was unaltered by the surface modification. **B:** The porosity of the artificial aggregates increased with a slight inflection at 15% volume loading, and was not significantly altered by the peroxide treatments. Lines are guide to the eye only, error bars represent one standard deviation (n = 3-5).

rather than surface chemistry. On drying, fibres may lock together, forming internal voids, at low loadings these are filled by kaolinite, but with increasing wood volume, these pores remain more and more open.

For the unmodified and lightly treated wood particles, the strength of the artificial aggregates increased until 15% mass loading, and then decreased, corresponding to a very low percolation threshold (Figure 3.10). The low percolation threshold is due to the high porosity and large particle size. The bleached wood does not increase the strength of the kaolinite but retains it until 10% volume loading. The reduction in percolation threshold for the bleached pulp is not clear, but maybe due to the reduction in surface area and surface functionality or porosity which may help in locking fibres together. The toughness increased dramatically with the wood fragments, and was much more significant than both the strength and modulus. The large change in toughness suggests that the network of bridged wood particles is able to absorb more energy before fracturing, due to the fibre like shape of the pulp fibres creating a scaffold (Figure 3.11). The bleached particles show reduced toughness, although the composites are tougher than the pure kaolinite artificial aggregates, due to the reduced fibre size.

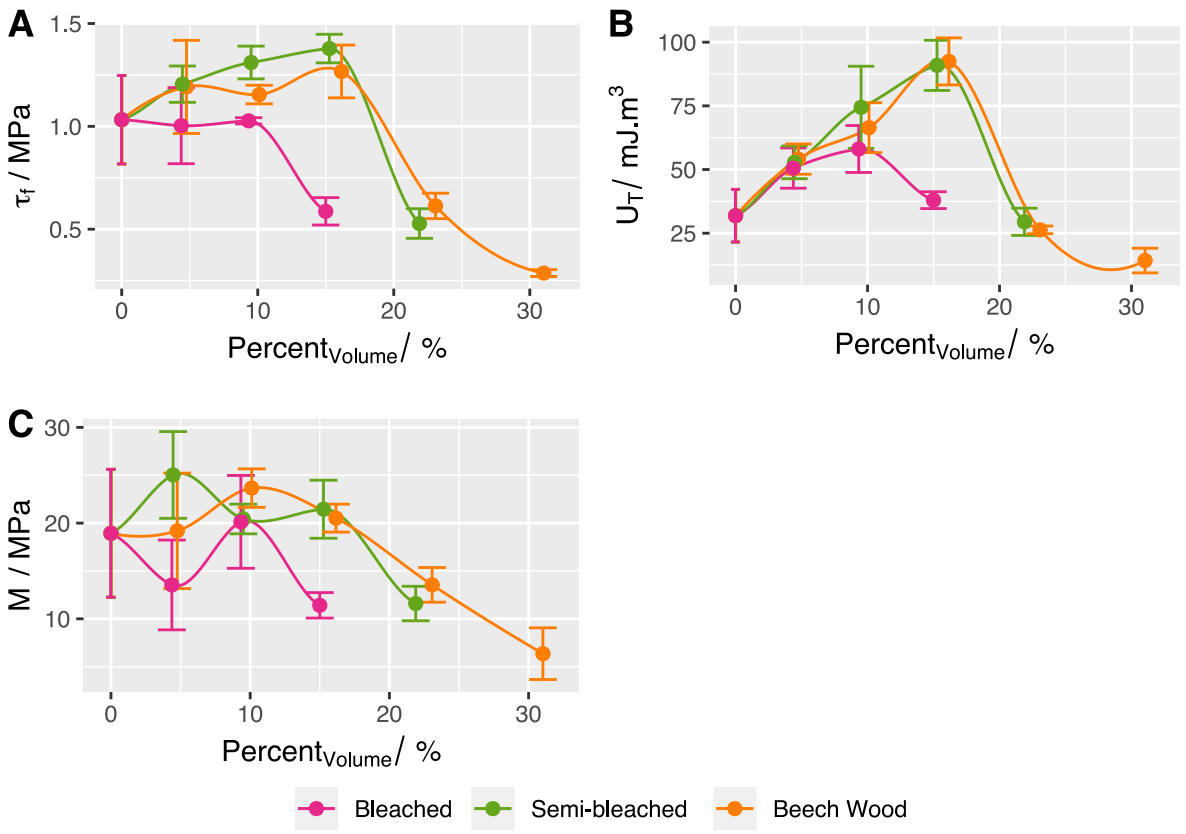

Figure 3.10: The mechanical properties of artificial aggregates with increasing wood chip compositions **A:** The maximum compressive strength of composites containing beech wood and semi-bleached beech wood plateaued around 15% volume, after which the compressive strength decreased, becoming non-cohesive. Fully bleached wood did not strengthen the composites and dropped rapidly in strength after 10% volume loading. **B:** The maximum strength increased to a maximum at 15% volume, except for that of the bleached pulp which decreased after 10% volume loading. **C:** The modulus followed the changes in strength, but the data was far noisier. Lines are guide to the eye only, error bars represent one standard deviation (n = 3-5).

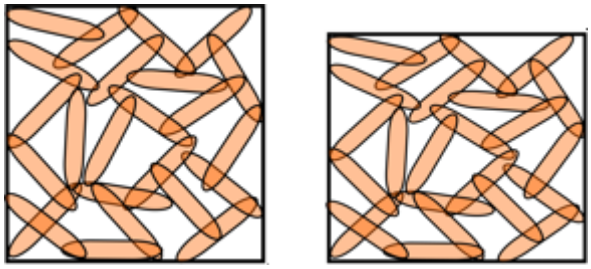

Figure 3.11: fibre-like particles can form a scaffold within the aggregate, making the composite more spongey, thereby increasing the toughness.

3.7 Discussion

The results of this study are a continuation of the findings from the last chapter. Cellulose is an important component of plant cell walls, adding strength and rigidity. Its fibre-like properties give materials such as paper high tensile strength, but fibres are less effective at providing high compressive strength. The compressive strength of the cellulose aggregates was very high at high cellulose loadings. This compressive strength indicates a high inter-particle strength between the fibres, and strong interlocking properties. The shape of the curve representing the mass loadings vs compressive strength indicates that the kaolinite weakens the cellulose-cellulose interactions. Despite the impressive compressive strength, cellulose is unlikely to be a good material for increasing the aggregate strength. It is likely that in natural systems the cellulose would phase separate and that the kaolinite-cellulose interactions that form would be weak and fragile. Cellulose is rapidly decomposed by soil organisms, so it is unlikely that cellulose would be protected from degradation by clay interactions. Many plant residue surfaces, especially those which have been formed by splitting or breaking, have exposed cellulose surfaces. This means that woody or cellulose rich residues may not interact strongly with kaolinite in the soil, which makes them more exposed to microbial decay.

Biochar, like lignin contains aromatic functionality, but biochar is largely more hydrophobic. The particles are rigid and completely insoluble in water. Evidence for biochar-clay interactions is minimal, but of minor importance because it is highly recalcitrant and increases the water holding capacity by the nature of its own porosity. In this study, the biochar behaved as if it was interacting with the clay particles, and did not produce a large porosity aggregate. The low porosity may originate from a low electrostatic charge, forming a dense sediment. The more angular particle geometry, which may form better interactions with the plate-like clay particles may enhance the formation of a dense sediment, which changes little on drying. This dense sediment may result in the formation of a stronger aggregate. Biochar aggregates were increased in strength in comparison to the kaolinite particles, until the percolation threshold was reached.

Wood chips were used to represent the naturally cleaved fragments of plant matter which exist as POM in agricultural and forestry soils. The surfaces and shapes of these particles are likely to be extremely variable, and cannot be treated as ideal particles. The particle size of these amendments

were large, and so the percolation threshold was reached at low loadings. Large, fibrous particles may enhance aggregate strength by forming a flexible network, which boosts strength by acting like a scaffold, held together with clay. By bleaching the particles, surface roughness was reduced and functional groups were oxidised. The reduction in surface roughness may prevent the particles from acting like a scaffold.

3.8 Conclusion

3.8.1 Cellulose

The mechanical strength tests clearly indicated that cellulose in low volumes was able to retain the strength of the pure kaolinite composite and increase the strength at high loadings. However, this may be due to its properties as a fibre, rather than its inter-particle binding strength. Fibres are able to transverse the dimensions of a composite forming a net, which particles are not able to do. This usually manifests itself as a greater tensile strength, however, the cellulose-cellulose interaction is so strong, it may impact the compressive strength too. Clay is often added to cellulose to encourage dispersion of cellulose particles, but the binding interaction is known to reduce the mechanical properties. (*169*) The almost exponential increase in strength, toughness and modulus observed with cellulose suggests that cellulose-cellulose interactions are considerably more strong than kaolinite-kaolinite or kaolinite-cellulose interactions. Cellulose may phase separate, and form strong interactions, excluding kaolinite. It is likely that the addition of cellulose to kaolinite rich soils would lead to the formation of cellulose enriched aggregates, due to their greater aggregate strength, disregarding the biological considerations. The mechanical properties of kaolinite or kaolinite:cellulose aggregates were not modified by the addition of glucose, suggesting a poor interaction of both glucose and cellulose with kaolinite surfaces. For this reason it is unlikely that kaolinite would sequester cellulose or sugar rich materials, and that the increase in aggregation in soils would be strong but transient.

3.8.2 Biochar

Despite the apparent hydrophobicity of biochar, and the limited hydrogen-bonding functionality, the addition of biochar to kaolinite resulted in the formation of strong composites. Small volumes of biochar were able to increase the strength of the composite and a plateau was reached, indicating that the kaolinite-biochar interactions which form a stable network were saturated. The percolation threshold was clearly marked, resulting in a large decrease in strength. Biochars tend to have relatively neutral zeta potentials, generally less than -9 mV, and have a much smaller negative charge than kaolinite. (*164*) This may result in the low porosity, which suggests a good packing density. A strong interaction in the solid may even be a result of hydrophobic interactions formed in the initial suspension. The capacity for hydrogen bonding interactions between kaolinite and biochar is limited, instead an increase in van der Waals type interactions is likely, due to the high surface area of the biochar. A percolation threshold was reached, in which biochar-biochar interactions and porosity created a weak network as the volume loading increased. This indicated that biochar-biochar interactions are weak, and that kaolinte-biochar interactions are favourable.

3.8.3 Wood fragments

Wood chips, including chips which were sequentially bleached with alkaline hydrogen peroxide treatment were found to have different mechanical properties. The addition of large fibres resulted in a strong increase in porosity, caused by large gaps formed from interconnected fibres, and a very low percolation threshold, around 15% volume loading. Wood chips were likely to form a criss-crossed network of particles, with cavities filled with kaolinite particles. Wood chips and chips with only a light surface modification were found to be strengthening up to 15% volume loading, however, heavily bleached wood chips were significantly weaker, only retaining the strength of the kaolinite until 10% volume loading. This is due to the removal of lignin and hemicellulosic residues from the wood surface, which are likely to contain the surface functionality most able to form strong bonds with kaolinite. A reduction in particle size and surface roughness may also contribute to a weakening of the composites however.

3.8.4 Part I and II: Relevance to soil science

From this study, it is clear that the mechanical properties of artificial aggregates are dependent on a number of factors which are interrelated. Porosity has been shown to strongly modify the mechanical behaviour of a number of composites and materials, but in these artificial aggregates the contribution of porosity to the mechanical properties is complex. The formation of porosity is related to the packing of both primary particles (individual particles) and the porosity formed between agglomerations (tactoids of kaolinite, micron sized aggregates of primary particles), and this depends on the sediment fabric in solution and the morphology and size of particles. The fabric which forms on drying will be more porous if strong electrostatic repulsion exists between particles in solution although in some cases this can result in strengthening, as observed in high pH kaolinite. For the design of soil amendments, it may be beneficial to add an amendment which may generate porous aggregates, as micropores are valuable reservoirs for water and nutrients, as well as habitats for microbiology. Porosity may be an inherent property of the amendment (wood chips) or generated between particles with mismatched morphology. Despite large increases in porosity, many particles were able to increase the strength of kaolinite aggregates, suggesting that porosity is not the dominant factor defining aggregate strength and that surface chemistry is an equally important consideration. That said, reductions in porosity result in much stronger interactions between particles. It is clear that surface chemistry plays an important role, hydrogen bonding type interactions are likely to be the strongest interactions which exist between clays and particulates in dry solids, although because of the localised and directional nature of the bond, the material formed may be more brittle. Hydrogen-bonding at surfaces is not always considered in DLVO calculations of natural materials, despite evidence that they can form at room temperature and in the presence of moisture. (*170*) A solid held together by van der Waals type interactions at surfaces may be less brittle. Hydrophobic materials such as biochar, with low hydrogen bonding capacity, are able to form strong networks with kaolinite, but this is due to the densification of the fabric on forming a suspension and a large surface area, resulting in a low porosity material held together with low strength but high contact area interactions.

The strength of an artificial aggregate is dependent on a number of factors, which include particle-

particle interactions, particle packing density and structure, the contact area between particles, the porosity and the percolation threshold. All of these factors are related to the nature of the amendment particulate and therefore there is considerable opportunity to enhance and optimise these properties. These experiments show that the clay – amendment interaction formed on a single wet and dry cycle is strongest at a particular clay:amendment ratio. These clay:amendment ratios could be used to determine the quantity of an amendment which may bring about greatest increase in aggregate mechanical stability. Alternatively, in soils where the clay content is limiting and where there is strong pressure on the soil to form strong aggregates (soil is mechanically perturbed), clays may naturally sequester amendments at a ratio that renders them strongest. I.e., aggregates containing low clay and high amendment are unstable, where as those closer to a clay:amendment ratio that results in the strongest aggregate will persist. Mechanical pressures such tillage, may select for aggregates with a particular clay:particulate ratio. The HDPE particles demonstrate that hydrogen bonding groups can increase the strength of composites. Amendments such as cellulose however, may be more likely to phase separate, forming stronger aggregates without clay which are highly susceptible to mineralisation. For particles with rough surfaces or irregular particle dimensions and shapes, estimating the inter-particle contact areas is impossible, and so the increase in strength per surface area of functional groups can only be estimated for composites with similar porosities containing particles with comparable shapes and sizes, such as the HDPE. However, this method can be used to determine the binding characteristics of two dissimilar particles, and that the line shape with increasing additive can provide information regarding the percolation threshold and the nature of inter-particle interactions. This method also takes into account the porosity which is developed by the addition of an additive, which appears to be an inherent property of the material. This also demonstrates clearly that the interactions between soluble materials and particulate materials are distinct and need to be considered separately in reference to soil function.

In the context of utilising biorefinery wastes, some clear strategies have been identified. Hydrogen bonding functionality may increase the mechanical strength of soil aggregates, and form stronger interactions with clay, thereby increasing the potential for carbon sequestration and resistance to soil erosion. Cellulose rich materials may only lead to transient increases in soil mechanical strength, but cellulosic materials may phase separate and would not be recommended. Lignin appears to form

a strong interaction with kaolinite, which increases with pH, due to partial dissolution. It also forms very porous aggregates and forms interactions with kaolinite which may increase in strength via the addition of soluble organic matter. Both lignin and biochar, have high surface areas, and due to the low electrostatic repulsion may help flocculate kaolinite via hydrophobic interactions. Biochar forms an aggregate with less inter-particulate porosity, which is likely to be a result of particle morphology and size, and represents a more recalcitrant form of carbon.

These experiments also have relevance to the issue of microplastics in soils. The use of plastics in agricultural and horticultural applications, residues in domestic compost production and plastic pollution has resulted in large quantities of microplastics being identified in soils. (*149*, *171*, *172*) These results show that oxidised microplastics may have a greater potential to be retained by soil clays, where as microplastics with similar surface chemistry to HDPE may not be retained, and may be transported to waterways at a faster rate.

Chapter 4

Water Stability of Artificial Aggregates

4.1 Abstract

Rain and irrigation subject soils to periodic wetting. The wetting of aggregates can be disruptive to soil structure, causing the breakdown of soil aggregates on wetting through slaking. Particulate organic matter, may stabilise aggregates to wetting but the mechanisms of this stability (particularly physio-chemical stabilisation) are not well studied. Slaking can be complex, and is thought to be the result of a number of different factors such as porosity, hydrophobicity, and inter-particulate binding strength. Attempts to quantify slaking stability, are numerous but there lacks a recognised methodology able to identify mechanistic elements. In this study, the stability of artificial aggregates containing kaolinite are tested using a custom-built imaging device with the aim of determining slaking kinetics and dispersion. This is done with the aim of identifying key mechanistic elements to slaking breakdown, which may occur over different time-scales.

Kaolinite was found to slake forming small water stable particles, with minimal dispersed material. The addition of particulate organic matter changed the slaking onset, duration and the amount of dispersed material. Hydrogen bonding interactions were found to be weak when wetted, and the formation of hydrophobic interactions was observed to stabilise slaking. Surface modified HDPE particles caused a large destabilisation, due to the high wettability and the formation of electrostatic repulsive forces. Hydrophobic interactions were weak and formed after a delay in some cases,

resulting in a deviation from sigmoidal slaking. HDPE particles stabilised kaolinite, despite having no functionality which could result in HDPE-kaolinite interactions. Samples with increased porosity were found to slake faster, although this was only observed over a large porosity range between samples of different types. Wood samples contained inherent porosity and likely swelled, destabilising aggregates, suggesting amendments with low internal porosity may form better amendments. Treating the wood with peroxide collapsed the structure, and increased the stability of the aggregate. Cellulose, biochar and wood particles resulted in the formation of dispersed material, likely to be the result of a disruption of kaolinite-kaolinite aggregations due to clays coating surfaces. Biochar was observed to delay slaking due to the formation of hydrophobic interactions, but this only occurred after significant loss of material by dispersion caused by a large internal porosity.

4.2 Introduction

The stability of soils, and aggregates within soils, are dependent not only on the strength of the interactions between particles and the mechanical properties of the bulk material, but on the stability of particles to once wetted or submerged in water. Aggregates which appear hard and resilient dry are not necessarily resilient when submerged in water or when soils become saturated by rain, flooding or irrigation and the amount of dry stable aggregates does not usually correlate well with water stable aggregates. (*80*). Soils can change dramatically on wetting, and this has major implications for soil management practices. The main cause of soil erosion is water erosion, which is estimated to result in a loss of 4.0 - 6.0 Pg C/year. (*173*) It is therefore essential that the underlying mechanisms which underpin aggregate stability in water are determined, and if these interactions can be strengthened by the addition of particulate organic matter.

Water stable aggregates are also a strong indicator of good soil health, which is usually attributed to biological factors such as plant roots, exudate producing soil biota and fungal mycelium present in carbon-rich temperate soils. (*174*, *175*) Exudates are often polymeric polysaccharides which have the ability to glue particulates together and are thought to be resistant to wetting. (*176*) Plant roots and fungal mycelium also form a net which physically retains material from being washed away. (*177*,

178) Microbial biofilms may also modify clay surfaces or bind particles together as do the various mucus produced by organisms such as worms. (*121*, *179*) Soil management practices such as no-till can dramatically enhance soil aggregate stability and the resistance of soils to slaking, due to the action of these organisms. (*77*) The role of abiotic processes, however, is not well understood, and it may be these initial abiotic interactions that determine which particles are in sufficient proximity to be glued together by biological means. Many studies have shown that the mineral composition of a soil significantly modifies microbial community structure and colonisation, and some species may preferentially colonise specific biogeochemical interfaces. (*180*) In the context of degraded soils, inter-particulate interactions may play a larger role in stabilising soils, especially if soil amendments are added.

There are a number of theories as to the main causes of aggregate instability in water, yet little empirical evidence exists to confirm the magnitude or action of these causes. Aggregate instability is likely related to factors such as internal porosity, the wettability of surfaces and heat of wetting, the forces between particulates and the nature of the electrolyte. (*181*, *182*) Because of the amorphous and highly variable nature of aggregates, the mechanisms of aggregate stability are likely to be soil specific and multifaceted. It also remains a technical challenge to measure some of these attributes of a natural aggregate or find naturally occurring aggregates with predictable and reproducible properties for study. (*183*) The suggestion that there may be one cause or indicator for aggregate stability in soils is misleading at best, especially where there is both a biological and physio-chemical contribution. In order to assess the contribution of each, model systems are used to investigate specific physio-chemical interactions. An assessment of the inter-particle interactions and their behaviour in water will help indicate which interactions can bring about stability allowing for more targeted studies of real aggregates. Particulate interactions dictate the behaviour of young or heavily degraded soils and form the infrastructure on which a more developed topsoil forms, so understanding these interactions may help in designing better soil amendments.

4.2.1 Determining soil aggregate stability and slaking.

There are a number of methods that are used to measure slaking stability, including rainfall simulation, dry sieving, wet sieving, ultrasonic vibration and clay dispersion. These methods are carried out using aggregates which are dry or moist and can be pre-sieved to meet a certain size requirement in order to remove some variability. A study which measured the aggregate stability of a soil, using different methods found soil aggregate stability indicators to poorly correlate with each other, suggesting that each method is sensitive to a different element of soil aggregate stability, and that a single measure or protocol may not be appropriate. (*80*) It has been suggested that the methodology or protocol used should be appropriate for the soil and the soil management practice, simulating the primary driver of soil aggregate breakdown. (*184*) Techniques show good reproducibility within soil types and for many studies, this is adequate. However, little mechanistic information can be extracted from these studies.

A number of observations have been made from field work which help to improve soil management practices but also provide some mechanical insight. For example, the clay content and type is known to have a strong effect on the nature and stability of aggregation. Clay soils tend to from more stable aggregates, as sandy soils loose structural stability on drying. (*185*) Soils with strongly swelling minerals (2:2 clays) can have low slaking stability as differential swelling can break up aggregates. Aggregate stability is known to increase with organic matter, but again, it is not clear if this is due to predominantly biological or physiochemical interactions or what kind of organic matter is stabilising. (*71*) Vegetation cover is highly correlated with stable aggregates, with root structures adding significant mechanical strength and exudates helping create water stable aggregates. In weathered soil, crystalline oxides and amorphous iron oxides give soils increased stability against slaking and promote the formation of water stable aggregates. Soil cations, particularly sodium are also known to play a strong role in the dispersion of clays and soils, and can cause soil sealing. However, studies of soil sodicity and aggregate stability have yielded some inconclusive evidence, especially in combination with with measurements of soil C. (*186*)

4.2.2 Aggregate composition

The composition and morphology of natural aggregates is hugely variable and complete characterisation of all the components present is practically impossible in most cases, especially in terms of the chemical composition of the organic matter present. (*64*) Broad statements can be made however, about the nature of aggregates and water stability. Hydrophobic aggregates tend to have greater stability in water, and this may largely be due to biological activity (worm casts are hydrophobic), but could also be due to the nature of the organic matter present. (*70*, *75*, *181*) With the exception of waxes, root material and lignin rich residues, plant residues are largely hydrophilic, and are likely to become more hydrophilic as they decompose. Chars and fungal/microbial debris could also contribute to hydrophobic materials and soluble organic matter, such as fatty acids can modify the surfaces of clay particles and enhance hydrophobicity. The stabilising effects may be due to a water repellence, slowing water ingress, hydrophobic interactions which form on wetting, or these hydrophobic residues may simply act as a glue. The existence of soils which have variable hydrophobicity/hydrophilicity are also known, thought to be caused by amphiphilic molecules such as phospholipids which rotate in response to their environment. It has also been suggested that molecules can become amphiphilic on decomposition. These amphiphilic molecules have been used to explain an interesting behaviour of some soils which become hydrophobic on drying but hydrophilic on wetting. The orientation of these molecules swap in response to the solvent environment, mediated by a coating on clay surfaces. However, direct evidence for these types of molecules operating on an aggregate scale has not been provided. Cementing agents such as carbonates or oxides are known to precipitate and bind together mineralogy, in mineral rich soils. This requires the formation of loose associations between materials before they can be bridged by precipitation, and the aggregates which form are often small (sand-sized) and hard, contributing little to soil structure. Removal of these oxides has been shown to cause minerals to disperse, but these soils may respond quickly to the addition of organic matter which can help to build more complex soil structure (*76*).

There is a clear distinction between tropical and temperate soils. The moist, carbon rich and biologically active temperate soils are generally more dynamic and have strong aggregate hierarchies. The biological contribution is also likely to be much higher, and therefore the physio-chemical

interactions are less defined. Although important in temperate soils, soil organic matter is not always present in high enough quantities in tropical soils to be a significant contributing factor of aggregate stability, but nevertheless may contribute to stability to some degree. Aggregate stability is often found to positively correlate with cation exchange capacity and the presence of elements such as Mn, Mg and P. Tropical soils such as oxisols appear to be stabilised predominantly by oxides. These soils usually contain homogeneous microaggregates and the aggregate hierarchy present in other soils are often not observed. (*55*, *185*, *187*)

4.2.3 Inter-particle forces

The movement of water through a porous, spatially heterogenous material like soil is complex. In the bulk soil, the movement of water is largely determined by topological aspects, capillary and gravitational forces, and the bulk surface properties of the soil matrix. (*42*, *188*) At the microscale, or in the topsoil, soil water can be extremely disruptive. For example, air trapped within pores is compressed as water moves into the soil by capillary action. The pressure which builds can overcome interparticle binding, and this forces particles apart breaking an aggregate into smaller aggregated particles, this is what is commonly referred to as 'slaking' and is often observed to worsen when soil is very dry or when wetting is rapid. (*39*, *189*) The internal porosity of aggregates is therefore thought to be a strong predictor of aggregate stability in water. This is also commonly used to explain why large aggregates, which have a higher probability of larger pores, are less water stable. Porosity is related to the soil texture and a greater volume of fine particulates is supposed to be beneficial for water stability, well packed fine particulates are thought to result in the formation of only extremely small pores which can restrict water penetration and potentially stop water infiltration (*190*). The rate of water ingress though a soil or aggregate is largely related to the affinity of water to the particle surfaces, which is often termed the soil matric-potential. Water is bound to surfaces largely by hydrogen bonding, and surfaces which contain pores or have large surface roughness can hold greater volumes of water. (*165*)

Dispersion of clays can also occur as surfaces are wetted and particles are separated. Electrostatic repulsion forces the particles apart, and individual particulates can break away. Dispersive slaking

is commonly observed in sodic soils, which contains a high level of soluble sodium. This reduces inter-particle interactions at clay surfaces and promotes dispersion. (*80*) The dissolution of salts away from the clay surfaces, which can act to shield charge, enhance the electrostatic repulsion and cause dispersion to occur, and so the degree of wetting can also influence slaking. This can also occur if aggregates are submerged in water with a low electrolyte concentration, the rapid diffusion of ions from the surfaces can cause osmotic pressures, which force clays apart. Water can also cause some minerals to swell, 2:1 clays strongly swell when wetted and this can cause materials to break apart, especially when particles are mixed - resulting in differential swelling which can cause large ruptures in the aggregate structure.

The most commonly discussed mechanisms for aggregate breakdown are summarised below (*4*, *80*, *165*)

- **Slaking** - the breakdown of an aggregate into microaggregates, caused by compression of entrapped air, and is thought to be strongly related to internal porosity, wettability and internal cohesion.
- **Differential swelling** - most common in soils containing swelling clays, differential swelling occurs when components swell at different rates, forming ruptures. This results in the formation of larger fragments which break away.
- **Raindrop impact** - Raindrops have been shown to strike aggregates with enough force to cause aggregates to breakdown, this is predominantly related to the cohesion between particles in the wet and dry state.
- **Dispersion** – Dispersion is the breakdown of aggregates and microaggregates into individual particles. This is caused by the wetting of particulate surfaces, and the formation of electrostatic repulsion between surfaces or the disruption of electrostatic attractive forces. Low electrolyte water is most effective at causing dispersion by electrostatic repulsion, and is common in aggregates containing negatively charged particles.

Few experiments on slaking stability are designed to isolate the effect of a single mechanistic variable, and differentiating each process in a single slaking event is a technical challenge. However, some

processes may occur over different time-scales. For example, dispersion may be slow and require time to occur, as water has to ingress throughout the aggregate. The formation of electrostatic interactions require the surfaces to be wetted, overcoming van der Waals forces and for bound ions to diffuse away from surfaces.

4.2.4 Imaging analysis

Measuring aggregate breakdown by experiments such as wet sieving, subject aggregates to both mechanical stress by collisions and abrasion with the sieve surface as well as the effects of water ingress into the aggregates to determine stability. This results in a measure of aggregate stability which cannot differentiate between mechanical stability and wetting stability and assumes that aggregate breakdown is identical in all aggregates. Wet sieving is sometimes carried out by hand, a skill requiring careful observation and technique. This makes it a difficult protocol to standardise and the variability between researchers may be high. Recently, wet sieving has been replaced by subjecting aggregates to calibrated ultra-sonic vibration, which means aggregate stability can be determined more precisely. (*64*) More complex protocols based on wet-sieving have been developed using water/solvent (ethanol) mixtures to modify the rate of wetting, or the use of salt solutions to determine the role of electrostatic interactions on slaking. These techniques are able to differentiate between processes however, they are labour intensive and the uptake of these methodologies has been limited. (*80*)

Water ingress and the breakdown of aggregates by the forces created by compressed air is related to both the porosity of the solid and the rate of wetting. 2:1 clays may also swell, which results in a swelling of the aggregate. Dispersion of clays, occurs over longer timescales, and are not generally measured by sieving measurements can be measured afterwards by turbidity measurements. More automated and analytically advanced methods of determining aggregate stability have been developed, for example using sonication to mechanically disrupt aggregates coupled with particle laser granulometry. (*191*) These techniques allow the particle sizes to be determined more accurately and remove the variability that comes with manually sieving aggregates. Techniques such as these could be manipulated to infer differences in bonding interactions. Recently, imaging aggregate breakdown

using image recognition and processing has been used to determine slaking kinetics. A camera was used to measure the change of an aggregates area once an aggregate was submerged in a petri-dish and imaged from above. The imaging data was found to be accurately described by a sigmoidal function (Gompertz function) and the maximum slaking potential was shown to correlate linearly to chemical attributes such as exchangeable sodium, pH, clay content, calcium/magnesium and total carbon/ nitrogen. Aggregates were found to be more stable in natural systems then in farmed land. Previous studies have modelled slaking breakdown to exponential functions, however, the Gompertz function appears to describe the breakdown kinetics of natural soil aggregates well. (*192*)

4.2.5 Slaking kinetics

The breakdown of soil aggregates may be the result of a number of processes acting simultaneously, but these processes may play out over different time-scales. Time resolved experiments, may be able to identify different mechanisms of aggregate breakdown, indicated by changes in slaking rate or the appearance of finer particulates.

The initial breakdown of aggregates may be 'explosive'. This is caused by the rapid build-up of pressure within an aggregate as water ingress compresses air pockets. This explosive slaking is likely to result in the release of large fragments quickly. Alternatively, slaking may also occur quickly, but by the release of small particles in a stream of material, this is more likely the result of fast wetting and the hydration of surfaces which cause stable microaggregates to break away. The material may also disperse as wetting the material causes a build-up of repulsive electrostatic forces which form a cloud of dispersed material as the solid wets. Dispersion may occur at a slightly longer timescale, requiring hydration of surfaces and the disruption of inter-particle interactions first. Strongly hydrophobic materials may resist wetting and form water stable aggregations via hydrophobic interactions. Slaking will be drawn out, occurring over a larger time-scale.

4.3 Methodology

Artificial aggregates were formed by drying clay and organic matter pastes in 1 cm^3 moulds as previously described. The paste was dried for 18 hours at 35 °C and artificial aggregates of similar dimensions were tested. Porosity, density and mechanical strength were also tested as part of a related study (see chapters 2 and 3), and this may be referred to in the discussion.

The slaking of individual artificial aggregates was monitored via a video camera to identify the rate and nature of slaking using a customised flow cell. The video files were converted into grey-scale stacks (1/second) and processed using ImageJ. To count the particles and the movement of material through the flow cell the following assumptions were applied:

- The velocity of the falling particles is constant and similar for each artificial aggregate tested. More buoyant or slower descending particles may have a greater residence time in the frames and may wrongly increase the particle counts, the analysed imaging area was minimised in order to reduce the residence time of more buoyant particles in the frame. This ensures that most particles enter and leave the recorded area within a second.

- Refractive index and particle colour does not interfere with measurements. The experimental set-up is designed to maximise the contrast between the particles and the background.

- The depth of field used is sufficient to observe all particles, and that the particle breaks apart in the centre of the imaging cell, so that particles that are further away do not appear significantly smaller.

These assumptions were validated or challenged by visual inspection of the videos. Instances where these assumptions do not hold are mentioned in the discussion. The artificial aggregates were found to have low mechanical strength and low slaking stability, and traditional slaking methods such as wet sieving were too forceful, resulting in fast degradation and could not be used as a comparison.

4.3.1 Slaking apparatus

The apparatus consisted of backlit acrylic box with a clear side and a top mounted sample holder where the artificial aggregate was introduced to water (Figure 4.1 and 4.2). Rubber seals were used in the device design but are not included in the figure images. The flow cell was backlit using a 25 W incandescent light bulb onto a white translucent acrylic plastic sheet. The white acrylic sheet acted as a diffuser, creating an even illumination of the sample cell. The illumination was inspected visually and using imageJ and the backlight was fixed at a certain distance using a wire bracket. The camera was mounted on a tripod at a set distance from the box, with the camera centred in respect to the box. Camera settings were adjusted as to focus on the back of the box, using a macro setting with sufficient depth of field to allow imaging of particles closer to the front of the acrylic box with reasonable resolution. An inlet/outlet tube was included in the flow cell design, which could be used to flow water around the aggregates and through the cell, however the stability of the aggregates was low, and a flow was not required. This flow may be helpful for more stable aggregates, or for slowly exchanging the solution for one containing salts or ethanol mixtures. It could also be used to control for either fast wetting (submersion – used here) or slow wetting (by slowly filling the sample chamber with water using a syringe). The experiment was run in a covered fume cupboard with the lights off. Additional screens were used to remove stray light and reflected light so the only light reaching the camera was from the back light.

An area 150 pixels square was taken for analysis, and a second area, 100 pixels square was taken from a region containing no particles to measure and correct for fluctuations in light intensity measurements of dispersion.

4.3.2 Interpretation of images

- **Particle counts:** Discrete particles which form on slaking can be counted and crudely sized by pixel area. Particle counts are used to determine breakdown kinetics and are plotted cumulatively until the aggregate is fully slaked. The cumulative particle count, can also be converted into a percentage slaked. Since all aggregates tested are of a similar volume, there is

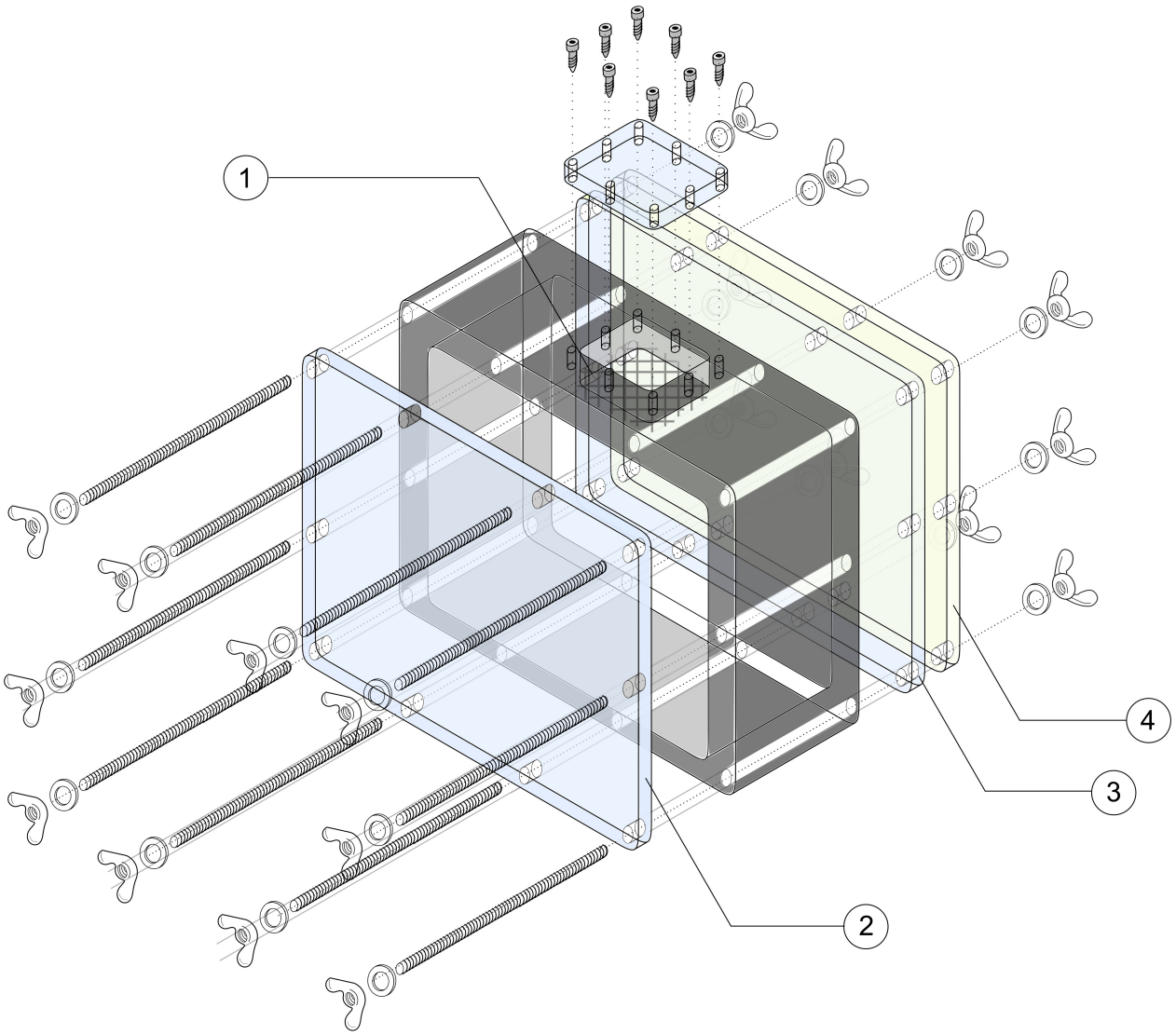

Figure 4.1: Technical drawing of imaging cell, consisting of 1: Exchangeable mesh to containing sample. 2: Clear acrylic front panel, 3: Clear acrylic viewing window with 4: white acrylic diffuser for incoming light.

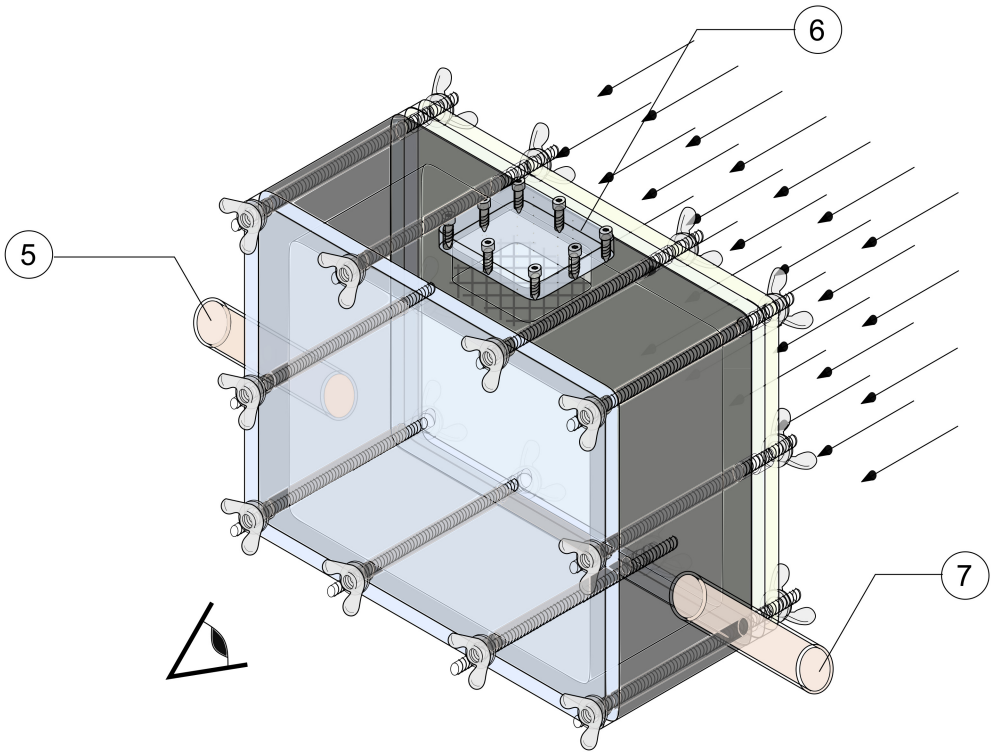

Figure 4.2: Technical drawing of assembled slaking cell with inlet and outlet hoses included. 5: Inlet hose from syringe pump, 6: sample cell, 7: outlet hose to waste.

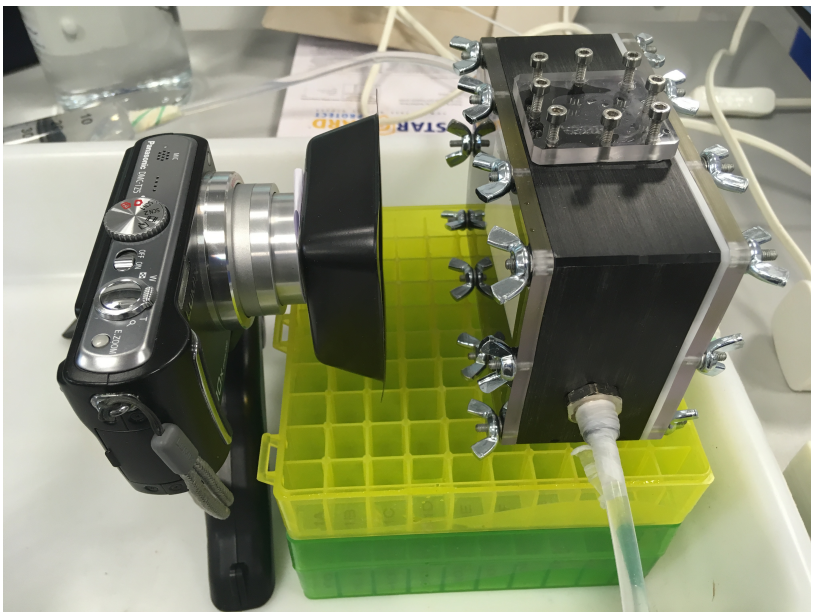

Figure 4.3: A photo of the experimental set-up consisting of a camera and the flow cell. The whole set up is kept in the dark whilst recording in order to block out stray light.

likely to be a linear and positive relationship between the size of particles formed and the rate of aggregate breakdown. A larger number of particle counts is also indicative of smaller particles being formed. Larger particles suggest the formation of water stable micro-aggregates.

- **Dispersion:** Dispersed material is formed when fine particulates become wetted, and electrostatic repulsion is formed between surfaces. Detection of dispersed material suggests that the clay has been destabilised. Alternatively dispersed material could form when clay coats surfaces as a thin layer, and this material forms a dispersion as clay is lost from a surface.

- **Slaking onset:** The slaking onset refers to the delay before any particles are observed. This parameter indicates the initial stability of the aggregate, which is thought to be related to total porosity, wettability and inter-particle binding.

- **Slaking duration:** The slaking duration gives the total stability of the wetted aggregate.

- **Slaking rate:** The cumulative particle counts can be used to calculate a slaking rate, the rate may be indicative of the strength of interactions between particles.

- **No/limited slaking:** This suggests that stable aggregations have formed which resist breakdown in water.

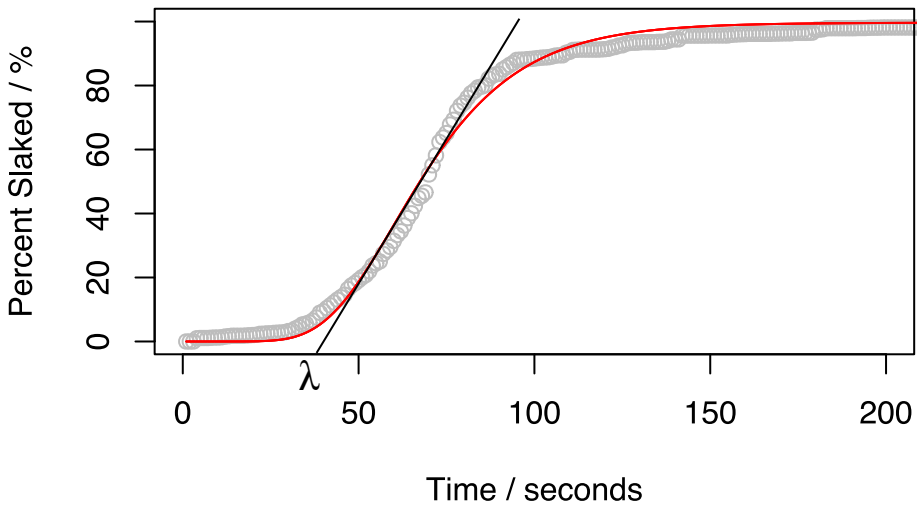

Figure 4.4: An example of Gompertz fitting to the slaking profile of kaolinite, the red line indicates the fitted function, the linear line represents the maximum slaking rate defined by μ. The lag-phase λ, is the point that the linear function crosses the x axis.

4.3.3 Gompertz model

Slaking kinetics have previously been fitted to the Gompertz function, which is a modified exponential function and can be written and modelled as:

$$\%Slaked = Ae^{-e^{\mu e/A(\lambda - t + 1)}} \tag{4.1}$$

Where A defines the maximum, t is time, μ defines the maximum gradient (here the maximum slaking rate) and λ is often called the lag-phase, and represents the position along the x axis where the linear gradient would cross at y = 0. Here, λ is a convenient variable for the offset. The Gompertz model presents a considerable advantage over a simple exponential which cannot provide an offset value. Graphs of slaking percent vs time were fitted to a Gompertz model using R, to attain parameters relating to the initial slaking stability and the maximum rate of slaking (Figure 4.4).

4.4 Results

Kaolinite artificial aggregates broke down rapidly ($<$ 100 s) into small discrete particles and little dispersion was observed. Slaking duration was measured to be 66 $\pm$ 13 s, with a delay (or onset) of 17 $\pm$ 6 s. Although it is possible to measure the particle size (measured in pixels) over time, the distribution was very large and no significant change occurred over the duration of slaking. Although the artificial aggregates had similar dimensions, the total amount of material present can also present an additional variable which may also give rise to higher error in measuring particle counts, especially when the particle sizes are small. To correct for this, and to compare the slaking kinetics, the graph can be replotted as a percentage of the total particle counts, or percentage slaked. Data presented as percent slaked gave extremely reproducible data and the line shapes were found to be near identical with three repeats. This suggests that large errors in particle counts are due to the variable mass or volume of material present in the initial sample, although it was not possible to correct for this by dividing the counts by the sample mass. It is difficult to obtain samples with identical sample volumes, as it is difficult to obtain real soil aggregates with identical volumes. Plotting data as a percentage slaked offers a more useful metric to compare the kinetics of aggregate breakdown, but this requires slaking to reach completion in a reasonable time-scale (minutes) or large amounts of image data will need to be processed.

In order to determine if the slaked material contained larger particles due to the formation of water stable aggregates, the particle size of both the slaked and the raw kaolinite material was compared. Particle size analysis of a dispersion of kaolinite in water versus the kaolinite after being dried and crushed showed that the particle size was reduced after wet/dry cycles (Figure 4.5). Measurements in a previous chapter showed that a kaolinite solution became more acidic following a wet/dry cycle, and this could lead to the formation of smaller, more dense particles caused by face-face stacking. The light scattering data suggests that the bulk of the kaolinite is dispersed as singular particles, but a large fraction exist as larger microaggregates.

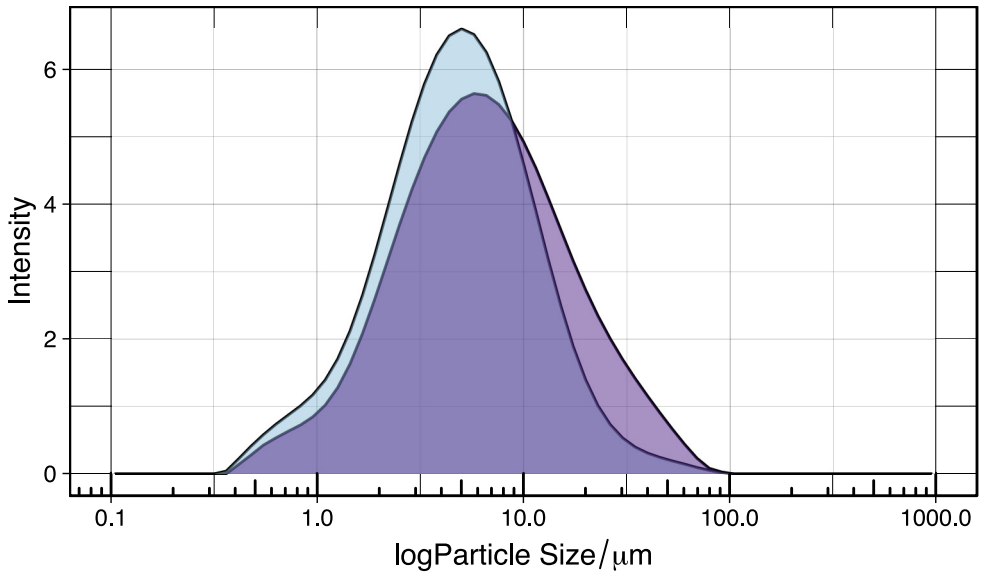

Figure 4.5: The particle size distribution of kaolinite as received (purple) and slaked kaolinite (blue) dispersed in DI water, showing a reduction in particle size following slaking.

4.4.1 Influence of restraining mesh on breakdown kinetics

A mesh restraint was able to retard large fragments of aggregate from leaving the cell and moving through to the view finder too quickly without fully breaking down. Reducing the rate of slaking by reducing the threshold size before particles can exit the sample chamber may help for comparisons of materials with similar slaking behaviour. This is because it reduces the number of particles which are present in each image, which may reduce errors due to overlaps and crowding. Additionally, more subtle changes in breakdown kinetics may be observed. In order to investigate the effect of the mesh size on particle counts and the slaking kinetics, a 1 mm mesh was compared with three horizontal wires which allowed for a more rapid unimpeded breakdown. The kaolinite sample was used as all samples investigated here contain kaolinite, additionally breakdown occurred in under 15 minutes when left submerged in water and fine particles were observed with little dispersion.

Figure 4.6, A shows that the mesh increases the number of particles that are counted, as the particles have to break down into smaller fragments before leaving the sample cell. The sample breakdown however, was prevented by the mesh, and the material was blocked from breaking down fully, extending the slaking to over 15 minutes (full experiment not shown). Slower slaking may help in analysing samples with more rapid slaking or with smaller differences in slaking behaviour.

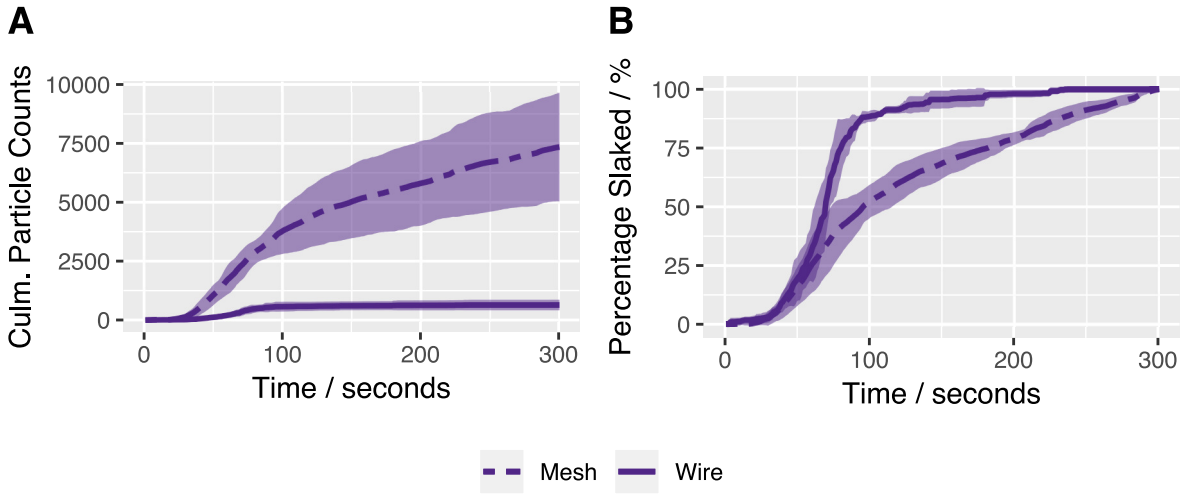

Figure 4.6: **A:** The cumulative particle counts are higher for kaolinite slaked using a mesh sample holder, due to the mesh retaining larger particles. **B:** The onset for both samples was similar and the plateau for the three wires samples occurred at a similar point for the intersect between the initial rapid rate of slaking and the slower rate of slaking. Errors are plotted as standard deviations and visualised as purple ribbons (n=3).

Using the cumulative particle counts, the percentage material slaked was calculated, which is more convenient to observe the change in breakdown kinetics (Figure 5, B).

The apparent onset of slaking was extremely comparable with a delay of < 10 seconds between the wire and mesh result. Slaking was found to be most rapid at the beginning of the experiment for both, followed by a plateau for the wire and a large change in rate of slaking for the mesh. The plateau of the second region with slower slaking was therefore considered to be the point at which the clay had been broken down fully into large particles, and the second region relates to a breakdown into finer material which can pass through the mesh. The duration of the first region using the mesh was also found to be around 66 seconds, identical to that of the 3 wire method, although higher errors were recorded (table 4.1). Since the sample in the mesh did not finish slaking in the time of the experiment, a calculation of percentage slaked is not accurate but presented here for a comparison of the line shape only.

The breakdown kinetics for kaolinite is simple, the onset represents a delay, in which the sample is wetted, followed by a rapid and almost linear slaking, which slows and plateaus rapidly. Particles are likely to be water stable aggregates, formed by strong face-face interactions, predominant in this kaolinite sample.

Sample	Onset /seconds	Plateau /seconds	Duration /seconds
Mesh restraint	27 ± 7	93 ± 16	66 ± 23
Wire restraint	17 ± 6	83 ± 10	66 ± 13

Table 4.1: The slaking characteristics of kaolinite artificial aggregates with a finer mesh. Slaking time was calculated from the intersect of the two tangents formed by the initial more rapid slaking and the second slow rate of slaking, due to the blockage formed in the mesh.

4.4.2 Bound electrolytes in kaolinite aggregates

Solutions of 0.1 M and 0.5 M NaCl and $CaCl_2$ were added as electrolytes on forming the artificial aggregates, the artificial aggregates were then slaked in DI water to test the effects of the adsorbed cations on resisting slaking. Initial trial experiments showed that there was large variation in the slaking behaviour of these materials and so a three-wire restraint was used. All samples made with the additional salts extended the slaking duration. Kaolinite without an added electrolyte fragmented quickly, larger particles were observed, and slaking finished within 250 seconds (Figure 5, A). When salts were present, the particles observed were smaller and were released more slowly.

The addition of 0.1 M NaCl or $CaCl_2$ reduced the slaking rate, and did not fully slake in the experimental timescale (15 minutes). However, the remains of the swollen artificial aggregates left in the sample container were not stable and were easily disrupted with a spatula. The slaking behaviours of the kaolinites amended with 0.1 M salt solution were extremely similar and it was impossible to differentiate them, although they may have behaved differently at longer timescales. This suggests that the rapid rate of slaking in the pure kaolinite sample is caused by extremely low electrolyte concentrations, which may increase the water potential and accelerate water ingress. The addition of 0.5 M NaCl or $CaCl_2$ also reduced the slaking rate, however, NaCl produced many more particles than $CaCl_2$. Sodium salts are known to destabilise clays and cause them to disperse and here sodium is found to extend slaking, however little dispersion was detected. Mechanical tests on these same aggregates suggest that no substantial change in fabric occurs on the addition of sodium salt, calcium however may promote edge-face interactions, which form larger particles as they slake. $CaCl_2$ increased the stability of the kaolinite so that a cohesive artificial aggregate could be obtained after 15 minutes of being submerged in water. The calcium ions retained by the kaolinite may be affected by the volume and conductivity of the water in the cell, and more stable artificial aggregates

are likely to be obtained when water has a higher electrolyte concentration. Analysis of the slaking profile can only be done in a qualitative manner as the samples with high concentrations of salt did not completely slake in the timescale of the experiment, limiting the information that can be inferred from this data (Figure 5, B). Kaolinite with 0.1 M $CaCl_2$ appears to have a single slaking rate, but the equivalent concentration of NaCl results in an initial slaking, similar to that of pure kaolinite, followed by a change in slaking rate. This may indicate that the dissolution of ions away from the kaolinite modifies the slaking rate. The same change in rate appears to be present with 0.5 M NaCl, but the transition is less obvious.

These experiments show that the slaking behaviour of kaolinite clays are significantly affected by high concentrations of salt, although at lower electrolyte concentrations, the slaking behaviour does not differ strongly with different salts. Adding NaCl as an electrolyte did not affect the mechanical properties of pure kaolinite, suggesting that the kaolinite fabric is not modified by the presence of sodium cations at low pH. This is thought to be due to the predominance of face-face stacking interactions, the formation of which is not affected significantly by indifferent ions such as $CaCl_2$. The slaking of aggregates containing $CaCl_2$ results in the formation of small particles (tactoids of kaolinite) formed by face-face interactions, but dissolution of $CaCl_2$ away from the surfaces of clays can slow the rate of slaking by reducing electrostatic repulsion. The addition of $CaCl_2$ resulted in a mechanical strengthening as a result of a change in fabric of the kaolinite. At low pH kaolinite forms tactoids, but the addition of $CaCl_2$ may promote edge-face interactions in the clay. Ca^{2+} is known to form stronger interactions at clay faces, and so the dissolution of calcium into the bulk solution may be slower than for $CaCl_2$. The presence of Ca^{2+} reduces electrostatic repulsion and potentially creates additional clay-clay interactions. Particle sizes also may appear bigger, as edge face interactions result in less dense micro-aggregations of kaolinite.

4.4.3 HDPE

HDPE particles with differing surface functionality were compared at 55% volume loading (30% HDPE mass loading). The unmodified HDPE particles had a d(0.5) of 89 μm, the modified particles contained COOH surface functionality and had a d(0.5) of 45 μm. The sample artificial aggregates

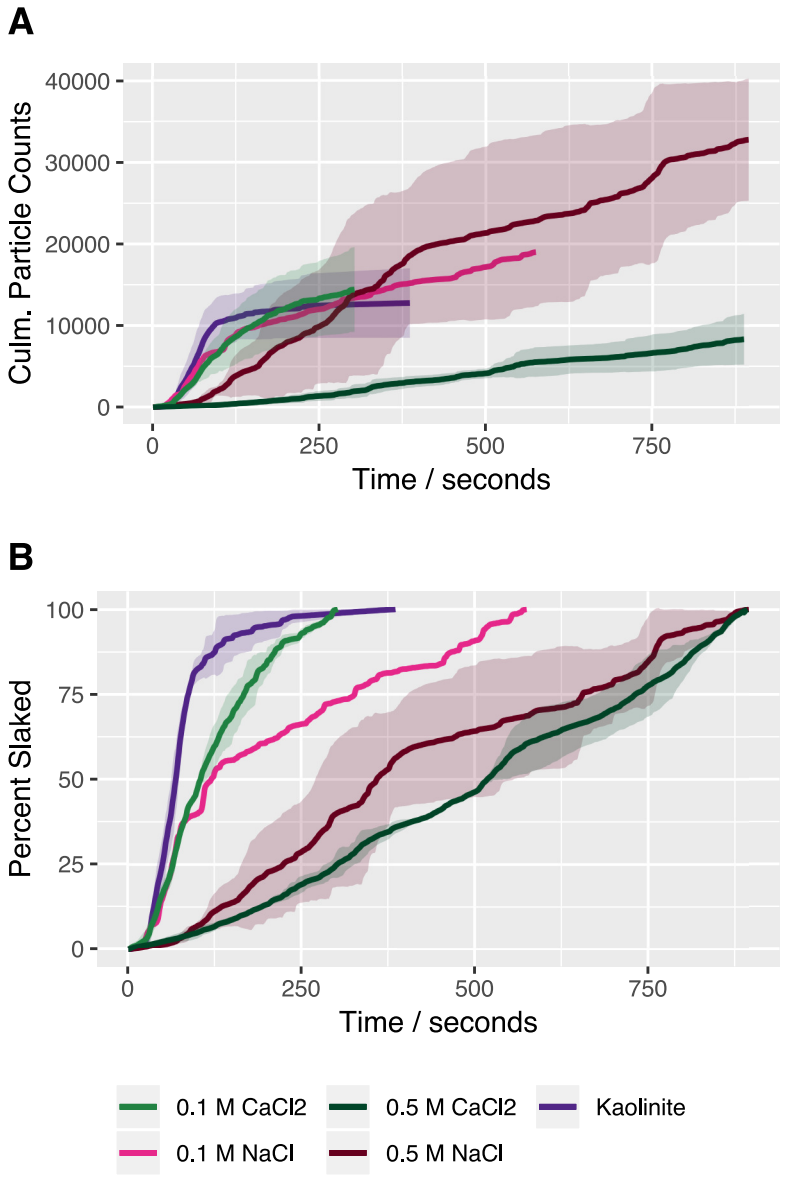

Figure 4.7: Kaolinite made with additional salt solutions showed very different slaking behaviour. **A:** The culmulative particle counts was highest for sodium salts and lowest for calcium. **B:** The slaking percentage is shown to illustrate line shapes, but is not quantitative since the samples did not slake in the timescale of the experiment. All samples represent three repeats except for 0.1 M NaCl which is a single measurement. Standard deviation either side is visualised as ribbons. Kaolinite without added salt is in purple, $CaCl_2$ is in green, NaCl is pink and dark red.

were held by 3 wires, which allowed for more rapid, complete slaking as initial observations on the slaking of the artificial aggregates suggested there was a large variation in slaking behaviour.

The slaking onset is thought to be related to the internal porosity, wettability and strength of particle interactions holding the aggregate together. The slaking onset for artificial aggregate containing COOH modified HDPE particles was marginally longer (6 seconds), which may reflect the reduced porosity of the modified HDPE artificial aggregates (33 %) as compared to kaolinite (42 %), and the reduction in surface area (HDPE particles are large and have less surface area than kaolinite) per volume. The unmodified HDPE artificial aggregates however, were found to have an intermediate porosity of 35%, but an almost immediate slaking onset. The immediate slaking of the HDPE artificial aggregates may be a result of weak inter-particle bonding which is unable to withstand internal pressures caused by water ingress. Additionally all samples initially broke down via the formation of small discrete particles. This suggests that inter-particle interactions are a bigger driver of slaking onset than porosity with these samples.

In addition to increasing the slaking offset, the slaking duration was marginally extended with the addition of 55% loading of surface-modified HDPE particles. This overall increase in slaking stability may just reflect a 10% reduction in porosity, although the observed mechanical strengthening (see 2.7) may indicate that stronger inter-particle interactions may contribute. The number of particles observed were also much higher than that for kaolinite, and therefore much smaller on average. Large particles were observed early on, however these particles quickly dispersed once they had reached the bottom of the sample cell. The amount of material which dispersed in the cell increased considerably with the modified HDPE as compared to kaolinite (Figure 4.8 **C**). Hydrogen-bonding interactions, the primary interaction between surfaces of kaolinite and modified HDPE are wetted easily, and are unlikely to resist water ingress, electrostatic repulsion is also likely to occur as both particles have a net negative charge. The line shapes were comparable for kaolinite and aggregates containing modified HDPE, suggesting similar slaking kinetics and a similar breakdown mechanism. There was no indication via a change in breakdown kinetics that the aggregate breakdown mechanism changed as dispersive forces evolved. This means dispersion follows slaking in this case. A decrease in slaking rate is observed with the addition of modified HDPE particles, however since the dispersed material was high, this cannot be considered an increase in slaking stability. The reduction in porosity and

surface area is likely to have been the primary driver of a longer slaking duration.

Unmodified HDPE particles were unstable in water, however the slaking duration was much extended (Figure 4.8), releasing a slow stream of fine particulates, which did not disperse considerably in the lower portion of the imaging area. The reduction in particulate size confirms that HDPE additives of both kinds disrupt the stable microaggregates formed by pure kaolinite. It would be expected that a reduction in kaolinite-kaolinite interactions would increase the slaking rate and increase dispersion. However, since unmodified HDPE contain no surface functionality able to bind to kaolinite, any stabilisation must be the result of hydrophobic interactions formed between the surfaces on wetting.

The slaking behaviour for an extended range of HDPE loadings was investigated. The slaking stability was found to increase as the loading of surface modified HDPE particles increased (Figure 4.9, **A**). Increasing the loading of modified HDPE particles increased the slaking duration and the slaking onset time, although the onset was not found to be strictly proportional to loading or porosity. The slaking duration however, increased as a function of loading almost linearly, suggesting a direct influence of the particle interactions in slaking stability. The particle counts were also greatly increased with respect to the kaolinite (Figure 4.9, **C**), suggesting the formation of smaller particles.

The addition of modified HDPE at different loadings had a significant impact on the amount of dispersed material (Figure 4.9). At 24% volume loading modified HDPE, dispersed material was observed more quickly due to the faster initial slaking, but less material was observed overall as compared to aggregates where the majority of the particulate volume was HDPE.

Figure 4.11 is a plot of the initial slaking rate (measured as percent slaked/second) as a function of HDPE loading. These values were obtained via a linear fit of the initial, more rapid slaking rate ($R^2 > 0.98$). There is a step-drop between 10% and 30% loading, indicating the change in rate with HDPE is non-linear. This means that it likely that at low loadings the rate is dominated by kaolinite, and at higher loadings it is dominated by the HDPE. Slaking rate may therefore be representative of a major phase, or like mechanical strength testing, is dependent on a percolation threshold.

The large increase in slaking stability observed by the addition of the unmodified HDPE particles suggests a powerful hydrophobic stabilisation on wetting (Figure 8, B). The unmodified HDPE

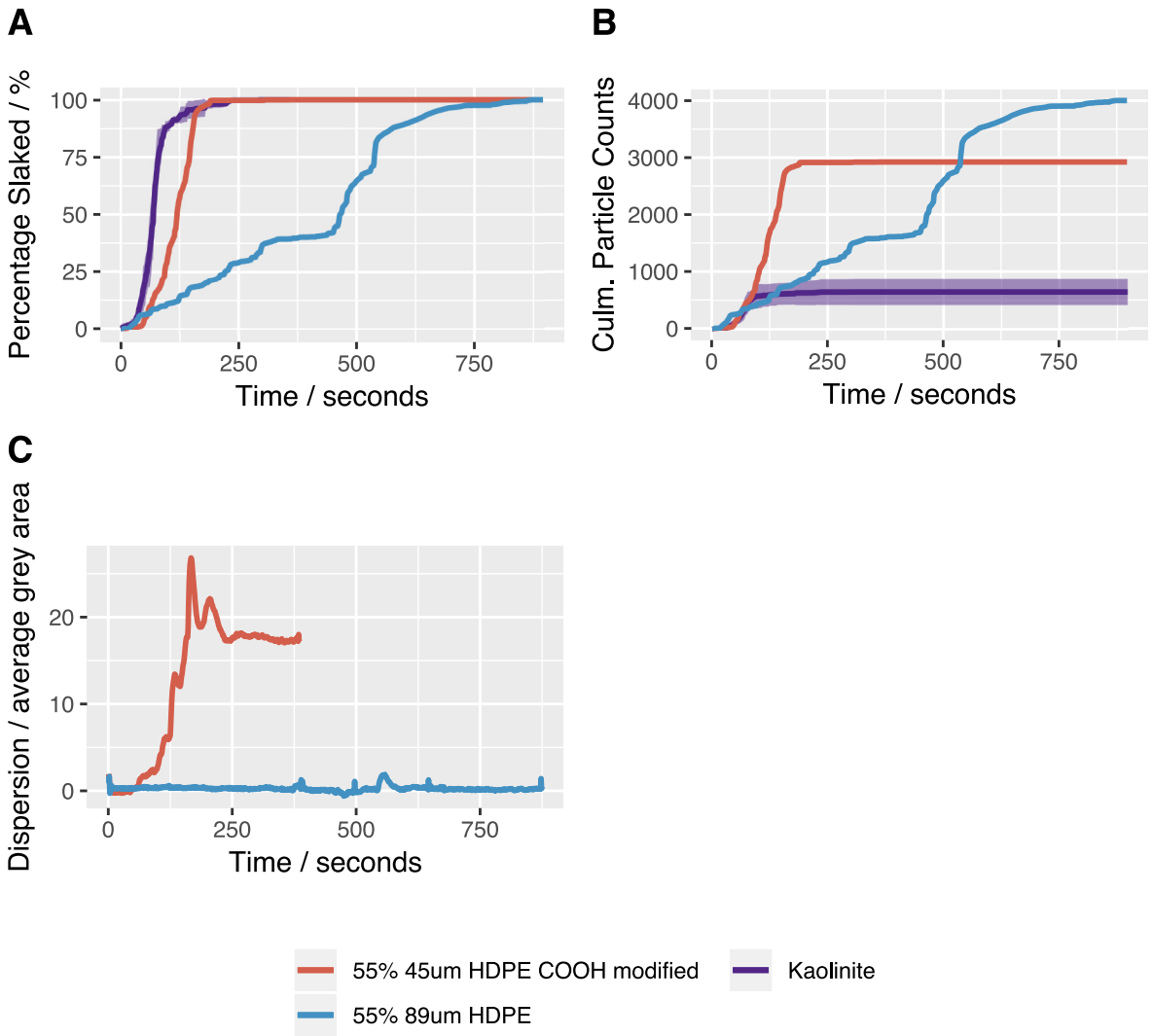

Figure 4.8: HDPE particles with and without COOH surface modification added at 55% volume loading were compared. **A:** The percent slaked showed that the slaking profile for the modified HDPE and kaolinite were similar **B:** The cumulative total particle counts for the modified HDPE were much higher for both, with kaolinite forming larger, more discrete particulates. **C:** The dispersion was measured to be considerably higher in artificial aggregates containing modified HDPE. The dispersion reached a maximum around 160 seconds. (A and B errors for kaolinite shown as purple ribbon, n = 3).

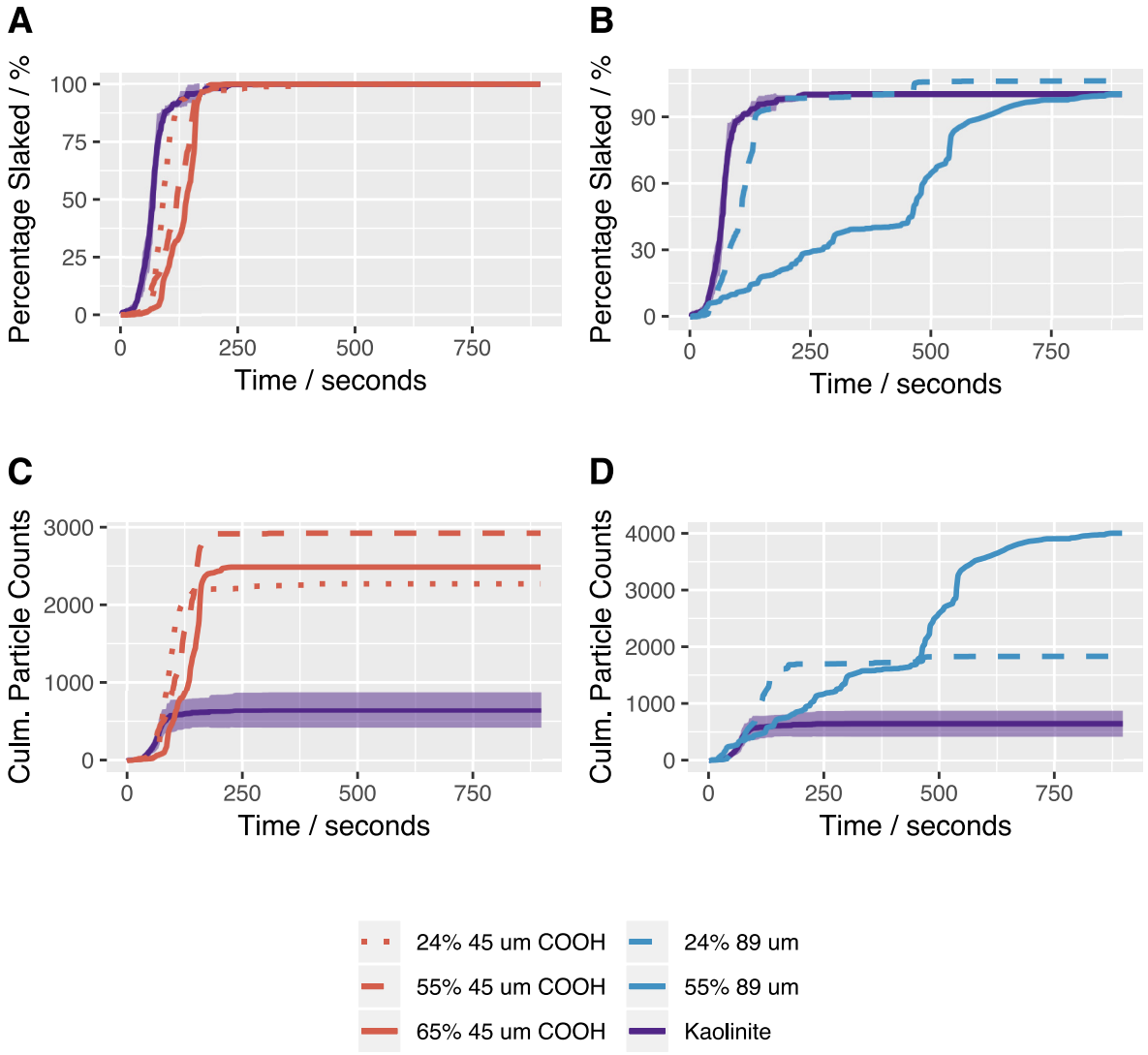

Figure 4.9: 24, 55 and 65 % volume loadings of surface modified HDPE artificial aggregates as compared to pure kaolinite, is shown as a percentage of material slaked **(A)** and as total particle counts **(B)**.Unmodified particles at 24, 55 % volume loadings are shown here, as percentage slaked **(B)** and total particle counts **(C)**, higher loadings (65%) were found to be stable to slaking and so no particles were imaged.

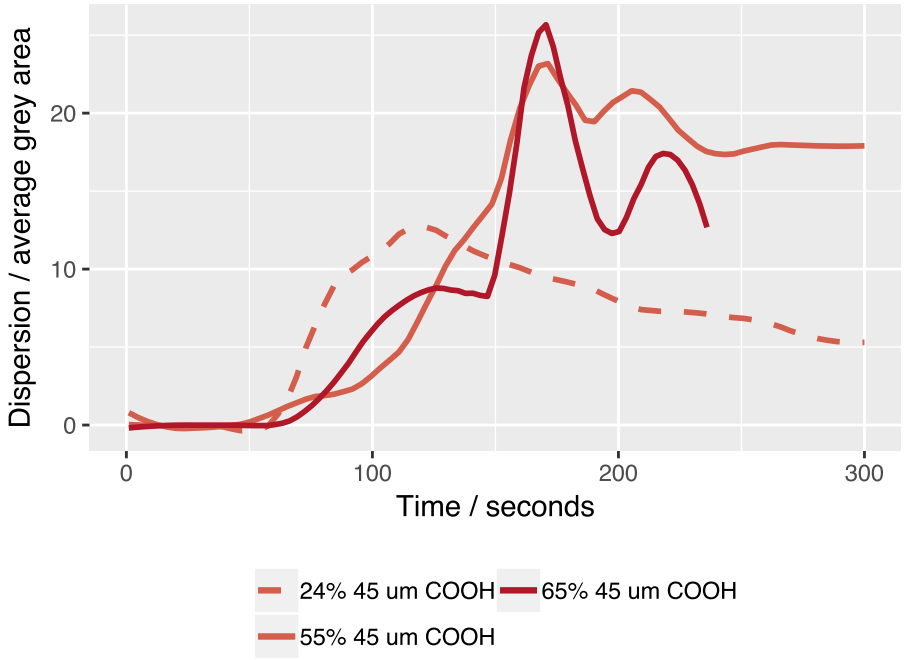

Figure 4.10: The dispersion of the COOH modified HDPE cubes. Dispersed material was observed more quickly at lower HDPE loadings. At loadings where modified HDPE was the main component ($>$ 50%) the dispersed material was very similar. Pure kaolinite had almost no dispersed material.

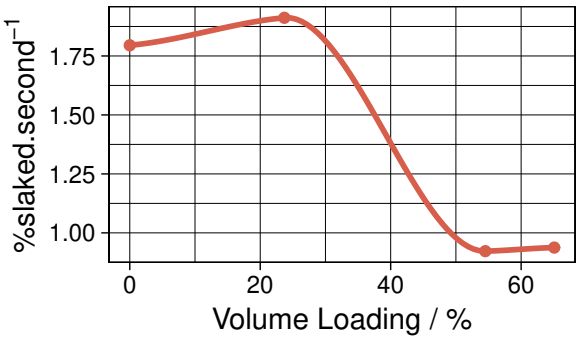

Figure 4.11: The slaking rates of COOH modified HDPE as a function of HDPE volume loading, the slaking rate transitioned from a more kaolinite-like slaking rate below 50% volume loading, to a slower rate at higher loadings. This is indicative of a percolation threshold.

was visually, extremely hydrophobic in powder form, resisting wetting and clumping when added to water. Despite this, HDPE aggregates formed well mixed pastes, and no phase separation was observed suggesting kaolinite was able to increase the wettability of HDPE. 24% HDPE extended the slaking time marginally, but above 55% HDPE loading the aggregates were extremely stable. At 65% loading, the artificial aggregates were stable submerged in water for 15 minutes, and so no slaking data was recorded. The 65% HDPE artificial aggregate was found to be swollen and almost gel-like, and soft to the touch, this suggests that the interactions are weak and associative and would likely be broken by mechanical disruption. Because the pure kaolinite artificial aggregate was almost fully slaked after a minute, this suggests that there is a strong hydrophobic interaction formed between the kaolinite and the HDPE particles when wetted. Mechanical testing showed a very weak interaction between HDPE and kaolinite, with artificial aggregates weakening in mechanical strength as a function of HDPE loading.

4.4.4 Lignin

A series of lignin:kaolinite aggregates were measured. Initial test observations indicated a more subtle variation in slaking behaviour and so a mesh was employed to slow slaking. The slaking profiles were very similar (Figure 4.12) with the aggregates initially slaking rapidly, followed by a prolonged and more gradual slaking period. Artificial aggregates containing higher lignin contents formed swollen gel-like materials which were unstable to violent shaking or to disruption with a spatula, but remained in the sample holder and could be handled. These aggregates are only semi-stable to slaking, and stability increased with higher lignin contents. The slaking onset was not significantly changed with the addition of lignin, despite a large increase in the porosity, and the particle size (measured in pixel area) was not found to change significantly from kaolinite. Spruce lignin was not as effective at reducing the slaking and formed weaker aggregates in mechanical tests. Spruce lignin appears however to be marginally more hydrophobic via crude wetting experiments (not shown).

The rate of initial rapid slaking, as with the rate of the proceeding slower slaking (not shown), was found to decrease as a function of lignin loading (Figure 4.13 **A**). Analysis of the duration of this slaking region suggests that the duration is controlled by the major volume phase as there is a large

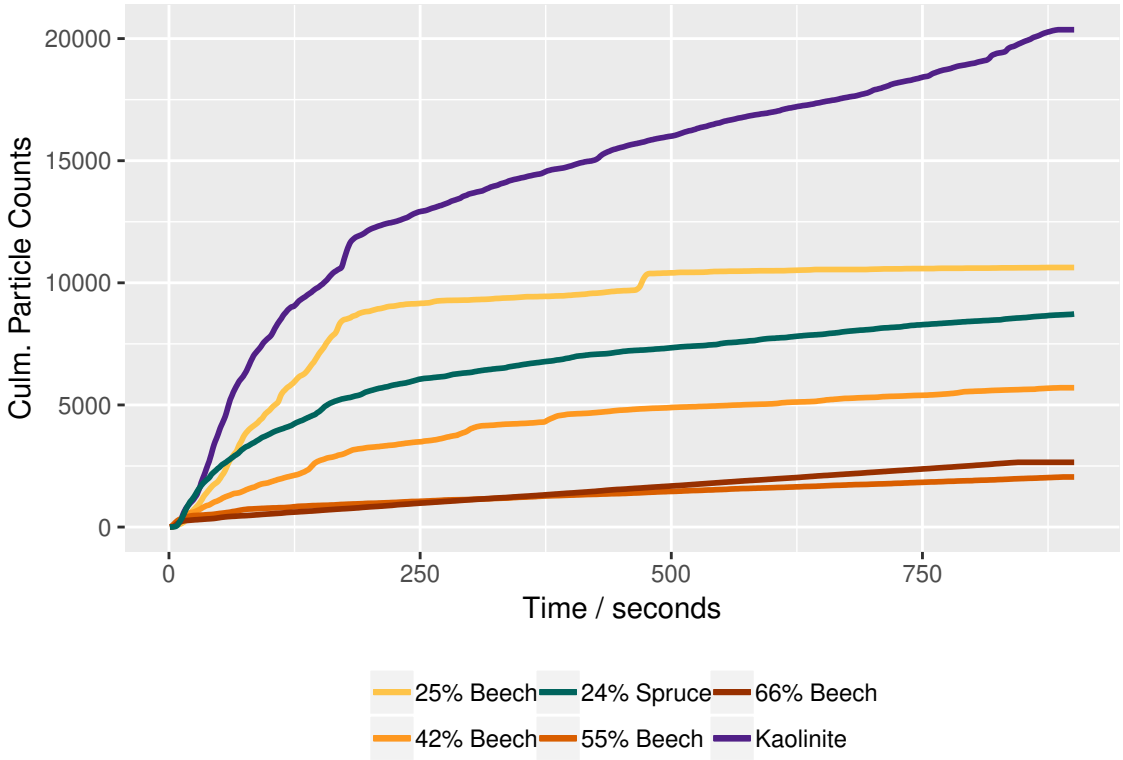

Figure 4.12: The cumulative particle counts for the lignin:kaolinite aggregates for which slaking rate and duration was calculated. Errors are omitted for clarity.

drop in duration around 50% lignin (Figure 4.13 **B**). The total particle counts decreases linearly as a function of lignin loading (Figure 4.13 **C**). The addition of 25% volume lignin resulted in a 50% reduction in the particles observed, suggesting that more kaolinite was retained than would be expected if only the kaolinite was slaked, but it is not clear if this is due to entrapment alone, or a stable interaction. The material collected after slaking was brown, and not enriched in kaolinite, suggesting that the slaked material contained both components. The change in slaking rate does indicate that lignin stabilises the kaolinite, and that this stabilisation increases with lignin loading, the rapid slaking is attributed to the kaolinite-kaolinite interactions, as this contribution to the slaking profile disappears as lignin becomes the dominant phase. This suggests that the initial rapid slaking duration (seconds) is a better indicator of the dominant volume phase, whereas slaking rate (particles/second) and total particle counts (counts) are a better indicator of the amount of the lignin present. In all cases, the composition of the aggregate is clearly dominant, with inter-particle interactions dominating slaking properties.

Particle size, measured in average pixel area, did not appear to change as measured using the image

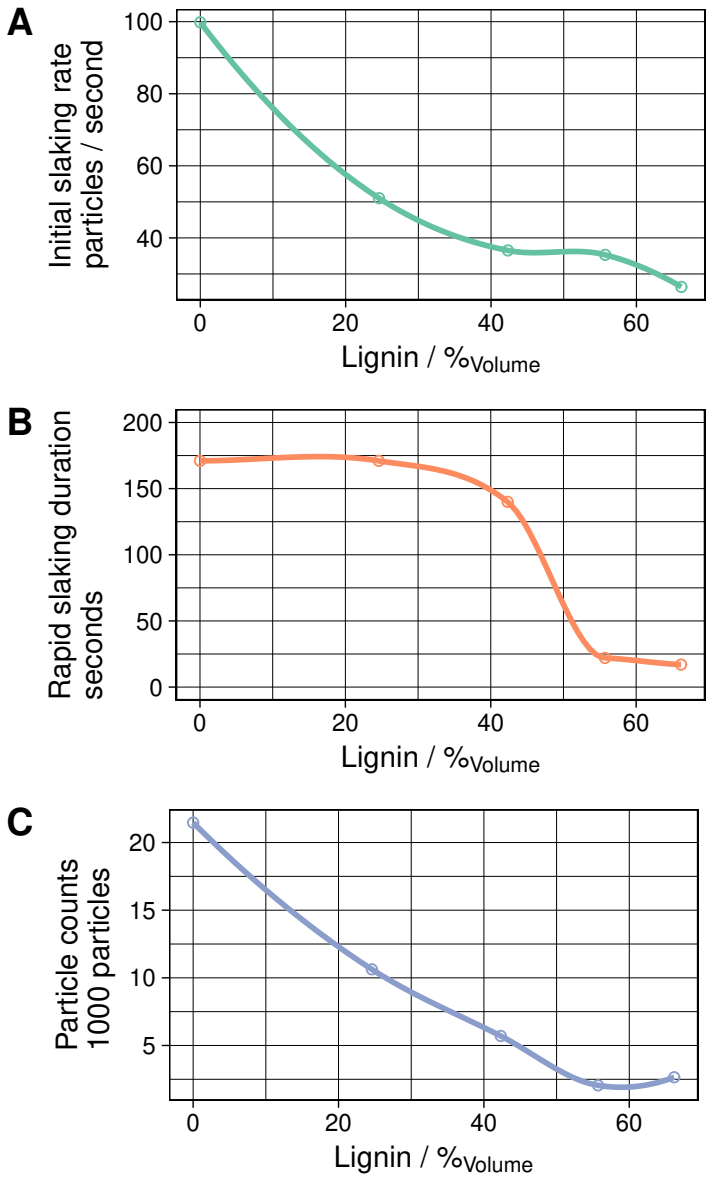

Figure 4.13: **A:**The initial slaking rate, appears to drop rapidly as the amount of lignin is added. **B:** The duration of the initial rapid slaking drops at around 50% lignin volume loading. **C:** Total particle counts at 900 seconds drops almost linearly with lignin loading, reaching a minimum around 50% loading.

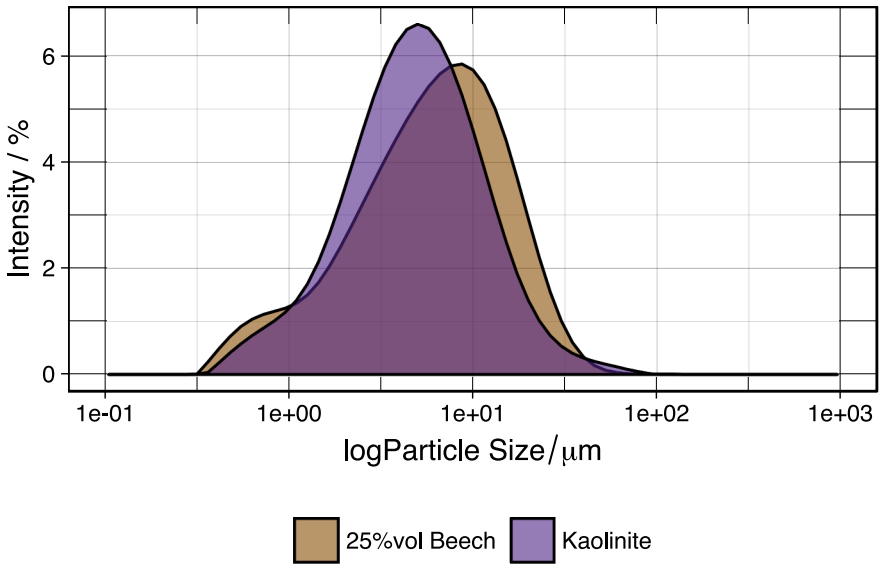

Figure 4.14: The particle size distribution of kaolinite and a 25% volume lignin aggregate, following complete slaking in DI water. Particle sizes increase with the addition of lignin, resulting in a d0.5 increase of 27%.

analysis, and particle size was pretty consistent over the duration of slaking. Particles were small however and the particles were too low resolution to be measured accurately. Pixel areas measured were between 4-8 pixels, and were at the very lower limits of the cameras resolution. In order to determine if particle sizes had changed considerably, fully slaked materials were analysed using static light scattering.

Kaolinite has a d(0.5) of 5.76 μm and a span of 2.46. Beech lignin has more heterogenous particle size with a d(0.5) around 10 μm. Adding 20% lignin to the artificial aggregates appears to increase the d(0.5) of the slaked material by 27% (Figure 4.14). In order to determine if this was due to the formation of stable aggregates on wetting and drying, the dispersed artificial aggregate was compared to a mixture of the powders. When measuring the powdered mix vs the artificial aggregate of a 20% lignin artificial aggregate, the particle size only increases marginally (this may account for refractive index, making the measurements more comparable) of 9 $\pm$ 1 %. Lignin:kaolinite mixtures therefor form water stable aggregates which are slightly larger than those formed by kaolinite alone. Because the particle size of lignin and kaolinite are relatively similar, it is not possible to say how the particles are aggregated.

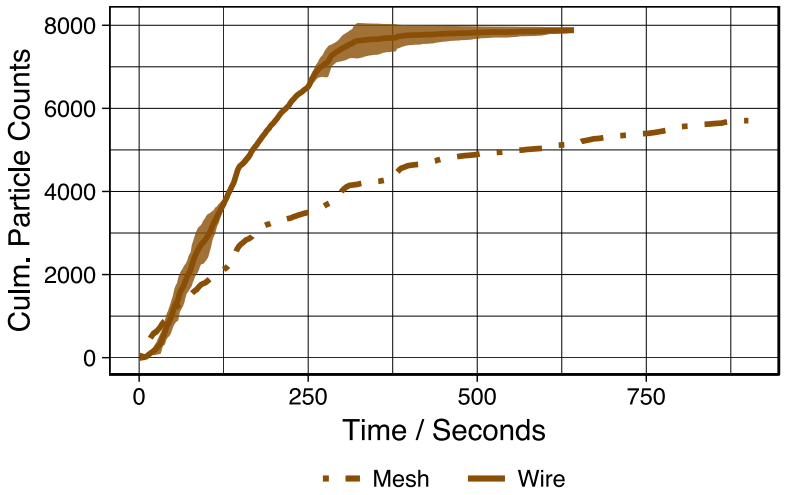

Figure 4.15: Comparing the slaking behaviour of a 42% beech lignin aggregate slaked using either a mesh or wire restraint. The plateau for the wire indicating complete slaking corresponds to a reduction in slaking rate for the aggregate held by a mesh restraint (indicated by black crossed lines).

4.4.5 Influence of restraining mesh on breakdown kinetics

The effect of a wire or mesh restraint on the slaking kinetics of a 42% beech aggregate was measured (Figure 4.15). The differences were very similar to that of kaolinite, and visual inspection of the line shapes indicated that the full slaking achieved using a wire restraint at around 330 seconds corresponded to a change in slaking rate to a slow linear slaking regime in the mesh profile.

4.4.6 Humic acids

Despite a strengthening of the aggregates containing 42% beech lignin, the slaking characteristics of cubes made with, or without humic acids were remarkably similar (Figure 4.16). Fewer particles were detected in the aggregates made with humic acids, but it is not clear if this is due to a difference in sample mass. The slaking kinetics however, were identical, suggesting no improvement in slaking stability despite evidence to suggest that humic acids play a role in aggregation in soils.

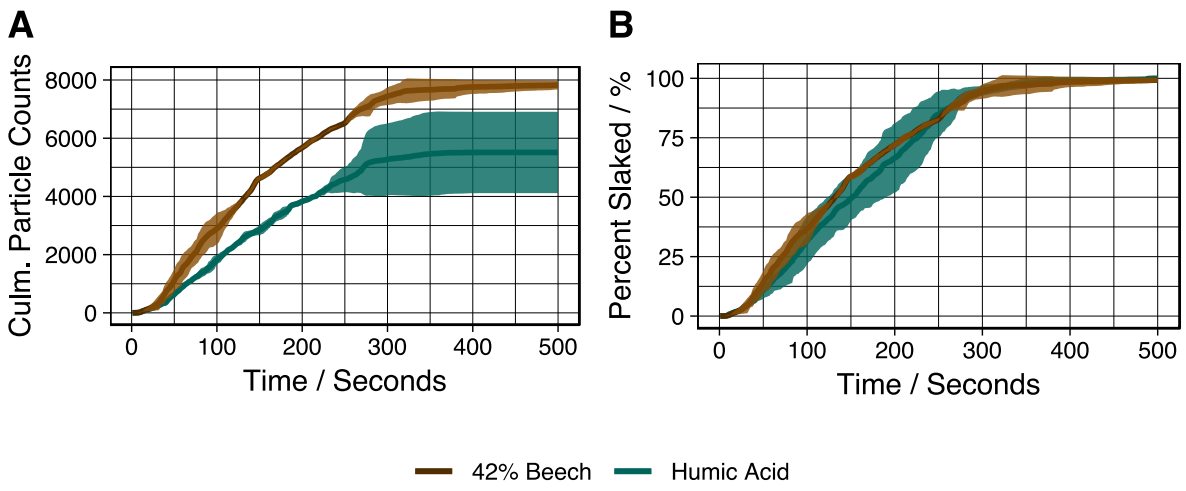

Figure 4.16: The addition of a concentrated humic acid solution to a 42%volume beech lignin cube was found not to change the slaking kinetics.

4.4.7 Cellulose

Cellulose pulp artificial aggregates were completely unstable in water, forming rapidly dispersing clouds of material very quickly. The recorded particle counts were much higher than those of kaolinite, and the slaking behaviour was extremely similar at all loadings (Figure 4.17, **A**). Slaking onset started later as cellulose content increased and slaking duration also increased with cellulose content. The mechanical strength tests showed that cellulose-cellulose interactions are far stronger than those of kaolinite-cellulose, and that artificial aggregates became much stronger at higher loadings. It seems clear that the slaking onset in this instance is strongly correlated with artificial aggregate strength. Dispersion of kaolinite occurs due to electrostatic repulsion on wetting, this can be via a change in pH or electrolyte concentration, alternatively if kaolinite particles are distributed on a surface, where face-face interactions have been disturbed, wetting may also cause the release of these particles. Since the dispersed material increases as a function of cellulose content, it could be that cellulose is the material, which is dispersed, and that the kaolinite is retained as individual particles. However, it is difficult to distinguish between the two materials. This material was not a stable suspension, but clouds which form and settle as particles fall to the bottom of the sample cell. This suggests that cellulose disrupts the kaolinite-kaolinite interactions, and all the interactions present are unstable to wetting.

The amount of dispersed material is strongly correlated to both particle counts and the percentage

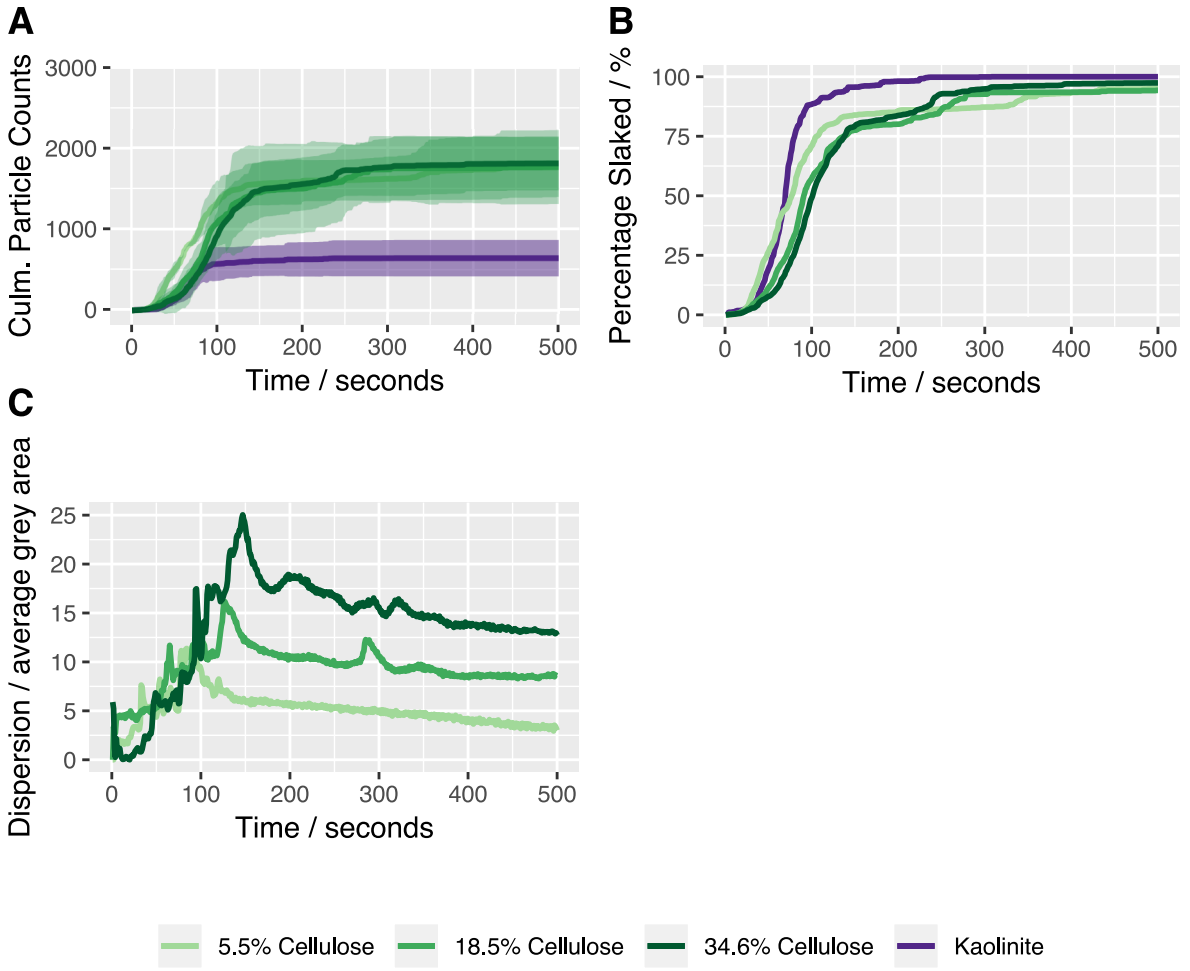

Figure 4.17: Slaking was very similar for all cellulose containing aggregates. **A:** The particle counts for cellulose containing aggregates was much higher than that for kaolinite. **B:** The slaking profile was not too disimilar from kaolinite, although there was a slight stabilisation in slaking rate. **C:** Dispersed material increased with increasing cellulose content, dispersed material reached a peak between 100 and 150 seconds, again, increasing with cellulose loading.

material slaked.

4.4.8 Biochar

Biochar is more hydrophobic than lignin. Pyrolysis reduces the oxygen content by driving off volatile aliphatics from the lignin, leaving a heavily crosslinked and aromatic carbon rich structure. (*193*) The onset of slaking is reduced linearly as biochar is added which may be due to an increase in porosity , despite an increase in hydrophobicity (Figure 4.19, **A**).

At low loadings (18.6 and 34.0 %), the total particle counts were very similar to that of the kaolinite, above this loading, smaller particles were observed. Analysis of the slaking profile suggested that even though the particle counts were extremely different, the slaking kinetics are very similar (Figure 4.18). The slowed slaking indicated biochar had a stabilisation effect, extending complete slaking by almost 100 seconds (Figure 4.19, **B**). The total slaking time for the maximum biochar loading (67.3%) exceeded 10 minutes but a large amount of fine particles and dispersed material was detected which reduced the accuracy of the measurements considerably. At 67.3% loading, the slaking duration increased, however the amount of dispersed material was substantial, and this cannot be considered an increase in aggregate stability, nor can the other loadings, which slaked with considerable dispersed material (Figure 4.18, **C**).

The initial slaking rate of all biochar amended samples was extremely similar to that of pure kaolinite, however slaking transitions to a slowed rate of slaking after about 100 seconds, where the exponential increase in particle counts is disrupted (Figure 4.18, **B**). This does not correspond to a change from slaking to dispersion as dispersed material was observed from almost immediately after the first particles had settled (Figure 4.18, **C**). The delayed slower rate of slaking may result hydrophobic interactions which form slowly between kaolinite and biochar, which may explain why the slower rate forms at the same time at each experiment. However, these hydrophobic interactions appear unable to stabilise the aggregate fully despite significant hydrophobicity and surface area. For the lignin samples, the rapid slaking rate transitioned to a slower slaking rate at 150 seconds for samples contain a majority of lignin, here, the rapid slaking rate is reduced to 100 seconds, suggesting

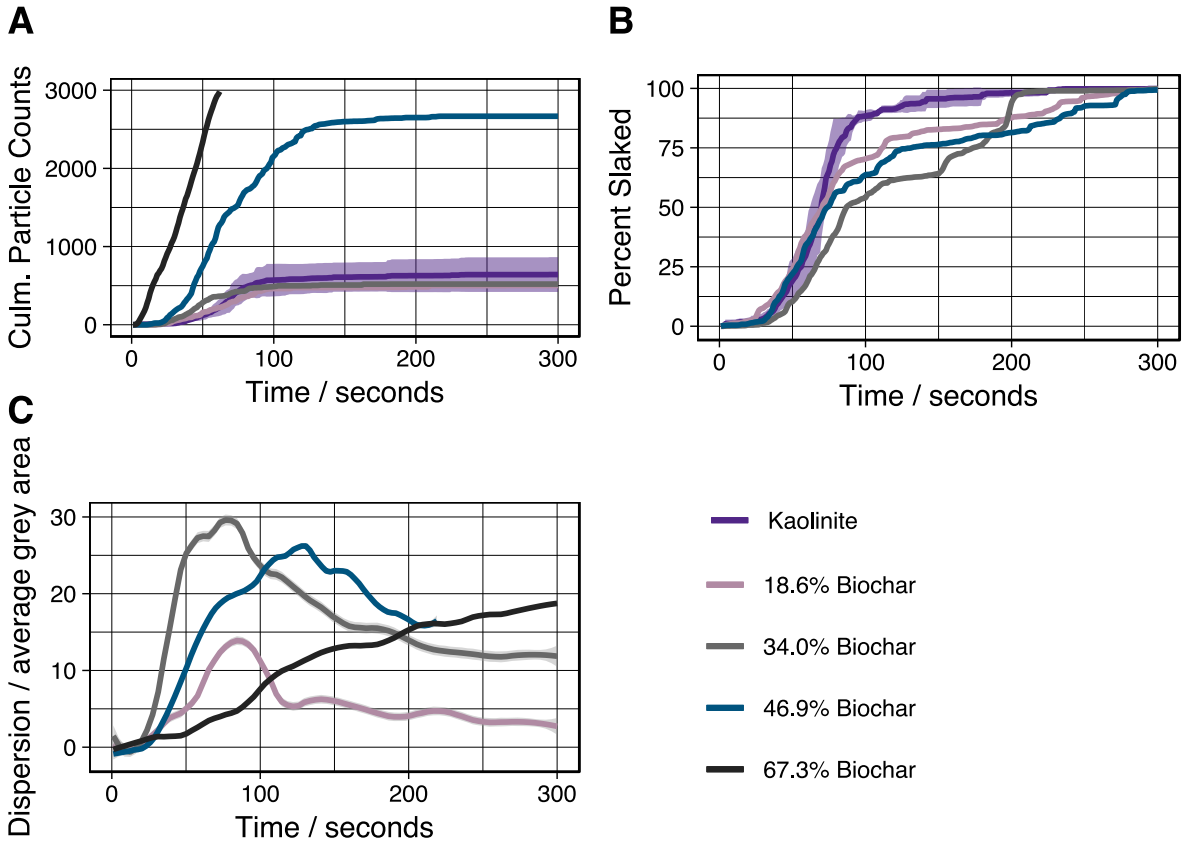

Figure 4.18: Biochar slaking, **A:** The cumulative particle counts at 200 seconds were extremely similar until loading approaches 50% volume biochar when particle counts increased dramatically, the highest loading (67.3%) produced a stream of dispersed material. **B:** Slaking profile of biochar loadings below 34%, slaking proceeded more slowly than pure kaolinite. **C:** There was a significant amount of dispersed material produced with increasing biochar loading, 67.3% volume loading biochar continued to produce biochar with a mean grey value exceeding 40 at 600 seconds.

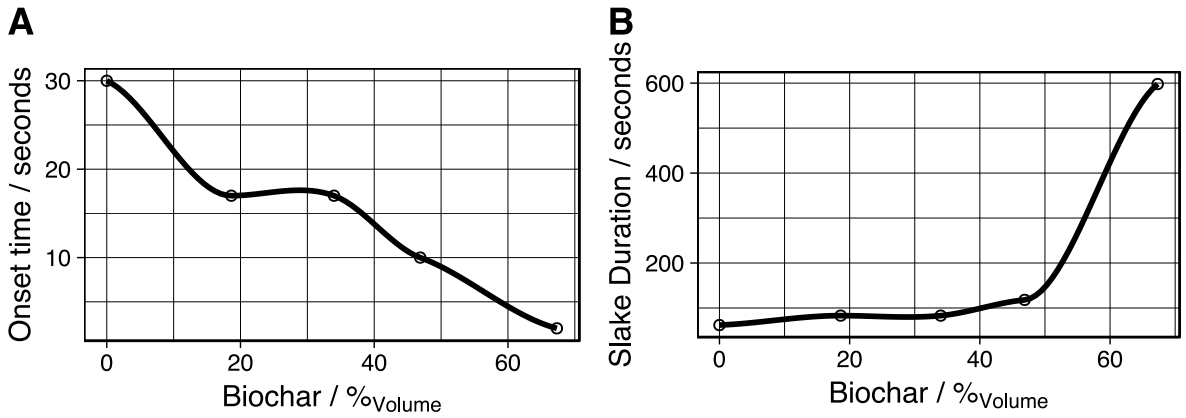

Figure 4.19: **A:** The onset time decreased with biochar loading. **B:** The duration of rapid slaking increased substantially as the volume of biochar exceeds 50% volume, due to the formation of a large amount of small particles.

that this may be the time for biochar to form hydrophobic stabilisation is reduced, and occurs at all loadings, possibly due to a much higher surface area, and the lack of hydrogen bonding functionality.

4.4.9 Beech wood fragments

The slaking behaviour of kaolinite amended with beech wood particles was observed to be very different from that of kaolinite (Figure 4.20). Beech wood amended artificial aggregates appeared to have two simultaneous modes of slaking, forming both discrete particles initially, similar to those formed by kaolinite, followed by a constant stream of dispersed material that flowed continuously. At 250 seconds slaking was catastrophic and large clumps were quickly formed likely to contain larger particles of wood. This was a challenge to measure using image analysis and the particle counts were measured at being considerably higher than those of kaolinite due to the stream of finer material. Analysis of the slaking profile was more useful, and beech wood amended artificial aggregates were found to have a characteristic slaking profile (Figure 4.20, **B**). At 30% $_{mass}$ loading beech wood appeared to extend the slaking duration although slaking began immediately. The slaking profile showed that the initial slaking was slower, and that more rapid slaking occurred at a longer timescale (250 seconds). The two rates of slaking, a slower initial rate and a secondary faster rate suggest that the slaking behaviour is more complex. Increasing the wood loading to 50%

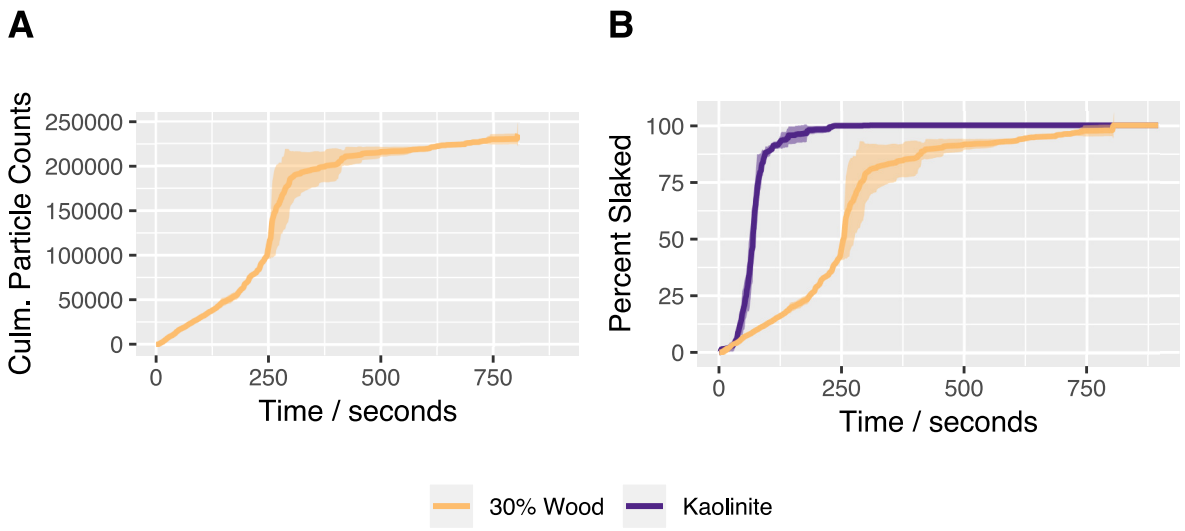

Figure 4.20: **A:** Wood pulps formed lots of material and counted particles far exceeded that of kaolinite (not shown) **B:** The slaking profiles are very different with wood amended kaolinite with a more distinct slaking profile.

$_{mass}$ resulted in an artificial aggregate which was quick to slake and dispersed material was present very quickly. This destabilisation may be the result of the much larger porosity of the 50% loaded artificial aggregate (61% porosity) as compared to the 30% loaded artificial aggregate (50%), and a reduction in mechanical binding strength. The presence of dispersed material also suggests that the kaolinite is not forming stable face-face structures, and is likely to be coating wood particles. The large clumps formed at the end suggest that the wood particles remain stable longer than the bulk kaolinite but this may be due to wood-wood interactions. These particles are also large, and so electrostatic repulsion between wood particles will not cause them to disperse.

4.4.10 Hydrogen peroxide bleached pulps

Wood pulp was treated with alkaline peroxide solutions at differing levels of severity in order to remove lignin from the surface as described in the previous chapter. Image analysis settings were modified to be less sensitive to finer particles, as to only measure discrete particles and not dispersed matter. The sensitivity was decreased but qualitative trends were easier to determine.

On reducing the sensitivity of the image analysis, in order to detect only the larger particles, the

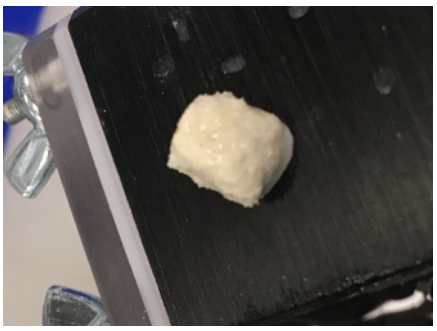

Figure 4.21: 30% hard treatment wood pulp formed a semi-stable aggregate which produced a constant stream of slaked material but retained its shape.

total particle counts for the untreated wood (Figure 4.22, **A**) were found to be similar to those of kaolinite. However, the amount of dispersed material was increased and observed much more quickly with the addition of both wood and treated wood. Dispersed material appeared as a stream from the sample, rather than forming at the bottom of the cell or from falling particles, with the bleached wood (30% Hard) producing a stream of dispersed material after around 30 seconds (Figure 4.22, **C**). Despite the presence of a greater amount of dispersed material, the amendments did increase the slaking duration and 30% Hard did not slake fully in the duration of the experiment (Figure 4.22, **B**). Instead of breaking down into particles, the 30% Hard treatment formed a cohesive artificial aggregate which slaked gradually from the outside as dispersed material, resembling a tablet dissolving from the outside (Figure 4.21).

The particle sizes (measured as pixel area) showed that the largest particles were observed at around 250 seconds for wood and the first mild treatment (Figure 4.22, **D**) . These particles were larger than those observed in kaolinite, and are therefore likely to contain wood particles. Following this release of larger particles, more dispersed material was observed (Figure 4.22, **C**). Wood amended kaolinite thus formed discrete particles initially, which are similar to those observed in pure kaolinite artificial aggregates (although significantly slowed), and then transitioned to a slaking which resembled a constant stream of more dispersed material, followed by the release of wood particles.

This could be interpreted as initial slaking forms as the result of kaolinite particles, followed by kaolinite associated with wood particles which slakes as a dispersion. This dispersed material is removed and weakens wood-wood interactions causing them to break away. Despite the colour change observed by the mild peroxide treatment, the light bleaching treatment did not result in a

major change in slaking behaviour. The hard peroxide treatment however, changed the behaviour of slaking considerably. Slaking duration was found to increase with the addition of the bleached pulps (hard treatment) from 10 to 30%, whereas beech wood particles were found to have poor slaking stability. The onsets for all particles were found to be zero, with some particles detected almost immediately. Porosity for all samples was greater than that of kaolinite and at 30% loading, artificial aggregates were found to have almost identical porosities, suggesting total porosity did not define the slaking characteristics in these samples. The bleached wood also resulted in the formation of the least mechanically strong artificial aggregates and so the increase in stability must be due to an interaction which forms on wetting. The peroxide treatment was shown to strongly reduce the surface area and porosity of the wood, which is likely to reduce the wettability of the surfaces. The collapse of the wood structure, is likely to result in a reduction in swelling of the wood particles and the water the artificial aggregate takes up. This may delay the rate of slaking, however, the kaolinite may play a small role in this stability, and is why a stream of material is observed coming from the aggregate as slaking continues.

4.4.11 Gompertz model

The maximum rate of slaking (μ) decreases with an increased volume with almost all the additives (Figure 4.23, **A**), suggesting all particulates were able to reduce the rate of slaking at some loading. The modified HDPE was found to maintain a higher slaking rate than the other amendments, due to a higher wettability and the instability of hydrogen bonding interactions in water. It is possible that the reduction in slaking rate with unmodified HDPE is linear, the result of a purely hydrophobic interaction. Biochar and cellulose, despite having quite dissimilar surface chemistries both reduced the maximum slaking rates considerably, and both created large amounts of dispersed material. This indicates the need to consider both dispersion and slaking rate, as both biochar and cellulose did not stabilise the aggregate.

The resistance to slaking requires both a reduction in repulsive forces and an increase in water stable interactions. Since the HDPE is net neutral, and contains no surface charge, electrostatic repulsion is minimal, and so hydrophobic interactions dominate. 42% lignin aggregates slaked

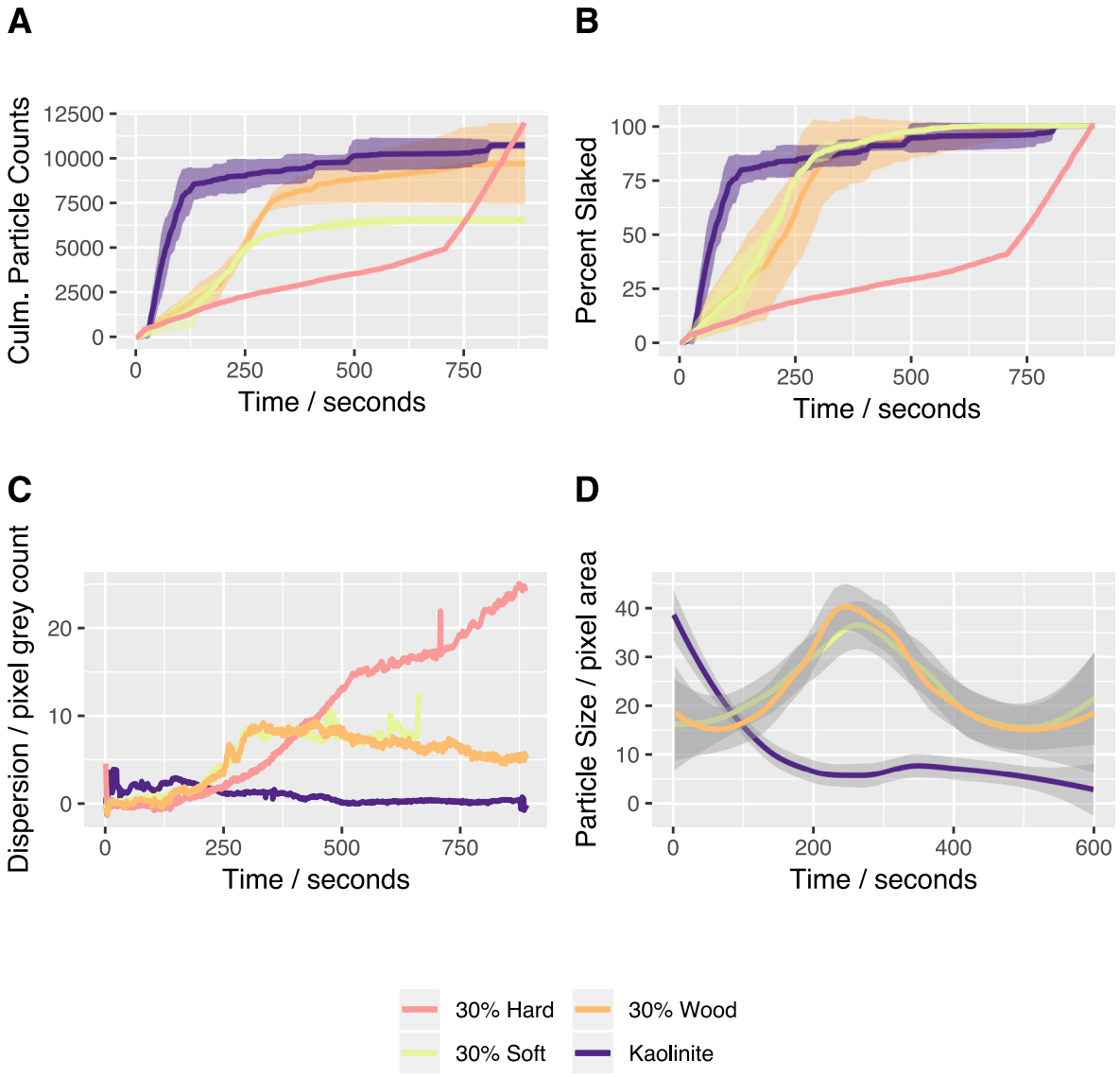

Figure 4.22: **A:**The cumulative particle counts were very similar, however, the values for the beech with soft and hard treatments may be artificially low, as the content of dispersed material may have masked the presence of particles. **B:** The percentage slaked showed that slaking duration was extended by the presence of treated and untreated wood particles, the harshest treatment resulted in a very different lineshape. **C:** Dispersion was high, and highest for the most bleached wood chips. **D**: Dispersed material observed in C was accompanied by an increase in the particle size of the slaked particles.

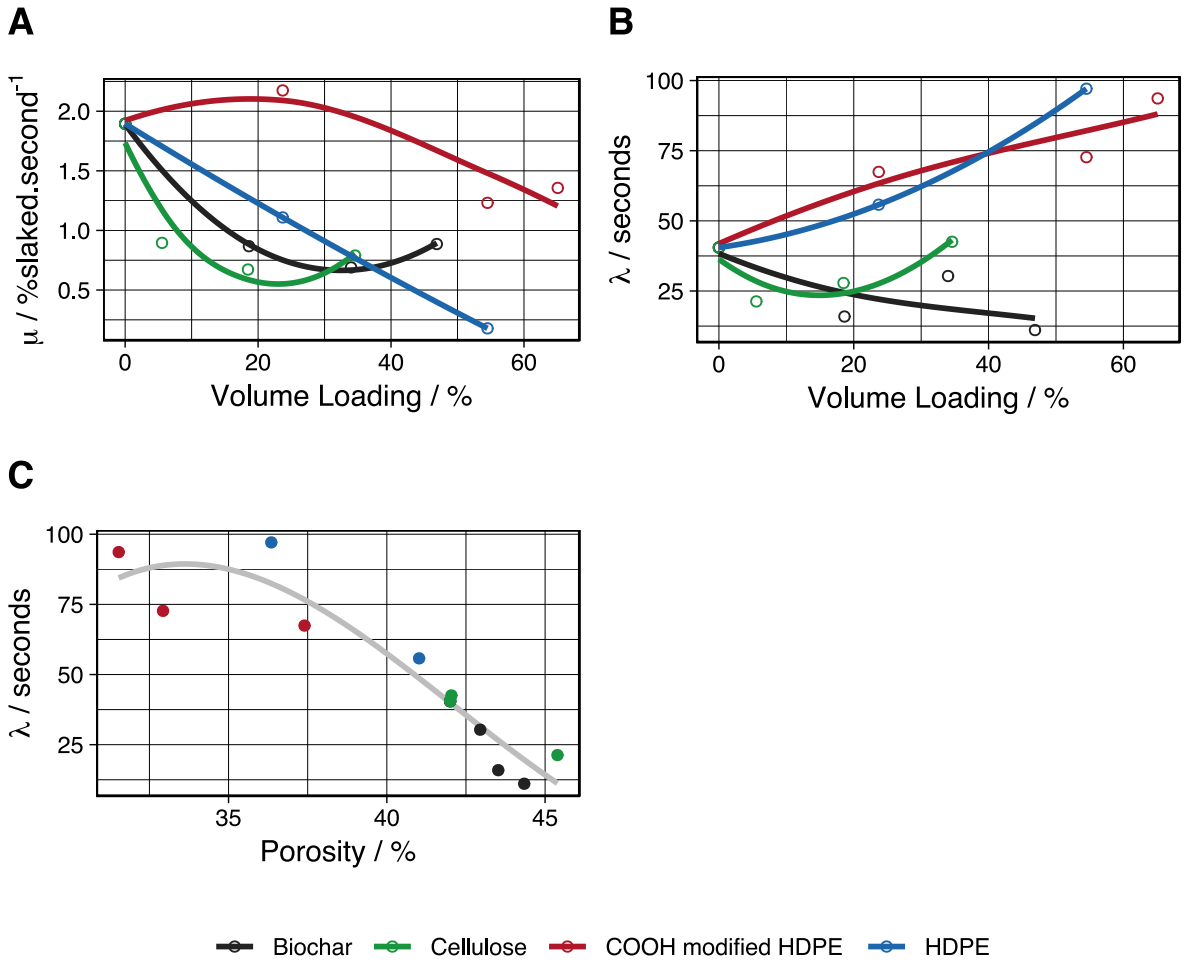

Figure 4.23: **A:** The maximum slaking rate, μ, was obtained via Gompertz line fitting. Slaking rate was highest in kaolinite samples, and those containing COOH modified HDPE. Biochar and cellulose particles had very similar slaking profiles. **B:** Lag time, λ, is also calculated using the same model and can be considered equivalent to the slaking onset mentioned previously. The offset was found to increase with samples containing HDPE particles, both modified and unmodified. Biochar and cellulose had a reduced offset. **C:** The offset was found to correlate strongly with porosity (here a third order polynomial has been fitted).

using a wire restraint was found to have a maxima at 0.46 % slaked/second, the lowest maximum slaking rate of any additive at this loading. Lignin is able to form hydrogen bonding interactions with the clay, which are considerably weakened by wetting, but may help retain an interaction as hydrophobic interactions are formed, which helps combat an electrostatic repulsive force. It appears that hydrophobic interactions occur over a longer timescale, and so are only stabilising if electrostatic repulsion is minimised and slaking is reduced. The extremely hydrophobic biochar contains a strongly hydrophobic surface, but the high surface area and negative charge means that electrostatic repulsion overcomes hydrophobic interactions before they form. This suggests that the role of hydrogen bonding in particulate interactions may be important for destabilising and stabilising aggregates with potential electrostatic repulsion, were particles held by only van der Waals type interactions are weak to water slaking, and may break down despite the presence of hydrophobic interactions.

4.5 Conclusions

Methodology: The instrument used here was designed to measure slaking kinetics. It was able to qualitatively reproduce the observed slaking behaviour of simple systems using particle counting and a measure of dispersion. The breakdown kinetics were in most cases simple, and could be fitted to a sigmoidal model such as a (Gompertz function) if required. The system is able to measure the number of observed particles, measure particle sizes where large particles are present, measure dispersion and slaking kinetics. Differences in sample volume or mass which result in large errors can be minimised by converting particle counts to percentage slaked, which gives highly reproducible slaking curves.

Kaolinite, although unstable to water, does not slake and then disperse, suggesting microaggregates of kaolinite are relatively water stable. It is known that strong van der Waals forces and H-bonding exists between kaolinite faces, and these are able to resist hydration forces. Edge-edge, or edge-face interactions are not as stable owing to a smaller contact area between particles, and these are likely to hydrate and fall apart. Kaolinite artificial aggregates have clearly defined slaking onset and slaking

duration. Kaolinite aggregates made with 0.1 M NaCl or $CaCl_2$ as an electrolyte, were found to increase the slaking duration by reducing electrostatic repulsion. Kaolinite aggregates made with 0.5 M $CaCl_2$ solution increased the slaking stability further to form a very stable aggregate, due to the strong affinity of Ca^{2+} for the kaolinite surface. Kaolinite made with NaCl, and low concentrations of $CaCl_2$ slaked into smaller and more numerous particles, suggesting a reduction in particle size.

HDPE particles are stabilising, despite having a destabilising effect on the mechanical strength, and at $65\%_{vol.}$ form water stable aggregates. HDPE is highly hydrophobic which can reduce the rate of water ingress, however, the long-term stability of the artificial aggregate suggests the interactions are stable and associative in nature. The hydrophobic HDPE particles, which increase the water repellence of the aggregate surfaces did not extend the slaking onset and particles appeared instantly. This occurred despite HDPE being less porous than kaolinite. The slaking became more linear at higher loadings, deviating from the S shape curve in kaolinite.

HDPE particles with surface modification were previously shown to increase the mechanical strength of artificial aggregates, these strong interactions were only able to extend the slaking duration by a small fraction. Additionally, the reduced porosity was not found to strongly effect the slaking stability. This demonstrates that polar surface groups such as alcohol and carboxylic acid functionality enhance the wettability of surfaces, these wetting forces move particles apart and allows electrostatic repulsion to dominate interparticle forces.

Lignin increased the slaking stability, aggregates with mass loadings over $50\%_{vol.}$ (around 20% mass loading) formed semi-stable aggregates which swelled considerably, but resisted breakdown. Again, porosity was not found to strongly impact the slaking. Lignin is negatively charged and contains some hydrophilic functionality, the gel-like material that forms is a result of a both hydrated surface functionality and electrostatic repulsion counteracted by a hydrophobic interaction which forms as the aggregate wets. This suggests that lignin would be an ideal soil amendment, as low loadings can increase mechanical strength and water stability. The interaction with clays is similar to the role of lignin in the plant cell wall, whereby it acts as a 'glue' and increases the stability of the material to water. (*194*) However, in the literature lignin is often deemed to be a hydrophobic polymer, in this case it seems to strongly interact with water but form interactions which are stable to wetting.

This is an important distinction, as lignin may not act to exclude water, but instead be acting as a water-tolerant glue/gel.

Cellulose pulp increases the mechanical strength of artificial aggregate composites significantly, but does so via cellulose-cellulose interactions. The lack of slaking stability is evidence to suggest that cellulose does not interact strongly under any conditions with kaolinite, the dispersed material increases with the increase in cellulose loading.

Biochar, which is strongly hydrophobic, was found not to be stable in water, and broke down initially in a very similar rate to pure kaolinite, but the rate was slowed after 80 seconds due to the formation of hydrophobic interactions. Biochar has been shown to increase the mechanical strength of artificial aggregates, despite the lack of hydrogen bonding surface functionality. Dispersion was high, however, and the overall stablity of the aggregates was poor.

Wood pulp was found to increase the mechanical strength of the artificial aggregates, via structural reinforcement of the cube rather than strong interparticle interactions. Lignin, hemicellulose, cellulose and waxy residues are likely to be present on the surface of wood pulp. Wood pulp was not effective for increasing the slaking stability of the kaolinite. Treating the surfaces of wood pulp with peroxide is used to remove lignin from the surfaces, but has also shown to reduce the surface area and porosity of the wood. It was thought that the reduction of lignin on the surface would decrease the surface affinity for kaolinite and increase its wettability, this means that the slaking stability should rapidly decrease. However, it was found that increasing the strength of the peroxide treatment helped to increase the stability of the aggregates. 30% wood pulp was found to stabilise the aggregate considerably. The stability of the aggregate was temporary, and a continuous stream of dispersed clay was observed. This suggests that the pulp effectively delayed the slaking rather than prevented it by forming a stable hydrophobic interaction with kaolinte. Instead it is likely that the reduction in pulp pore space and surface roughness brought about by harsh bleaching prevents rapid wetting of the aggregate, and possibly allows weak associative interactions between bleached wood fibres. The stream of material is predominantly kaolinite, which is gradually released from the aggregate. The lack of discrete particles indicates that kaolinite coats the particles and so mixing with wood disrupts the formation of more stable kaolinite tactoids.

Kinetic elements: The simple systems studied here have large variations in sample composition and porosity, but are otherwise very similar. The slaking offset, the delay before slaking is observed, was thought to be strongly related to both the porosity and the sample wettability, but no strong evidence for this was found within specific examples. The formation of hydrophobic interactions appears to be slow, and results in a deviation from a sigmoidal line shape to one that is more linear. Significant dispersion was observed in samples amended with cellulose, biochar, modified-HDPE and wood. Kaolinite forms water stable tactoids on drying, and these are disrupted by the addition of particulates which can result in the formation of dispersed material.

Chapter 5

Are Particulate Interactions Able to Generate Stable Aggregates over Wet/Dry Cycles in an Artificial Soil?

5.1 Abstract

Organosolv lignin has been shown to increase the mechanical strength of artificial kaolinite-based aggregates at loadings of up to 45 % volume loading (20 % mass loading). These aggregates also demonstrated increased stability in water, becoming water stable at loadings above 45 % volume loading lignin content. This suggests that kaolinite based aggregates containing around 45 % volume loading lignin are likely to show increased mechanical strength and water stability; as a result, lignin-kaolinite aggregates may accumulate in soils subjected to repeated mechanical stress and wet/dry cycles. The aim of this study was then to investigate if artificial soils, amended with organosolv lignin, would accumulate lignin in a stable aggregated fraction after rigorous and prolonged mechanical seiving and repeated wet and dry cycles, due to the formation of aggregates with increased resistance to these stresses. Artificial soils were based on the analysis of a degraded sub-Saharan African soil (Ghana) which contains low clay content of predominantly kaolinite and iron oxides. The results of this study showed that although the addition of lignin increased the

aggregation of these soils, lignin was not present at higher concentrations in aggregated material compared to unaggregated material, or that lignin was not present in aggregates at a particular 'optimum' concentration representing a material with superior strength and water stability.

Lignin was instead found to accumulate in aggregates as a function of lignin loading, suggesting aggregation in these systems in non-specific and non-selecting. Soils containing no iron oxide contained less aggregated material, but the lignin concentration in the aggregates was unaffected, demonstrating that aggregation in these systems is driven by soil texture only. However, soils containing bentonite as the primary clay mineral were found to accumulate lignin at higher contents in the aggregated size fraction, as compared to kaolinite. It is not clear if this increase in lignin in the aggregate size fraction of bentonite soils is due to strong surface interactions which exist between lignin and bentonite, as the accumulation may also be attributed to shrink/swell properties or a greater surface area.

Key Findings:

- Aggregation in synthetic soils increased with lignin content, the increase in aggregation was higher between 0- 2.5% mass loading than between 2.5 -5%, this suggests a saturation of inter-particle interactions or a limit on the amount of aggregated material formed under the conditions of the experiment.
- Repeated wet/dry cycles (up to 10 times) resulted in very subtle changes to the materials retained in the sieve fractions and no significant evolution of soil structure was observed.
- Iron oxide and clay accumulated in the aggregate size fraction, along with the highest concentration of exchangeable cations. Synthetic soils without iron oxide were found to accumulate less material in aggregated size fractions, the lignin content (mass percent) did not change in aggregated size fraction despite the removal of iron oxide. This suggests that the aggregated size fraction is formed by the aggregation of fine particulates, of which, the chemical characteristics are relatively unimportant.
- This methodology does not consider that stable micro-aggregates may form that are sand sized.

- The cation exchange capacity was unchanged with the addition of beech organosolv lignin, but increased slightly with spurce organosolv lignin, due to a higher concentration of carboxylic acid groups.

5.2 Introduction

Soils in the tropics, which contain weathered minerals and low clay contents are particularly susceptible to erosion on conversion to agriculture. These soils occur where there is high humidity and/or higher temperatures, and soil carbon is quickly lost. As a result of a reduction in plant cover, soil erosion can accelerate and soils can become desertified. (*173*) One strategy that can be employed to recover soils in a bad state of soil degradation is to add a soil amendment which creates beneficial soil structure. This can be in the form of traditional soil amendments such as plant residues or manure. Alternatively, processed agricultural residues or products of industrial biorefineries may be used. Farmers who provide materials to biorefineries could feasibly utilise the waste from biorefineries, which are often cheap and have low value, to restore organic matter. Industrial biproducts may present an opportunity for soil restoration, as additional processing of a solid waste may vastly increase the soil restoration properties, with little additional investment, and materials will be available on large scales. (*195*) However, the mechanistic elements which determine the efficacy of a soil amendment for improving a degraded soils remain largely unknown. Without this knowledge, soils can only be improved by trail and error, and more advanced soil amendments may only evolve slowly.

Wet/dry cycles are known to create soil structure in both natural and artificial soils (*49*, *196*), creating or disrupting soil structure through the physio-chemical means, or by biological processes. (*70*) Despite the prevalence of studies attributing the evolution of soil structure to cycles of wetting and drying, the mechanistic aspects of this process is not well understood. (*197*) Organo-mineral interactions in soil form under constrained circumstances, with soluble molecules only accessing mineral surfaces where water is present, and solid particles only meeting surfaces which have exposed sites and have even less spacial mobility. Preferential retention of specific forms of carbon on mineral

surfaces has been demonstrated, although the nature of this preferential retention is not always clear. For example, kaolinite soils were shown by ^{13}C NMR spectroscopy and pyrolysis-GC/MS to retain more polysaccharides, where as smectite containing soils contain more aromatic functionality (*198*). This was attributed to organo-mineral interactions, but other factors such as the nature of the fauna, microbial community, soil material properties and environmental factors may have a larger role. Field studies and adsorption studies of soluble organic matter indicate a clear difference in binding strength of certain chemical functionality, however, the importance of this difference in binding affinity for the function of soils and carbon cycling may not be substantial.

Beech lignin has been shown to increase the mechanical strength and toughness of clay aggregates and has been shown to form aggregates with high water stability at similar mass/volume loading. The aim of this experiment was to see if lignin would therefore accumulate in clay rich aggregates by the action of strong mechanical and water pressures, due to the increase in strength or water repellence of these materials. If mechanical disruption by sieving only retained aggregates with increased strength, and disruption by water only retained aggregates with increased slaking stability, then repeated sieving and wet/dry cycles should result in a soil which has accumulated aggregated material which is both strong and water stable. The formation of these enhanced, or optimised aggregates by the selection of material with stronger mechanical and slaking resistance may represent a new equilibrium in the soil structure. This may also present a likely mechanism in which to design soil amendments with preferential soil structure building properties.

This hypothesis was tested on an artificial soil containing high quartz sand and quartz silt content, soils which have low organic matter content and may respond well to the application of a soil amendment. The action and 'behaviour' of particulate organic matter when added to soil is not well understood. In this study, the following questions are asked:

- Does the action of mechanical sieving and submersion result in the accumulation of materials which are stronger and more water resilient?
- Does lignin accumulate in aggregates containing kaolinite, and is binding specific to clay minerals?

- How does the soil structure change over repeated wet/dry cycles?

In order to answer these questions, artificial soil systems were used, which are sterile. Biological effects can be considered separately.

5.3 Experimental design

Artificial soils are useful models, as the composition can be easily modified. In order to investigate the role of iron oxide and 2:1 vs 2:2 clays, two additional artificial soils were made containing no iron oxide (replaced by quartz silt) and another containing bentonite instead of kaolinite. Repeated wet/dry cycles followed by vigorous mechanical sieving was carried out in order to combine the effects of water and mechanical disruption.

5.4 Methodology

Kaolinite was obtained from PotteryCrafts Ltd, Stoke in Trent, UK, and was used as received. Quartz (Silica Sand) was also obtained through PotteryCrafts with a high purity (99.5 % SiO_2) and was pre-seived to below 63 μm. Iron oxide was obtained via Scarva, Banbridge, County Down, UK and contained 80.0 % Fe_2O_3 with some aluminium and silicon oxide impurities. Acid washed sand (50-70 mesh size) was obtained through Sigma Aldrich (now Merck). Sericite Mica was obtained via The Soap Kitchen and was used as received. Artificial soils consisted of the following minerals mixed together (see Table 5.1): 80 g Quartz coarse sand, 13 g fine quartz (silt), 5 g kaolinite*, 1 g of mica, 1 g of iron oxide**.

* Kaolinite was replaced by the same mass of bentonite for bentonite artificial soils

** To study the effect of iron oxide on aggregation, one soil contained no iron oxide, and was replaced by an equal mass (1g) of fine quartz silt.

	Component added / g					
Experiment	Quartz (sand)	Fine-quartz (silt)	Kaolinite (clay)	Mica (mineral)	Iron oxide (oxides)	Beech Lignin
0 % lignin	80.0	13.0	5.0	1.0	1.0	0.0
0.5 % lignin	80.0	13.0	5.0	1.0	1.0	0.5
1.0 % lignin	80.0	13.0	5.0	1.0	1.0	1.0
2.5 % lignin	80.0	13.0	5.0	1.0	1.0	0.5
5.0 % lignin	80.0	13.0	5.0	1.0	1.0	5.0

Table 5.1: Mineral mixtures which were added to make up the artificial soils used in these experiments.

5.4.1 Artificial soils and wet and dry cycles

100 g of the artificial soils (without lignin) was mixed for 4 hours in a rotary mixer until solids appeared to be homogenously mixed. 100 mls of 0.01 M $CaCl_2$ was added as a background electrolyte and the amendment (lignin) was added. Mixing is continued for a further 4 hours on a rotary mixer until the mixture was completely wetted. Soils were then dried to constant weight at 40 °C. The soil formed a solid cohesive mass which was broken up by hand and lightly crushed. The crushed samples were wetted, left for 1 hour and dried in a fan oven at 30 °C for 18 hours.

Soil was sieved for 30 mins at with a Retsch AS 200 basic sieve shaker, amplitude of 70. This was found by trial and error to be sufficient time to distribute material through the sieve without causing excessive breakdown of the most stable aggregates by abrasion rather than fracturing of the aggregates by vibration. Soils were removed from the sieve and brushed into weighing boats. The soil fractions were weighed and remixed. The soils were then re-wetted and left for 1 hour before being dried in a 30 °C oven for 18 hours and re-sieved.

5.4.2 Characterisation techniques

UV/vis spectroscopy: Lignin was washed from each soil fraction using acetone. 1 g of soil material was used per size fraction. The soil was shaken in a sealed centrifuge tube with 10 ml of spectroscopy grade acetone. The solutions were centrifuged, filtered and diluted quickly as to reduce evaporation of acetone. The concentration was measured using UV/vis in a sealed cuvette (to prevent evaporation) and quantified using a prepared standard of sequential lignin dilutions.

CHNS: CHNS was carried out using a Vario MICRO CUBE by Elementar using Helium as a carrier

gas and oxygen for combusion. A tungsten (IV) combustion column and a copper wire reduction column was used, operating at 1150 °C and 850 °C respectively. An adsorption column operating at 40 to 210 °C was then used and species were detected using a thermal conductivity detector (TCD) operating at 60 °C. Lignin and soil fractions were analysed using CHNS, the lignin content of each soil fraction was back calculated using the %C obtained from the CHNS measurement and the %C of pure lignin.

ATR-FTIR: Attenuated total reflectance Fourier transform Infrared spectroscopy (ATR-FTIR) is a surface sensitive technique sensitive to (0.5 - 5.0 μm) beyond the surface. Powders and aggregates were used without further preparation in order to retain fragile particle-particle interactions. An Agilient Cary 630 FTIR Spectrometer using 32 scans and a resolution of 2 cm^{-1} was used.

Cation Exchange Capactiy: A modified silver thiourea method was used to measure the cation exchange capactity and the exchangeable cations for the artificial soils. This modified method corrects for chemical instability of the exchange solution, which minimises silver sulphide precipitation. (*199*) 15.2 g of thiourea is dissolved in 1400 ml of DI water, then 3.397 g of $AgNO_3$ in 300 ml is added very slowly (with stirring). 200 ml of 1M ammonium acetate solution is added. The solution is made up to 2 L with ammonium acetate. 1 g was used per soil and samples were measured in triplicate.

5.5 Results

5.5.1 The formation of soil structure with wet and dry cycles

Wet and dry cycles, followed by sieving were repeated ten times for a soil amended with 0, 1 and 5 % beech lignin in order to observe any changes the distribution of material in each size fraction, and to determine if an equilibrium was reached. Figure 5.1 shows the build-up of soil structure over 10 cycles for the highest lignin loading. The material in the largest sieve sizes (above 420 µm) reached a stable mass after a single cycle, despite the larger aggregates visibly breaking in the wetting cycle. The material in the larger of the intermediate sieves (420 – 250 µm) containing

mostly sand continued to accumulate mass gradually over 10 cycles, which may accumulate mass from the size fractions below, suggesting a small increase in smaller size fractions. The material in the finest sieves ($<$ 177 µm) also reached an equilibrium after only a few cycles. Results from soils containing 0 % and 1 % lignin showed a similar trend albeit with less material in the aggregated fractions. The lack of soil development with repeated wet and dry cycles suggests that interactions occur quickly, do not accumulate strongly and that material is well mixed. The artificial soils were observed to break up quickly and material did not move much between the largest sieve size fractions over the sieving cycle.

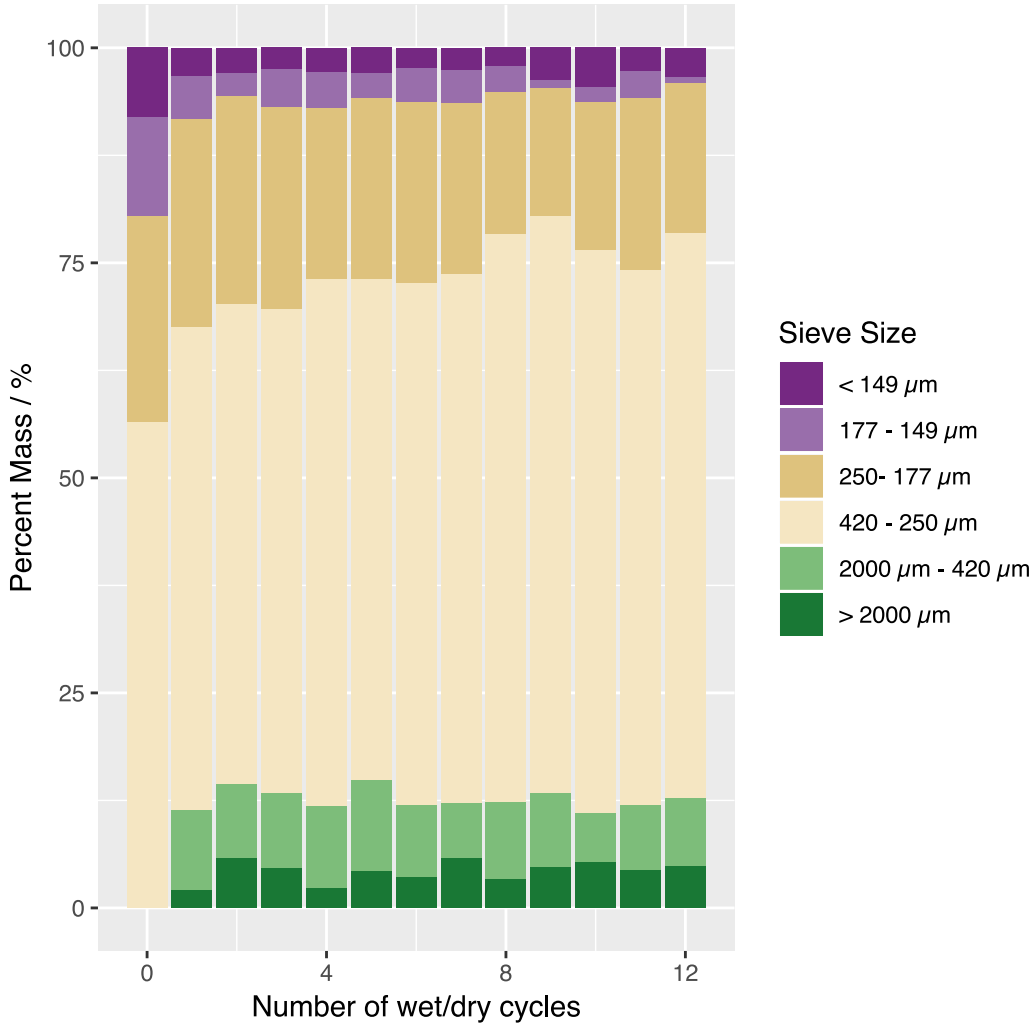

Figure 5.1: An artificial soil containing 5% beech lignin was subjected to repeated wet and dry cycles and rigourous mechanical disruption using a sieve shaker. The sieved material exceeding 420 µm (green) consisted of aggregated material, the middle size fractions containing material between 420 - 177 µm (sandy colours) contained predominantly coarse sand, the smallest size fractions $<$ 177 µm contain fine powders.

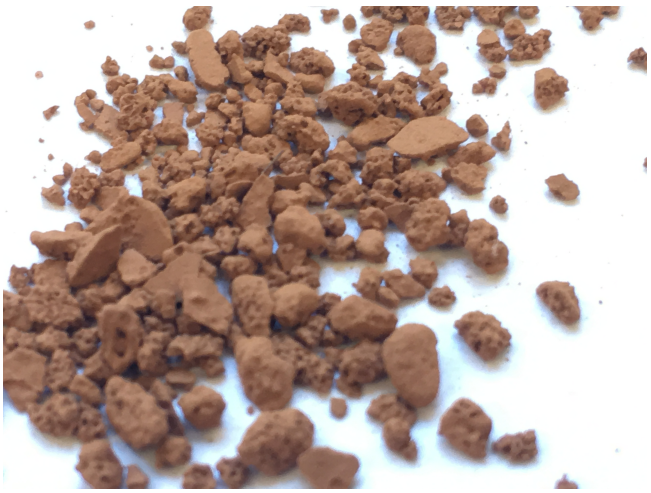

Figure 5.2: Photograph of the aggregated material which forms after wet and dry cycles and sieving. Blocky aggregates were formed which resembled real soil aggregates.

5.5.2 Aggregation and lignin loading

The material retained in the uppermost ($>$ 420 µm size) sieve fractions, contained no loose material material and constituted a number of flattened aggregates of similar size (Figure 5.2). After three wet/dry and sieve cycles, the material in the uppermost sieves was found to be greater at higher lignin loading (Figure 5.3). The relationship between lignin loading and the material aggregated in the uppermost sieves was non-linear, the enhancement in lignin aggregation is greater at lower loadings. This may be the result of a saturation of inter-particle interactions or a limit on the amount of aggregated material that can form with only weak, associative surface interactions in a fine particle mix. There is also a large percentage of coarse sand which makes the soil more brittle and may set the upper limit to aggregate strength. The increase in material in the 'microaggregate' (420-2000 µm) range did not change considerably on repeated wet/dry cycles, the largest change was observed with the more fragile macroaggregates ($>$ 2000 µm). Soils with no added lignin retained 5.4 % soil mass in the largest two sieves, at 5% mass loading, 13.1 % of the soil mass was retained in the largest two sieves. Smaller aggregates are known to have higher stability to slaking whereas larger and looser aggregates are often only stable in dry conditions (*200*).

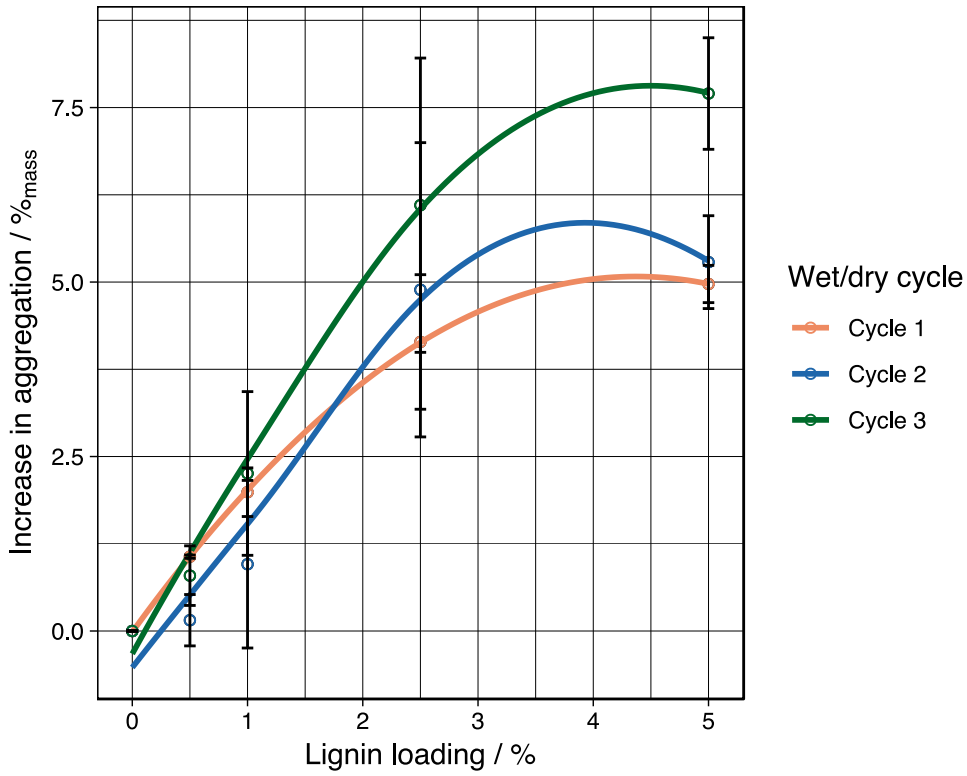

Figure 5.3: The increase in the mass of soil in the aggregated size fractions (2000 – 420 µm) increases with increasing lignin loading, shown here for three wet/dry cycles. The rate of increase is higher between 0 and 2.5 % lignin than between 2.5 - 5 % lignin. Error bars represent one standard deviation (n=3) and lines are a guide to the eye only.

5.5.3 Lignin distribution within soil fractions

The increase in aggregation due to the addition of lignin suggests a role for lignin as an aggregating/gluing or cementing agent. This may be due to the lignin binding minerals in the soil, creating stable aggregates. It was then of interest to see if lignin was therefore enriched in the aggregate size fraction. Figure 5.4 shows that lignin does not accumulate in the aggregated size fraction as compared to the unaggregated material in the smallest sieve sizes. However, lignin is found to be at considerably lower concentrations in the sand sized fractions. The mass of lignin distributed in each size fraction was proportional to the mass loading in the total soil, which indicates that lignin remains well distributed throughout the soil fraction after 3 wet/dry cycles. No heterogeneity is created by the formation of strong inter-particle interactions, which is why the soil does not develop strongly over wet/dry cycles. Sand has a low surface area, and as a result low amounts of lignin accumulated in the sand sized fraction. This also suggests that lignin does not accumulate in stable aggregates at a mass or volume loading which creates more mechanically strong or water stable aggregates. The rapid and extreme wet/dry cycles used in this experiment may be too harsh to allow the accrual of stable aggregates, and the accumulation of lignin in aggregated fractions. It is possible the lignin content may change with increasing wet/dry cycles, however the 'steady-state' observed after 10 cycles suggest that the artificial soils are not changing substantially.

5.5.4 Mineral composition of aggregates

XRF showed that iron and minerals with a high Al content (clay) accumulated in the larger aggregated size fractions, and was slightly reduced in the lower size fractions. There also appeared to be an accumulation of potassium, magnesium and calcium in the aggregated size fractions, which may suggest that these cations were important for aggregation, but may also be associated with minerals with high CEC such as the clay and iron oxides (Figure 5.5)

The presence of clay can be indicated by an increased aluminium content, which appeared in the aggregated size fractions. This was a clear indication that kaolinite, the predominant clay, is important for aggregation. K, present in high concentrations in kaolinite (6.54%) and mica (22.90%) and Mg,

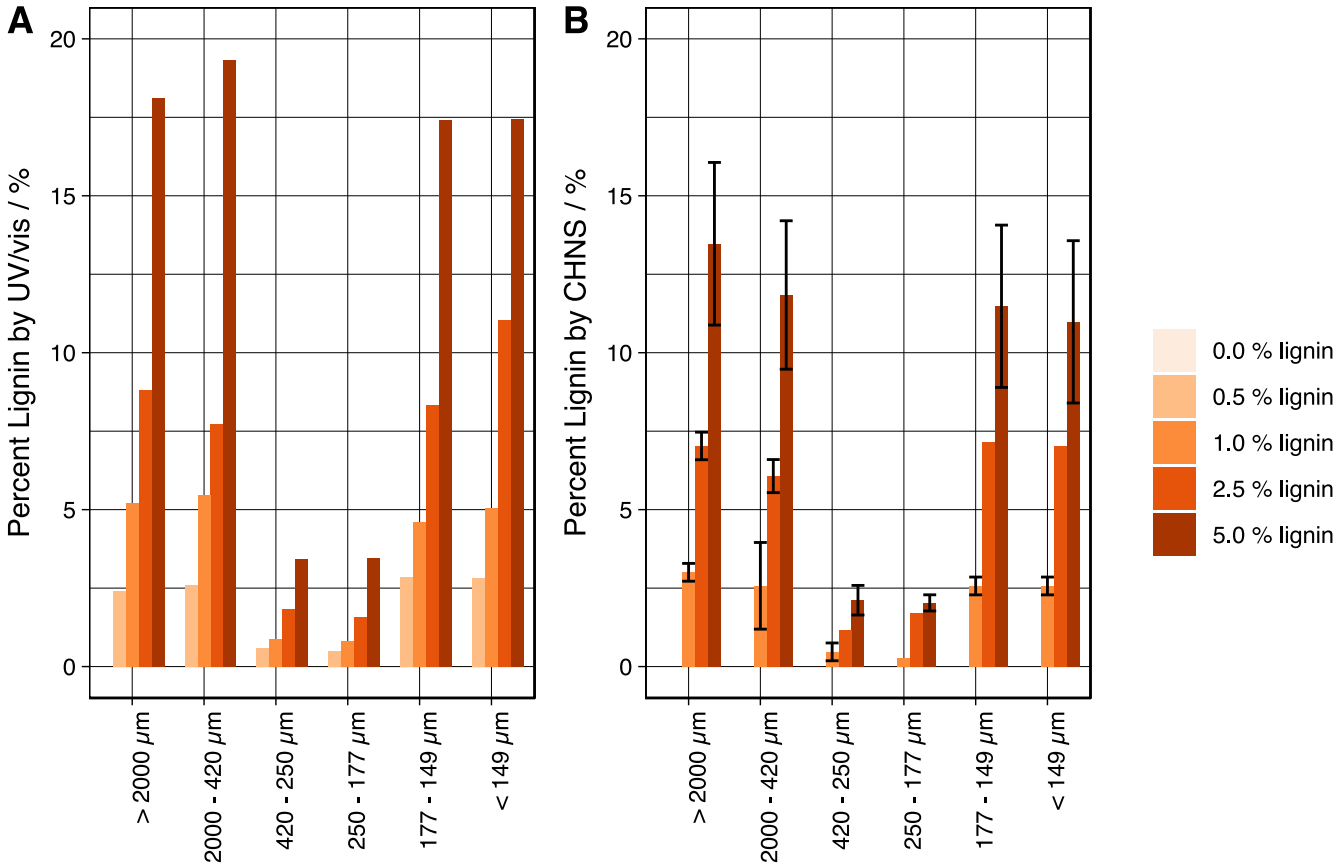

Figure 5.4: The lignin distribution between size fractions as measured by CHNS and UV-visible spectrscopy. Lignin content is higher in the aggregated size fraction, and the unaggregated size fractions, as compared to the material enriched in sand. Lignin determined by CHNS was much lower than that determined by UV-vis spectroscopy. Considering the mass balance of each fraction, total lignin was overestimated by UV-vis by 1 – 1.5 % for 5 % lignin samples, CHNS underestimated by 1 % for 5 % loading. This may be due to a slight bathochromic shift in the lignin spectra due to an increase in pH. In CHNS, complete combustion of soil organic matter with high ash (or mineral) content is often incomplete. The errors were higher for CHNS, possibly reflecting the heterogeneity of the smaller sample masses sampled. Both measurements were complimentary.

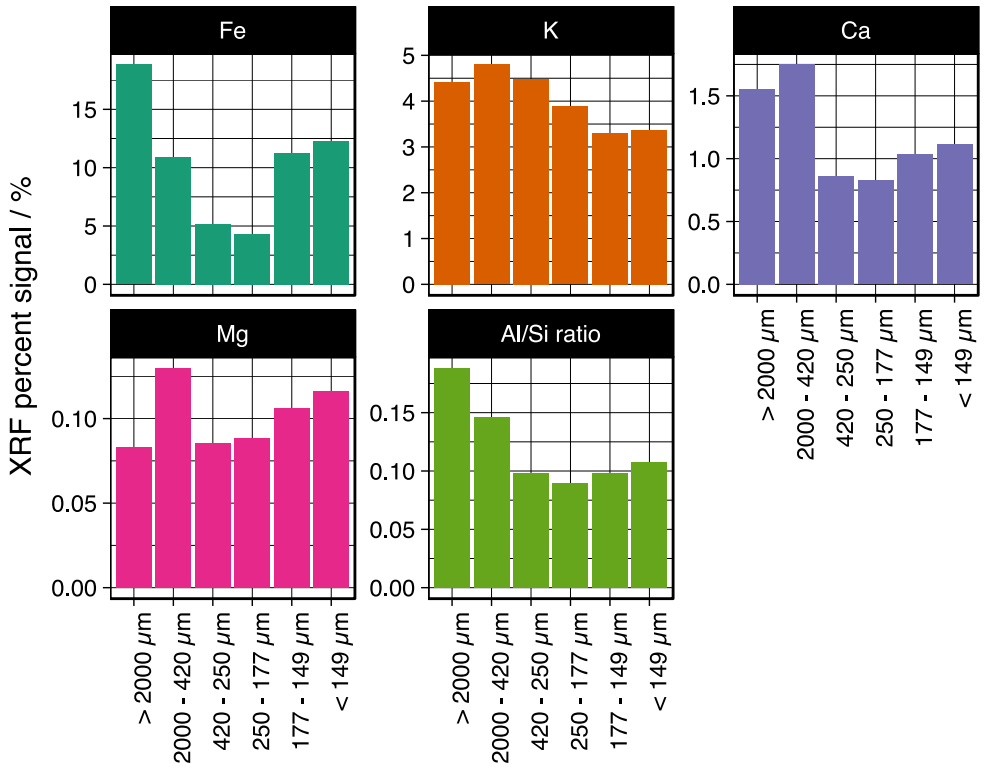

Figure 5.5: Elemental distribution with XRF, concentrations go from high (top left) to low (bottom right). Fe, representative of the iron oxide distribution was highest in the most aggregated size fraction. The exchangable cations Mg and Ca were enriched in more aggregated size fractions, with Ca significantly enriched in comparison to K. Mg was enriched in the smaller of the aggregated size fractions, indicating high levels of mica. The alumina/silicon ratio was used to indicate the clay content, a higher ratio suggesting an enrichment in kaolinite

enriched in mica (1.56%), were useful indicators of both kaolinite and mica. K was relatively evenly distributed, as compared to Ca, which may be an indication of a redistribution of exchangeable cations. Ca^{2+}, which is added as an electrolyte, has a strong affinity for clay surfaces, and may accumulate where there is high cation exchange. K^{+}, an indifferent electrolyte may not act in a similar way. This may also indicate that mica is well distributed. Mg, another indicator of mica, is also well distributed, although a particularly high concentration may exist in the smaller of the aggregated size fractions.

5.5.5 Particle size distribution

DMSO was used to wash each soil sieve size fraction to remove the lignin, and the particle size distribution of the mineral components were measured. Coarse sand was distributed in all but the smallest sieve fraction, accounting for the majority of the material in the central size fractions (Figure (5.6, **A**). Smaller aggregated size fractions (420-2000 μm), were found to have a higher sand content, higher sand contents may increase the brittleness of aggregates, and so larger aggregates may just reflect material with lower sand content. The d(0.5), which indicates the average particle size of the clay/silt sized material $<$ 100 μm, showed that the aggregated size fractions contained more clay (kaolinite and mica) sized material, and that the material in the lower sieves with unaggregated material is likely to be predominantly quartz silt.

A positive correlation was observed between the lignin content in the sieve fraction and the percentage of fine particles, a similar correlation was observed between the calculated specific surface area (from static light scattering measurements) and lignin content of the sieve fraction. This suggests that lignin can be found were clay is abundant. Correlation may not be linear however, and surface area may not be the predominant driver of lignin content.

5.5.6 Iron oxide and aggregation

Iron oxide, which constitutes less that 1% of the total mass of the soil was found, via XRF, to accumulate in the aggregates. An additional artificial soil with no iron oxide added was tested,

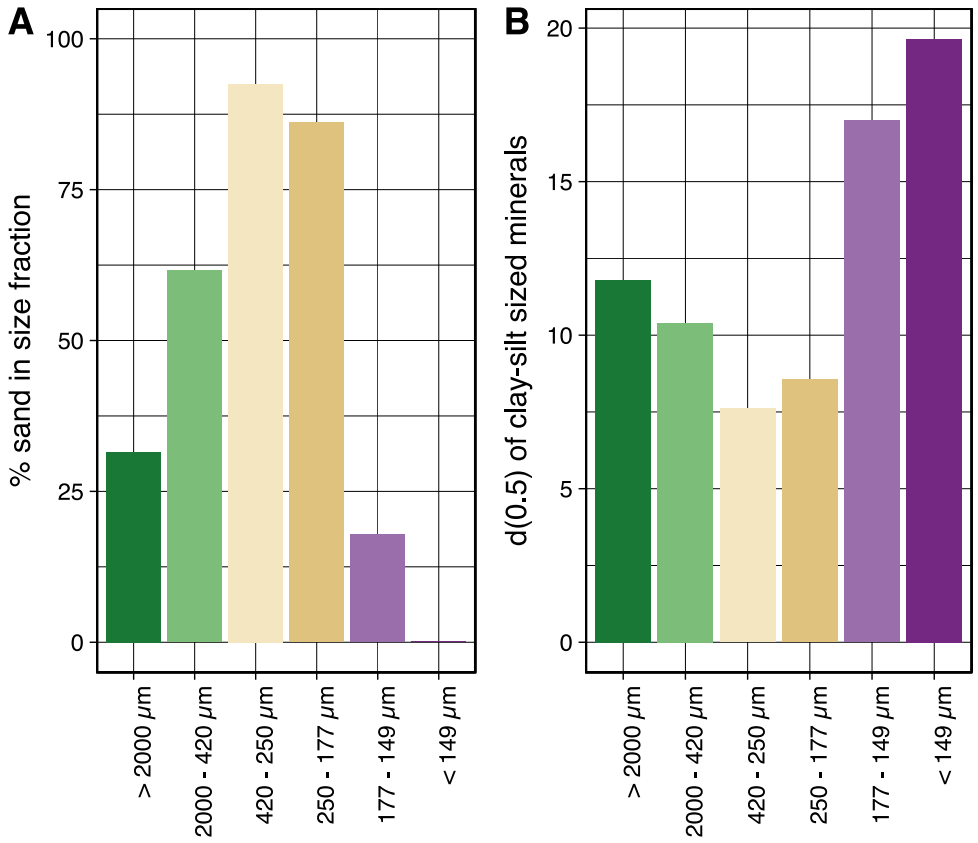

Figure 5.6: Static light scattering was used to determine the particle size distributions of minerals, following a DMSO wash to remove lignin. **A**: The size fraction relating to coarse sand was used to determine the sand content of each size fraction. Sand accounts for 86 % and 93 % of the material in the central sieves, and appears to be normally distributed within the sieve fractions. **A**: The d(0.5) of each fraction was calculated, ommiting material which is sand sized ($>$ 100 µm). The largest material was observed in the sieve, corresponding to material enriched in quartz silt.

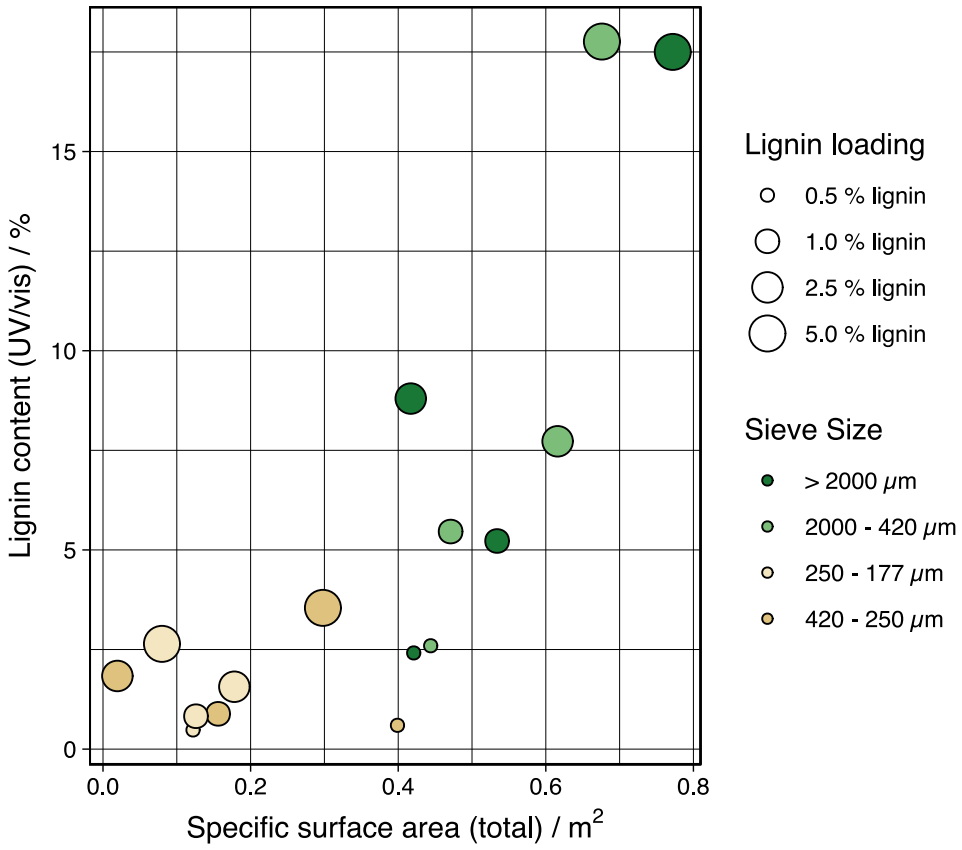

Figure 5.7: The total specific surface area or each sieve fraction, calculated from particle size measurements, were found to correlate with the lignin measured by UV/vis to be present in each sieve fraction. This suggests that lignin is associated with smaller particles due to the small surface area, and the specificity of this interaction may be minimal

whereby the 1 g of iron oxide was replaced by 1 g of quartz silt. It was found that the amount of material that was aggregated reduced after 3 cycles, from 12.5 $\pm$2.1, to 10.7 $\pm$1.7, and that the evolution of soil structure (the build up of aggregates with wet/dry cycles was significantly reduced. The distribution of lignin within the aggregates remained unchanged, suggesting that iron oxide enhances aggregate formation, adding to the amount of fine material that can form stable aggregates.

5.5.7 Bentonite

The addition of Bentonite, instead of kaolinite was found to have profound effects on the aggregation, and also the rate of soil formation (Figure 5.8. Initially the mass of aggregated material for bentonite soil was significantly higher than that of kaolinite, 15.5 $\pm$1.3 % and 9.3$\pm$0.3 % respectively. However, repeated wet and dry cycles reduced the amount of aggregated material for the Bentonite to 10.3$\pm$3.6 after three cycles. Despite this reduction in aggregation, lignin was found to be significantly higher in the aggregated size fraction as compared to the bulk soil, suggesting a preferential accumulation of lignin in aggregated size fractions. The driving force which allows lignin to accumulate in the aggregated size fractions may be due to surface chemistry or a greater slaking stability, that allows lignin-bentonite aggregates to remain stable when wetted.

5.5.8 Spectroscopic evidence of inter-particulate interactions

The generation of artificial aggregates also allowed for a spectroscopic investigation of particulate-particulate interactions, or particulate orientation/organisation in artificial aggregates. FTIR was used, initially to try and indicate the composition of each fraction, by identifying signals from each component of the soil, and to look for perturbations in the signals that might indicate bonding interactions. ATR-FTIR was carried out using whole aggregates, in order to retain any interactions which may be disrupted on crushing. Quantitative compositional analysis using FTIR was proven to be too complex and could not be achieved by deconvolution of signals, as there was significant overlap in almost all of the spectra from multiple species and there was additional effects from

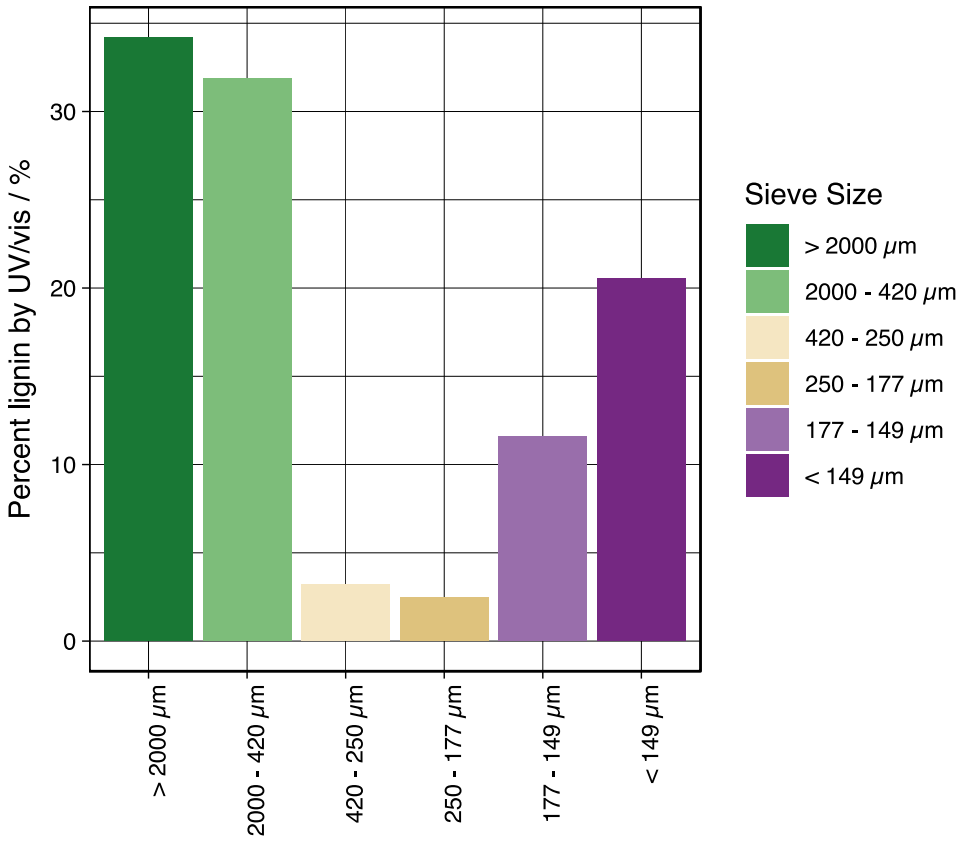

Figure 5.8: Artificial soils where kaolinite was replaced by bentonite resulted in large changes to the soil structure and lignin distribution. Lignin was found to accumulate in aggregated size fractions, concentrations of lignin were higher than in the bulk of the soil, suggesting a stable interaction between bentonite and lignin was formed.

changes in particle size and sample heterogeneity. Ratios of lignin and kaolinite powders were made in triplicates, and only a small contribution from lignin signals were observed in the FTIR spectra. This is because clays contain a high density of polarisable groups which makes them more sensitive for FTIR spectroscopy, and so using FTIR to indicate lignin content was abandoned. Kaolinite and mica, contains signals between 3600 and 3700 cm^{-1}, which are well separated from the most convoluted region. These signals are assigned to internal and external υ(O-H stretches), and may be used to indicate inter-particulate binding. 3620 cm^{-1} is usually assigned to an inner O-H stretch, which means it is unlikely to be affected by inter-particulate binding (*201*) and so changes in the external O-H stretch relative to the external peak might be used to infer hydrogen bonding interactions.

The aggregate size fractions resolved peaks which were unrecognisable as any of the minerals present in the soil. Signals for clay and mica O-H stretches became more resolved as material is less aggregated (finest material), this was observed in the O-H stretching region and in the lower wave-number region where signals attributed to υ(Si-O) are observed. This is evidence for a strong hydrogen bond interaction occurring between lignin and the clays. The enhancement of the lignin signals and decrease in kaolinite/mica signals in sieve fractions which are more aggregated suggests that lignin may act as a surface coating, since ATR-FTIR is a surface sensitive technique.

5.5.9 SEM of artificial aggregates

SEM was used to look at the aggregated size fractions of a unamended soil and a 5% beech lignin soil. Aggregated material with 5% beech lignin were significantly larger than the unamended soil but no structural organisation was identified. Grains were blocky and consisted of a mix of fine particles and lignin. Sand grains were found to be heavily encrusted with particles which resembled both lignin and clay particles suggesting that lignin was able to glue minerals to the surface (Figure 5.9).

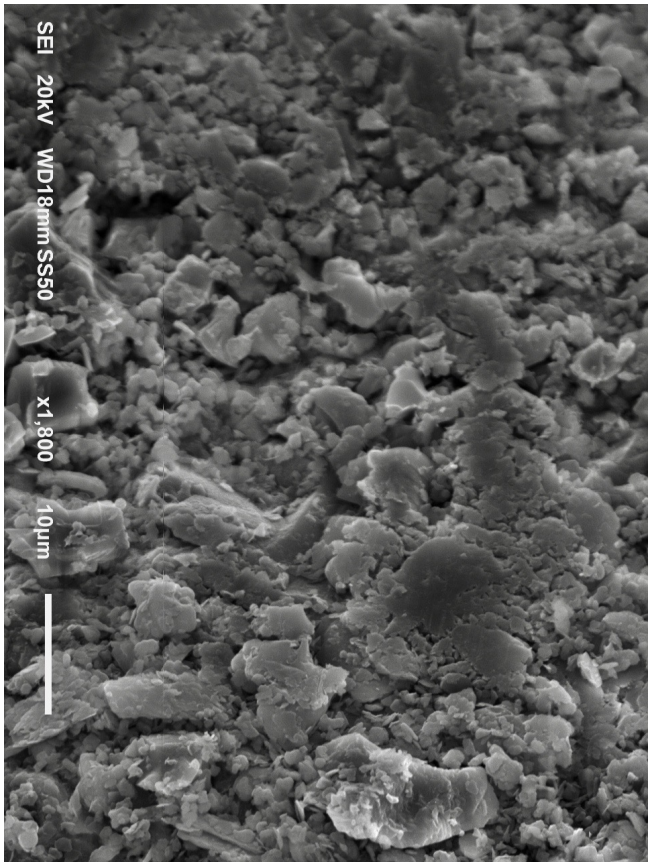

Figure 5.9: SEM image of the surface of a sand grain, which is encrusted with material which resembles lignin, quartz silt and kaolinite.

5.5.10 Cation exchange capacity

The cation exchange capacity was measured for all soils. CEC values were low and was determined largely by the clay present. CEC was measured to be around 10 cmols.kg^{-1}, with no significant differences at any beech lignin loading. 5% spruce lignin however, increased the CEC of kaolinite based soils from 10.19±0.17 to 10.83±0.77 cmols.kg^{-1}. The increased CEC of the spruce lignin is a result of a higher carboxylic acid content (see A.1). Bentonite soils had a higher CEC, with 5% spruce bentonite soils measured as 13.31±0.32 cmols.kg^{-1}. The other eulted cations (Na^+, Mg^{2+}, K^+, Ca^{2+}) were measured and a slight increase in the concentration of all cations was indicated as lignin was added, possibly due to cation exchange with lignin protons.

5.6 Conclusion

The aim of this study was to demonstrate that clays in soil accumulate particulate organic matter based on the accumulation of materials which increase mechanical strength and prevent slaking. Kaolinite and lignin were used in this study, as they have previously been shown to have increased mechanical strength and water resistance at ratios around 50:50 volume. This study showed that kaolinite rich aggregates formed by repeated wet/dry sieving and mechanical disruption did not accumulate lignin at mass concentrations higher than that of the bulk soil, or at levels which result in higher mechanical strength or slaking stability. This indicated that kaolinite-lignin interactions are not retained preferentially, and that lignin content in aggregates is based on mixing and lignin loading only. Artificial soils with bentonite instead of kaolinite were, however, shown to accumulate lignin at higher levels than in unaggregated material, suggesting the formation of aggregates with heterogenous composition in comparison to that of the bulk soil can occur and that the abiotic accumulation of particulates is likely to occur in soils rich in 2:2 clays.

It was found that despite an increase in aggregation resulting from additional lignin loading, lignin did not appreciatively accumulate in aggregated material in respect to the bulk material. This suggests that disruptive forces caused by water and mechanical stress do not preferentially select out material which is more resistant to these pressures, and that particulate solids remain well mixed. This

suggests that the weak interactions which cause adhesion of surfaces are not different enough to cause an enrichment of lignin in the kaolinite rich aggregates. This challenges the assumption that organic particulates may preferentially aggregate with more reactive surfaces in real soils, and that the distribution of carbon in soils may be controlled more by deposition and mixing than chemical structure. It was also found that organosolv lignin did not contribute significantly to an improvement of CEC, spruce organosolv lignin was found to have a higher CEC then beech organosolv, due to the presence of additional carboxylic acid groups.

The artificial aggregates generated in this study also served as model aggregates, used to study particulate interactions between lignin and soil minerals. Some of these experiments are included in chapter 7. Since these studies were carried out on abiotic systems, the biological component is missing. The biological component to aggregate formation is important, as a number of organisms produce exudates which act as a glue, additionally, soil organic matter is used as a food source, and is degraded by microbial life.

Chapter 6

How lignin modifies the microbial communities in a sandy soil

6.1 Abstract

Organic residues and soil amendments are known to modify the microbial and fungal communities present in the soil, acting as a source of food and habitat. (*4*) Microbial ecology plays an important role in creating and modifying soil structure, cycling nutrients and breaking down organic matter. Lignin is a natural component in many soils, so it is expected that when added to soils the lignin may break down. The motivation of this experiment was to see how lignin, added as a soil amendment could modify the microbial and fungal composition of the soils, particularly to see if the additional substrate would reduce diversity, favouring more specialist (mainly fungal) species. Lignin breakdown has been studied, and it is known that nitrogen availability and the availability of additional, more easily accessible carbon sources (such as sugars) are key factors that determine lignin decomposition. (*202*, *203*) In this experiment, organosolv lignin was applied to a sandy soil, containing low moisture content and low organic matter. Soils such as these could benefit from more biologically recalcitrant organic matter in order to build soil structure and retain nutrients. Organosolv lignin, despite resembling lignin residues found in soil, presents a more recalcitrant substrate for microbial and fungal communities compared to biomass which contains around 20% lignin. Additional nitrogen

and cellobiose was added as additional substrates, which may accelerate lignin decomposition or modify microbial community structure further. It was found that the addition of lignin reduced the microbial functioning of the soil considerably, in all experiments where lignin was present metabolic activity was greatly reduced. Where lignin was not added, microbial communities functioned well. This suggests that lignin is not a good substrate to add to sandy soils containing low amounts of organic matter. Few species are able to make use of lignin as a substrate, and low molecular weight fragments present may be toxic.

6.2 Introduction

The decomposition of organic matter is as important as photosynthesis for the cycling of carbon in natural ecosystems. The breakdown of organic materials in soils depends largely on the composition of the substrate, but also factors such as nitrogen availability, moisture and temperature (*204*). This is because these factors influence the metabolic action of the soil ecology, the primary drivers of soil organic matter decomposition. Microbial communities in soil not only influence the breakdown of soil organic matter, but the microbial communities themselves are modified by the abundance and type of organic matter in a soil. (*205*, *206*) Healthy soil communities are also able to create and modify soil structure, and so soil carbon and soil biology are inextricably linked. (*204*)

6.2.1 Fungal/microbial degradation of lignin

Of the three main plant biopolymers (cellulose, hemicellulose and lignin), lignin is the most resistant to microbial decomposition. Fewer soil organisms have the enzymatic tools to degrade polyphenols in comparison to the ubiquitous cellulases used to degrade hemicellulose and cellulose, and so it is thought to be more 'recalcitrant'. (*207*, *208*) Lignin presents a challenging substrate due to combined aromaticity and heterogeneity, lignin degradation is also known to liberate small soluble phenolic compounds which can bind and hinder enzyme functioning. (*209*) For this reason, lignin was once thought to be the primary source of the 'humic substances' found in soil. However, recent

evidence suggests that lignin can be metabolised relatively quickly (within 5 years), despite increased lignin content resulting in reduced decomposition rates. (*210*)

Wood-rotting saprophytic basidiomycetes, such as white and brown rot fungi have long been observed to degrade lignin. They work by secreting extracellular oxidative enzymes (oxidoreductases) such as ligninase, laccase, lignin peroxidase and manganese peroxidase to breakdown lignin in cell walls. (*211*, *212*) Filamentous fungi utilise holes and channels in the wood such as the xylem and phloem to penetrate the surface wood, and so wood breakdown is also dependent on the substrate morphology. (*213*, *214*). Fungi such as lignin decomposing basidiomycetes, are known to produce large amounts of water insoluble exudates, which can enhance soil aggregation when present in soils. (*215*)

Streptomyces is another known lignin degrader utilising peroxidase type enzymes. Lignin degradation is usually lower in bacteria, resulting in the formation of a low amount of acid soluble material. (*216*) Non-filamentous bacteria such as Pseudomonas spp. can degrade soluble lignin fragments, however, they often lack the extracellular enzymes required to break down polymeric lignin. Actinobacteria, a-Proteobacteria or g-Proteobacteria have been shown to degrade lignin, along with specialised bacteria living in the digestive organs of wood eating insects such as termites. (*217*). Less is known about Archea, but it is likely that they too are able to produce lignin degrading enzymes. (*207*) Lignin degradation, especially in woody biomass is unlikely to occur due to the efforts of a single organism, instead a consortia of organisms working symbiotically is more efficient. (*207*) For this reason, litter rich in a multitude of more difficult substrates is likely to produce a more dynamic and rich soil ecosystem. (*218*)

6.2.2 The role of soil consitutents

The ratio of carbon to nitrogen is known to strongly affect the rate of degradation of carbon in soils, N is a requirement of microbial growth and can be limiting. Evidence suggests that nitrogen (N) plays a major role in the control of lignin decomposition in soil, especially as lignin is associated with very little N. However, the rate of decay of lignin and its relationship with nitrogen is not straight forward, and studies have been contradictory. (*219*) Some studies have shown that fungi require low

levels of available N to begin lignin decomposition, and that a source of more easily metabolisable C is required. (*203*) It is not clear how the addition of N in the form of fertiliser might effect lignin decomposition. Applied N has been shown to reduce decomposition of high lignin plant litters, possibly due to a shift in microbial community structure. (*203*) However, studies have also shown that in soils with low N, additional N enhances lignin decomposition. (*220*) There is also evidence to show that the soil mineral phases may control the rate of decomposition of lignocellulosic materials, especially the presence of Al or Fe oxides/hydroxides. (*221*).

6.3 Experimental design and methodology

A sandy loam soil taken from an agricultural field in Herefordshire, UK was used as a model soil. The pH was measured to be mildly acidic (pH 6.5), SOM content was low, only 3.4 % of the soils mass was combustible material as measured by TGA. CEC was measured as mentioned previously, and found to be 5.95 $\pm$ 0.21 cmols.kg^{-1} which is very low. The presence of large amounts of quartz and iron oxide was confirmed by XRF. The particle size distribution was determined to be 14.7 % clay, 22.0 % silt, 22.6 % fine sand, 38.7 % medium and 2.1 % coarse sand by the pipette method. The soil was sieved to remove any large plant debris and gravel, and mixed thoroughly. The sieved soil was kept in a moist and dark environment until use. 5.0 g of soil was used for each microcosm experiment and the following treatments were applied to give a fully factorial set of experiments:

The following treatments were applied:

- Beech organosolv lignin was added at 0, 1 or 5 % of the soil mass.
- Urea was added, to attain N concentrations of 0, 9.867 and 19.734 $mg_N.g^{-1}$ soil
- Cellobiose was added at 0, 0.768 and 1.536 $mg.g^{-1}$ soil

The urea added was used to increase the C:N ratio of the lignin artificially. The C:N ratio ranges from very high (no urea added) to very low in order to stimulate lignin degradation. C:N ratios of

the added carbon and nitrogen ranged from 1 to over 20. Urea is an extremely common fertiliser and has been shown to effect community structure at loadings of 0.5 mg/g, at higher concentrations urea may become more toxic, and so urea was added gradually over the first days of the experiment. (*222*) Soils were then incubated for 30 days at 20 °C in a humidity stabilised desiccator.

6.3.1 CHNS, moisture content

CHNS analysis was carried out as detailed in Chapter 5. Moisture content was determined by weighing before and after drying in a 50 °C oven for 48 hrs.

6.3.2 Metabolic activity

A measure of the metabolic activity of the soils was estimated based on the quantification of adenosine triphosphate (ATP), which also gives a measure of the amount of viable cells present in the soil. 45 µg subsamples of soil were taken and cells were extracted in a 96-well plate. Sterile phosphate buffer saline solution (PBS) was added at a soil to solution ratio of 1:1 and briefly vortexed, a further 450 µL of PBS was added. The soil solutions were vortexed at 250 rpm for 10 minutes and left to settle. The supernatants were collected and diluted for ATP analysis in a separate 96-well plate. ATP measurements were carried out using the BacTiter-GloTM Microbial Cell Viability Assay kit. ATP is measured using luminescence which forms as a result of the binding of a thermostable luciferase enzyme to ATP in the presence of oxygen and magnesium. A 1:2 ratio of BacTiter-GloTM reagent to soil extract solution was used, luminenscence was detected using a BioTek Synergy2 plate reader. Samples were measured for 7 minutes with readings taken every 1.15 minutes and exposure time set to 0.5 seconds, and standardised against a control. Luminescence was converted to ATP (nmol g^{-1}) at pH 7 using a previously obtained calibration, where d is the dilution factor (10 fold dilution) (6.1).

$$ATP = \frac{Luminescence_{sample} - Luminescence_{control}}{1416.8} \times d \tag{6.1}$$

6.3.3 HSQC of lignin extracts

Lignin and associated soluble organic matter was extracted from representative samples from microscosm experiments by extraction with acetone. The acetone solutions were collected until the acetone solutions were clear (5-6 times). Extracts were carried out so the concentration of lignin in each sample was roughly equivalent. Beech lignin was added to 0% mass lignin before extractions to use as a control. Acetone was removed by rotary evaporation and lignin was re-dissolved in d-DMSO for 2D HSQC NMR. HSQC of 5 lignins were extracted from 1% and 5% samples with high ATP counts.

6.4 Results

6.4.1 Microbial response to lignin addition

ATP counts by the end of the 30 day incubation were all extremely low, except for samples with high N loadings and low lignin loadings which were recorded to have the highest ATP counts around 100 nmol.g^{-1}. ATP counts exceeding 30 nmol.g^{-1} were only observed for soils containing no lignin and the maximum nitrogen loading. ATP counts drastically reduced as the amount of lignin added increased, with the maximum loading resulting in no ATP counts being recorded. ATP counts did not correlate with moisture content.

Note: The objectives of this experiment initially included extraction of genetic material for 16S and 30S for microbial profiling, using T-RFLP (terminal restriction fragment length polymorphism). However, the amplification of material by PCR was extremely problematic. This may be due to the low amount of genetic material extracted as indicated by the reduction in ATP counts or the presence of low molecular weight lignin fragments, which may hinder extraction of genetic material.

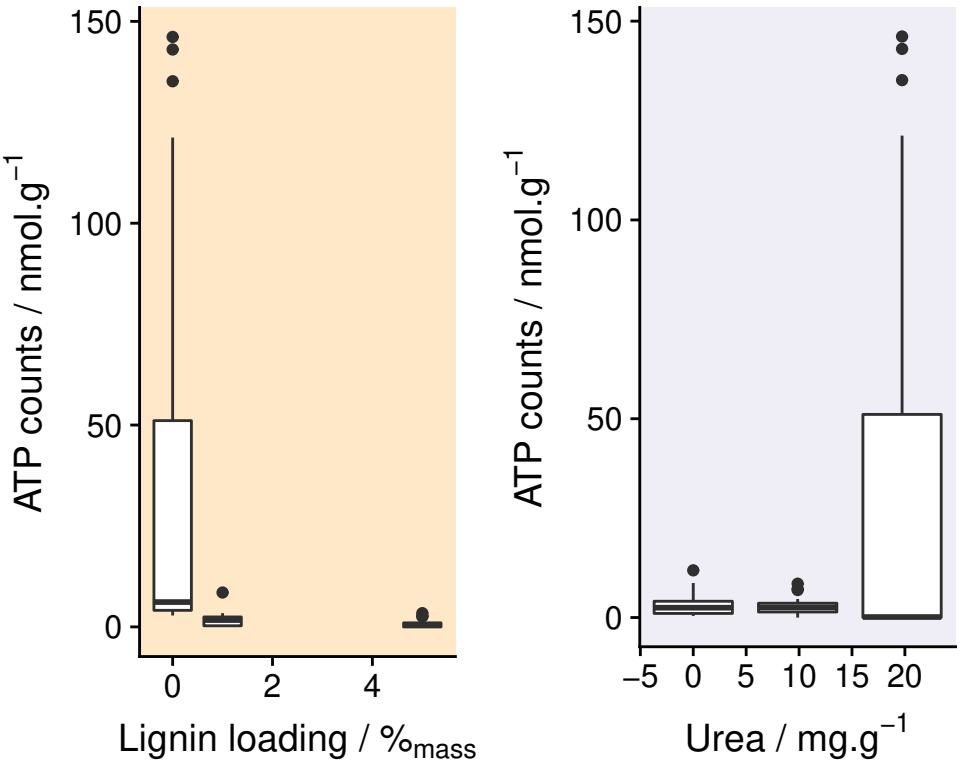

Figure 6.1: ATP counts were reduced drastically by the addition of lignin, conversely, ATP counts were much higher in soils with additional N. Soils with no lignin and high N additions were recorded to have the highest ATP counts.

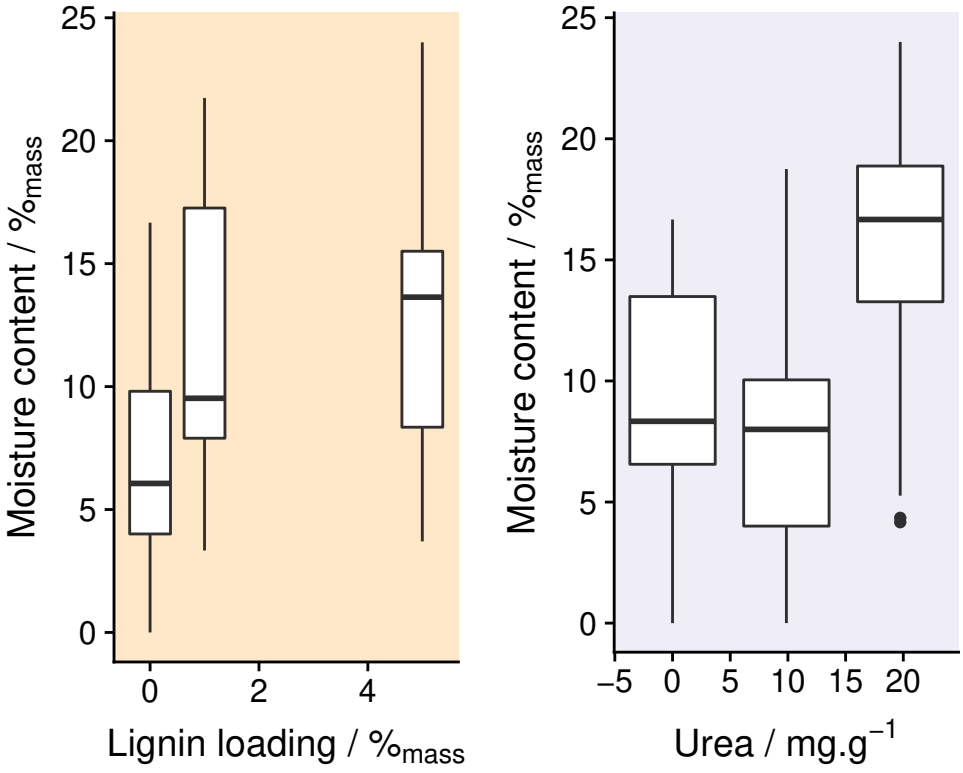

Figure 6.2: The moisture content of soil microcosm experiments increased with both lignin addition and urea added.

6.4.2 Moisture content

Soils were oven dried overnight to obtain moisture values. Values were found to be around 10% with high variability. Moisture content did increase with lignin content, suggesting lignin helped soils retain moisture. Soils without lignin had a moisture content of 6.8 $\pm$ 5.3, the addition of 1 and 5% lignin increased moisture content to 11.9 $\pm$ 5.6 and 13.3 $\pm$ 5.5 respectively. Urea was also found to increase moisture content(Figure 6.2).

6.4.3 Elemental analysis and mass loss

The soil microbial community is expected to utilise carbon present in the soil, or in the lignin to maintain metabolic activity. CHNS analysis was used, to determine how much carbon and nitrogen was lost upon the addition of lignin to these soils. Carbon loss was calculated based on the amount of C before and after microcosm experiments. Carbon loss was found to be higher in samples containing high levels of lignin, despite reduced ATP counts. This loss of C was reflected in the

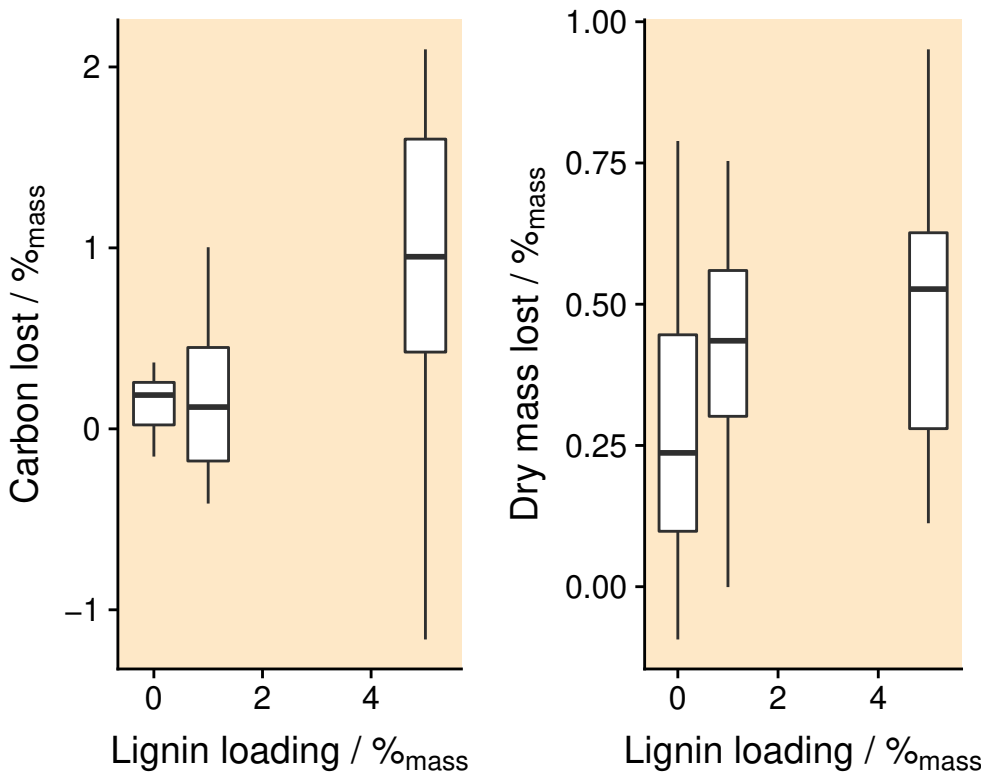

Figure 6.3: Increasing the amount of lignin added to the soil increased the amount of carbon lost by the soil, indicating that likely lignin was slowly degraded in these microcosm experiments, despite the very low ATP counts. There was extremely high variance in the values obtained for 5% lignin loading which could not be explained by other measured variables such as N, cellobiose or moisture. Similarly the dry mass loss was higher when lignin was present, dry mass loss did not exceed 0.5 % of the soils mass.

change in dry weight which reduced by around 0.5 % mass over the course of the experiment (Figure 6.3). N content did not change over the microcosm experiments. There appears to be a negative linear relationship between mass loss and ATP, and a modest increase in mass loss with lignin. This means that some lignin may have been metabolised or lost, but that microbial activity was reduced as a result.

6.4.4 Lignin HSQC

The HSQC of each lignin was measured and integrals of important signals were normalised to the largest $S_{2,6}$ signal in the aromatic region, as S lignin may be more difficult to degrade then other components of lignin. Additionally, the signals could be normalised to the intense MeO signal. The region δ_C 50 - 90 and δ_H 2.5 -6 ppm was used to indicate microbial or fungal degradation. Microbial

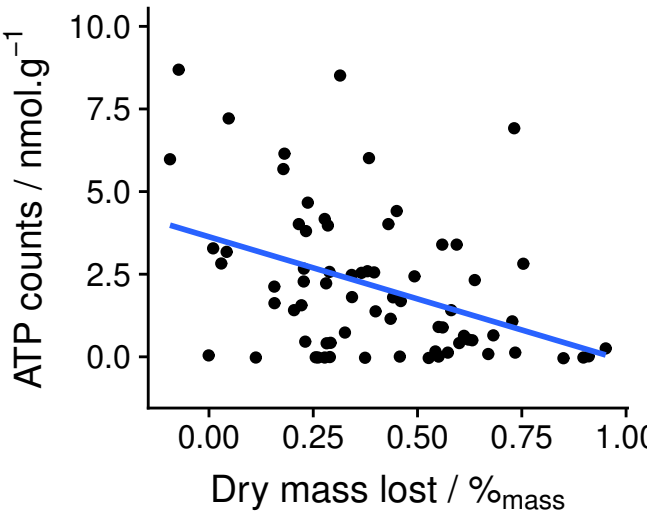

Figure 6.4: A negative correlation between ATP counts and dry mass loss was observed, suggesting microbial communities were able to metabolise some material, but that this had a negative effect on overall microbial function or abundance.

and fungal degradation usually proceeds by the oxidative cleavage of β-aryl ether bonds, which are present in the region described above. Normalised to either the S signal intensity or the MeO peak the signals for the β-O-4' did not appear to change significantly for the extracted lignin, at any lignin loadings. This suggests that lignin had not undergone significant degradation in the 30 days, and the carbon and mass loss was likely to originate from the loss of soil organic matter present in the soil. Represnetative HSQC spectra can be found in the appendix (see A.1).

6.5 Conclusion

Lignin is known to be a difficult substrate for microbial and fungal communities to degrade, and only few specialised species are able to use lignin as a source of energy. Its biological recalcitrance might make lignin the ideal soil amendment in the humid topics where soil organic matter or soil amendments are turned over rapidly. However, the impact of this material on the microbial community is an important consideration, since the soil depends upon the soil ecosystem for cycling nutrients and overall soil health. Here, lignin was found to drastically reduce the metabolic activity of a series of soils of a sandy agricultural soil over 30 days incubation. Microbial communities responded well to additional N, in the form of urea, but N was not able to activate the degradation of lignin. Moisture

content was increased by the addition of lignin, suggesting soils were able to retain more water in the presence of lignin, however, this appeared not to effect the ATP counts. Both carbon losses (by CHNS) and dry mass loss was higher at higher lignin contents. HSQC NMR showed that lignin had not been significantly altered, and that the loss of carbon and mass is likely to be due to the loss of alternative substrates such as microbial negromass, residual SOM, which may have been encouraged by the addition of N and cellobiose. The presence of high concentrations of lignin, and low microbial biomass, meant that the extraction and amplification of biological material for meta-genomic analysis was problematic. It is likely, however, that the microbial activity was significantly reduced by the addition of lignin, even with the addition of additional sources of organic matter, and nitrogen. This suggests that the wide-spread application of technical lignin on agricultural soils may strongly modify and reduce the microbial community and ecosystem functioning. Since the health of a soil is dependent on the biological resilience and diversity, the addition of a lignin amendment may not be recommended without additional innoculants for example, which can counteract the negative effects of lignin.

Chapter 7

Investigating Organosolv Lignin - Kaolinite Interactions using Solid Statets NMR

7.1 Abstract

The interactions which occur between particles in soil are weak, and easily disturbed. Fragile associations at surfaces can result in the formation of stable structures which bring about soil structure. Observing these interactions without disturbing the structure is a technical challenge. Solid-state NMR is a non-destructive technique which is capable of providing information on undisturbed solids. Here, the lignin-mineral interaction observed in previous chapters was investigated using solid state MAS ^{1}H NMR and T_1 spin-lattice relaxation experiments. No clear chemical shifts could be observed from the heterogenous polymer on contact with the clay, but a reduction in signal intensity of the aromatic region was observed in non-aggregated fractions of synthetic soils. The T_1 of aliphatic protons was faster than aromatic protons in artificial aggregates, and this may be attributed to methoxy groups at the surface of lignin. T_1 experiments with water indicated that lignin did not act as a hydrophobic barrier, as a strong interaction with water was indicated.

7.2 Introduction

Solid state NMR is perhaps one of the only non-destructive methods which is able to provide information on the chemical environment of molecules in a solid, and is therefore well placed for studying subtle or weak interactions between particulates. It has also been employed for the study of the interaction of water with solids such as clays, and molecules at the solid-liquid interface (*223*). Unfortunately, strong dipolar interactions can cause spectra to be broad, resulting in the loss of information. The dipolar coupling constant is strong between nuclei which are close in space and of a similar gyromagnetic ratio, for this reason ^{1}H-^{1}H is stronger than ^{1}H-^{13}C. When molecules are fixed in a solid, the dipolar interaction is strengthened, as compared to solution phase where molecular rotation causes dipolar coupling to average to zero. Fortunately, nuclear dipole-dipole interactions can be averaged in solids if spun at 54.74° to the magnetic field, using a technique called magic angle spinning (MAS). Using this technique some of the signal resolution can be recovered. Additionally, lineshape analysis, spin-lattice (T_1)and spin-spin (T_2) relaxation has been used to indicate the interactions of water (or D_2O) with clay surfaces. Information regarding the distribution, diffusion rates and even orientation of water molecules on the surface of clays has been demonstrated at a range of water contents. (*224*)

Spin-lattice relaxation (T_1) is a decay constant which describes the recovery of the z component of the nuclear spin magnetization to its thermodynamic equilibrium, and is considered to be a first-order process. T_1 is determined by measuring the recovery of the NMR signal over time (Equation 7.1), where Mt is the magnetization at time t and Mo is the magnetization at equilibrium:

$$M_t = M_0(1 - e^{-t/T_1}) \tag{7.1}$$

The process can be slow (on the order of seconds), as energy exchange between dipoles is weak, and molecular reorganisation may need to occur to allow energy to be dissipated. The presence of paramagnetic ions can cause rapid relaxation due to the presence of unpaired electrons, which have a magnetic moment 10^3 times greater than that of the nucleus. T_1 spin-lattice relaxation also occurs more effectively when the frequency of molecular motion is closer to that of the NMR frequency,

typically $10^6 - 10^8$ cycles/second. In polymer chemistry, T_1 spin-lattice relaxation is used to indicate molecular rigidity and is particularly sensitive to high-frequency side chain motions. (*225*) (*226*) It is also particularly sensitive to the molecular environment of water.

7.3 Methodology

Solid state magic angle spinning (MAS) NMR was carried using a Brucker Spectrospin (200 MHz) spectrometer with a Bruker HP WB 73B MAS 4BL CP BB WVT probe. Samples were lightly packed into 2.5 mm rotors, and were referenced against Tetramethylsilane (TKS) in order to determine chemical shifts.

Synthetic soils were generated as described in chapter 5. Synthetic aggregates were generated as described in chapter 2.

7.4 Statement of originality

Data included in this section includes T_1 data obtained by Dongxun Lyu and included in a BSc report 'A study of the water behaviour at organic-inorganic interfaces using spectroscopy methods'. This data was re-analysed and interpreted for this section, and the findings outlined here are original.

7.5 ^{1}H MAS NMR of synthetic soils

The synthetic soils size fractions were freeze-dried before analysis to remove any residual water. The lineshape for each size fraction was broad, but resembled lignin. (*227*) Signals were assigned based on the solution phase organosolv beech and spruce lignin ^{1}H NMR spectra (Figure 7.1 and 7.2). The two broad signals were assigned as aromatic - around 7.5 ppm, and aliphatic (with a large contribution from MeO groups) at around 4.5 ppm. Spinning side-bands were present at spin speeds up to and including 6000 Hz. The peaks were fitted to Lorentzian-Gaussian functions using

Mestrenova v.12 to obtain peak positions, intensities and the areas in order to determine if signals in the aromatic or aliphatic regions were modified in the presence of minerals due to interactions at the surface. Most notably, there was no observable shift in peak positions however, the signal was broad, and subtle interactions might be masked. The contribution to the total signal from the aromatic region was less for material in the finest fractions (non-aggregated =29 % aromatic) as compared to aggregated size fractions (33% aromatic), which was closer to lignin. Lignin was washed from the size fractions and compared by solution NMR. Lignin was found to be identical in different size fractions, so different spectra must result from a interaction or interference from clay minerals, rather than a fractionation. In order to determine the contribution of surface hydroxyl groups on clay, the aggregates were soaked in deuterated water for 24 hours and freeze-dried. No observable change in peak intensities or line shape was observed, indicating the contribution from exchangeable protons was negligible. ^{1}H MAS NMR of the size fractions was not sensitive enough to indicate any molecular interactions, especially as the concentration of lignin was low and lignin was amorphous, resulting in a broad signal. These experiments were repeated with spruce organosolv lignin, and bentonite lignin, and no changes in the spectra were observed in aggregated fractions.

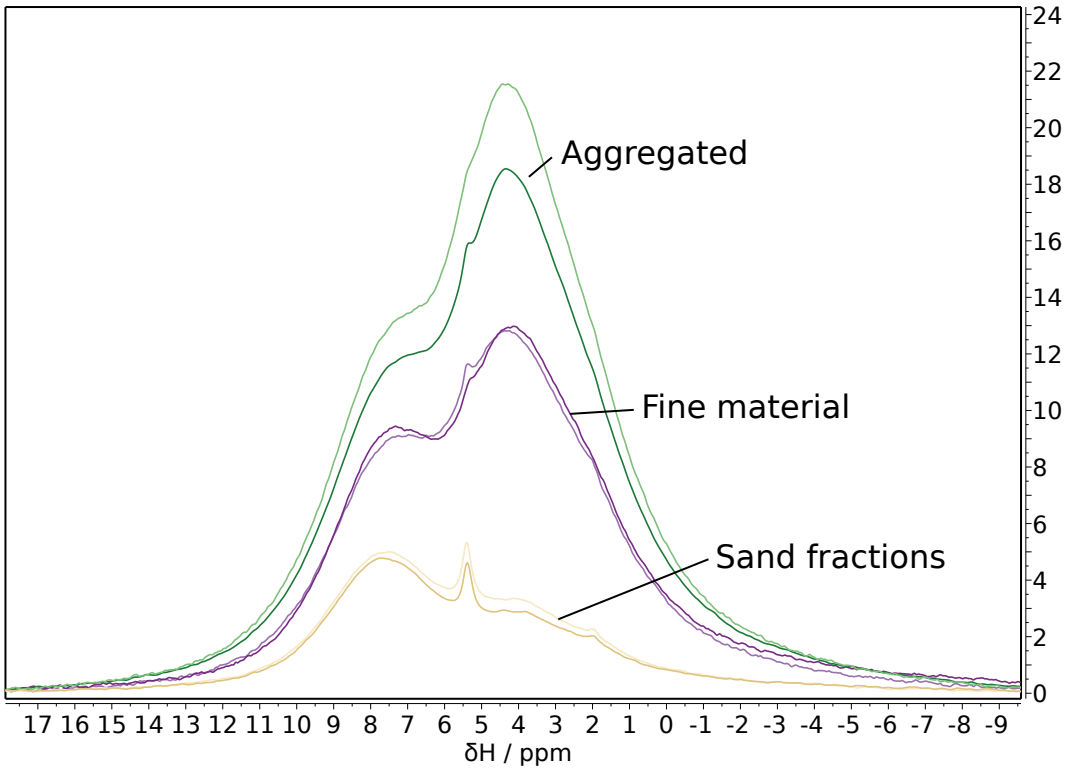

Figure 7.1: The ^{1}H MAS NMR spectra of the size fractions of the synthetic soils, normalised to the proton concentration present, obtained from CHNS measurements. The broad line-shape originates from protons on the lignin, with some minor contributions from clays.

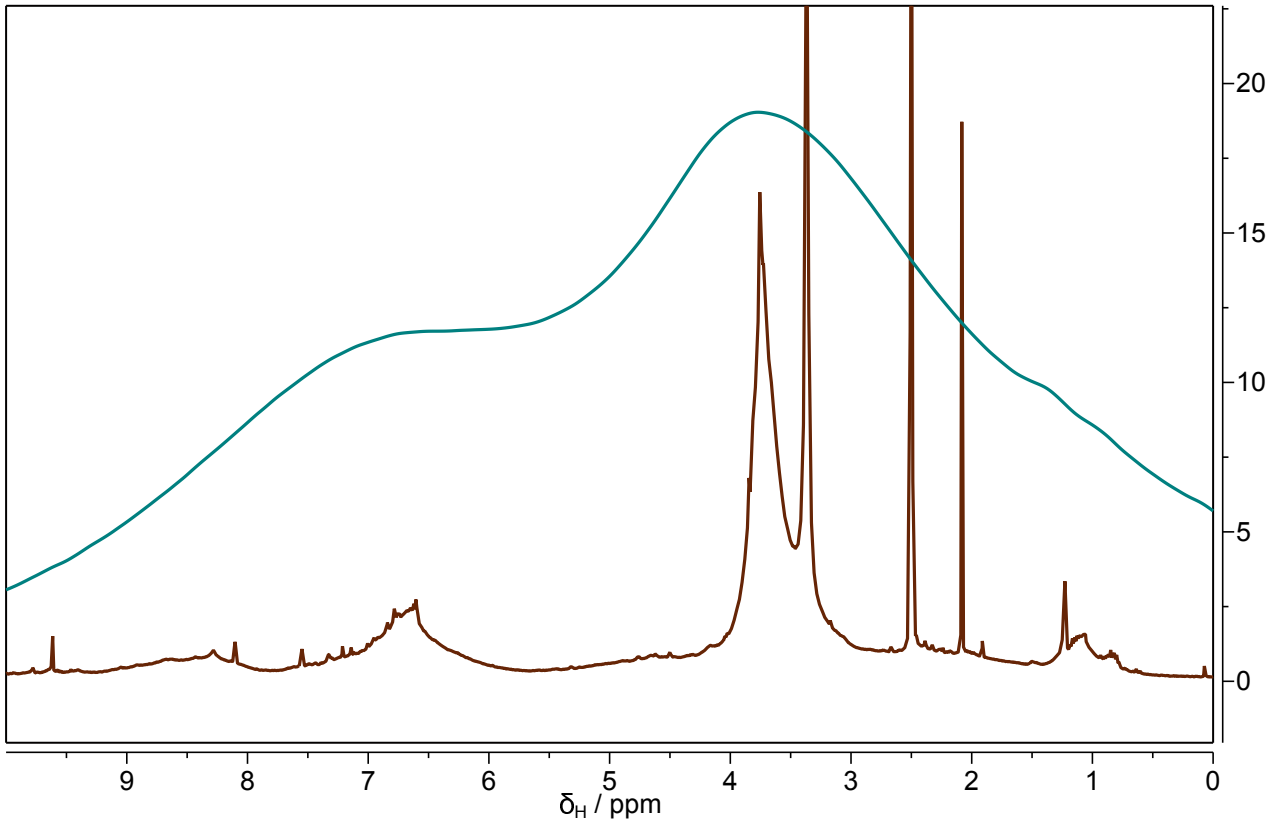

Figure 7.2: The ^{1}H solution state NMR spectra (dark brown) of beech organosolv lignin as compared to the solid state ^{1}H MAS NMR spectra (dark blue), showing the significant broadening effects. The y axis is an arbitary intensity unit which has been scaled to see both spectra. Signals above 5.5 ppm are from aromatic protons, below 5.5 the protons are generally more aliphatic. Sharp peaks are from residual water (3.35 ppm) and DMSO which was used to reference the spectra at 2.50 ppm.

7.6 T_1 relaxation NMR of synthetic soils

The T_1 was measured for the aliphatic and aromatic component and analysed as a single exponential function. The T_1 for the aromatic region was distinct from the aliphatic regions in all cases, in the size fractions despite the uniform T_1 of pure lignin. The aromatic region had a T_1 of 400 ms, whereas the T_1 for the aliphatic region appeared to be more sensitive to the molecular environment and had a T_1 of around 200 ms. The faster relaxation time may be due to the increased mobility of the aliphatic groups, particularly the methoxy groups. Interference from minerals in this region was extremely small. In the presence of clay, in the aggregated material, the T_1 for the aliphatic region increased to 340 ms, suggesting a slower relaxation on mixing with minerals. This suggests that a component of the aliphatic signal, likely the methoxyl groups, are molecularly more constrained on contact with the clay, and may be forming binding interactions with the clay surfaces. However, paramagnetic groups present on the clay surface may not be in close enough proximity to allow for rapid relaxation. Non-covalent interactions between lignin and hemicellulose are thought to be important for the structural stability of cellulose, and the role of methoxy groups has been suggested. (*112*) It is possible that these groups play a similar role in binding clays.

7.7 T_1 and T_2 relaxation of synthetic aggregates on wetting

The T_1 and T_2 was measured for a series of lignin:kaolinite mixtures at different moisture contents, ranging from 0 to 20 weight percent water. A single T_1 and T_2 was measured for each experiment, and was considered in relation to the majority phase contributing to the signal.

7.7.1 Kaolinite, lignin and bentonite

The signal for dry kaolinite was weak, and so on wetting, the signal intensity increased significantly. Water signals dominated the T_1 for wetted samples. The T_1 for pure water is very high (measured as 2.397 s for this instrument), and so the addition of water was expected to increase the T_1 substantially. However, this was not observed up to the maximum of 20 % moisture, T_1 remained

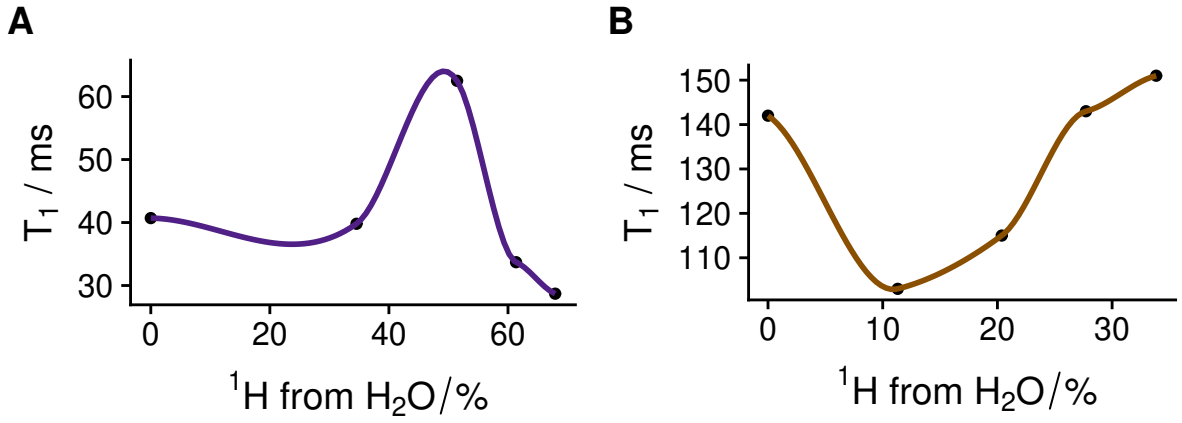

Figure 7.3: The T_1 for kaolinite and lignin as water content was increased from 0 - 20$\%_{wt.}$. **A**: Kaolinite appears to reach a maxima when the number of protons contributing to the signal contributes 50%. **B**: Adding water to the lignin reduced the T_1, the water molecules cause rapid relaxation of the majority phase - lignin.

below 60 ms, close to that of dry kaolinite, even when over 50% of the signal was from water (Figure 7.3, **A**). This suggests a strong water-kaolinite interaction, paramagnetic ions in the kaolinite may cause fast relaxation of protons in water. A maxima was observed when the protons from water reached 50%. Literature has found that a monolayer of water forms on kaolinite around 20% relative humidity, around 2% weight water (*228*). However, this data was obtained for very low surface area kaolinite. It is possible that the maxima represents a transition from monolayer coverage to multilayer coverage or the formation of droplets.

Lignin is proton rich compared to the clays, and the signal from lignin was dominant ($>$ 60%) at the water contents tested (Figure 7.3, **B**). Lignin has a low surface area, and it was calculated that there was enough water to fully wet the lignin surface below 5% moisture content. The T_1 of lignin was around 140 ms, the addition of water caused the T_1 to drop, the addition of more water caused the T_1 to rise again, towards that of bulk water or lignin. The addition of a small amount of lignin may result in a loosening of the molecular configuration and the decreased rigidity may result in a lower T_1 (*226*). The T_1 and the signal from lignin is dominated by the oxygenated aliphatic region, with an extremely strong signal from MeO groups. The change in T_1 may reflect the changes in this region. At high moisture contents, a network of protons is prevalent and the T_1 tends towards an average of all the T_1s in the system. The T_1 increases again as more free water is added to the

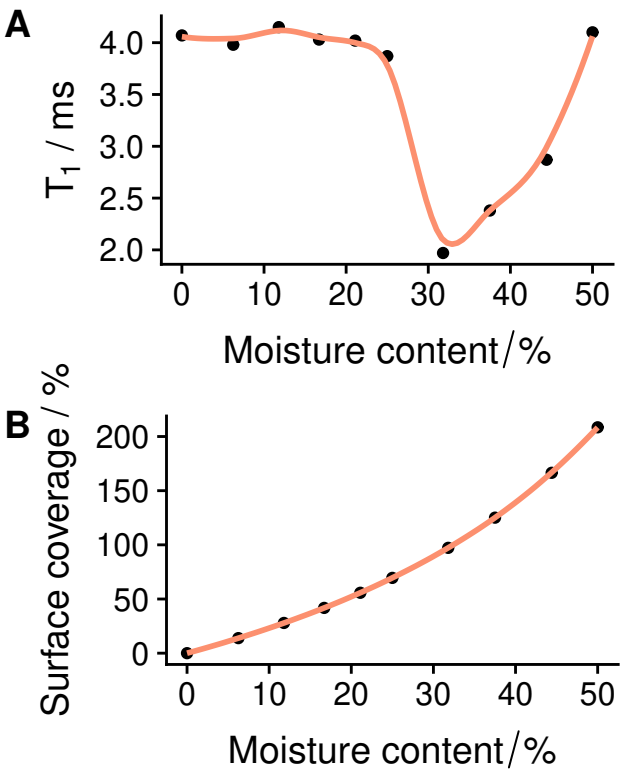

Figure 7.4: **A**:The T_1 for bentonite, which drops dramatically around 30% moisture content. This appears to correspond to a transition from monolayer to multilayer water coverage as indicated by calculations made in **B**.

system.

In order to test the hypothesis that a large change in T_1 is indicative of a transition from a monolayer to multilayer water, bentonite was also tested as a function of moisture content. The T_1 of bentonite was extremely low, 4 ms, such a fast relaxation is due to the presence of paramagnetic ions. Signal intensity was also very small. The addition of moisture did not change the T_1, until 30% moisture content at which point the T_1 becomes extremely rapid, reaching a minima at 2 ms (Figure 7.4 **A**). Further addition of water results in an increase in the T_1 value. This drop coincides with the transition from a monolayer surface coverage of water to a multilayer coverage based on calculated values (Figure 7.4 **B**).

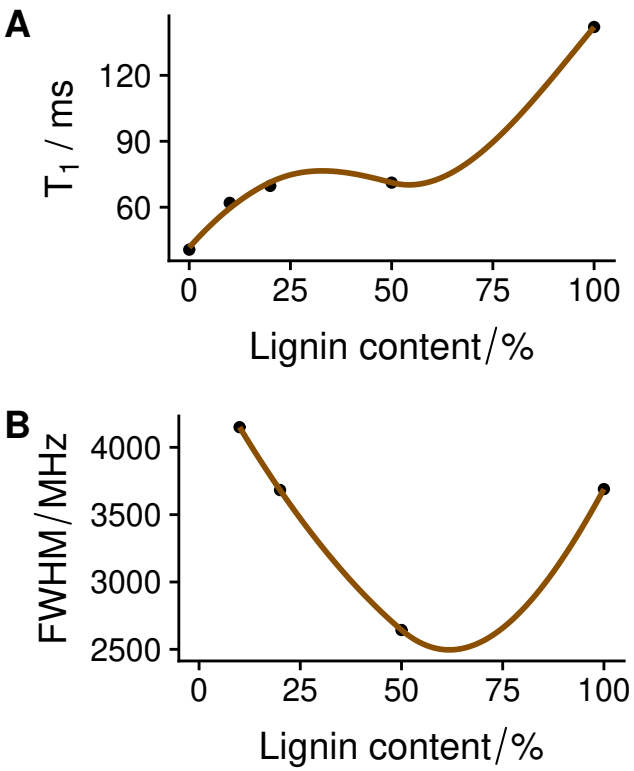

Figure 7.5: **A**:The T_1 and **B**: FWHM of for kaolinite:lignin artificial aggregate blends.

7.7.2 Kaolinite-lignin blends

Artificial aggregates containing mixtures of lignin and kaolinite were used to observe the changes in T_1 which accompany the mixing of the two materials. The bulk of the protons are lignin in this case, since the signal from kaolinite is so low. The T_1 appeared to increase with the addition of lignin, with the increase being more significant as the lignin content exceeded 50%. The FWHM also reached a minima around 50% loading. The T_1 demonstrates that kaolinite:lignin interactions are occuring up to 50% loading, since the T_1 is closer to that of kaolinite. Beyond 50% the T_1 approaches that of pure lignin. The increase in FWHM as lignin exceeds 50% also indicates that lignin has a slower rate of relaxation due to fewer interactions with kaolinite.

The T_1 data was replotted as a function of the contribution of lignin protons to the total signal. If T_1 simply represented the individual components contribution to the total signal, a linear relationship would be expected (grey line : Figure 7.6). This was not observed, instead it appears that the T1 of lignin:kaolinite mixutres are much lower than would be expected, suggesting a rapid relaxation, likely to be caused by the interaction of lignin protons with paramagnetic ions on the mineral surface.

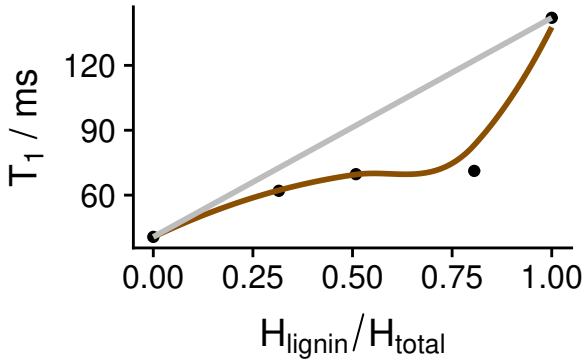

Figure 7.6: **A**:The T_1 data replotted as a function of the percentage protons originating from lignin. A 1:1 ratio would be expected if there was no changes in T_1 for the individual components (grey line), however, the data suggests that lignin has a reduced T_1 in the presence of kaolinite.

Kaolinite-lignin blends and moisture

The T_1 of the same lignin-kaolinite blends were measured as a function of moisture content. The FWHM was decreased considerably at 10 % moisture content for all lignin:kaolinite ratios. The T_1 measurements were significantly altered by the presence of water. Figure 7.7 **A** shows the measured T_1 data at different moisture contents. The relaxation time was much more rapid than would be expected from a combination of the two materials, without an interaction. The expected T_1s were calculated by multiplying the T_1 of the pure component (lignin or kaolinite) by the contribution of that material to the total protons (7.2) at each moisture content.

$$T_{1calc.} = (T_{1kaolinite} \times^1 H_{kaolnite}) + (T_{1lignin} \times^1 H_{lignin}) \tag{7.2}$$

The calculated T_1 data is presented in Figure 7.7 **B** and the differences between **A** and **B** are presented in Figure 7.8.

The reduction in T_1 in the mixtures as compared to the single components suggests an interaction which causes more rapid relaxation of the protons, predominantly those in the lignin. Lignin has already been shown to have two components to the T_1, probably from aromatic and aliphatic protons, which may exist in different spin reservoirs on mixing with clay. The majority of the protons in lignin come from aliphatic protons, and it is likely that it is these protons which are responsible for the

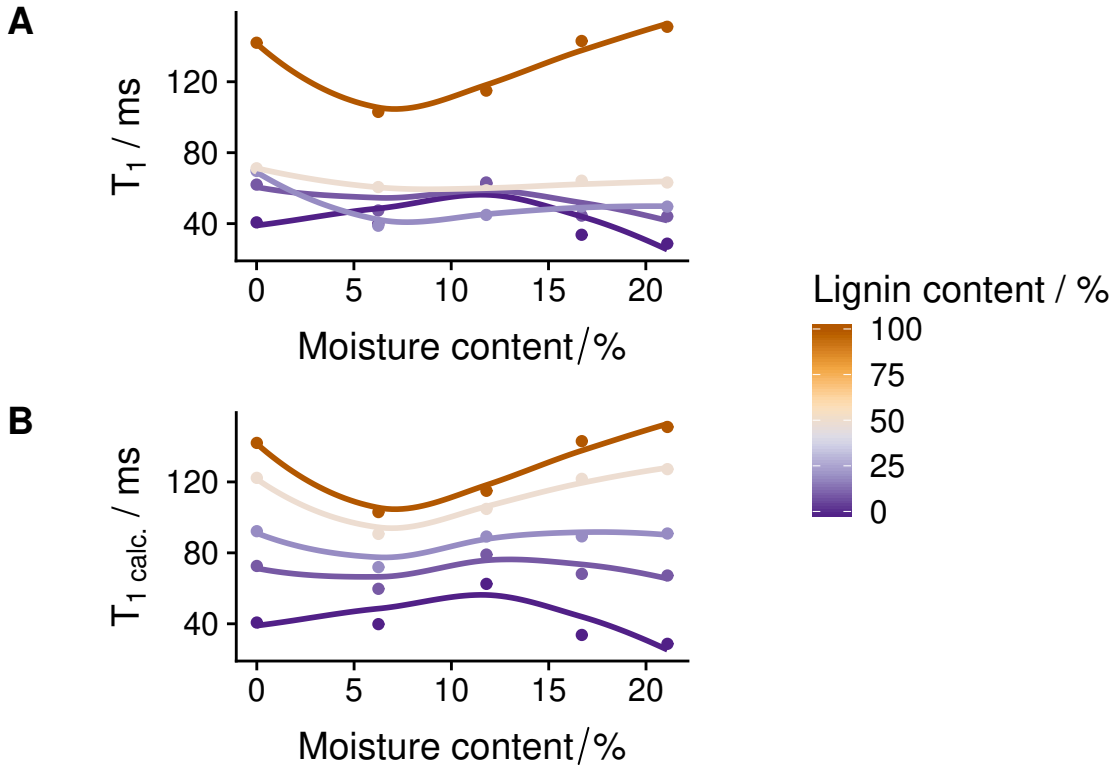

Figure 7.7: **A**:The T_1 data as measured, showing line shapes and features which are similar to the majority phase. **B**: The calculated T_1 data if the T_1 was just a combination of the T_1 from each component. The difference between **A** and **B** is the change in T_1 due to an interaction

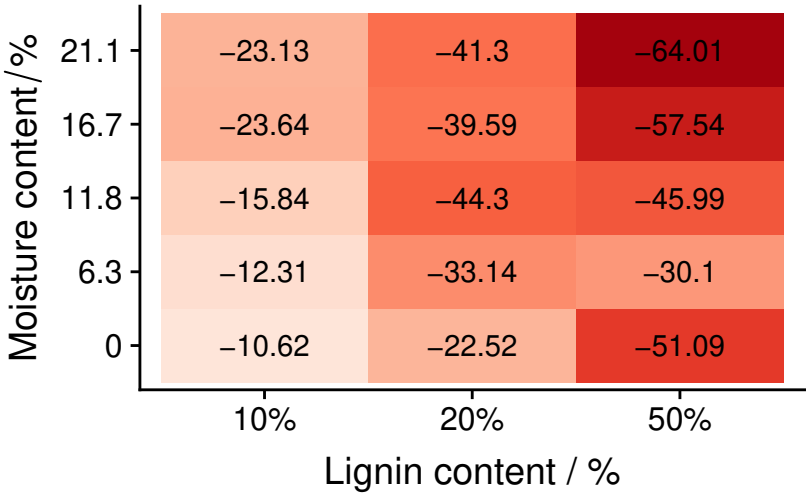

Figure 7.8: The difference between the recorded and the calculated T_1 values for kaolinite-lignin mixtures at different moisture contents. All values are negative, meaning the recorded T_1s are much smaller (faster) than expected.

changes in T_1. The deviation from the calculated T_1 deviates most strongly at higher lignin and moisture contents, suggesting that both of these components are responsible for a strong increase in the rate of relaxation. The strong reduction in T_1 demonstrates that lignin is not acting as a hydrophobic barrier, and is not preventing the ingress of water. Water repellence would likely not result in the strong decrease in T_1, as the T1 of lignin would remain more or less unchanged. The strong reduction in T_1 suggests that lignin is strongly interacting with the water.

7.8 Conclusion

MAS NMR spectroscopy was not able to fully resolve peaks observed in solution state NMR for organosolv lignin. The peaks which were resolved were broad and featureless, and chemical shift data could not be obtained in order to determine any molecular interactions with clay surfaces. Spin-lattice relaxation (T_1) is a technique often applied to polymers and is sensitive to molecular environment, and was employed for this study. T_1 data indicated that the role of protons in the aliphatic region may undergo more rapid relaxation on contact with clay. The aliphatic region contains a strong contribution from methoxy groups which may cover the exterior of the lignin particle and present a point of contact with the surface of clays. The T_1 of mixtures of kaolinite, lignin

and water were measured as a single weighted average of the T_1 of multiple components, as fitting multiple exponentials to a single set of data points is reliant on the estimation of too many unknown variables. However, the T_1 could be determined in context of the majority phase, to illustrate the interactions between the three components. Lignin was not found to be particularly hydrophobic, as water strongly reduced the measured T_1s. A strong reduction of the T_1 of lignin:kaolinite mixtures was found to occur on wetting, which would not be expected if lignin was acting as a hydrophobic barrier, as an increase in T_1 occurs as the concentration of unbound water increases.

Chapter 8

Conclusion

The preceding chapters illustrate the importance of particulates for forming stable soil aggregates, and demonstrate that there are simple methods which can be used to determine how well a particulate may interact with a soil. Using uni-axial compression tests and observing slaking can help infer characteristics of a particulate in a soil which may help or hinder the build up of soil structure.

Hydrogen bonding interactions are important for strength, but poor for slaking stability.

The importance of polar or hydrogen bonding surface chemistry was clearly demonstrated by experiments using HDPE and surface modified HDPE particles as additives. Both particles were able to form cohesive aggregates with kaolinite. However, the modified HDPE, which contains COOH surface functionality, formed much stronger aggregates. Unmodified HDPE lacks hydrogen bonding functionality and this resulted in a significantly weaker aggregate. Lignin, which contains both hydrophobic character and polar groups was found to strengthen kaolinite, but the strengthening effect was smaller in comparison to HDPE, due to the lower density of polar groups. In slaking experiments, these hydrogen bonding interactions were not stable to water, and resulted in the formation of dispersed kaolinite and a destabilisation of the aggregates, especially in the case of the COOH surface modified HDPE. The additional functionality increases the wettability of the surfaces, and hydration of this functionality may reduce the strength of the inter-particle interaction. Aggregates containing unmodified HDPE without surface modification were stable in water, despite weak interactions with the clay. This hydrophobic binding, appears to be important for aggregate stability in

soils. This places materials with both a degree of hydrophobicity resulting from aliphatic/aromatic groups, and hydrogen bonding functionality as strong candidates for amendments which may form strong interactions, but retain stability once submerged in water.

Hydrophobic effects drive aggregate stability in water, but take time to evolve.

Materials with hydrophobic chararcter such as unmodified HDPE, lignin and biochar were able to reduce the slaking rate, due to hydrophobic interactions. However, these interactions occurred after a delay, and did not always result in a stable aggregate. HDPE contains no additional functionality which could interact with clay, and so stabilisation was purely hydrophobic in character, resulting in a slow rate of slaking which was linear with time. Biochar and lignin, which contained more porosity and smaller particle size took longer to slow slaking, additional electrostatic and hydration effects are also present, which weaken the stabilising effect.

Microporosity is not as important as fabric morphology and composition in determining strength, but does effect the percolation threshold.

Aggregates formed of spherical or irregular-shaped particles, especially without any confining pressures, will contain inter particulate porosity. Porosity was found to reflect the sedimentation morphology of kaolinite, which was retained on drying. Porosity appears to be linked to the particulate and is not strongly altered by modifying the drying rate in the case of lignin. The reduction of porosity by compression or the formation of semi-soluble lignin particles results in a large increase in strength, due to the formation of more contact points, and so optimising a particle to pack well or to have 'soft edges' might help in forming strong interactions. This also reduces the percolation threshold, an important parameter which determines when an amendment no longer contributes to the strengthening of an aggregate. With fine particles, electrostatic repulsion may result in the formation of open, less dense fabric, which dries with a higher microporosity. Reducing electrostatic repulsion may also result in the formation of stronger fabrics.

Organo-mineral interactions between particulates may not be strong enough to cause aggregates to be enriched in particulate organic matter in comparison to the bulk soil.

Lignin appeared to increase the mechanical strength and water stability of kaolinite based-artificial

aggregates. It was thought that in a soil which underwent cycles of sieving and wetting, the increase in strength and water stability might cause aggregates to become enriched in lignin and kaolinite. In the presence of other soil minerals however, lignin appeared to bind non-specifically to surfaces and lignin was not found to be enriched in the aggregated fractions, despite an enrichment of kaolinite. If the kaolinite was replaced by bentonite however, the aggregates became enriched. The proportion of lignin in aggregates was representative of the lignin present in the bulk soil. This suggests that strong environmental pressures in real soils may not cause lignin to bind kaolinite preferentially.

Lignin is not strongly hydrophobic and does not exclude water from aggregates.

Wetted lignin aggregates were found to form semi-stable aggregates, but were visibly swollen with water. This gel-like aggregate held moisture when removed from water, and did not display any hydrophobic tendencies. T_1 results indicated that on wetting, there was less free water than would be expected, suggesting a strong water interaction on binding. This is not to say that hydrophobic interactions cannot form with kaolinite surfaces. It is likely that the wetted kaolinite-lignin fabric is held by hydrophobic interactions and hydrated hydrogen bonds, which are only semi-stable due to the high water content.

Lignin-kaolinite interactions are complex, and can take many forms.

Lignin-kaolinite interactions were formed in this study by wet and dry cycles. The wet paste which is formed, may contain enough water to allow particles sufficient mobility to reorientate, overcome repulsive forces and form interactions between particles. Clay and lignin, are likely to orientate themselves to minimise the amount of hydrophobic surface area exposed to water and to minimise repulsive forces. This means that more hydrophobic lignin patches may form hydrophobic interactions with silica surfaces, with the more hydrophilic surfaces orientating into solution. On drying, this sediment structure may be largely fixed in position. On drying electrostatic repulsion is overcome and particles can interact at surfaces. The dried aggregate derives it's strength from this initial fabric which is formed.

Kaolinite-HDPE interactions were made stronger via the addition of polar surface functionality. Polar surfaces may form strong hydrogen bonding interactions with the kaolinite particles. These stronger

interactions are more directional than van der Waals interactions, and are likely to be more brittle. Lignin is a heterogeneous material containing a variety of functional groups which could feasibly bind to the mineral surfaces. Polar groups are likely to orientate outwards into the solution, but can also form hydrogen bonds with clay edge and surface sites on drying. Increasing the pH increases the solubility of lignin, and this may allow functional groups to extend further out into solution. These soluble edges of the particles will allow for stronger interactions with kaolinite surfaces. Finding spectroscopic evidence for these interactions is a technical challenge.

Lignin dissolved in acetone, or fragments of lignin dissolved in water, were shown to bind to kaolinite surfaces. Lignin dissolved in acetone was added to kaolinite, and the solvent removed. The ATIR-FTIR showed large changes in regions associated with both the octahedral and tetrahedral surfaces, these indicate that lignin dissolved in acetone was able to form strong hydrogen bonds with surface hydroxyls on both faces. Lignin treated with peroxide to generate soluble lignin fragments were fractionated into 'humic' and 'fulvic' acids based on pH solubility and found to interact similarly with kaolinite surfaces. Differences in binding to iron oxide or kaolinite reflected the difference in mineral surface area. This evidence suggests that soluble lignin binds to surfaces, but that binding is limited and non-specific. Ca^{2+} had no effect, on the strength of aggregates suggesting weak associative binding in all cases with little contribution from electrostatic or cation-bridging interactions. However, ATR-FTIR analysis of insoluble lignin in kaolinite-lignin artificial aggregates showed that Si-O signals were perturbed only, suggesting hydrophobic type interactions with the kaolinite silica surface, which may shield these signals from the surface sensitive ATR-FTIR. Studies have shown that silica surfaces can bind aromatic compounds such as polystyrene, possibly via π-interactions, although the adsorption of small molecules on silica surfaces is still mainly attributed to hydrogen bonding interactions with hydroxyl groups. (*229*) Lignin was also found to bind to quartz silt, on the surface of sand and strongly with bentonite, suggesting that clay-lignin interactions are strongly associated with silica surfaces. The silica face contains a lower density of surface hydroxyl groups (4.6 OH/nm^2) than the alumina face (12.5 OH/nm^2), and so the preference for binding on the silica face must be driven by hydrophobic interactions in solution. Additionally, hydroxyl groups associated with the alumina face and edges were not perturbed. (*170*) Studies using solid state NMR could not resolve lignin functional groups in order to determine binding interactions, however

a role of the methoxy groups was indicated. It is possible that clays orientate the more hydrophobic surfaces (silica) on the lignin surface, with alumina faces facing outwards and this is retained on drying. Since the formation of the dry sediment is dominated by hydrophobic interactions, the number of polar or hydrogen bonding interactions may be small, and so the increase in strength is modest.

Technical lignins reduce microbial functioning in degraded soils.

The addition of lignin, even with additional sources of nitrogen and easy metabolisable carbon tends to reduce the metabolic function of microbial communities in a degraded soil. Additionally, the lignins studied here have low CEC and so may not do much to enhance microbial activity or the availability of nutrient cations to plants.

Biochar forms interactions with kaolinite, but they are not particularly stable in water.

Biochar is very hydrophobic, and this may lead to the formation of kaolinite-biochar interactions which are driven by the hydrophobic interactions in the sediment. Mixing biochar with kaolinite reduced the water repellency of biochar considerably, and so kaolinite may disperse and coat the biochar particles. This results in a strengthening of kaolinite interactions, due to the disruption of the formation kaolinite tactoids with weak inter-aggregate pores, and a more open fabric. The hydrogen-bonding capacity of biochar is poor, and so the strengthening of the aggregates must be due to a higher density of Van der Waal interactions, and a strengthening of the kaolinite fabric. The disruption of the kaolinite fabric, results however, in an aggregate which is unstable in water. Kaolinite tactoids do not swell, and appear partially stable in water, the coating of biochar particles results in individual particles which are susceptible to dispersion. The fine particle size and reduction of stable kaolinite tactoids results in a solid which slakes with a high amount of dispersed material. It was observed that hydrophobic interactions begin to slow the slaking, but the formation of stable hydrophobic interactions takes time possibly as explosive slaking from the entrapment of air subsides.

8.1 Integrating knowledge

These findings can be applied to the design of particulate amendments, but can also be considered with respect to the stability of natural aggregates. Few studies consider the surface chemistry of particulates in natural soils. It is a technical challenge to analyse the surface chemistry of particulate organic matter, because of the large heterogeneity. There are also few experiments that consider surface chemistry to be an important factor, as there are no studies which have made this observation. The particulate organic matter studied in this thesis are unlikely to be found as discrete particles in real soil. The wood fragments investigated in Chapter 3 were sequentially bleached, in order to replicate some form of fungal or bacterial decay. In this case, the particles were large and the surface roughness and the arrangement of the particles was likely to play a large role. This masked the surface chemistry contribution to the mechanical strength.

Plant roots are known to have a strong effect on soil properties. The role of plant roots and microbes has been studied, for the importance of these attributes for stabilising soils. It was found that plant roots are best for stabilising macroaggregates, smaller microaggregates were likely to be microbially engineered, and were found to be more important in dried conditions, roots in wetter conditions. Legacy of dead plant roots is large. however, the microbial effect takes months to take effect in incubation studies, possibly years in the field, and so the role of additional amendments could really change the story. This study, did however, find that soil aggregates were stable without plant roots in wet conditions, but did not suggest that this might be due to abiotic effects (*178*)

Few soil amendments based on lignin have been trailed, including soluble amino-acid containing biopolymers, these modified polymers are likely to be expensive however, and probably cannot be applied at high loadings, which could sink more carbon.

8.2 Future Work

More work is needed in order to derive a model that can quantitatively explain these findings, relating surface chemistry and particle size to mechanical strength and slaking stability. Unfortunately, even

with simple systems such as this containing only two particles, the complexity of this model would be high and susceptible to anomalies originating from the non-uniform nature of the particulates. This model would have to be able to integrate measurements of surface chemistry (functional group density), surface charge (zeta potential), particle size and particle shape and be able to predict how the sedimentation behaviour, internal porosity and inter-particle interactions form. At this point it is not yet possible to determine how all these factors are linked.

One of the major limitations to this study is that the biological contribution to aggregate stability has been ignored, in order to determine the physio-chemical attributes of aggregate formation. Microbial and fungal inoculates could be added to the artificial aggregates and incubated, and the changes in aggregate strength and slaking stability may provide additional information regarding the aggregate stabilising effects of microbial and fungal communities.

Alternatively, this approach can be treated from the point of view of soil engineering, where qualitative trends and not mechanistic or quantitative data is required. It would be interesting to compare aggregate stability measurements in the lab, with observations made in the field.

Bibliography

(*1*) Lal, R. (2001). Soil degradation by erosion. *Land Degradation & Development 12*, 519–539.

(*2*) Borrelli, P., Robinson, D. A., Fleischer, L. R., Lugato, E., Ballabio, C., Alewell, C., Meusburger, K., Modugno, S., Schütt, B., Ferro, V., Bagarello, V., Oost, K. V., Montanarella, L., and Panagos, P. (2017). An assessment of the global impact of 21st century land use change on soil erosion. *Nature Communications 8*, 2013.

(*3*) Pimentel, D. (2006). Soil Erosion: A Food and Environmental Threat. *Environment, Development and Sustainability 8*, 119–137.

(*4*) Totsche, K. U., Amelung, W., Gerzabek, M. H., Guggenberger, G., Klumpp, E., Knief, C., Lehndorff, E., Mikutta, R., Peth, S., Prechtel, A., Ray, N., and Kögel-Knabner, I. (2018). Microaggregates in soils. *Journal of Plant Nutrition and Soil Science 181*, 104–136.

(*5*) Bach, E. M., Williams, R. J., Hargreaves, S. K., Yang, F., and Hofmockel, K. S. (2018). Greatest soil microbial diversity found in micro-habitats. *Soil Biology and Biochemistry 118*, 217–226.

(*6*) Theng, B. K., Ristori, G. G., Santi, C. A., and Percival, H. J. (1999). An improved method for determining the specific surface areas of topsoils with varied organic matter content, texture and clay mineral composition. *European Journal of Soil Science 50*, 309–316.

(*7*) Yudina, A. V., Fomin, D. S., Kotelnikova, A. D., and Milanovskii, E. Y. (2018). From the Notion of Elementary Soil Particle to the Particle-Size and Microaggregate-Size Distribution Analyses: A Review. *Eurasian Soil Science 51*, 1326–1347.

(*8*) Bormann, H. (2010). Towards a hydrologically motivated soil texture classification. *Geoderma 157*, 142–153.

(*9*) Grandy, A. S., Strickland, M. S., Lauber, C. L., Bradford, M. A., and Fierer, N. (2009). The influence of microbial communities, management, and soil texture on soil organic matter chemistry. *Geoderma 150*, 278–286.

(*10*) Basma, A. A., Al-Homoud, A. S., Husein Malkawi, A. I., and Al-Bashabsheh, M. A. (1996). Swelling-shrinkage behavior of natural expansive clays. *Applied Clay Science 11*, 211–227.

(*11*) Attou, F., Bruand, A., and Le Bissonnais, Y. (1998). Effect of clay content and silt-clay fabric on stability of artificial aggregates. *European Journal of Soil Science 49*, 569–577.

(*12*) Mackinnon, I. D. R. (1993). Kaolinite Particle Sizes in the ¡2 µM Range Using Laser Scattering. *Clays and Clay Minerals 41*, 613–623.

(*13*) Detellier, C., and Letaief, S. In *Developments in Clay Science*, 2nd ed.; Elsevier Ltd.: 2013; Vol. 5, pp 707–719.

(*14*) Cheng, H., Liu, Q., Yang, J., Ma, S., and Frost, R. L. (2012). The thermal behavior of kaolinite intercalation complexes-A review. *Thermochimica Acta 545*, 1–13.

(*15*) Chikazawa, M., and Takei, T. In *Powder Technology*; Elsevier: 2010, pp 325–334.

(*16*) Gupta, V., Hampton, M. A., Stokes, J. R., Nguyen, A. V., and Miller, J. D. (2011). Particle interactions in kaolinite suspensions and corresponding aggregate structures. *Journal of Colloid and Interface Science 359*, 95–103.

(*17*) Šolc, R., Gerzabek, M. H., Lischka, H., and Tunega, D. (2011). Wettability of kaolinite (001) surfaces — Molecular dynamic study. *Geoderma 169*, 47–54.

(*18*) Tombácz, E., and Szekeres, M. (2006). Surface charge heterogeneity of kaolinite in aqueous suspension in comparison with montmorillonite. *Applied Clay Science*, DOI: `10.1016/j.clay.2006.05.009`.

(*19*) Chen, H., Koopal, L. K., Xiong, J., Avena, M., and Tan, W. (2017). Mechanisms of soil humic acid adsorption onto montmorillonite and kaolinite. *Journal of Colloid and Interface Science 504*, 457–467.

(*20*) Yu, C. Y., Chow, J. K., and Wang, Y. H. (2016). Pore-size changes and responses of kaolinite with different structures subject to consolidation and shearing. *Engineering Geology*, DOI: 10.1016/j.enggeo.2016.01.007.

(*21*) Wang, Y. .-.-H., and Siu, W. .-.-K. (2006). Structure characteristics and mechanical properties of kaolinite soils. II. Effects of structure on mechanical properties. *Canadian Geotechnical Journal 43*, 601–617.

(*22*) Gupta, V., and Miller, J. D. (2010). Surface force measurements at the basal planes of ordered kaolinite particles. *Journal of Colloid and Interface Science 344*, 362–371.

(*23*) Chorom, M., and Rengasamy, P. (1995). Dispersion and zeta potential of pure clays as related to net particle charge under varying pH, electrolyte concentration and cation type. *European Journal of Soil Science 46*, 657–665.

(*24*) Wan, J., and Tokunaga, T. K. (2002). Partitioning of clay colloids at air-water interfaces. *Journal of Colloid and Interface Science*, DOI: 10.1006/jcis.2001.8132.

(*25*) Rao, F., Ramirez-Acosta, F. J., Sanchez-Leija, R. J., Song, S., and Lopez-Valdivieso, A. (2011). Stability of kaolinite dispersions in the presence of sodium and aluminum ions. *Applied Clay Science*, DOI: 10.1016/j.clay.2010.10.023.

(*26*) Keller, W., and Matlack, K. (1990). The pH of clay suspensions in the field and laboratory, and methods of measurement of their pH. *Applied Clay Science 5*, 123–133.

(*27*) Choudhury, C., and Bharat, T. V. Wetting Induced Collapse Behavior of Kaolinite: Influence of Fabric and Inundation Pressure. *Canadian Geotechnical Journal 0*, DOI: 10.1139/cgj-2017-0297.

(*28*) Pillai, R. J., Robinson, R., and Boominathan, A. In *Indian Geotechnical Conference - 2010 GEOtrendz*, 2010, pp 271–274.

(*29*) Peng, Y., Wang, W., and Cao, J. (2016). Preparation of Lignin-Clay Complexes and Its Effects on Properties and Weatherability of Wood Flour/Polypropylene Composites. *Industrial and Engineering Chemistry Research 55*, 9657–9666.

(*30*) Barré, P., Fernandez-Ugalde, O., Virto, I., Velde, B., and Chenu, C. (2014). Impact of phyllosilicate mineralogy on organic carbon stabilization in soils: Incomplete knowledge and exciting prospects. *Geoderma 235-236*, 382–395.

(*31*) German, W. L., and Harding, D. A. (1969). The adsorption of aliphatic alcohols by montmorillonite and kaolinite. *Clay Minerals 8*, 213–227.

(*32*) Arnarson, T. S., and Keil, R. G. (2000). Mechanisms of pore water organic matter adsorption to montmorillonite. *Marine Chemistry 71*, 309–320.

(*33*) Sutton, R., and Sposito, G. (2005). Molecular Structure in Soil Humic Substances: The New View. *Environmental Science & Technology 39*, 9009–9015.

(*34*) Greenland, D. J. Interactions Between Humic and Fulvic Acids and Clays., 1971.

(*35*) Jiang, T., Hirasaki, G. J., and Miller, C. A. In *Energy and Fuels*, 2010.

(*36*) Feng, X., Simpson, A. J., and Simpson, M. J. (2005). Chemical and mineralogical controls on humic acid sorption to clay mineral surfaces. *Organic Geochemistry 36*, 1553–1566.

(*37*) Barhoumi, M., Beurroies, I., Denoyel, R., Saïd, H., and Hanna, K. (2003). Coadsorption of alkylphenols and nonionic surfactants onto kaolinite. *Colloids and Surfaces A: Physicochemical and Engineering Aspects 219*, 25–33.

(*38*) Newcomb, C. J., Qafoku, N. P., Grate, J. W., Bailey, V. L., and De Yoreo, J. J. (2017). Developing a molecular picture of soil organic matter-mineral interactions by quantifying organo-mineral binding. *Nature Communications 8*, DOI: 10.1038/s41467-017-00407-9.

(*39*) Kaiser, M., Kleber, M., and Berhe, A. A. (2015). How air-drying and rewetting modify soil organic matter characteristics: An assessment to improve data interpretation and inference. *Soil Biology and Biochemistry 80*, 324–340.

(*40*) Aquino, A. J., Tunega, D., Schaumann, G. E., Haberhauer, G., Gerzabek, M. H., and Lischka, H. (2011). The functionality of cation bridges for binding polar groups in soil aggregates. *International Journal of Quantum Chemistry*, DOI: 10.1002/qua.22693.

(*41*) Piccolo, A. (2001). the Supramolecular Structure of Humic Substances. *Soil Science 166*, 810–832.

(*42*) Doerr, S., Shakesby, R., and Walsh, R. (2000). Soil water repellency: its causes, characteristics and hydro-geomorphological significance. *Earth-Science Reviews 51*, 33–65.

(*43*) Kleber, M., Sollins, P., and Sutton, R. (2007). A conceptual model of organo-mineral interactions in soils: Self-assembly of organic molecular fragments into zonal structures on mineral surfaces. *Biogeochemistry 85*, 9–24.

(*44*) Horne, D. J., and McIntosh, J. C. In *Journal of Hydrology*, 2000.

(*45*) Heister, K., Höschen, C., Pronk, G. J., Mueller, C. W., and Kögel-Knabner, I. (2012). NanoSIMS as a tool for characterizing soil model compounds and organomineral associations in artificial soils. *Journal of Soils and Sediments 12*, 35–47.

(*46*) Schmidt, M., Torn, M., and Abiven, S. (2011). Persistence of soil organic matter as an ecosystem property. *Nature 478*, 49–56.

(*47*) Eusterhues, K., Rumpel, C., and Kogel-Knabner, I. (2005). Organo-mineral associations in sandy acid forest soils: importance of specific surface area, iron oxides and micropores. *European Journal of Soil Science 56*, 050912034650049.

(*48*) Lavelle, P., Spain, A., Blouin, M., Brown, G., Decaëns, T., Grimaldi, M., Jiménez, J. J., McKey, D., Mathieu, J., Velasquez, E., and Zangerlé, A. (2016). Ecosystem engineers in a self-organized soil: A review of concepts and future research questions. *Soil Science 181*, 91–109.

(*49*) Pronk, G. J. (2011). Biogeochemical interfaces in natural and artificial soil systems. *Thesis*.

(*50*) Balan, E., Calas, G., and Bish, D. L. (2014). Kaolin-group minerals: From hydrogen-bonded layers to environmental recorders. *Elements 10*, 183–188.

(*51*) Ito, A., and Wagai, R. (2017). Data Descriptor: Global distribution of clay-size minerals on land surface for biogeochemical and climatological studies. *Scientific Data 4*, 1–11.

(*52*) LAL, R. (1987). Managing the Soils of Sub-Saharan Africa. *Science 236*, 1069–1076.

(*53*) Feller, C., and Beare, M. H. (1997). Physical control of soil organic matter dynamics in the tropics. *Geoderma 79*, 69–116.

(*54*) Wattel-Koekkoek, E. J. W., Buurman, P., van der Plicht, J., Wattel, E., and van Breemen, N. (2003). Mean residuence time of soil organic matter associated with kaolinite and smectite. *European Journal of Soil Science 54*, 269–278.

(*55*) Six, J., Feller, C., Denef, K., Ogle, S. M., De Moraes Sa, J. C., and Albrecht, A. (2002). Soil organic matter, biota and aggregation in temperate and tropical soils - Effects of no-tillage. *Agronomie 22*, 755–775.

(*56*) Murphy, B. W. (2014). Soil organic matter and soil function - Review of the literature and underlying data. Effects of soil organic matter on functional soil properties., 155.

(*57*) Fujisaki, K., Chevallier, T., Chapuis-Lardy, L., Albrecht, A., Razafimbelo, T., Masse, D., Ndour, Y. B., and Chotte, J. L. (2018). Soil carbon stock changes in tropical croplands are mainly driven by carbon inputs: A synthesis. *Agriculture, Ecosystems and Environment 259*, 147–158.

(*58*) Wattel-Koekkoek, E. J. W., and Buurman, P. (2014). Mean Residence Time of Kaolinite and Smectite-Bound Organic Matter in Mozambiquan Soils. *Soil Science Society of America Journal*, DOI: 10.2136/sssaj2004.1540.

(*59*) Denef, K., and Six, J. (2005). Clay mineralogy determines the importance of biological versus abiotic processes for macroaggregate formation and stabilization. *European Journal of Soil Science 56*, 469–479.

(*60*) Paustian, K., Lehmann, J., Ogle, S., Reay, D., Robertson, G. P., and Smith, P. (2016). Climate-smart soils. *Nature 532*, 49–57.

(*61*) Lehmann, J., Gaunt, J., and Rondon, M. Bio-char sequestration in terrestrial ecosystems - A review., 2006.

(*62*) Lehmann, J., Rillig, M. C., Thies, J., Masiello, C. A., Hockaday, W. C., and Crowley, D. (2011). Biochar effects on soil biota – A review. *Soil Biology and Biochemistry 43*, 1812–1836.

(*63*) Lehmann, J., and Kleber, M. (2015). The contentious nature of soil organic matter. *Nature 528*, 60–68.

(*64*) Hedges, J., Eglinton, G., Hatcher, P., Kirchman, D., Arnosti, C., Derenne, S., Evershed, R., Kögel-Knabner, I., de Leeuw, J., Littke, R., Michaelis, W., and Rullkötter, J. (2000). The molecularly-uncharacterized component of nonliving organic matter in natural environments. *Organic Geochemistry 31*, 945–958.

(*65*) Dungait, J. a. J., Hopkins, D. W., Gregory, A. S., and Whitmore, A. P. (2012). Soil organic matter turnover is governed by accessibility not recalcitrance. *Global Change Biology 18*, 1781–1796.

(*66*) Kögel-Knabner, I., Guggenberger, G., Kleber, M., Kandeler, E., Kalbitz, K., Scheu, S., Eusterhues, K., and Leinweber, P. (2008). Organo-mineral associations in temperate soils: Integrating biology, mineralogy, and organic matter chemistry. *Journal of Plant Nutrition and Soil Science 171*, 61–82.

(*67*) Ashagrie, Y., Zech, W., Guggenberger, G., and Mamo, T. (2007). Soil aggregation, and total and particulate organic matter following conversion of native forests to continuous cultivation in Ethiopia. *Soil and Tillage Research 94*, 101–108.

(*68*) Chan, K. (2001). Soil particulate organic carbon under different land use and management. *Soil Use and Management 17*, 217–221.

(*69*) Cambardella, C. A., and Elliott, E. T. (2010). Carbon and Nitrogen Dynamics of Soil Organic Matter Fractions from Cultivated Grassland Soils. *Soil Science Society of America Journal*, DOI: 10.2136/sssaj1994.03615995005800010017x.

(*70*) Denef, K., Six, J., Bossuyt, H., Frey, S. D., Elliott, E. T., Merckx, R., and Paustian, K. (2001). Influence of dry–wet cycles on the interrelationship between aggregate, particulate organic matter, and microbial community dynamics. *Soil Biology and Biochemistry 33*, 1599–1611.

(*71*) Tisdall, J. M., and Oades, J. M. (1982). Organic matter and water-stable aggregates in soils. *Journal of soil science 33*, 141–163.

(*72*) Oades, J., and Waters, A. (1991). Aggregate hierarchy in soils. *Australian Journal of Soil Research 29*, 815.

(*73*) Vrdoljak, G., and Sposito, G. (2002). Soil aggregate hierarchy in a Brazilian oxisol. *Developments in Soil Science*, DOI: 10.1016/S0166-2481(02)80054-X.

(*74*) Brady, N. C; Weil, R. R., *The Nature and Properties of Soils*. Macmillan Publishing Co.: New York, 1974.

(*75*) HAYNES, R. J., and SWIFT, R. S. (1990). Stability of soil aggregates in relation to organic constituents and soil water content. *Journal of Soil Science*, DOI: 10.1111/j.1365-2389.1990.tb00046.x.

(*76*) Pinheiro-Dick, D., and Schwertmann, U. (1996). Microaggregates from Oxisols and Inceptisols: Dispersion through selective dissolutions and physicochemical treatments. *Geoderma*, DOI: 10.1016/S0016-7061(96)00047-X.

(*77*) Blanco-Canqui, H., and Lal, R. (2004). Mechanisms of carbon sequestration in soil aggregates. *Critical Reviews in Plant Sciences 23*, 481–504.

(*78*) Sarker, T. C., Incerti, G., Spaccini, R., Piccolo, A., Mazzoleni, S., and Bonanomi, G. (2018). Linking organic matter chemistry with soil aggregate stability: Insight from13C NMR spectroscopy. *Soil Biology and Biochemistry 117*, 175–184.

(*79*) Martens, D. A. (2000). Plant residue biochemistry regulates soil carbon cycling and carbon sequestration. *Soil Biology and Biochemistry 32*, 361–369.

(*80*) Almajmaie, A., Hardie, M., Acuna, T., and Birch, C. (2017). Evaluation of methods for determining soil aggregate stability. *Soil and Tillage Research 167*, 39–45.

(*81*) Etzler, F. M., and Drelich, J. (2012). Atomic Force Microscopy for Characterization of Surfaces, Particles, and Their Interactions. *Developments in Surface Contamination and Cleaning: Detection, Characterization, and Analysis of Contaminants 4*, 307–331.

(*82*) Yariv, S., and Cross, H. In *Geochemistry of Colloid Systems*; Springer Berlin Heidelberg: Berlin, Heidelberg, 1979; Chapter 8, pp 335–377.

(*83*) Besseling, N. A. M. (1997). Theory of Hydration Forces between Surfaces. *Langmuir 13*, 2113–2122.

(*84*) Hu, F., Xu, C., Li, H., Li, S., Yu, Z., Li, Y., and He, X. (2015). Particles interaction forces and their effects on soil aggregates breakdown. *Soil and Tillage Research 147*, 1–9.

(*85*) Yu, Z., Zhang, J., Zhang, C., Xin, X., and Li, H. (2017). The coupling effects of soil organic matter and particle interaction forces on soil aggregate stability. *Soil and Tillage Research*, DOI: 10.1016/j.still.2017.08.004.

(*86*) Luo, Y. X., Li, H., Ding, W. Q., Hu, F. N., and Li, S. (2018). Effects of DLVO, hydration and osmotic forces among soil particles on water infiltration. *European Journal of Soil Science*, DOI: 10.1111/ejss.12672.

(*87*) Yu, H., Zeng, G., Huang, H., Xi, X., Wang, R., Huang, D., Huang, G., and Li, J. (2007). Microbial community succession and lignocellulose degradation during agricultural waste composting. *Biodegradation 18*, 793–802.

(*88*) Hou, J., Li, H., Zhu, H., and Wu, L. (2009). Determination of clay surface potential: a more reliable approach. *Soil Science Society of America Journal 73*, 1658.

(*89*) Ebrahimi, D., Whittle, A., and Pellenq, R.-M. (2016). Effect of Polydispersity of Clay Platelets on the Aggregation And Mechanical Properties of Clay at the Mesoscale. *Clays and Clay Minerals 64*, 425–437.

(*90*) Liu, J., Lin, C.-L., and Miller, J. D. (2015). Simulation of cluster formation from kaolinite suspensions. *International Journal of Mineral Processing 145*, 38–47.

(*91*) Keller, T., Arvidsson, J., Schjønning, P., Lamandé, M., Stettler, M., and Weisskopf, P. (2012). In situ subsoil stress-strain behavior in relation to soil precompression stress. *Soil Science 177*, 490–497.

(*92*) Patel, S., Kaushal, A. M., and Bansal, A. K. (2006). Compression physics in the formulation development of tablets. *Critical Reviews in Therapeutic Drug Carrier Systems 23*, 1–66.

(*93*) Bellamy, L. J., Nordon, A., and Littlejohn, D. (2008). Effects of particle size and cohesive properties on mixing studied by non-contact NIR. *International Journal of Pharmaceutics 361*, 87–91.

(*94*) Berkowitz, B., and Ewing, R. P. (1998). Percolation theory and network modeling applications in soil physics. *Surveys in Geophysics 19*, 23–72.

(*95*) Simpson, D. C., and Evans, T. M. (2016). Behavioral thresholds in mixtures of sand and kaolinite clay. *Journal of Geotechnical and Geoenvironmental Engineering 142*, 04015073.

(*96*) Singer, M. J., Southard, R. J., Warrington, D. N., and Janitzky, P. (1992). Stability of Synthetic Sand-Clay Aggregates after Wetting and Drying Cycles. *Soil Science Society of America Journal 56*, 1843.

(*97*) Miller, F. P., Wilding, L. P., and Holowaychuk, N. (1971). Canfield Silt Loam, a Fragiudalf: II. Micromorphology, Physical, and Chemical Properties. *Soil Science Society of America Journal*, DOI: 10.2136/sssaj1971.03615995003500020041x.

(*98*) Lindbo, D. L., and Veneman, P. L. (1993). Micromorphology of selected Massachusetts fragipan soils. *Soil Science Society of America Journal*, DOI: 10.2136/sssaj1993.03615995005700020025x.

(*99*) Munkholm, L. J., Heck, R. J., Deen, B., and Zidar, T. (2016). Relationship between soil aggregate strength, shape and porosity for soils under different long-term management. *Geoderma 268*, 52–59.

(*100*) Dexter, A. R., and Kroesbergen, B. (1985). Methodology for determination of tensile strength of soil aggregates. *Journal of Agricultural Engineering Research 31*, 139–147.

(*101*) Zhang, H. (1994). Organic matter incorporation affects mechanical properties of soil aggregates. *Soil and Tillage Research*, DOI: 10.1016/0167-1987(94)90085-X.

(*102*) Hu, F., Xu, C., Li, H., Li, S., Yu, Z., Li, Y., and He, X. (2015). Particles interaction forces and their effects on soil aggregates breakdown. *Soil and Tillage Research 147*, 1–9.

(*103*) Reyes-Rivera, J., Soto-Hernández, M., Canché-Escamilla, G., and Terrazas, T. (2018). Structural characterization of lignin in four cacti wood: implications of lignification in the growth form and succulence. *Frontiers in Plant Science 9*, 1–16.

(*104*) Suhas, Carrott, P. J. M., and Ribeiro Carrott, M. M. L. (2007). Lignin–from natural adsorbent to activated carbon: a review. *Bioresource technology 98*, 2301–12.

(*105*) Vanholme, R., Demedts, B., Morreel, K., Ralph, J., and Boerjan, W. (2010). Lignin Biosynthesis and Structure. *Plant Physiology 153*, 895–905.

(*106*) Del Río, J. C., Marques, G., Rencoret, J., Martínez, Á. T., and Gutiérrez, A. (2007). Occurrence of naturally acetylated lignin units. *Journal of Agricultural and Food Chemistry 55*, 5461–5468.

(*107*) Ragauskas, A. J. et al. (2014). Lignin valorization: improving lignin processing in the biorefinery. *Science (New York, N.Y.) 344*, 1246843.

(*108*) Constant, S., Wienk, H. L., Frissen, A. E., Peinder, P. D., Boelens, R., Van Es, D. S., Grisel, R. J., Weckhuysen, B. M., Huijgen, W. J., Gosselink, R. J., and Bruijnincx, P. C. (2016). New insights into the structure and composition of technical lignins: A comparative characterisation study. *Green Chemistry 18*, 2651–2665.

(*109*) Janesko, B. G. (2014). Acid-catalyzed hydrolysis of lignin β-O-4 linkages in ionic liquid solvents: a computational mechanistic study. *Physical chemistry chemical physics : PCCP 16*, 5423–33.

(*110*) Hage, R. E., Brosse, N., Chrusciel, L., Sanchez, C., Sannigrahi, P., and Ragauskas, A. (2009). Characterization of milled wood lignin and ethanol organosolv lignin from miscanthus. *Polymer Degradation and Stability 94*, 1632–1638.

(*111*) El Hage, R., Brosse, N., Sannigrahi, P., and Ragauskas, A. (2010). Effects of process severity on the chemical structure of Miscanthus ethanol organosolv lignin. *Polymer Degradation and Stability 95*, 997–1003.

(*112*) Kang, X., Kirui, A., Dickwella Widanage, M. C., Mentink-Vigier, F., Cosgrove, D. J., and Wang, T. (2019). Lignin-polysaccharide interactions in plant secondary cell walls revealed by solid-state NMR. *Nature Communications 10*, 347.

(*113*) Giummarella, N., Pu, Y., Ragauskas, A. J., and Lawoko, M. (2019). A critical review on the analysis of lignin carbohydrate bonds. *Green Chemistry 21*, 1573–1595.

(*114*) Chatel, G., and Rogers, R. (2014). Review: oxidation of lignin using ionic liquids - an innovative strategy to produce renewable chemicals. *ACS Sustainable Chemistry & Engineering 2*, 322–339.

(*115*) Kögel-Knabner, I. (2002). The macromolecular organic composition of plant and microbial residues as inputs to soil organic matter. *Soil Biology and Biochemistry 34*, 139–162.

(*116*) Sariyildiz, T., and Anderson, J. M. (2005). Variation in the chemical composition of green leaves and leaf litters from three deciduous tree species growing on different soil types. *Forest Ecology and Management 210*, 303–319.

(*117*) DeAngelis, K. M., Allgaier, M., Chavarria, Y., Fortney, J. L., Hugenholtz, P., Simmons, B., Sublette, K., Silver, W. L., and Hazen, T. C. (2011). Characterization of trapped lignin-degrading microbes in tropical forest soil. *PLoS ONE 6*, DOI: 10.1371/journal.pone.0019306.

(*118*) Bugg, T. D. H., Ahmad, M., Hardiman, E. M., and Singh, R. (2011). The emerging role for bacteria in lignin degradation and bio-product formation. *Current opinion in biotechnology 22*, 394–400.

(*119*) Bi, R., Lawoko, M., and Henriksson, G. (2016). Phoma herbarum, a soil fungus able to grow on natural lignin and synthetic lignin (DHP) as sole carbon source and cause lignin degradation. *Journal of Industrial Microbiology and Biotechnology 43*, 1175–1182.

(*120*) Geib, S. M., Filley, T. R., Hatcher, P. G., Hoover, K., Carlson, J. E., Jimenez-Gasco, M. D. M., Nakagawa-Izumi, A., Sleighter, R. L., and Tien, M. (2008). Lignin degradation in wood-feeding insects. *Proceedings of the National Academy of Sciences of the United States of America 105*, 12932–7.

(*121*) Hong, H. N., Rumpel, C., Henry des Tureaux, T., Bardoux, G., Billou, D., Tran Duc, T., and Jouquet, P. (2011). How do earthworms influence organic matter quantity and quality in tropical soils? *Soil Biology and Biochemistry 43*, 223–230.

(*122*) Mao, J., Olk, D. C., Fang, X., He, Z., and Schmidt-Rohr, K. (2008). Influence of animal manure application on the chemical structures of soil organic matter as investigated by advanced solid-state NMR and FT-IR spectroscopy. *Geoderma 146*, 353–362.

(*123*) Puttaso, A., Vityakon, P., Rasche, F., Saenjan, P., Treloges, V., and Cadisch, G. (2013). Does Organic Residue Quality Influence Carbon Retention in a Tropical Sandy Soil? *Soil Science Society of America Journal 77*, 1001.

(*124*) Hall, S. J., Silver, W. L., Timokhin, V. I., and Hammel, K. E. (2016). Iron addition to soil specifically stabilized lignin. *Soil Biology and Biochemistry 98*, 95–98.

(*125*) Kim, S., Gopalakrishnan, K., and Ceylan, H. (2011). Moisture Susceptibility of Subgrade Soils Stabilized by Lignin-Based Renewable Energy Coproduct. *Journal of Transportation Engineering 138*, 1283–1290.

(*126*) Xiao, C., Bolton, R., and Pan, W. L. (2007). Lignin from rice straw Kraft pulping: Effects on soil aggregation and chemical properties. *Bioresource Technology 98*, 1482–1488.

(*127*) Au, P. I., and Leong, Y. K. (2016). Surface chemistry and rheology of slurries of kaolinite and montmorillonite from different sources. *KONA Powder and Particle Journal 2016*, 17–32.

(*128*) Martin, R. T. (1975). Fabric of consolidated kaolinite. *Clays and Clay Minerals 23*, 17–25.

(*129*) Zhao, J., Chen, S., Hu, R., and Li, Y., *Aggregate stability and size distribution of red soils under different land uses integrally regulated by soil organic matter, and iron and aluminum oxides*, 2017; Vol. 167.

(*130*) Norgren, M., and Edlund, H. (2014). Lignin: Recent advances and emerging applications. *Current Opinion in Colloid & Interface Science 19*, 409–416.

(*131*) Frangville, C., Rutkevičius, M., Richter, A. P., Velev, O. D., Stoyanov, S. D., and Paunov, V. N. (2012). Fabrication of environmentally biodegradable lignin nanoparticles. *ChemPhysChem 13*, 4235–4243.

(*132*) Ahvazi, B., Cloutier, É., Wojciechowicz, O., and Ngo, T.-D. (2016). Lignin Profiling: A Guide for Selecting Appropriate Lignins as Precursors in Biomaterials Development. *ACS Sustainable Chemistry & Engineering 4*, 5090–5105.

(*133*) Kannangara, M., Marinova, M., Fradette, L., and Paris, J. (2016). Effect of mixing hydrodynamics on the particle and filtration properties of precipitated lignin. *Chemical Engineering Research and Design 105*, 94–106.

(*134*) Kang, S., and Xing, B. (2007). Adsorption of dicarboxylic acids by clay minerals as examined by in situ ATR-FTIR and ex situ DRIFT. *Langmuir 23*, 7024–7031.

(*135*) Gascó, G., and Méndez, A. (2005). Sorption of Ca2+, Mg2+, Na+ and K+ by clay minerals. *Desalination 182*, 333–338.

(*136*) Torre, M., Rodriguez, A. R., and Saura-calixtot, F. (1992). Study of the interactions of calcium ions with lignin , cellulose , and pectin. *Journal of Agricultural and Food Chemistry 40*, 1762–1766.

(*137*) Liu, X., Lu, X., Sprik, M., Cheng, J., Meijer, E. J., and Wang, R. (2013). Acidity of edge surface sites of montmorillonite and kaolinite. *Geochimica et Cosmochimica Acta 117*, 180–190.

(*138*) Zhu, W. (2013). Equilibrium of Lignin Precipitation The Effects of pH, Temperature, Ion Strength and Wood Origins Equilibrium of Lignin Precipitation. *Telephone + 46*, 31–772.

(*139*) Nistor, M.-T., Chirila, O., Cazacu, G., Totolin, M., and Vasile, C. (2014). Solution properties of some modified lignins. *Cellulose Chemistry and Technology*.

(*140*) Duval, A., and Lawoko, M. (2014). A review on lignin-based polymeric, micro- and nano-structured materials. *Reactive and Functional Polymers 85*, 78–96.

(*141*) Laurichesse, S., and Avérous, L. (2014). Chemical modification of lignins: Towards biobased polymers. *Progress in Polymer Science 39*, 1266–1290.

(*142*) Huang, Y., Wang, W., Xing, L., Han, G., Liu, J., and Fan, G. (2016). Exploring on aqueous chemistry of micron-sized lignite particles in lignite-water slurry: Effects of pH on humics dissolution. *Fuel*, DOI: `10.1016/j.fuel.2016.04.117`.

(*143*) van den Berg, L. J., Shotbolt, L., and Ashmore, M. R. (2012). Dissolved organic carbon (DOC) concentrations in UK soils and the influence of soil, vegetation type and seasonality. *Science of the Total Environment 427-428*, 269–276.

(*144*) Borggaard, O. K., Raben-Lange, B., Gimsing, a. L., and Strobel, B. W. (2005). Influence of humic substances on phosphate adsorption by aluminium and iron oxides. *Geoderma 127*, 270–279.

(*145*) Naveed, M., Brown, L. K., Raffan, A. C., George, T. S., Bengough, A. G., Roose, T., Sinclair, I., Koebernick, N., Cooper, L., Hackett, C. A., and Hallett, P. D. (2017). Plant exudates may stabilize or weaken soil depending on species, origin and time. *European Journal of Soil Science 68*, 806–816.

(*146*) Al Bakri, A. M. M. et al. (2011). Chemical Reactions in the Geopolymerisation Process Using Fly Ash-Based Geopolymer: A Review. *Journal of Applied Sciences Research 7*, 1199–1203.

(*147*) Melton, I. E., and Rand, B. (1977). Particle interactions in aqueous kaolinite suspensions. *Journal of Colloid and Interface Science*, DOI: 10.1016/0021-9797(77)90292-2.

(*148*) Andrady, A. L. (2011). Microplastics in the marine environment. *Marine Pollution Bulletin 62*, 1596–1605.

(*149*) Nizzetto, L., Bussi, G., Futter, M. N., Butterfield, D., and Whitehead, P. G. (2016). A theoretical assessment of microplastic transport in river catchments and their retention by soils and river sediments. *Environmental Science: Processes & Impacts 18*, 1050–1059.

(*150*) Rillig, M. C. (2012). Microplastic in terrestrial ecosystems and the soil? *Environmental Science and Technology 46*, 6453–6454.

(*151*) Torvinen, K., Pettersson, F., Lahtinen, P., Arstila, K., Kumar, V., Österbacka, R., Toivakka, M., and Saarinen, J. J. (2017). Nanoporous kaolin-cellulose nanofibril composites for printed electronics. *Flexible and Printed Electronics*, DOI: 10.1088/2058-8585/aa6d97.

(*152*) Alves, L., Ferraz, E., and Gamelas, J. (2019). Composites of nanofibrillated cellulose with clay minerals: A review. *Advances in Colloid and Interface Science 272*, 101994.

(*153*) Castro, D. O., Karim, Z., Medina, L., Häggström, J. O., Carosio, F., Svedberg, A., Wågberg, L., Söderberg, D., and Berglund, L. A. (2018). The use of a pilot-scale continuous paper process for fire retardant cellulose-kaolinite nanocomposites. *Composites Science and Technology*, DOI: 10.1016/j.compscitech.2018.04.032.

(*154*) Zhang, R., Li-Mayer, J. Y. S., and Charalambides, M. N. (2018). Development of an image-based numerical model for predicting the microstructure–property relationship in alumina

trihydrate (ATH) filled poly(methyl methacrylate) (PMMA). *International Journal of Fracture 211*, 125–148.

(*155*) Bondeson, D., Mathew, A., and Oksman, K. (2006). Optimization of the isolation of nanocrystals from microcrystalline cellulose by acid hydrolysis. *Cellulose 13*, 171–180.

(*156*) Fontaine, S., Bardoux, G., Benest, D., Verdier, B., Mariotti, A., and Abbadie, L. (2004). Mechanisms of the Priming Effect in a Savannah Soil Amended with Cellulose. *Soil Science Society of America Journal 68*, 125.

(*157*) Di Lonardo, D. P., De Boer, W., Klein Gunnewiek, P. J., Hannula, S. E., and Van der Wal, A. (2017). Priming of soil organic matter: Chemical structure of added compounds is more important than the energy content. *Soil Biology and Biochemistry 108*, 41–54.

(*158*) Puget, P., Angers, D. A., and Chenu, C. (1998). Nature of carbohydrates associated with water-stable aggregates of two cultivated soils. *Soil Biology and Biochemistry*, DOI: 10.1016/S0038-0717(98)00103-5.

(*159*) De Boer, W., Folman, L. B., Summerbell, R. C., and Boddy, L. (2005). Living in a fungal world: Impact of fungi on soil bacterial niche development. *FEMS Microbiology Reviews 29*, 795–811.

(*160*) Gunina, A., and Kuzyakov, Y. (2015). Sugars in soil and sweets for microorganisms: Review of origin, content, composition and fate. *Soil Biology and Biochemistry 90*, 87–100.

(*161*) Foston, M. (2014). Advances in solid-state NMR of cellulose. *Current Opinion in Biotechnology 27*, 176–184.

(*162*) Fernandes, A. N., Thomas, L. H., Altaner, C. M., Callow, P., Forsyth, V. T., Apperley, D. C., Kennedy, C. J., and Jarvis, M. C. (2011). Nanostructure of cellulose microfibrils in spruce wood. *Proceedings of the National Academy of Sciences*, DOI: 10.1073/pnas.1108942108.

(*163*) Smith, P. (2016). Soil carbon sequestration and biochar as negative emission technologies. *Global Change Biology 22*, 1315–1324.

(*164*) Mukherjee, A., Zimmerman, A. R., and Harris, W. (2011). Surface chemistry variations among a series of laboratory-produced biochars. *Geoderma 163*, 247–255.

(*165*) Suliman, W., Harsh, J. B., Abu-Lail, N. I., Fortuna, A. M., Dallmeyer, I., and Garcia-Pérez, M. (2017). The role of biochar porosity and surface functionality in augmenting hydrologic properties of a sandy soil. *Science of the Total Environment 574*, 139–147.

(*166*) Vogel, C., Babin, D., Pronk, G. J., Heister, K., Smalla, K., and Kögel-Knabner, I. (2014). Establishment of macro-aggregates and organic matter turnover by microbial communities in long-term incubated artificial soils. *Soil Biology and Biochemistry 79*, 57–67.

(*167*) Zhang, X., Qu, T., Mosier, N. S., Han, L., and Xiao, W. (2018). Cellulose modification by recyclable swelling solvents. *Biotechnology for Biofuels 11*, 1–12.

(*168*) Ding, G. C., Pronk, G. J., Babin, D., Heuer, H., Heister, K., Kögel-Knabner, I., and Smalla, K. (2013). Mineral composition and charcoal determine the bacterial community structure in artificial soils. *FEMS Microbiology Ecology 86*, 15–25.

(*169*) Yadav, P., Chacko, S., Kumar, G., Ramapanicker, R., and Verma, V. (2015). Click chemistry route to covalently link cellulose and clay. *Cellulose 22*, 1615–1624.

(*170*) Wu, X., Sacher, E., and Meunier, M. (1999). The effects of hydrogen bonds on the adhesion of inorganic oxide particles on hydrophilic silicon surfaces. *Journal of Applied Physics 86*, 1744–1748.

(*171*) de Souza Machado, A. A., Lau, C. W., Till, J., Kloas, W., Lehmann, A., Becker, R., and Rillig, M. C. (2018). Impacts of Microplastics on the Soil Biophysical Environment. *Environmental Science & Technology 52*, 9656–9665.

(*172*) Rillig, M. C., Ingraffia, R., and de Souza Machado, A. A. (2017). Microplastic Incorporation into Soil in Agroecosystems. *Frontiers in Plant Science 8*, 8–11.

(*173*) Lal, R. (2004). Carbon sequestration in dryland ecosystems. *Environmental Management 33*, 528–544.

(*174*) Paul, E. A. (2016). The nature and dynamics of soil organic matter: Plant inputs, microbial transformations, and organic matter stabilization. *Soil Biology and Biochemistry 98*, 109–126.

(*175*) Kallenbach, C. M., Grandy, A. S., Frey, S. D., and Diefendorf, A. F. (2015). Microbial physiology and necromass regulate agricultural soil carbon accumulation. *Soil Biology and Biochemistry 91*, 279–290.

(*176*) Albalasmeh, A. A., and Ghezzehei, T. A. (2014). Interplay between soil drying and root exudation in rhizosheath development. *Plant and Soil 374*, 739–751.

(*177*) Abiven, S., Menasseri, S., Angers, D. A., and Leterme, P. (2007). Dynamics of aggregate stability and biological binding agents during decomposition of organic materials. *European Journal of Soil Science 58*, 239–247.

(*178*) Blankinship, J. C., Fonte, S. J., Six, J., and Schimel, J. P. (2016). Plant versus microbial controls on soil aggregate stability in a seasonally dry ecosystem. *Geoderma 272*, 39–50.

(*179*) Six, J., Bossuyt, H., Degryze, S., and Denef, K. (2004). A history of research on the link between (micro)aggregates, soil biota, and soil organic matter dynamics. *Soil and Tillage Research 79*, 7–31.

(*180*) Ding, G. C., Pronk, G. J., Babin, D., Heuer, H., Heister, K., Kögel-Knabner, I., and Smalla, K. (2013). Mineral composition and charcoal determine the bacterial community structure in artificial soils. *FEMS Microbiology Ecology 86*, 15–25.

(*181*) Zaher, H., and Caron, J. (2011). Aggregate slaking during rapid wetting: Hydrophobicity and pore occlusion. *Canadian Journal of Soil Science 88*, 85–97.

(*182*) Hu, B., Wang, Y., Wang, B., Wang, Y., Liu, C., and Wang, C. (2018). Impact of drying-wetting cycles on the soil aggregate stability of Alfisols in southwestern China. *Journal of Soil and Water Conservation 73*, 469–478.

(*183*) Rabot, E., Wiesmeier, M., Schlüter, S., and Vogel, H. J. (2018). Soil structure as an indicator of soil functions: A review. *Geoderma 314*, 122–137.

(*184*) Herrick, J. E., Whitford, W. G., De Soyza, A. G., Van Zee, J. W., Havstad, K. M., Seybold, C. A., and Walton, M. (2001). Field soil aggregate stability kit for soil quality and rangeland health evaluations. *Catena*, DOI: 10.1016/S0341-8162(00)00173-9.

(*185*) Lomeling, D., Modi, A. L., Kenyi, S. M., Kenyi, M. C., Silvestro, G. M., and Yieb, J. L. (2016). Comparing the Macro-aggregate Stability of Two Tropical Soils : Clay Soil (Eutric Vertisol) and Sandy Loam Soil (Eutric Leptosol). *Interntional Journal of Agriculture and Forestry 6*, 142–151.

(*186*) Levy, G. J., Mamedov, A. I., and Goldstein, D. (2003). Sodicity and water quality effects on slaking of aggregates from semi-arid soils. *Soil Science 168*, 552–562.

(*187*) Alekseeva, T. V., Sokolowska, Z., Hajnos, M., Alekseev, A. O., and Kalinin, P. I. (2009). Water stability of aggregates in subtropical and tropical soils (Georgia and China) and its relationships with the mineralogy and chemical properties. *Eurasian Soil Science 42*, 415–425.

(*188*) Beven, K., and Germann, P. (1982). Marcopore and water flow in soils. *Water Resources Research 18*, 1311–1325.

(*189*) Goebel, M. O., Woche, S. K., and Bachmann, J. (2012). Quantitative analysis of liquid penetration kinetics and slaking of aggregates as related to solid-liquid interfacial properties. *Journal of Hydrology 442-443*, 63–74.

(*190*) BISSONNAIS, Y. (1996). Aggregate stability and assessment of soil crustability and erodibility: I. Theory and methodology. *European Journal of Soil Science 47*, 425–437.

(*191*) Rawlins, B. G., Wragg, J., and Lark, R. M. (2013). Application of a novel method for soil aggregate stability measurement by laser granulometry with sonication. *European Journal of Soil Science*, DOI: 10.1111/ejss.12017.

(*192*) Fajardo, M., McBratney, A. B., Field, D. J., and Minasny, B. (2016). Soil slaking assessment using image recognition. *Soil and Tillage Research 163*, 119–129.

(*193*) Kim, D., Lee, K., and Park, K. Y. (2016). Upgrading the characteristics of biochar from cellulose, lignin, and xylan for solid biofuel production from biomass by hydrothermal carbonization. *Journal of Industrial and Engineering Chemistry 42*, 95–100.

(*194*) Lima, T. R., Carvalho, E. C., Martins, F. R., Oliveira, R. S., Miranda, R. S., Müller, C. S., Pereira, L., Bittencourt, P. R., Sobczak, J. C., Gomes-Filho, E., Costa, R. C., and Araújo,

F. S. (2018). Lignin composition is related to xylem embolism resistance and leaf life span in trees in a tropical semiarid climate. *New Phytologist*, DOI: 10.1111/nph.15211.

(*195*) Ontl, T. A., Cambardella, C. A., Schulte, L. A., and Kolka, R. K. (2015). Factors influencing soil aggregation and particulate organic matter responses to bioenergy crops across a topographic gradient. *Geoderma 255-256*, 1–11.

(*196*) Pires, L. F., Cooper, M., Cássaro, F. A. M., Reichardt, K., Bacchi, O. O. S., and Dias, N. M. P. (2008). Micromorphological analysis to characterize structure modifications of soil samples submitted to wetting and drying cycles. *Catena 72*, 297–304.

(*197*) Seguel, O., and Horn, R. (2006). Structure properties and pore dynamics in aggregate beds due to wetting-drying cycles. *Journal of Plant Nutrition and Soil Science 169*, 221–232.

(*198*) Wattel-Koekkoek, E. J. W., Van Genuchten, P. P. L., Buurman, P., and Van Lagen, B. (2001). Amount and composition of clay-associated soil organic matter in a range of kaolinitic and smectitic soils. *Geoderma 99*, 27–49.

(*199*) Dohrmann, R. (2006). Cation exchange capacity methodology II: A modified silver-thiourea method. *Applied Clay Science 34*, 38–46.

(*200*) Regelink, I. C., Stoof, C. R., Rousseva, S., Weng, L., Lair, G. J., Kram, P., Nikolaidis, N. P., Kercheva, M., Banwart, S., and Comans, R. N. (2015). Linkages between aggregate formation, porosity and soil chemical properties. *Geoderma*, DOI: 10.1016/j.geoderma.2015.01.022.

(*201*) Spence, A., and Kelleher, B. P. (2012). FT-IR spectroscopic analysis of kaolinite–microbial interactions. *Vibrational Spectroscopy 61*, 151–155.

(*202*) Yanni, S. F., Whalen, J. K., Simpson, M. J., and Janzen, H. H. (2011). Plant lignin and nitrogen contents control carbon dioxide production and nitrogen mineralization in soils incubated with Bt and non-Bt corn residues. *Soil Biology and Biochemistry 43*, 63–69.

(*203*) Talbot, J. M., and Treseder, K. K. (2012). Interactions between lignin, cellulose, and nitrogem drive litter chemistry - decay relationships. *Ecology 93*, 345–354.

(*204*) McGuire, K. L., and Treseder, K. K. (2010). Microbial communities and their relevance for ecosystem models: Decomposition as a case study. *Soil Biology and Biochemistry 42*, 529–535.

(*205*) Rabbi, S. M. F., Daniel, H., Lockwood, P. V., Macdonald, C., Pereg, L., Tighe, M., Wilson, B. R., and Young, I. M. (2016). Physical soil architectural traits are functionally linked to carbon decomposition and bacterial diversity. *Scientific Reports 6*, 33012.

(*206*) Reardon, C. L., and Wuest, S. B. (2016). Soil amendments yield persisting effects on the microbial communities-a 7-year study. *Applied Soil Ecology 101*, 107–116.

(*207*) Cragg, S. M., Beckham, G. T., Bruce, N. C., Bugg, T. D., Distel, D. L., Dupree, P., Etxabe, A. G., Goodell, B. S., Jellison, J., McGeehan, J. E., McQueen-Mason, S. J., Schnorr, K., Walton, P. H., Watts, J. E., and Zimmer, M. (2015). Lignocellulose degradation mechanisms across the Tree of Life. *Current Opinion in Chemical Biology 29*, 108–119.

(*208*) Shamim, G., Sandra, Y. F., and Joann K., W. In *Lignin*, 2014.

(*209*) Ahmad, M., Taylor, C. R., Pink, D., Burton, K., Eastwood, D., Bending, G. D., and Bugg, T. D. H. (2010). Development of novel assays for lignin degradation: comparative analysis of bacterial and fungal lignin degraders. *Molecular bioSystems 6*, 815–821.

(*210*) Waksman, S. A. (1936). Humus Origin, Chemical Composition, and Importance in Nature. *Soil Science 41*, 395.

(*211*) Ruiz-Dueñas, F. J., and Martínez, Á. T. (2009). Microbial degradation of lignin: How a bulky recalcitrant polymer is efficiently recycled in nature and how we can take advantage of this. *Microbial Biotechnology 2*, 164–177.

(*212*) Worrall, J. J., Anagnost, S. E., and Zabel, R. a. (1997). Comparison of wood decay among diverse lignicolous fungi. *Mycologia 89*, 199–219.

(*213*) Martínez, Á. T., Speranza, M., Ruiz-Dueñas, F. J., Ferreira, P., Camarero, S., Guillén, F., Martínez, M. J., Gutiérrez, A., and Del Río, J. C. (2005). Biodegradation of lignocellulosics: Microbial, chemical, and enzymatic aspects of the fungal attack of lignin. *International Microbiology 8*, 195–204.

(*214*) Arantes, V., and Goodell, B. (2014). Current understanding of brown-rot fungal biodegradation mechanisms: A review. *ACS Symposium Series 1158*, 3–21.

(*215*) Caesar-TonThat, T. C., and Cochran, V. L. (2000). Soil aggregate stabilization by a saprophytic lignin-decomposing basidiomycete fungus I. Microbiological aspects. *Biology and Fertility of Soils 32*, 374–380.

(*216*) Hatakka, A. In *Biopolymers Online*, Steinbüchel, A., and Hofrichter, M., Eds.; Wiley-VCH Verlag GmbH & Co. KGaA: Weinheim, Germany, 2005, pp 129–145.

(*217*) Brune, A. (2007). Woodworker's digest. *Nature 450*, 487–488.

(*218*) Cortes-Tolalpa, L., Jiménez, D. J., de Lima Brossi, M. J., Salles, J. F., and van Elsas, J. D. (2016). Different inocula produce distinctive microbial consortia with similar lignocellulose degradation capacity. *Applied Microbiology and Biotechnology 100*, 7713–7725.

(*219*) Gul, S., Yanni, S. F., and Whalen, J. K. In *Lignin*, Lu, F., Ed.; Nova Science Publishers, Inc: 2014; Chapter 14, pp 376–416.

(*220*) Allison, S. D., LeBauer, D. S., Ofrecio, M. R., Reyes, R., Ta, A. M., and Tran, T. M. (2009). Low levels of nitrogen addition stimulate decomposition by boreal forest fungi. *Soil Biology and Biochemistry*, DOI: `10.1016/j.soilbio.2008.10.032`.

(*221*) Miltner, A., and Zech, W. (1998). Beech leaf litter lignin degradation and transformation as influenced by mineral phases. *Organic Geochemistry 28*, 457–463.

(*222*) Staley, C., Breuillin-Sessoms, F., Wang, P., Kaiser, T., Venterea, R. T., and Sadowsky, M. J. (2018). Urea amendment decreases microbial diversity and selects for specific nitrifying strains in eight contrasting agricultural soils. *Frontiers in Microbiology 9*, 1–13.

(*223*) Simpson, A. J., Kingery, W. L., Shaw, D. R., Spraul, M., Humpfer, E., and Dvortsak, P. (2001). The Application of 1 H HR-MAS NMR Spectroscopy for the Study of Structures and Associations of Organic Components at the Solid - Aqueous Interface of a Whole Soil. *Environmental Science & Technology 35*, 3321–3325.

(*224*) Weiss Jr., C. A., and Gerasimowicz, W. V. (1996). Interaction of water with clay minerals as studied by 2H nuclear magnetic resonance spectroscopy. *Geochimica et Cosmochimica Acta 60*, 265–275.

(*225*) Kawai, T. (1961). Study on the Internal Motions of Some Acryl- and Methacryl-group High Polymers by Pulsed NMR Method. *Journal of the Physical Society of Japan*, DOI: 10.1143/JPSJ.16.1220.

(*226*) Savy, D., and Piccolo, A. (2014). Physical-chemical characteristics of lignins separated from biomasses for second-generation ethanol. *Biomass and Bioenergy 62*, 58–67.

(*227*) Gil, A. M., Lopes, M. H., Neto, C. P., and Rocha, J. (1999). Very high-resolution H-1 MAS NMR of a natural polymeric material. *Solid State Nuclear Magnetic Resonance 15*, 59–67.

(*228*) Hatch, C. D., Wiese, J. S., Crane, C. C., Harris, K. J., Kloss, H. G., and Baltrusaitis, J. (2012). Water Adsorption on Clay Minerals As a Function of Relative Humidity: Application of BET and Freundlich Adsorption Models. *Langmuir 28*, 1790–1803.

(*229*) Parida, S. K., Dash, S., Patel, S., and Mishra, B. (2006). Adsorption of organic molecules on silica surface. *Advances in Colloid and Interface Science 121*, 77–110.

(*230*) Pu, Y., Cao, S., and Ragauskas, A. J. (2011). Application of quantitative31P NMR in biomass lignin and biofuel precursors characterization. *Energy and Environmental Science 4*, 3154–3166.

(*231*) Özcan, A., Ömeroğlu, Ç., Erdoğan, Y., and Özcan, A. S. (2007). Modification of bentonite with a cationic surfactant: An adsorption study of textile dye Reactive Blue 19. *Journal of Hazardous Materials 140*, 173–179.

(*232*) Bhatt, A. S., Sakaria, P. L., Vasudevan, M., Pawar, R. R., Sudheesh, N., Bajaj, H. C., and Mody, H. M. (2012). Adsorption of an anionic dye from aqueous medium by organoclays: equilibrium modeling, kinetic and thermodynamic exploration. *RSC Advances 2*, 8663.

Appendix A

Appendix

A.1 Lignin characterisation

The following analysis was carried out on lignin samples taken from bulk 1 kg tubs of organosolv beech and spruce lignin provided by Fraunhofer CBP.

A.1.1 Gel permeation chromatography

GPC analysis was carried out using a G7800A Agilent 1260 Infinity GPC/SEC Multi Detector Suite with A6000M and A3000 columns. DMSO containing 1 g/ml LiBr was used as the mobile phase and solvent. Pullulan standards were used to calculate MWs and calibrate the detectors. Refractive index was used for analysis. 20 mg of lignin was dissolved in 1.5 ml of DMSO/LiBr solution and filtered to remove any undissolved solids (no undissolved solids were visible).

	Mp	Mn	Mw	PD
Beech	1186	953	2230	2.34
Spruce	1514	1117	4779	4.28

Table A.1: Molecular weight distribution by GPC of beech and spruce Organosolv lignin. Peak molecular weight (Mp) , number average molecular weight (Mn), number average molecular weight (Mw) and polydispersity (PD).

A.1.2 Elemental analysis

CHNS analysis of lignin showed extremely low N content (Table A.1.2) in both lignins, nitrogen in the spruce lignin was below the detection limits. Otherwise, the composition of the two lignins were remarkably similar.

	C%	H%	N%
Beech	66.35	5.85	0.35
Spruce	66.24	5.86	$<$0.10

Table A.2: CHN elemental analysis for beech and spruce Organosolv lignin.

A.1.3 Lignin HSQC

HSQC of beech and spruce lignin was used to determine the key structural subunits present in lignin, here p-Xylene was used as an internal standard, to obtain more quantitative measurements via integration of signals (Figure A.1) Beech lignin was found to contain both S and G subunits, whereas spruce lignin contained only G. Beech lignin contained a higher β-O-4' signal and interunit linkages as compared to spruce.

A.1.4 ^{31}P NMR analysis

^{31}P NMR was used to quantitatively determine the hydroxyl groups of beech and spruce lignin by using a phosphorous tag which can be measured quantitatively using ^{31}P NMR. ^{31}P labelling NMR carried out as described in Y. Pu, S. Cao, and A. J. Ragauskas, Energy Environ. Sci., 2011, 4, 3154 (*230*). A stock solution of 1.6:1 anhydrous pyridine and *d*-chloroform was used to prepare two other solutions. Around 20 mg/ml of cyclohexanol was dissolved in 50 μL stock solution per sample. A second solution of 5.6 mg/ml of chromium (III) acetylacetonate (relaxation agent) was added to another 50 μL of stock solution. Vacuum dried lignin (10 mg, 24 hours drying), 100 μL of stock solution, 50 μL of cyclohexanol solution, 50 μL of the phosphitylating agent (TMDP) and 50 μL of the relaxation reagent solution was added. 1 ml of solution was transferred to a Shigemi tube.

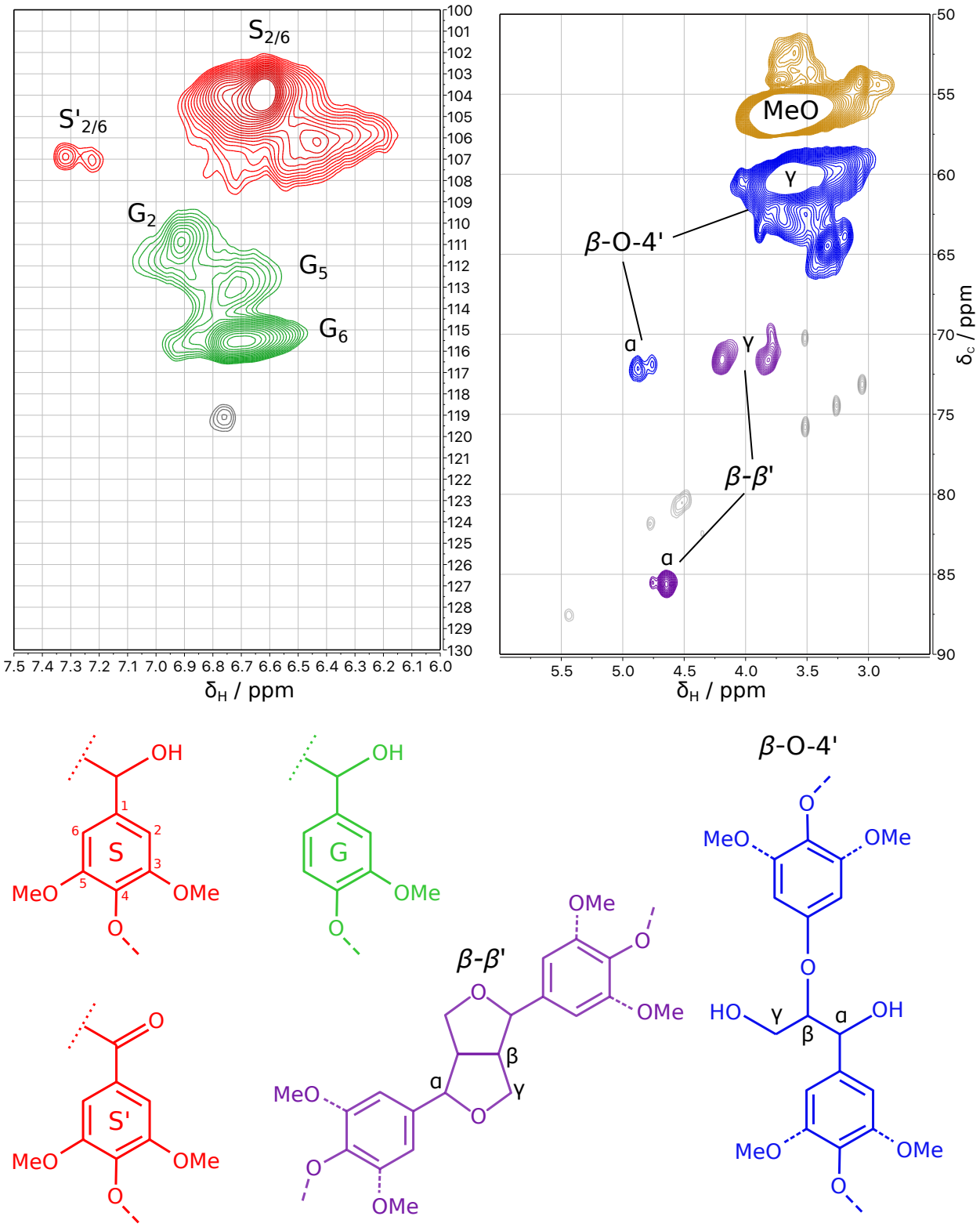

Figure A.1: The 2D HSQC NMR of beech organosolv lignin dissolved in *d*-DMSO, showing the aromatic region (left) and the oxygenated aliphatic regions (right) with colour coded chemical structures. The main subunits, syringyl (S) and guaiacyl (G) are shown along with the main linkages, β-O-4' aryl ether linkage and the $\beta - \beta'$ resinol linkage.

NMR experiments were run on a Bruker Advance 500 MHz NMR. Peak areas were normalised to the cyclohexanol signal and corrected for variations in the mass of the lignin added to the solution.

Beech lignin appears to have much less aliphatic hydroxyl groups, but a high number of β-O-4' linkages were detected. Spruce lignin appeared to me much more aliphatic in character, with considerably less β-O-4' remaining. The slightly higher concentration of carboxylic acid signals suggests that the spruce lignin may be more acidic in solution (tableA.1.4).

	Aliphatic OH mmols/g	β-O-4' mmols/g	G mmols/g	Carboxylic acid mmols/g
Beech	1.08	2.09	0.76	0.05
Spruce	1.51	0.84	1.92	0.08

Table A.3: Quantitative ^{31}P NMR analysis of organosolv beech and spruce lignin.

A.1.5 Soluble lignin NMR

In order to determine the interactions of particulates with clays, and the effects of these interactions on aggregate strength and stability, the particulates need to behave as discrete particles with consistent surface properties and particle size. Since lignin dispersed in an aqueous solution adjusted to pH 7 appeared to be partially soluble, it was of interest to see which fraction of the lignin was solubilised, particularly if it had chemical functionality which allowed it to become more soluble.

^{1}H NMR was used to indicate and quantify the functionality present in the soluble lignin fraction as a function of pH (Figure A.2). As the pH increases, the lignin soluble in the aqueous phase is more aliphatic in character and is likely to contain many more intact β-O-4' linkages. The methoxy signals increase as do signals from aromatic moieties as the pH increases. This suggests that the soluble lignin is mostly small aliphatic lignin fragments, rather than heavily modified fragments. As the beech lignin is an extracted technical lignin, it may be that condensed lignin is likely to have a higher molecular weight and contain more acid groups, which are soluble at higher pH values. However, at low pH, the amount of soluble lignin isolated was extremely low, the isolated material may have been very fine particles rather than soluble material. Native lignin is insoluble in water until a high pH is reached due to its high Mw and chain length, however lignin fragments in the soil are likely to be short and heavily chemically modified by extracellular enzymes.

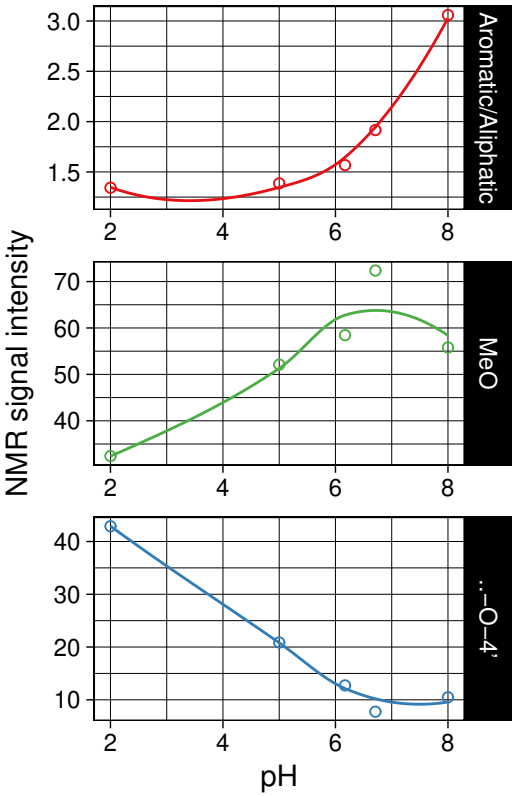

Figure A.2: Soluble extracts of aqueous lignin at various pH were extracted and redissolved in *d*-DMSO for ^{1}H NMR. Top: The ratio of signal intensity aromatic/fatty(aliphatic) increases, acid-soluble lignin is therefore more aliphatic than aromatic. Middle: Methoxy groups are found on aromatic rings, and are present in solution at higher pH. Lower: The signal from β-0-4' is much higher at lower pH too, indicating less chemically modified lignin are acid soluble. Additionally the peak for COOH also increases with pH. Note: at low pH the amount of soluble material was extremely low and repeated washings were used to obtain enough material for NMR. It may be that this material was fine particulates, rather than fully dissolved.

A.2 Adsorption isotherms

Adsorption isotherms are extremely powerful tools for determining adsorption phenomena for soluble molecules on solid sorbents. The Langmuir equation A.1, was used to fit a model to obtain values for Q_m, the maximum adsorption capacity (mg g^{-1}), and K_L, the Langmuir adsorption constant (ml g^{-1}). C_e is the concentration of lignin at equilibrium (mg/ml) and Q_e is the equilibrium adsorption capacity (mg g^{-1}). The Langmuir model assumes energetically homogeneous binding and equal surface coverage of the adsorbent. Alternatively, the Freundlich model can be used. This model accounts for multi-site adsorption and heterogeneous surface coverage via the heterogeneity factor $1/n$. (*231*) (*232*)

$$Q_e = \frac{Q_m K_L C_e}{1 + K_L C_e} \tag{A.1}$$

$$Q_e = K_F C_e^{\frac{1}{n_F}} \tag{A.2}$$

A.2.1 Absorption isotherms

Lignin is insoluble in aqueous solutions, and only sparingly soluble at high pH. Lignin was dissolved in acetone to monitor the adsorption of kaolinite to lignin and an absorption isotherm was generated. Adsoption experiments were carried out at room temperature after equlibriating at 25 °C for 24 hrs on a automatic vibrational shaker. UV-vis was used to quantify lignin in solution using an absorption maxima at 400 nm.

The fitted data gave Q_m to be 0.614 mg g^{-1}, and K_L as 2.51 ml g^{-1} using the Langmuir model. The Freundlich model gave the constants K_F to be 0.534 ml g^{-1} and n to be 1.641. An n_F value greater than 1 suggests that the adsorption is a favourable physical process, rather than chemisorption. (*232*) Langmuir and Freundlich models gave a residual sum-of-squares (RSS) of 0.008737 andl 0.008869 respectively, demonstrating that both models were good fits for the data. The Langmuir model was slightly better with a lower RSS.

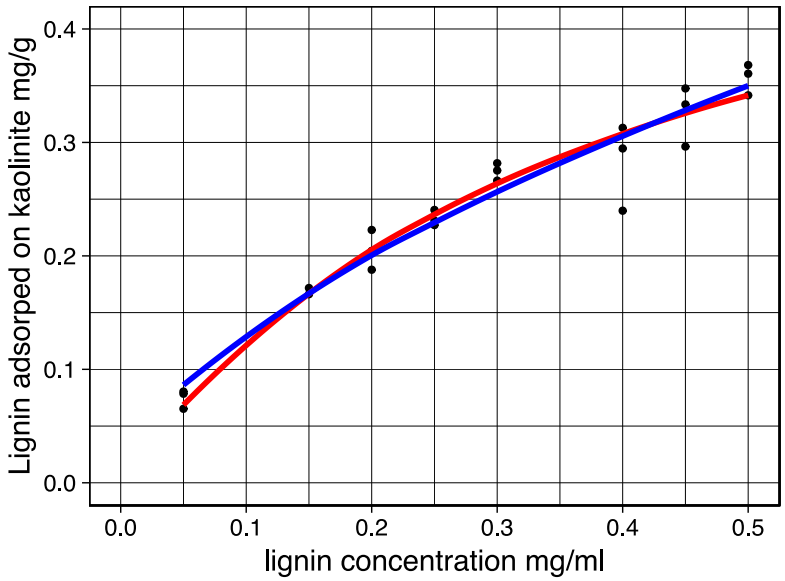

Figure A.3: The adsorption isotherm for organosolv lignin dissolved in acetone on kaolinite clay, the data was fitted to a Langmuir model (red) and a Freundlich model (blue). Langmuir model was used to obtain the equilibrium constant K_L and the maximum absorption Q_e per g of kaolinite where as Freundlich model was used to determine equilibrium constant K_F and the dimensionless heterogeneity factor n.

A.2.2 Artificial Humic and Fulvic Acids

The generation of artificial humic and fulvic acids was carried out as follows. 2.5 g of lignin was added to a large 1 L glass reactor and 500 ml of DI water was added. The suspension was adjusted to pH 12 using NaOH and heated to 50 °C. After the temperature had equilibrated, 20 ml of DI water was added slowly over a period of 3.5 hours. The reaction was stopped by adding ice cold water and removing the heating. Humic and fulvic acids were separated by pH solubility. Fulvic acids were removed by centrifuge and filtration after adjusting the pH to 2, the remainder was adjusted to pH 7 and centrifuged and filtered to remove solids. Salts were removed from the synthetic humic and fulvic acids by dialysis, then material was freeze-dried to obtain very fine powders. The samples were weighed and re-dissolved in DI water to obtain a stock solution of humic and fulvic acid solutions. The solutions were sequentially diluted and added to 1g of kaolinite or iron oxide. Adsorption isotherms were genearted using UV-vis spectroscopy using an absorption at 280 nm. A background electrolyte of 0.01 or 0.005 M $CaCl_2$ was added to test the effect of additional calcium. Kaolinite was washed first with 0.01 M $CaCl_2$ and then washed twice with DI water. The kaolinite was oven dried at 35 °C.

Experiment	$[CaCl_2]/mM$	Langmuir RSS	Freundlich RSS
Kaolinite fulvic acid	10	3.87E-05	2.35E-04
	5	8.49E-05	2.87E-04
Iron oxide fulvic acid	10	2.98E-05	7.80E-05
	5	1.27E-04	1.42E-04
Kaolinite humic acid	10	5.74E-03	5.87E-03
	5	9.20E-03	8.92E-03

Table A.4: Residual sum-of-squares (RSS) values for isotherms fitted with Langmuir and Freundlich models

Results

The adsorption isotherms with background electrolytes of 10 or 5 mM $CaCl_2$ were near identical in all cases and so only the results for the 10 mM $CaCl_2$ are presented graphically (Figure A.4 and A.5). The quality of the fits were compared using residual sum-of-squares (RSS). The Freundlich model was a considerably better fit than the Langmuir model for fulvic acid on kaolinite, which may indicate a patchy adsoption due to the heterogeneity of the kaolinite surface. On iron oxide however, the Langmuir isotherms were marginally better. The Langmuir and Freundlich models were both good fits for the humic acids on kaolinite (Table A.2.2).

The higher Q_e value for humic acids (0.66 - 0.90 mg g^{-1}) as compared to fulvic acids (0.26 - 0.30 mg g^{-1}) demonstrates a much higher mass loading of humic acids on kaolinite surfaces, however, this may reflect the probable higher molecular weight of humic acids compared to fulvic acids (Figure A.4). Kaolinite has a higher binding affinity for fulvic acids than iron oxide, which may only reflect the differences in surface areas (iron oxide = 9.50 m^2/g, kaolinite = 13.40 m^2/g) which suggests a very weak and non-specific binding (Figure A.5). n values were all > 1, suggesting that the binding was not homogeneous however, as no evidence for multi-layer adsorption was indicated.

The pH and the concentration of Ca^{2+} remained constant with the addition of the humic and fulvic acids. Kaolinite is able to buffer the pH (pH = 4.60 $\mp$ 0.07) at all concentrations, although no Ca^{2+} is exchanged and higher concentrations of both humic and fulvic acids are progressively more acid. Adsorption by electrostatic interactions and cation bridging is more favourable at low pH, so this data is likely to represent a near-maxima in the adsorption of these compounds.

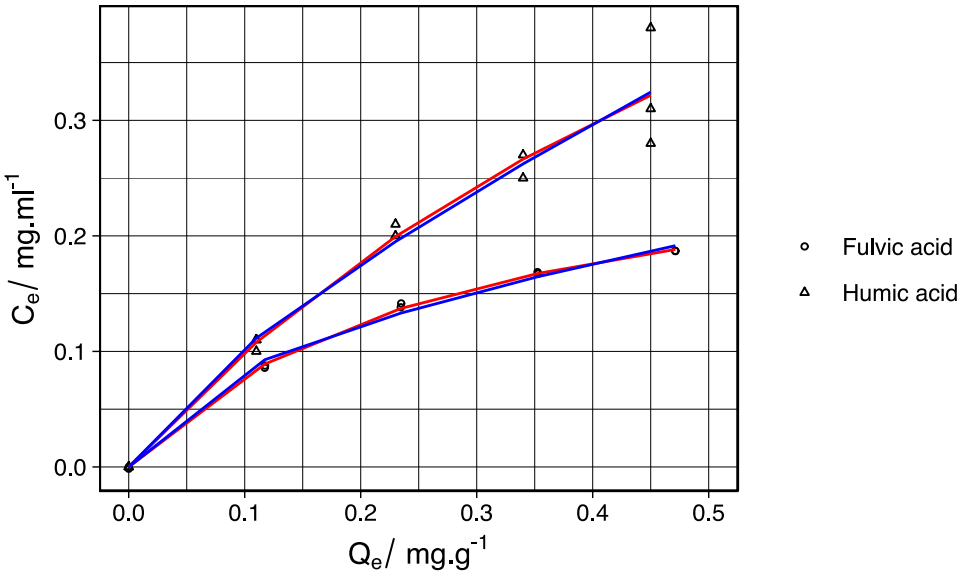

Figure A.4: The adsorption isotherm for lignin derived 'humic' and 'fulvic' acids on kaolinite clay, the data was fitted to a Langmuir model (red) and a Freundlich model (blue). Humic acids were found to have a higher adsorption. Langmuir model was used to obtain the equilibrium constant K_L and the maximum absorption Q_e per g of kaolinite where as Freundlich model was used to determine equilibrium constant K_F and the dimensionless heterogeneity factor n. Measurements were made in triplicate.

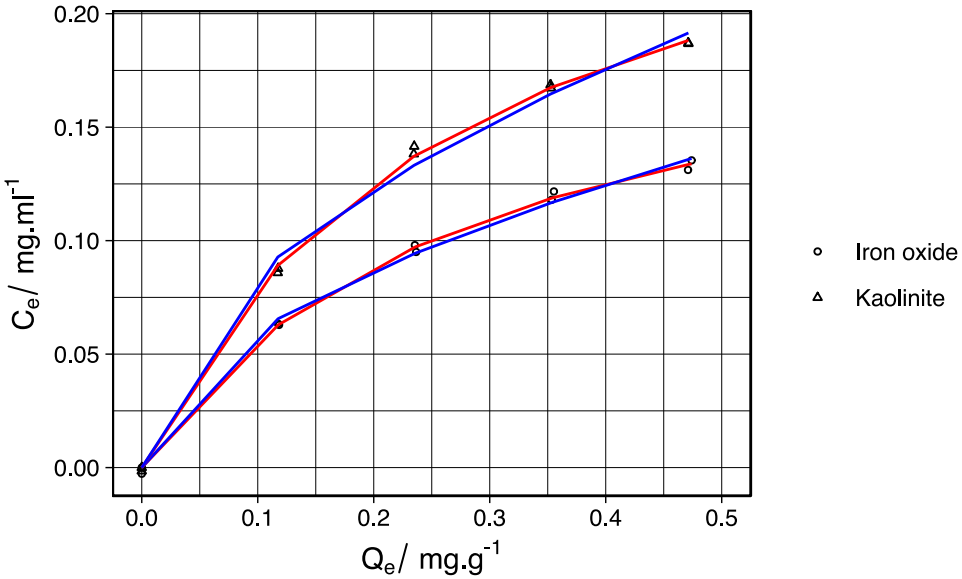

Figure A.5: The adsorption isotherm for lignin derived 'fulvic' acids on kaolinite and iron oxide, the data was fitted to a Langmuir model (red) and a Freundlich model (blue). Kaolinite was found to be a stronger adsorbent of fulvic acids. Measurements were made in triplicate.